MAX-PLANCK-GESELLSCHAFT

Max Planck Institute for Dynamics and Self-Organization

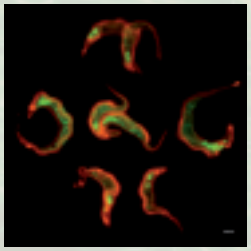
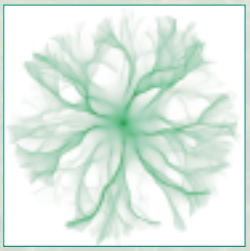
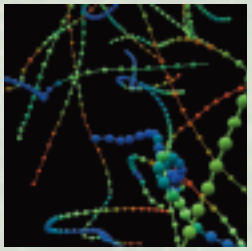
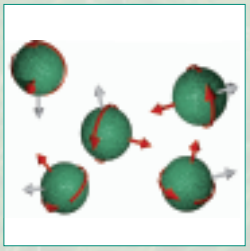
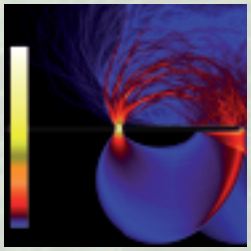
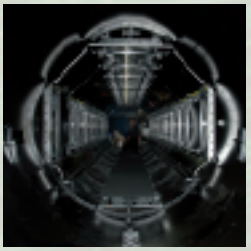

Research Report 2008

Max Planck Institute for Dynamics and Self-Organization
Bunsenstraße 10 – D-37073 Göttingen – www.ds.mpg.de

Editing: Dr. Kerstin Mölter
Photos: Prof. Dr. Markus Engstler, Dr. Ragnar Fleischmann, Peter Goldmann, Dr. Artur Kubitzek, Hans-Herbert-Krull
Design & Layout: dauer design, Göttingen
Printed by: Goltze Druck, Göttingen

Max Planck Institute
for Dynamics and Self-Organization

Research Report 2008

DIRECTORS

Prof. Dr. Theo Geisel (Managing Director)
Prof. Dr. Eberhard Bodenschatz
Prof. Dr. Stephan Herminghaus

SCIENTIFIC ADVISORY BOARD

Prof. Dr. William Bialek, Princeton University, USA
Prof. Dr. David K. Campbell, Boston University, USA
Prof. Dr. Jerry P. Gollub, Haverford College, USA
Prof. Dr. Pierre C. Hohenberg, New York University, USA
Prof. Dr. Alexei R. Khokhlov, Moscow State University, Russia
Prof. Dr. Boris I. Shraiman, University of California, Santa Barbara, USA
Prof. Dr. Uzy Smilansky, Weizmann Institute of Science, Israel
Prof. Dr. Sandra M. Troian, Princeton University, USA
Prof. Dr. Cynthia Volkert, Georg August University Göttingen, Germany

Contents

Introduction

Max Planck Institute for Dynamics and Self-Organization

MAX-PLANCK-GESELLSCHAFT

As recent decades have brought considerable progress in the understanding of simple temporal and spatiotemporal systems exhibiting complicated dynamics, it also proves to be a promising aim to tackle the dynamics of complex matter, where a large number of intimately coupled and possibly highly disparate entities often conspire to generate unanticipated structure and dynamics at higher levels of integration. Biology, in particular cell biology, provides many examples, but one also finds self-organization far from equilibrium e.g. in the pattern formation of a dewetting liquid film, the collective dynamics of eddies in a thunderstorm cloud, or the complex signaling of neurons in the brain. The mission of the Max Planck Institute for Dynamics and Self-Organization (MPIDS) is the investigation of the physics of such phenomena. Founded in 2003 as the successor of the former Max Planck Institute for Fluid Dynamics, it combines expertise from fluid dynamics, soft condensed matter physics, and nonlinear dynamics. The institute presently comprises three departments which jointly study various aspects of non-equilibrium complex systems.

Considerable attention is devoted to pattern formation phenomena in media as different as convection in fluids, the visual cortex of the brain, or the signaling of cell colonies. While the microscopic properties of the systems are quite disparate, certain aspects of the emerging structures are often strikingly similar. Finding the general principles underlying the commonality of the non-linear processes is at the center of this research.

The realm of life and biology intensively exploits such processes. As a further complication, however, biological systems are strongly influenced by discrete events (gene expression, mutations, etc.), have active components (molecular motors, transport, etc.), and operate on many scales and in a stochastic or disordered environment; e.g. molecular mechanisms are operative below the micron scale. The fluid dynamics of biological systems is affected by large macromolecules or other self-assembling structures and components. Due to the small dimensions some aspects of the comparably simple continuous descriptions may break down and molecular scale properties must be considered.

Our current research also includes medical applications of concepts of self-organization (in cellular signaling, neuronal dynamics in the brain, cardiac fibrillation, and the spread of epidemics), which necessitate a dedicated interdisciplinary approach. The research programs of the departments are embedded in collaborations with the *Bernstein Center for Computational Neuroscience* (BCCN), the *International Collaboration for Turbulence Research* (ICTR), and the Faculties of Physics and Medicine at the University of Göttingen.

In the past year we have formed interdepart-

mental topical groups, which focus on four areas of common interest and aim at strengthening the collaborations among the departments and independent junior research groups (IJRG). The presentation of our research activities in the next section follows the structure of these groups.

The institute was able to broaden its scope by attracting three IJRGs, the *Network Dynamics Group* headed by Marc Timme, the *Group of Nonlinear Dynamics* and *Arrhythmias of the Heart* led by Stefan Luther, and the recently established group of Björn Hof for the *Onset of Turbulence and Complexity*. Another independent junior research group was created by the Department of Nonlinear Dynamics in the BCCN Göttingen (Alexander Gail) and is presently hosted by the German Primate Center (DPZ) in Göttingen for practical reasons. The institute also has increased the number of its independent junior fellows; there are currently three Bernstein Fellows associated with the Department of Nonlinear Dynamics and one Bernstein Fellow associated with the Department of Fluid Dynamics, Pattern Formation, and Nanobiocomplexity. These fellows at the advanced postdoctoral level can define their own research program and profit from varying collaborations. They were all appointed in competitive selection processes.

The institute had to cope with an increasing demand on laboratory and office space. It is presently divided into three separate locations. The departments of Theo Geisel, Stephan Herminghaus, part of Eberhard Bodenschatz's department, and two independent junior research groups are located at the original campus of the MPI for Fluid Dynamics close to downtown Göttingen. The IJRG of Stefan Luther is hosted in the building of the MPI for Experimental Medicine, providing it with the proximity to its medical partners. Another part of Eberhard Bodenschatz's department is accommodated at the Max Planck Institute for Biophysical Chemistry adjacent to the site where the first part of our new building is already completed. This includes the experimental hall, which accommodates the turbulence wind tunnel and other fluid dynamics experiments, a computational facility, and a clean room. The latter is instrumental for many of the microfluidic and nanoscale experiments, which are planned in the near future. The second and main part of the new building will provide space for all departments and service groups and is scheduled for completion in 2010. It will reunite the institute in stimulating vicinity of the Max-Planck Institute for Biophysical Chemistry and the University Campus.

Göttingen, January 2008

Theo Geisel, Eberhard Bodenschatz, Stephan Herminghaus

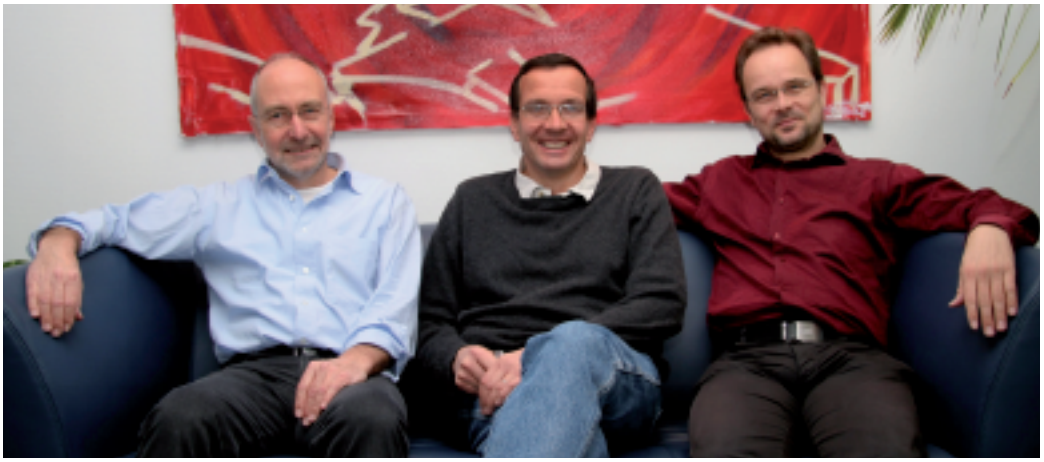

Department of Nonlinear Dynamics

Theo Geisel

The Department of Nonlinear Dynamics is the theory department of the Institute. Its research is motivated by such questions as: How do the neurons in our brain cooperate when we perceive an object or perform a task? How does the dynamics of such networks depend on their topology? What are the general principles governing the formation of patterns and neuronal representations in the cortex? What are the dynamical properties of mesoscopic systems and how can they be described semiclassically? Are there statistical principles underlying human travel and can they be used to forecast the geographical spread of epidemics?

These questions typically address the complex dynamics of spatially extended or multicomponent nonlinear systems which still hold many surprises. As an example, we found unstable attractors in networks of spiking neurons, a phenomenon which would neither have been guessed nor understood without mathematical modelling and which many physicists consider an oxymoron. They have a full basin of attraction, but due to their unstable character they allow the network to switch easily and rapidly between different attractors under external stimulation. They may play a functional role in the central nervous system by providing it with a high degree of flexibility in order to respond to frequently changing tasks.

The example illustrates the need and the role of mathematical analysis for the understanding of complex systems in nature. The concepts and methods developed previously in nonlinear dynamics and chaotic systems can now help us clarify the dynamics and function of spatially extended and multicomponent natural systems. On the other hand, rigorous mathematical analysis of the dynamics of such systems often cannot rely on mainstream recipes but poses new and substantial challenges. In particular, neural systems exhibit several features that make them elude standard mathematical treatment: The units of the network e.g. communicate or interact at discrete times only and not continuously as in many-body theory in physics. There are significant interaction delays, which make the systems formally infinite-dimensional. Complex connectivities give rise to novel multi-operator problems, for which we have devised new methods based on graph theory so as to obtain rigorous analytic results.

We have also previously applied graph theory in our work on quantum chaos. Similarly we used random matrix theory not only in quantum mechanical systems, but also for the stability matrices of synchronized firing patterns in disordered neural networks. Neuronal spike trains may be considered as stochastic point processes and so may energy levels of quantum chaotic systems. This list demonstrates to which extent cross-fertilization among our various areas of research is possible; in fact, it has often been substantial for our progress. The scientists of this department feel that the breadth of existing research activities and the opportunity of intense scientific exchange are key prerequisites for the success of our work. These features are also important for establishing and sustaining a culture of analytic rigor in theoretical studies which attempt to work in proximity to biological experiments.

Theoretical studies of complex systems are scientifically most fruitful when analytical approaches to mathematically tractable and often abstract models are pursued in close conjunction with comprehensive computational modeling and advanced quantitative analyses of experimental data. The department thus naturally has a strong background in computational physics and operates considerable computer resources. Research for which this is essential besides the network dynamics mentioned above includes e.g. studies of pattern formation in the developing brain, the dynamics of spreading epidemics, and transport in mesoscopic systems.

The Department of Nonlinear Dynamics was created by the Max Planck Society in 1996, when the focus of the institute was on mesoscopic systems. With the opening of two new experimental departments in the institute in 2003 this focus has changed; our group is therefore shifting its accents and tackling new subjects in the interest of a coherent research program. Besides, this department has initiated and hosts the federally (BMBF) funded Bernstein Center for Computational Neuroscience Göttingen, in which it cooperates with advanced experimental neuroscience labs in Göttingen. With the help of this funding the department has created the positions of Bernstein Fellows, independent junior fellows who can define their own research program and profit from varying collaborations. Our group is closely connected with the Faculty of Physics, it is financed to a large part by the Max Planck Society and to a smaller part by the University of Göttingen through its Institute for Nonlinear Dynamics.

Prof. Dr. Theo Geisel
studied Physics at the Universities of Frankfurt and Regensburg, where he received his doctorate in 1975. After postdoctoral research at the MPI for Solid State Research in Stuttgart and at the Xerox Palo Alto Research Center he became Heisenberg Fellow in 1983. He had appointments as Professor of Theoretical Physics at the Universities of Würzburg (1988-1989) and Frankfurt (1989-1996), where he also acted as a chairperson of the Sonderforschungsbereich Nichtlineare Dynamik before becoming director at the MPI for Fluid Dynamics (now MPI for Dynamics and Self-Organization) in 1996. He also teaches as a full professor in the Faculty of Physics of the University of Göttingen; he initiated and heads the Bernstein Center for Computational Neuroscience Göttingen.

Dr. Dirk Brockmann
studied theoretical physics at Duke University, NC and the Georg-August-University of Göttingen where he received his Diploma in the Institute for Theoretical Physics under the supervision of Reiner Kree in 1995. In 1996 he joined the Department of Nonlinear Dynamics and received his PhD in 2003 where he now leads a group of 6 students. In the fall of 2007 he was appointed Associate Professor for Complexity in the Department of Engineering Sciences and Applied Mathematics and the Northwestern Institute for Complex Systems at Northwestern University. He will join the faculty at Northwestern in summer 2008.

Dr. Ragnar Fleischmann
studied physics at the Johann-Wolfgang-Goethe University in Frankfurt am Main and received his PhD in 1997. The thesis was awarded the Otto-Hahn-Medal of the Max-Planck-Society. From 1997 to 1999 he was Postdoc in the group of Theo Geisel at the Max-Planck-Institut für Strömungsforschung and from 1999 to 2000 in the group of Eric Heller at Harvard University. Since 2000 he works as a scientific staff member in the Department for Nonlinear Dynamics and as deputy institute manager of the Max-Planck-Institute for Dynamics and Self-Organization.

Dr. Denny Fliegner
studied physics at the University of Heidelberg and received his doctoral degree in theoretical particle physics in 1997. From 1997 to 2000 he was a Postdoc at Karlsruhe University working on parallel computer algebra and symbolic manipulation in high energy physics. He joined the group of Theo Geisel at the Max-Planck-Institut für Strömungsforschung as an IT coordinator in 2000.

Dr. J. Michael Herrmann
studied mathematical physics and computer science at the University of Leipzig where he obtained his doctorate with a thesis on artificial neural networks. He did postdoctoral research at NORDITA (Copenhagen), RIKEN (Wako) and the Max-Planck-Institut für Strömungsforschung before becoming Assistant Professor at the Institute for Nonlinear Dynamics of the University of Göttingen and adjunct scientist at the Max Planck Institute for Dynamics and Self-Organization. He is a founding member and principal investigator of the Bernstein Center for Computational Neuroscience Göttingen as well as a member of the Center of Informatics at the University of Göttingen. In 2008 he starts working as a Lecturer at the University of Edinburgh.

Dr. Tsampikos Kottos
received his PhD in theoretical solid-state physics from the University of Crete in 1997. In 1997 he received a US European Office of Air Force Research and Development Fellowship. In the same year, he received the Feinberg Fellowship and joined the Quantum Chaos group of U. Smilansky at the Weizmann Institute of Science, Israel. In 1999 he moved to Germany as a postdoctoral research fellow in the group of T. Geisel at the MPI for Dynamics and Self-Organization in Göttingen. In 2005 he has become an Assistant Professor at Wesleyan University, USA. He continues working with a part-time appointment as an adjunct scientist in the Department of Nonlinear Dynamics. Dr. Kottos was recently awarded the 2006 International Stefanos Pnevmatikos Award given biannually to outstanding young researchers in the field of nonlinear phenomena.

Dr. Holger Schanz
studied physics at the Technical University of Dresden and graduated in 1992. He worked towards his PhD in the groups of Werner Ebeling (Humboldt University Berlin) and Uzy Smilansky (The Weizmann Institute of Science, Rehovot, Israel) and received his doctorate from the Humboldt University in 1996. After two years as a Postdoc at the Max Planck Institute for Physics of Complex Systems in Dresden, he joined the group of Theo Geisel at the Max-Planck-Institut für Strömungsforschung in Göttingen. He was Assistant Professor at the Institute for Nonlinear Dynamics of the University of Göttingen, and adjunct scientist at the Max Planck Institute for Dynamics and Self-Organization. In November 2006 he left academia to work as a consultant in mathematical finance.

Dr. Annette Witt
studied mathematics at the Humboldt-University Berlin and received her doctorate in theoretical physics from the University of Potsdam in 1996. Her thesis was awarded the Otto-Hahn-Medal of the Max Planck Society. Annette worked as a postdoctoral researcher at the University of Potsdam, the Istituto Nationale di Ottica Applicata (Florence, Italy), the GeoResearch Center Potsdam, the Environmental Change Research Centre (London, U.K.) and King's College London. She has recently joined the Department of Nonlinear Dynamics of the MPIDS where she develops statistical tools for time series analysis with applications to neuroscience.

Research Group Theoretical Neurophysics

The Research Group Theoretical Neurophysics was established in 2004 by the appointment of Fred Wolf on the associate professor level (W2) by the President of the Max Planck Society. Wolf's Group is an integral part of the Department of Nonlinear Dynamics and studies theoretical neuroscience problems from the dynamics of neuronal encoding in single neurons to the self-organization of large-scale networks in the brain. It comprises researchers with backgrounds mostly in theoretical physics and closely collaborates with experimental neuroscience laboratories at Duke and Carnegie Mellon University (USA), the Hebrew University (Israel) and the Universities of Göttingen and Jena. It is supported by the Human Frontier Science Program, the German Israeli Research Foundation and the BMBF.

Dr. Fred Wolf
studied physics and neuroscience at the University in Frankfurt, where he received his doctorate in theoretical physics in 1999. After postdoctoral research at the MPI für Strömungsforschung (Göttingen) and the Interdisciplinary Center for Neural Computation of the Hebrew University of Jerusalem (Israel), he became a research associate at the MPI für Strömungsforschung in 2001. Since 2001 he spent various periods as a visiting scientist at the KITP (Santa Barbara, USA). In 2004 he became head of the research group of Theoretical Neurophysics at the MPIDS. He is a founding member of the Bernstein Center for Computational Neuroscience Göttingen and faculty member of several Physics and Neuroscience PhD programs at the University of Göttingen and of the International Max Planck Research School Neurosciences.

Bernstein Fellows

Dr. Armin Biess
studied physics at the Universities of Ulm and Heidelberg with major interest in theoretical physics. He received a doctorate in Applied Mathematics in 2004 from the Weizmann Institute of Science, Israel, and conducted postdoctoral research in the Mathematics Department of this institute. In January 2008 he joined the Max Planck Institute for Dynamics and Self-Organization and Bernstein Center for Computational Neuroscience Göttingen as a Bernstein Fellow.

Dr. Babette Dellen
studied physics at the University of Cologne, Germany, and at Washington University in St. Louis, USA. She received a Diplom in theoretical physics in 2001 (University of Cologne) and a doctorate in physics in 2006 (Washington University in St. Louis). In 2006, she joined the Bernstein Center for Computational Neuroscience, Göttingen, as a postdoctoral researcher. She became a Bernstein Fellow in the Max Planck Institute for Dynamics and Self-Organization in January 2008.

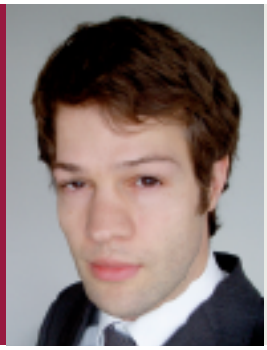

Dr. Fabian Theis
obtained MSc degrees in mathematics and physics in 2000 at the University of Regensburg. He received a PhD degree in physics from the same University in 2002 and a PhD in computer science from the University of Granada in 2003. Thereafter he headed the Signal Processing & Information Theory group at the Institute of Biophysics in Regensburg and joined the MPIDS and BCCN Göttingen as a Bernstein Fellow in 2006. He accepted an offer to head the Computational Modeling in Biology group at the Institute of Bioinformatics of GSF, Munich in 2007 and continues working part-time as a Bernstein Fellow at the MPIDS.

Dr. Tzvetomir Tzvetanov
studied physics at the Université Louis Pasteur (ULP, Strasbourg, France) and the University of Manchester (UK). He received an M.Sc. in physics in 1998 and a PhD in neuroscience in 2003 from the Université Louis Pasteur. From 2004 to 2007 he has been a postdoctoral researcher at the German Primate Center in Göttingen. He became a Bernstein Fellow in the Max Planck Institute for Dynamics and Self-Organization and the Bernstein Center for Computational Neuroscience Göttingen in 2007.

Department of Dynamics of Complex Fluids

Stephan Herminghaus

We investigate mechanisms of self-organization and self-assembly by studying selected complex fluid model systems. Our interest ranges from fundamental aspects of dissipative collective behavior to the physics of prototype bio-systems. Consequently, a wide scope of methods is employed including analytical statistical theory, advanced simulation tools and cutting edge experimental techniques. What is most intriguing to us is the question whether there are general common 'principles' behind the various instances of structure formation and emergence in open systems.

On the fundamental side, wet granular materials have proved to be versatile model systems for studying collective behavior in systems violating detailed balance on the microscopic level. Their particular charm is their being right at the border triangle of interfaces, complex fluids, and systems far from thermal equilibrium, thereby rejoining fields of expertise of different subgroups of the department. On the complex side, biological matter and bio-systems are the most intricate systems we are studying, but we concentrate on those which are simple enough to be described by physical and physico-chemical principles. This includes the dynamics of actin filaments in microchannels, the gelation of thrombin/fibrinogen systems, the self-assembly of DNA/poly-electrolyte systems, and the hydrodynamics of microbial behavior on the molecular scale.

Other projects are spanning the range from complex soft interfaces to the generation of artificial micro- and nano-devices, which play important roles as building blocks of the systems mentioned above. It is this range, between fundamentals and bio-systems, which has seen the largest productivity in patent disclosures in the last two years. These projects, which are mainly concerned with the development of unconventional concepts in microfluidic systems, are strongly fertilized by the insight we gain in non-equilibrium systems, and pushed by the need for soft manipulation techniques for our bio-related projects.

Recently, there have been substantial fluctuations in our personnel. Holger Stark has taken a chair for theoretical physics at the TU Berlin, and Ralf Seemann has received a professorship at the Saarland University. Jürgen Vollmer has joined the group, strengthening our theoretical activities in the field of physics far from thermal equilibrium. With the new CARS setup run by Kristian Hantke, which enables material specific confocal microscopy without flourescence staining, the department substantially widens its spectrum of available microscopy techniques.

Prof. Dr. Stephan Herminghaus received a PhD in Physics from the University of Mainz in 1989. Postdoctoral stay at the IBM Research Center in San Jose, California (USA), in 1990 . Habilitation at the University of Konstanz in 1994. Head of an independent research group at the MPI for Colloids and Interfaces, Berlin, from 1996 until 1999. Full professor at the University of Ulm from 1999 until 2003. Since 2003 Director at the MPI for Dynamics and Self-Organization, Göttingen. Since 2005, additional appointment as an adjunct professor at the University of Göttingen. Appointed as Professeur Invité at Université Paris VI for the winter term 2006/7.

Dr. Christian Bahr
studied Chemistry at the Technical University Berlin and received his PhD in 1988. Research stays and postdoctoral work took place at the Raman Research Institute (Bangalore, India) and the Laboratoire de Physique des Solides of the Université Paris-Sud (Orsay, France). After his Habilitation for Physical Chemistry at the Technical University Berlin in 1992, he moved 1996 to the Physical Chemistry Institute of the University Marburg as a holder of a Heisenberg-Fellowship. 2001-2004 he worked as a software developer in industrial projects. In 2004 he joined the group of Stephan Herminghaus at the MPI for Dynamics and Self-Organization. Research topics comprise experimental studies of soft matter, especially thermotropic liquid crystals, phase transitions, structures of smectic phases, thin films, interfaces and wetting.

Dr. Martin Brinkmann
studied Physics and Mathematics at the Free University of Berlin between 1990 and 1998 where he received his Diploma in Physics. After an internship at the Dornier Labs (Immenstaad, Lake Constance) in 1999 he joined the theory group of Prof. Reinhard Lipowsky at the MPI of Colloids and Interfaces (Potsdam, Germany) to work on wetting of chemically patterned substrates. In 2003 he received his doctorate from the University of Potsdam. During a postdoctoral stay in the Biological Nanosystems Group at the Interdisciplinary Research Institute in Lille (France) he explored wetting of topographic substrates as a possible way to manipulate small liquid droplets. Since the beginning of 2005 he investigates wetting of regular and random geometries in the department Dynamics of Complex Fluids at the MPI for Dynamics and Self-Organization.

Dr. Manfred Faubel
Physics studies at the University of Mainz (diploma 1969), and in Göttingen (PhD in 1976). Postdoctoral stays at the Lawrence Berkeley Laboratory, 1977, and in Okasaki at the Institute for Molecular Sciences in Japan, 1981. Employed by the MPI für Strömungsforschung since 1973. Molecular beams studies of rotational state resolved scattering cross sections for simple benchmark collision systems, such as Li^+-H_2, He-N_2 and for reactive F-H_2 scattering. Since 1986 exploration of the free vacuum surface of liquid water microjets. Photoelectron spectroscopy of aqueous solutions with synchrotron radiation at BESSY/Berlin (1999 to present), and, by laser desorption mass spectrometry of very large ions of biomolecules from liquid jets in vacuum (in a collaboration with MPI-BPC).

Dr. Kristian Hantke
started his Physics study at the Philipps-University Marburg in 1996 and received the Bachelor of Science in Physics at the UMIST, Manchester in 2000 after an Erasmus internship. In 2001 he joined the semiconductor-physics group of Prof. W. Rühle in Marburg, where he worked on the optical properties of dilute III-V nitrides. He received his Diploma in 2002 and his PhD in Physics in 2005. After studying the optical injection of spin currents during a post-doctoral stay at the Philipps-University in Marburg he joined the group of Prof. S. Herminghaus at the MPI for Dynamics and Self-Organization in 2007. As technical laboratory assistant he is responsible for the operation of a new CARS setup in combination with a confocal microscope.

Dr. Thomas Pfohl
studied Chemistry at the Johannes-Gutenberg University, Mainz, and received his doctorate in Physical Chemistry from the University of Potsdam in 1998. After his postdoctoral research at the Materials Research Laboratory, University of California, Santa Barbara, from 1998 to 2000, he became a research assistant at the Department of Applied Physics at the University of Ulm from 2000 until 2004. In 2001 he received a research funding to lead his "Independent Emmy Noether Junior Research Group" by the DFG. Since 2004 he is project leader "Biological Matter in Microfluidic Environment" at the Department "Dynamics of Complex Fluids" at the Max-Planck-Institute of Dynamics and Self-Organization.

Prof. Dr. Ralf Seemann
studied physics at the University of Konstanz where he received his diploma in 1997. The diploma work was carried out at the MPI of Colloids and Interfaces in Berlin-Adlershof. He received his doctorate in 2001 from the University of Ulm where he experimentally studied wetting and rheological properties of complex fluids. In 2003 he received the science award of Ulm. During a stay as postdoctoral researcher at the University of California at Santa Barbara, he explored techniques to structure polymeric materials on the micro- and nano-scale. Since 2003 he is a group leader at the MPI for Dynamics and Self-Organization, Göttingen. Ralf Seemann was appointed as professor at the Saarland University in 2007. Among others he is concerned with wetting of topographic substrates, wet granular media, and discrete microfluidics.

Dr. Habil. Jürgen Vollmer
studied physics at the University of Utrecht (NL). In 1990 he joined Prof. Harri Thomas group at the Universität Basel (CH), where he worked on applications of transient chaos, and became interested in the phase behaviour and kinetic properties of microemulsions. He pursued postdoctoral studies on the foundations of statistical transport theory and on the kinetics of complex fluids in Essen, Brussels and Mainz, where he was a Schloessmann research fellow of the MPG from 2001-2002. In 2003 he joined the AG Komplexe Systeme at the Philipps Universität Marburg, and since April 2007 he is a member of the department Dynamics of Complex Fluids at the MPIDS. In 2001 Jürgen Vollmer obtained his habilitation in Theoretical Physics from the University of Essen, and he was head of the AG Komplexe Systeme in Marburg in the academic year 2004/05.

Associated Scientist

apl. Prof. Dr. Folkert Müller-Hoissen
received his doctorate in theoretical physics from the University of Göttingen in 1983. After postdoc positions at the MPI for Physics in Munich and the Yale University in New Haven, USA, he returned to the University of Göttingen as a Wissenschaftlicher Assistent, passed the Habilitation in 1993 and became a Privatdozent. Since 1996 he carries on his research in mathematical physics at the MPI.

Department of Fluid Dynamics, Pattern Formation and Nanobiocomplexity

Eberhard Bodenschatz

The self-organization of complex systems impacts all levels of our everyday lives. The complexity of these systems should not be mistaken for the meaning of the word "complicated", but rather reflects the robust properties of a system that emanate from its highly nonlinear properties. The dynamics of complex systems is prescribed by a set of external parameters and by the fact that they are not in equilibrium – they only function when energy is 'consumed', i.e., used and dissipated as heat. The behavior itself can range from being well structured to highly disordered. Due to the nonlinearities, small changes in parameters can lead to a complete change in structure and dynamics. This can be most easily seen, for example, in the biology of a cell, where the expression of a few molecules can alter the behavior of a cell with, sometimes dire, consequences to the whole organism. Although different in detail, the temporal and spatial structure of many systems can often be described by general principles.

It is the topic of the Laboratory of Fluid Dynamics, Pattern Formation and Nanobiocomplexity (LFPN) to uncover and understand these principles. In our approach we are relying heavily on methods from the fields of nonlinear dynamics, pattern formation, and non-equilibrium statistical mechanics. The laboratory has two groups: one is led by the Scientific Director Eberhard Bodenschatz and the other on Cardiac Dynamics by the Independent Junior Research Group Leader Stefan Luther. The independent research group was established in the summer of 2007 by positions and startup funds from LFPN.

The topics of research of LFPN are focused on well-defined problems in the physics of fluid dynamics and of cell biology. We investigate experimentally and theoretically pattern formation, spatiotemporal chaos, and turbulence in thermal convection. In collaboration with researchers from the International Collaboration for Turbulence Research (ICTR.eu) we study particle dynamics in the fully developed turbulence of simple and complex fluids with its implication to fundamental theories, but also to practical issues like turbulent mixing and transport.

A highlight of the year 2008 is the newly established Göttingen Turbulence Facility. In biological physics we are especially interested in the spatio-temporal dynamics of intracellular and intercellular processes. At the level of a cell we conduct experiments using microfluidic devices to probe and to understand quantitatively the dynamics of intracellular molecular networks involved in chemotaxis. At the level of cells to the whole organ, we are studying the complex dynamics of cardiac fibrillation and its control.

Our research has been and will continue to be truly interdisciplinary from engineering, material science, geophysics, and applied mathematics, to chemistry, biology, and medicine. The research of LFPN is connecting seamlessly to that of the other two Departments, of the three Independent Junior Research Groups, and of the Max-Planck-Fellow.

Prof. Dr. Eberhard Bodenschatz
was born on April 22, 1959 in Rehau. He received his doctorate in theoretical physics from the University of Bayreuth in 1989. In 1991, during his postdoctoral research at the University of California at Santa Barbara, he received a faculty position in experimental physics at Cornell University. From 1992 until 2005, during his tenure at Cornell he was a visiting professor at the University of California at San Diego (1999-2000). In 2003 he became a Scientific Member of the Max Planck Society and an Adjunct Director (2003-2005)/ Director (since 2005) at the Max Planck Institute for Dynamics and Self-Organization. He continues to have close ties to Cornell University, where he is Adjunct Professor of Physics and of Mechanical and Aerospace Engineering (since 2005).

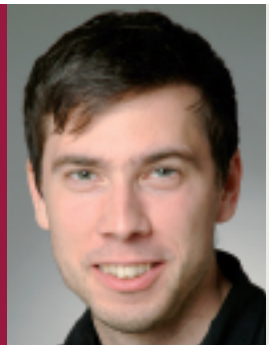

Prof. Dr. Carsten Beta
Carsten Beta studied Chemistry at the Universities of Tübingen and Karlsruhe and at the Ecole Normale Supérieure in Paris (France). In 2001, he joined the Department of Gerhard Ertl at the Fritz Haber Institute of the Max Planck Society in Berlin and in 2004 received his doctorate in Physical Chemistry from the Free University Berlin. He then moved to the US as a postdoctoral research fellow in the group of Eberhard Bodenschatz at Cornell University and as a visiting scientist at the University of California at San Diego. Since 2005 he was a group leader at the Max Planck Institute for Dynamics and Self-Organization in Göttingen and recently became a Junior Professor for Biological Physics at the University of Potsdam.

Dr. Gregory Bewley
received his bachelor's degree from Cornell University in mechanical engineering in 2000. He was awarded a PhD from Yale University in 2006 for observing inertial waves in rotating turbulence using liquid helium, and for discovering how to visualize quantized vortices in superfluid helium, while under the supervision of professor K.R. Sreenivasan. He continued these experimental investigations as a post doc at the University of Maryland, before joining the Max Planck Institute for Dynamics and Self-organization in 2007.

Dr. Azam Gholami
received her BSc from Sharif University in Tehran and her MSc from Institute for advanced studies in Basic Sciences (IASBS), in Zanjan, Iran. In 2003, she started her graduate work in Physics at Hahn-Meitner Institute (Berlin) working with Prof. E. Frey studying polymer physics and modelling cell motility, receiving her degree in 2007 from Ludwig-Maximilian-Universität of München. In January 2008, she joined the Bodenschatz group in Max-Planck Institute for Dynamics and Self-Organization as a post-doctoral research associate to work on actin filament dynamics at oil-water interface.

Dr. Mathieu Gibert
received his M.D. (2004) and Ph.D (2007) in Physics from the Ecole Normale Supérieure in Lyon (France). During his Ph.D he introduced the new and promising experimental configuration of Turbulent Thermal Convection in a vertical channel and was involved in the first Lagrangian measurements of temperature, velocity and local heat flux in the classical Rayleigh-Bénard turbulent flow ("smart particle" project). In October 2007 he became a member of the MPI for Dynamics and Self-Organization, and joined the Bodenschatz group as a post-doctoral research associate. He is now working on experimental techniques (Eulerian and Lagrangian) to retrieve velocity and acceleration and will focus on the effects of particle size and density on their motion in the context of fully developed turbulent flows.

Dr. Stefan Luther
Stefan Luther received his doctorate in experimental physics from the University of Goettingen in 2000. From 2001 – 2004 he was a research associate at the University of Enschede, The Netherlands, where he worked on turbulent multiphase flow. From 2004 - 2007 he was visiting scientist at Cornell University, Ithaca NY, USA and research group leader at the Max Planck Institute for Dynamics and Self-Organization. Since 2007 he is Independent Junior Research Group Leader.

Gisa Luther
studied physics at the Universities of Hannover and Oldenburg and graduated in 1996. From 1997 to 2001, she worked for Bull GmbH in Langen near Frankfurt as assistant project manager in software engineering and system integration. In 2002, she joined WestLB Systems GmbH in Muenster as project manager in software engineering. Since 2004, she has been working as scientific staff member at the Max Planck Institute for Dynamics and Self-Organization and visiting scientist at Cornell University, Ithaca NY, USA.

Dr. habil Holger Nobach
received his doctorate in electrical engineering from the University of Rostock in 1997. During his postdoctoral research, between 1998 and 2000 on an industrial research program with Dantec Dynamics in Copenhagen and between 2000 and 2005 at the Technical University of Darmstadt, he developed measurement techniques for flow investigations. Since 2005 he is a scientist at the Max Planck Institute for Dynamics and Self-Organization, at the Cornell University and Göttingen. In 2007 he habilitated at the University of Darmstadt. He works on experimental investigation of turbulent flows with improved and extended optical measurement systems.

Dr. Walter Pauls
received his M.D. (2003) from the University of Bielefeld and Ph.D (2007) in Physics from the University of Nice-Sohia Antipolis (France). His dissertation work dealt with singularities of incompressible inviscid flows. In October 2007 he became a member of the MPI for Dynamics and Self-Organization, joining the Bodenschatz group as a post-doctoral research fellow.

Dr. Gabriel Seiden
Born in Haifa, Israel. Earned his B.A. degree in physics in 2000 from the Technion-Israel Institute of Technology, where he also studied for his direct-track PhD in physics. His dissertation theme was the phenomenon of pattern formation in rotating suspensions. He is currently a postdoc researcher working with Eberhard Bodenschatz at the Max Planck Institute for Dynamics and Self-Organization. His current research is on topologically and optically induced spatial forcing in thermal convection experiments.

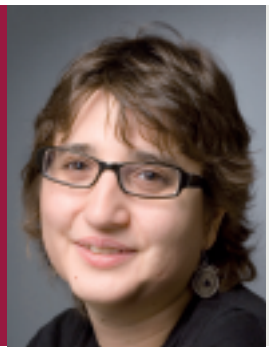

Dr. Mireia Torralba Cuello
received her Ph.D in Physics from Universitat de Barcelona (Spain) in 2007. During her Ph.D she performed an experimental study of the oscillatory flow of a Newtonian and a non Newtonian fluid. She also characterized lateral instabilities in Saffman-Taylor fingers subjected to different perturbations. She joined the group of professor Bodenschatz in the MPI for Dynamics and Self-Organization as a postdoctoral research associate in September 2007. She is currently working on turbulent flow and rheological characterization of dilute polymeric solutions.

Dr. Haitao Xu
received his Ph.D in Mechanical Engineering from Cornell University in 2003. His dissertation work is on collisional granular flows. In September 2003, he joined Eberhard Bodenschatz group as a post-doctoral research associate in the Laboratory of Atomic and Solid-State Physics at Cornell University and worked on experimental investigation of fluid turbulence. Since August 2006 he is a scientist at the Max Planck Institute for Dynamics and Self-Organization, Göttingen.

Bernstein Fellow

Dr. Andreas Neef
received his Diploma in physics in 2000 from the University of Jena, Germany. He joined the MRC Laboratory of Molecular Biology, Cambridge (UK) as a visiting scientist to work on retinal neurons and then went on to do his PhD at the Research Centre Jülich, Germany, where he received his doctorate from Cologne University in 2004. After being a postdoctoral researcher at the Institute for Biological Information Processing I in Jülich (2004) and at the Bernstein Center for Computational Neuroscience, Göttingen he became a Bernstein Fellow associated with the Department of Fluid Dynamics, Pattern Formation, and Nanobiocomplexity in 2006.

Associated Scientist

PD Dr.Reinhard Schinke
received his doctorate in theoretical physics from the University of Kaiserslautern in 1976. After a one year postdoctoral position at the IBM research laboratory in San Jose (Cal.) he took a position at the MPI für Strömungsforschung in the department for Atomic and Molecular Interactions in 1980.
He received his habilitation in theoretical chemistry from the Technical University of Munich in 1988. His research centers around the understanding of elementary processes in the gas phase like chemical reactions, photodissociation and unimolecular reactions. He is author of the monography "Photodissociation Dynamics" (Cambridge University Press, 1993) and received the Max-Planck research award in 1994 and the Gay-Lussac/Humboldt award in 2002.

Independent Junior Research Group Network Dynamics

Marc Timme

Many complex, multi-dimensional systems are organized as networks that are connected in a complicated way and exhibit non-trivial cooperative dynamics. Such systems are as diverse as networks of communicating nerve cells in our brains, millions of computers wired up to the internet and socially interacting humans that pass information or viruses to each other. In the Network Dynamics Group we investigate the fundamental principles underlying the connectivity structures of complex networks and their relation to the collective dynamics and functions that emerge.

Current research focuses on theoretical and computational neuroscience, where we try to answer whether and how networks of nerve cells that are strongly heterogeneous, exhibit a complicated wiring diagram, and often communicate over delayed pathways, can still exhibit spatio-temporal patterns of signals (spikes) that are precisely timed. In recent years, these spike patterns have been experimentally detected in various neuronal systems with unprecedented precision. They correlate with internal and external stimuli (events) and are thus considered key elements of neural computation and processing in the brain. Their dynamical origin, however, is unclear.

Addressing this open problem, we recently conceptualized and theoretically developed a reverse perspective onto network dynamical systems: Inverse methods not only yielded a way to determine the set of potential networks that exhibit a predefined spike pattern, they also proved useful for inferring, in general network dynamical systems, the connectivity structure of a network from its dynamical response properties. Other key problems of computational neuroscience studied include the coordination of spike times across networks, the plasticity of synaptic connections that induce adaptation and learning, and methods for the detection of timing relations between spikes of individual cells and collective signals (local field potentials) in experimental data.

A second major field of research in the group is modern statistical physics, with emphasis not only on random matrix applications to network synchronization, but also on many-particle systems with complex equilibria (where we study key questions of physics, aspects of graph theory, algebra and computation) and, established recently, fundamental aspects of large non-equilibrium systems as well as the dynamics of (human) contact patterns in complex networks.

Last but not least, we intensively work on the mathematical foundations of basically all of the above-mentioned science questions. Whereas this is necessary to secure progress in the scientific problems addressed, mathematical novelties that arise in this way are also worth studying in their own right. The new concept of Unstable Attractors that emerge in neural network models and an algebraic feature that arises from the Potts model of statistical physics and is useful for symbolic computation are important examples. The general mathematical perspective in fact constitutes a common basis for all of the problems investigated in the group.

The Network Dynamics Group was established in October 2006 by Dr. Marc Timme. It is funded by a grant of the Max Planck Society but we also secured a significant third-party funding by the German Ministry for Education and Research (BMBF). As of 2008, the research team consists of the group leader, two postdoctoral researchers, five doctoral students, one Diploma student and one student assistant. The current ten-person research team is not only highly cross-disciplinary, with experience in neuroscience, medicine, physics and computer science, but also internationally assembled, with members coming from Brazil, Canada, Germany, India and Russia.

Dr. Marc Timme
studied physics at the University of Würzburg, Germany, at the State University of New York at Stony Brook, USA, and at the University of Göttingen, Germany. He received an MA in physics in 1998 (Stony Brook) and a doctorate in theoretical physics in 2002 (Göttingen). After working as a postdoctoral researcher at the Max Planck Institute for Dynamics and Self-Organization, Göttingen, from 2003, he was a research scholar at the Center of Applied Mathematics, Cornell University, USA, from 2005 to 2006. In October 2006 he became the head of the independent research group Network Dynamics of the Max Planck Society. He is a faculty member at the Georg August University School of Science (GAUSS) and a founding member of and a principal investigator at the Bernstein Center for Computational Neuroscience (BCCN) Göttingen.

Dr. Raoul-Martin Memmesheimer
studied physics at the Technical University Kaiserslautern, the Ludwig Maximilian University Munich and the Friedrich Schiller University Jena. He received his diploma in theoretical physics in 2004 with a thesis in gravitational theory at the FSU Jena. From 2004 to 2007 he did his doctoral thesis on „Precise Spike Timing in Complex Neural Networks“ at the Max Planck Institute for Dynamics and Self-Organization and the Bernstein Center for Computational Neuroscience Göttingen. He is now a postdoctoral researcher in the Network Dynamics Group.

Dr. Dmitri Bibitchkov
studied physics at the Moscow Engineering Physics Institute, Russia, and at the University of Göttingen, Germany, and neurobiology at the Weizmann Institute of Science in Rehovot, Israel. He received a Diploma in physics in 2000 (Göttingen) and a PhD in neurobiology in 2006 (Rehovot). Since 2006 he is working as a postdoctoral researcher at the Max Planck Institute for Biophysical Chemistry. He is a fellow of the Bernstein Center for Computational Neuroscience (BCCN) Göttingen and an associate member of the independent research group Network Dynamics at the Max Planck Institute for Dynamics and Self-Organization.

Independent Junior Research Group Nonlinear Dynamics and Cardiac Arrhythmias

Stefan Luther

Cardiac arrhythmias are the leading cause of morbidity and mortality in industrialized countries. They occur due to the complex interplay of mechanical and electrical properties on the cellular, tissue, and organ levels. However, the detailed mechanisms of electromechanical instabilities leading to arrhythmias are not well understood – and thus therapies for many heart rhythm disorders remain largely ineffectual. The key question remains: How are cardiac arrhythmias induced, sustained, and eventually terminated?

A comprehensive understanding of cardiac arrhythmias faces three major challenges. First, a theoretical model is needed that incorporates key features on all relevant spatial and temporal scales. A direct numerical simulation of such a multi-scale system (e.g. for bifurcation analysis and control) is beyond available computing powers and therefore an efficient numerical approach is mandatory. Second, rapid progress in the development of modern imaging techniques for turbid biological media provides a wealth of quantitative data. These data need to be systematically integrated into a meaningful knowledge of the complete system. Third, model evaluation and analysis is needed to validate the model's performance and level of complexity, and to compare different models with each other and with measured data. Nonlinear dynamics provides a conceptual framework to address these challenges.

The group is developing numerical models and experimental techniques to study cardiac dynamics on cellular, tissue, and organ level. Our experiments span a wide range of biological complexity. We are developing and maintaining cell cultures as a simplified but well-defined model system. Merging techniques from cell biology and microfluidics will allow us to control the cellular environment and induce heterogeneities and anisotropies. In this system, we are studying the dynamics of phase singularities, their creation, interaction, and termination.

On the other hand, we are studying numerically and experimentally the onset and termination of fibrillation in tissue and whole heart preparations. The termination of fibrillation is of paramount importance for clinical applications. At present the only effective therapy for treating fibrillation is an implantable defibrillator using cardioversion, which requires high-energy electric shocks that reset the entire muscle. It is painful for the patient and can cause tissue damage. We are currently developing and validating a novel approach to terminate fibrillation using low-energy, pulsed, far-field stimulation. Our experimental in vitro results has demonstrated a high efficacy in terminating sustained AF. Using low energies, the method is expected to be painless and not harmful to the tissue.

Cardiac arrhythmias are a highly interdisciplinary field of research entailing expertise in mathematics, physics, computer science, biology, physiology, and medicine. The group is collaborating with R.F. Gilmour Jr. (Cornell, NY), V. Krinsky (INLN, Nice), G. Hasenfuss, L. Maier und U. Parlitz (University of Göttingen).

The group has been started in April 2007 by Dr. Stefan Luther in Göttingen.

Dr. Stefan Luther
Stefan Luther received his doctorate in experimental physics from the University of Göttingen in 2000. From 2001–2004 he was a research associate at the University of Enschede, The Netherlands, where he worked on turbulent multiphase flow. From 2004 - 2007 he was visiting scientist at Cornell University, Ithaca NY, USA and research group leader at the Max Planck Institute for Dynamics and Self-Organization. Since 2007 he is Independent Junior Research Group Leader.

Dr. Alexander Ahlborn
studied Physics at the Georg-August-University of Göttingen in the group of Prof. U. Parlitz. In Mai 2007 he received his Ph.D dealing with chaos control and chaos synchronization. In July 2007, he joined the group of Dr. Stefan Luther as a post-doctoral researcher at the Max-Planck-Institute for Dynamics and Self-Organization, Göttingen.

Gisa Luther
studied physics at the Universities of Hannover and Oldenburg and graduated in 1996. From 1997 to 2001, she worked for Bull GmbH in Langen near Frankfurt as assistant project manager in software engineering and system integration. In 2002, she joined WestLB Systems GmbH in Muenster as project manager in software engineering. Since 2004, she has been working as scientific staff member at the Max Planck Institute for Dynamics and Self-Organization and visiting scientist at Cornell University, Ithaca NY, USA.

Independent Junior Research Group Onset of Turbulence and Complexity

Björn Hof

The dynamics encountered in nonlinear systems are often extremely complex and disordered. The probably most familiar and at the same time most relevant example is the turbulent motion of fluids. Turbulent and disordered flows arise on many different scales ranging from the formation of stars and galaxies to flows in the atmosphere, rivers and blood vessels. At a first glance the only way to approach such complex problems seems to look at statistical properties such as fluctuations, mean profiles etc.

When studying particular flows more closely one surprisingly finds that even in the highly nonlinear regime almost regular, recurring structures can be observed. Thus we can easily detect patterns when looking at clouds, ocean-waves or the surface of the sun. Why are we able to distinguish patterns despite the extremely large flow speeds and temperature gradients present? Is it possible to link such observations to the equations describing the system? Can we gain an understanding of turbulence on a more fundamental level, going beyond a purely statistical one? These are key questions motivating our research.

Concepts from nonlinear dynamics are particularly useful to make progress in this direction. Here a disordered system is viewed in terms of underlying unstable states which are exact solutions to the governing equations. Due to the instability of these states the system can never quite settle down onto a particular one of them. The complex behaviour observed then results from the system in turn being drawn towards individual states along their stable manifolds and eventually being repelled along the unstable direction before visiting the next one etc. In order to probe these ideas we are carrying out carefully controlled experiments in a number of configurations. We closely collaborate with theoretical and numerical groups at the Philipps Universität Marburg, LIMSI Paris, TU Delft and Georgia Tech.

In future we would like to exploit the new insights we gained into the turbulent dynamics to control and relaminarize flows by manipulating the relevant structures. In addition to traditional fluid systems we also study viscoelastic fluids where different phenomena prevail. Our studies here range from highly viscoelastic flows where a new dynamical mechanism (elastic turbulence) is encountered to dilute polymer solutions, which are known to substantially decrease the flow resistance. By applying advanced velocity measurement techniques that enable us to resolve velocity fields in full time resolution we hope to gain new insights into these problems.

The group has been started by Dr. Björn Hof in November 2007 and is currently in its 'setting up phase'. In March 2008 one postdoc and two PhD students will be joining the group.

Dr. Björn Hof
studied physics at the Universities of Marburg and Manchester. He received his PhD in physics from the University of Manchester (UK) in 2001. From 2001 to 2003 he was a research associate at the University of Manchester where he studied transition to turbulence in pipe flow. From 2003 to 2005 he continued his investigation of pipe flow as a research associate at the Delft University of Technology. In 2005 he took up an appointment as RCUK fellow at the School of Physics, University of Manchester. Since 2007 he is the leader of an independent junior research group at the Max Planck Institute for Dynamic and Self-Organization.

Dr Alberto de Lozar
studied physics at the Universidad de Sevilla (Spain) finishing in 2001. During the last year of his studies he joined a research group at this University where he investigated numerically a model for catalyzed chemical reactions dynamics. In 2001 he got a PhD scholarship from the Graduiertenkollege "Non Equilibrium Phenomena and Phase Transitions in Complex Systems". He received his PhD in physics from the Universitaet Bayreuth in 2005. The title of his thesis was "Liquid crystal dynamics: defects, walls and gels". In 2006 he started his research in Fluid Mechanics as a Research Associate at the University of Manchester (UK). His investigations include carefully performed experiments combined with computer simulations. From 2008 he will start as a Research associate at the Max Planck Institute for Dynamic and Self-Organization.

Max Planck Fellow Group
Polymers, Complex Fluids and Disordered Systems

Annette Zippelius

Very complex behaviour of physical systems can originate from very simple ingredients. In our research group we try to understand how macroscopic complexity appears in the collective behaviour of strongly interacting many particle systems. Polymers, for instance, can be idealized as hard spheres (monomers) linked together randomly in a network. Even though this is an extremely idealized point of view, many macroscopic properties of polymer melts, solutions or gels can be understood from this model, for example the random localization of particles in the gel as well as rheological properties.

The behaviour of a simple system can become very complex as soon as it is pushed out of equilibrium. A granular fluid is a prototype of such a system which is relatively simple in the equilibrium limit (where it is an elastic hard sphere gas) and extremely complex as soon as dissipation is switched on, showing for instance clustering instabilities, correlations between translation and rotation or highly nongaussian energy distributions.

Complexity can also be induced by disorder. Disorder is present in most, if not all, systems encountered in reality and its influence is often such that it can not be neglected. To the contrary, even infinitesimal disorder can lead to effects which are absent in an idealized ordered state. A particular challenge is disorder in low dimensions, a typical example being the spin glass. Here, the nature of the low temperature phase is far from being understood. Recent development of new methods and tools has made significant progress possible in this area.

Our research group consists of the head of the group, one postdoctoral researcher and three PhD students in physics. Additionally, we have several diploma students who work on related projects.

Prof. Dr. Annette Zippelius
studied physics in Munich and Boulder (Colorado) and received her PhD in 1977 in Munich. She was a postdoc in Harvard and Cornell. In 1983 she became a scientific staff member at the Forschungszentrum Jülich. Since 1988 she is a full professor in the Faculty of Physics at the University of Göttingen and became a Max Planck research fellow in 2006.

PD Dr. Timo Aspelmeier
studied Physics in Göttingen and Edinburgh and received his PhD in 2000 in Göttingen. He was a Postdoc at Virginia Tech from 2000 to 2001 in the group of Beate Schmittmann and Royce Zia and from 2002 to 2004 in the group of Alan Bray and Michael Moore in Manchester. He returned to Göttingen in 2004 where he obtained his Habilitation in 2006 and became a member of the Max Planck Fellow group in 2007. He currently works on equilibrium and nonequilibrium statistical physics of complex liquids and disordered systems.

Emeritus Group Molecular Interactions

Jan Peter Toennies

Together with the late Hans Pauly (1928–2004) we came to Göttingen in 1969 from the University of Bonn to establish the new research direction of molecular beam investigations of chemical elementary collision processes. In the following years the Institute became one of the leading centers both for experimental and theoretical research in determining with unprecedented precision the van der Waals forces between atoms and molecules. These forces are of fundamental importance for understanding both the static and dynamic properties of gases, liquids and solids and their phase transitions.

In the course of these studies our group observed in the late 1970's that in the free jet expansions used to produce the molecular beams in the above experiments, helium gas expansions behaved in a remarkable way. Instead of the usual rather narrow velocity distributions of $\Delta v/v \approx 10\%$, the helium atom beam velocities were extraordinarily sharp and nearly monoenergetic with $\Delta v/v \leq 1\%$. This unexpected observation was found to be related to the extremely weak interatomic forces between He atoms, with the consequence that their collision cross section at the ultra-low ambient temperatures in the expanding gas rises to 255.000 A^2, more than 4 orders of magnitude larger than the cross section at room temperature.

These nearly monoenergetic helium atom beams have found widespread applications. In expansions with small concentrations of molecules the excess of helium atoms serves to cool the molecules down to temperatures of several degrees K. This became a great boom for molecular spectroscopy since at these temperatures the hot bands that otherwise obscure the molecular spectra are eliminated. Our group exploited the helium atom beams for exploring the structures and vibrations at the surfaces of solid crystals. In complete analogy to neutrons which are routinely used to study the structures and phonon dispersion curves inside solids, helium atoms were found to be the ideal method for investigating the structures and phonons at solid surfaces, which are not accessible with neutrons. The study of over 200 different surfaces by helium atom scattering (HAS) and the complimentary method of inelastic electron scattering (EELS) have lead to a much more profound knowledge of how atoms and molecules interact with metal surfaces, which is of basic importance for understanding catalysis.

In the following years we became even more fascinated by this unusual element helium. At first sight a helium atom appears to be extremely simple or perhaps since they are chemically inert, we should say, aloofly noble. With only two electrons in a closed shell most of its properties are well understood. But as soon as one assembles more than one helium atom wondrous phenomena appear. For one it is the only substance which when cooled down to the lowest temperatures remains liquid and does not freeze. Moreover it is the only substance which exhibits superfluidity, a collective quantum phenomena similar to superconductivity. In its superfluid state below 2.2 K liquid helium flows without friction, just as the electron in a superconductor flows without resistance.

Thus it was natural to ask if small clusters and droplets of helium might also exhibit superfluidity and how this might be detected. It had been speculated, since they could be superfluid, that upon scattering the projectile atoms might pass right through them without any interaction. Instead we found that atoms and molecules were trapped in the droplet's interior. This opened up the possibility to employ the spectroscopy of these molecules to interrogate the physical properties of helium droplets. Much to our astonishment the sharp spectral features of the embedded molecules indicated that the molecules rotate freely as if they were in a vacuum and not at all strongly hindered as expected for an ordinary liquid. Subsequent experiments revealed that this remarkable behaviour was related to the superfluidity of these droplets and has since been accepted by the science community as a new microscopic manifestation of superfluidity. Helium nanodroplets are now being used in more than 25 laboratories worldwide as a uniquely cold (0.15–0.37 *K)* and gentle matrix for high resolution molecular spectroscopic investigations of atoms, molecules, and "Taylor made" clusters, their chemical reactions, and their response to photoexcitation. Our group used this technique to provide the first evidence that para-hydrogen molecules which, like *He* atoms are spinless bosons, can also exhibit microscopic suerfluidity.

Our most recent experiments have been directed at exploring the nature of small pure clusters ($N \leq 100$) of helium and hydrogen molecules. To this end we developed an apparatus to study the matterwave diffraction of cluster beams from nanostructured transmission gratings. In collaboration with the theory group of Prof. G.C. Hegerfeldt at the University of Göttingen these experiments, for example, lead to the precise measurement of the size of the He_2 dimer and of the van der Waals interactions of a number of atoms and molecules with solid surfaces. Unexpected magic numbers were found in larger clusters ($N \leq 50$), which have led to the first insight into the elementary excitations of these nano-sized superfluids.

At the present time we are collaborating with several groups in the U.S., Spain and Russia to better understand the superfluid response of small pure para-H_2 clusters. We hope soon to understand how these small entities, manage to behave as if they were partly liquid, partly solid, superfluid and perhaps even supersolid.

Prof. Dr. Dr. h.c. mult. J. Peter Toennies
Studied physics and chemistry at Brown University, Providence,USA where he received his Ph.D.in 1957. He came to Germany in 1957 where he was a postdoc and "Assistent" 1957-1965 in Wolfgang Paul's Physics Institute in Bonn. After his habilitation (1965) he was a Dozent until becoming director at the MPI Strömungsforschung in Göttingen (1969-2002). Since 1971 Associate Professor at the University of Göttingen and Adjunct Professor at the University of Bonn.

Topical Group

Pattern Formation and Cooperative Phenomena

Pattern Formation in non-equilibrium systems and cooperative behavior in collective systems are fascinating, ubiquitous and often interlinked. They occur in systems as diverse as flocks of birds, neuronal networks, the stock exchange market, the 'mexican wave' in a sports stadium, ventricular fibrillation of a heart muscle, convection, or the mesoscale ordering in complex fluids. Given the amazing phenomenological similarities sometimes found among quite diverse systems, it can be fruitful to ask whether there is a general principle at work. For example, is it possible to predict collective phenomena of many coupled sub-systems solely from their properties and from the characteristics of the coupling? Fundamental to this research area is the question whether it is possible to achieve a broad understanding of such systems based on general mathematical theory that can quantitatively capture generic behavior.

It is instructive to consider some of the typical characteristics of such systems. One is the emergence of dynamically self-generated length scales due to a symmetry breaking mechanism. This is often encountered, e.g., in phase separation scenarios, in fluid dynamics, but also in biological and chemical systems. Another is the transfer of a broken symmetry from one subsystem to another, as typical for self-assembling systems. Convection phenomena and mesoscale pattern formation in liquid crystals involve both types of phenomena: the length scale of the pattern reflects the system dimensions, while its exact position may be chosen freely by the system, and thus represents an additional (dynamically) broken symmetry. Phenomena like solitary waves are not only found in shallow water, but are also encountered in many different excitable media, like coupled systems of myocardiocytes in the heart muscle and neurons in the brain, or in the crowd of spectators in a stadium. It is intriguing to study phase separation and swarming phenomena by using unifying concepts, such as the Potts model, in order to elaborate on the inherent similarities and differences of the corresponding systems.

There are in general two main directions which must be pursued. On the one hand, there are certainly many striking phenomena of pattern formation and collective behavior in very complex 'real' systems which still await their discovery, such as signaling patterns in living cells, or even in the brain, where the signaling pattern will govern the function of the system. A systematic search for such phenomena is thus very important. On the other hand, there is a need for suitable model systems, which are sufficiently complex to show the phenomena of interest, yet are still simple enough for a detailed and quantitative understanding of their dynamics and self-organization is believed to be possible. Both of these directions of research are designed to push and inspire the development of novel theoretical concepts, trying to find mathematical descriptions with minimum intricacy, but a maximum of predictive power.

Quantitative Universality of Pattern Formation in the Visual Cortex

F. Wolf
M. Kaschube, M. Schnabel, T. Geisel, M. Huang, L. Reichl, W. Keil,
S. Löwel (U Jena), L. White (Duke U, USA), D. Coppola (Randolph-Macon College, USA)

The occurrence of universal quantitative laws in a strongly interacting multi-component system indicates that its behavior can be elucidated through the identification of general mathematical principles rather than by the detailed characterization of its individual components. We recently discovered that universal quantitative laws govern the spatial layout of orientation selective neurons in the visual cortex in three mammalian species separated in evolution by more than 50 million years. Most suggestive of a mathematical structure underlying this universality, the average number of pinwheel centers per orientation hyper-column in all three species is statistically indistinguishable from the constant π. We show that mathematical models of neural pattern formation can reproduce all observed universal quantitative laws if non-local interactions are dominant, indicating that non-local interactions are constitutive in visual cortical development. These and other results demonstrate that mathematical principles can shape the organization of the brain as powerfully as an organism's genetic make-up.

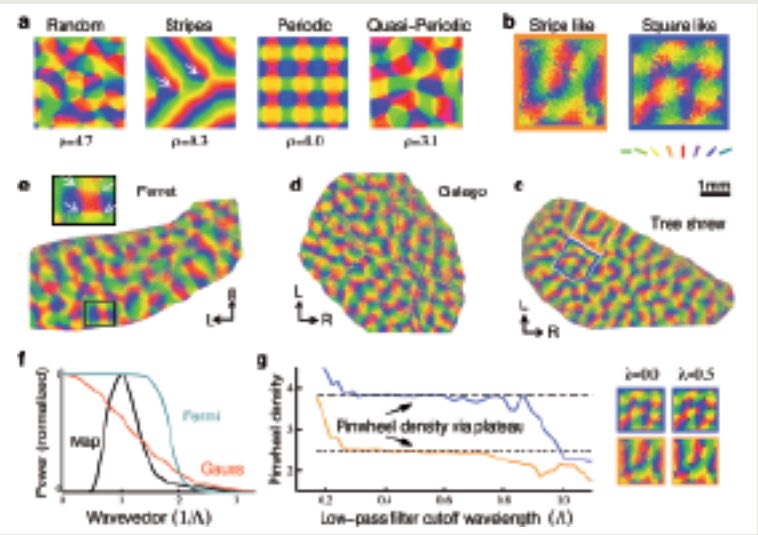

Figure 1: Patterns of pinwheels in the visual cortex: Spatial distribution and analysis. a, Synthetic orientation maps of equal column spacing but widely different pinwheel densities ρ. Displayed are solutions of different models. Colors code preferred orientations as indicated by the bars in b. White arrows mark two pinwheels. b, High (blue frame) and low (orange frame) pinwheel density regions in tree shrew visual cortex. c-e, Optically recorded orientation maps in tree shrew (c), galago (d), and ferret (e) visual cortex. Regions shown in b are marked in c. Four pinwheels are marked by white arrows in the magnified region in e (black frame). f, Fermi- (as opposed to conventional Gaussian-) filtering efficiently eliminates high frequency noise without deteriorating the signal. This is illustrated by comparing the radially averaged power spectrum of the galago map in d (high-pass filtered; normalized) with Gaussian and Fermi filter kernels in frequency representation. Fermi filtering effectively implements a cutoff in the frequency domain. g, Operational definition of pinwheel density ρ: Value of the 'plateau' region where the spatially averaged pinwheel densities independent of low-pass cutoff wavelength exemplified for the two maps from b.

Probing universality in the brain

The laws governing strongly interacting multi-component systems frequently detach from the detailed nature of microscopic interactions resulting in the robustness of collective properties and in their insensitivity to external and internal perturbations. Quantitative laws exhibiting such insensitivity are called universal because they characterize an entire class of systems rather then an individual system in all its specific detail. In biological systems, measurements precise enough to uncover universal quantitative laws are rarely performed and might appear misguided, when qualitatively new types of cellular and molecular components and interactions are continuously being discovered. Nevertheless, universality may play important roles in living systems. Neuronal, immune and genetic networks are strongly interacting multi-component systems and universal behavior, particularly the robustness associated with it, may often be beneficial for the functioning of the organism.

To examine the functional architecture of the visual cortex for signatures of quantitative universality we developed image analysis

methods for the automated detection, localization and counting of so called pinwheel defects, point-like orientation singularities of high abundance of orientation prefrence mapsaround which stimulus orientations are represented in a radial fashion (Fig.1). Using these tools we studied orientation preference maps in the visual cortex of three species widely separated in mammalian evolution, tree shrew (order scandentia), galago (order primate) and ferret (order carnivora). These species diverged evolutionarily more than 50 million years ago, occupy distinct ecological niches on different continents, and exhibit qualitative and quantitative differences in the anatomical and neurophysiological organization of the retina and central visual structures.

Universal pinwheel statistics

We found that fundamental statistical properties of orientation preference maps were surprisingly similar in the three species. Fig. 2a shows that the frequency of occurrence of pinwheels per mm^2 is proportional to the inverse hypercolumn size; Fig. 2b graphs pinwheel densities as a function of hypercolumn size for 26 hemispheres in tree shrew, 9 in galago, and 82 in ferret. Whereas the average column spacing and thus the average hypercolumn size varied by more than a factor of 2 across species, the average pinwheel density was virtually identical. In tree shrew, we observed an average pinwheel density of 3.12 ± 0.04, in galago a similar average 3.18 ± 0.09, and in ferret an average pinwheel density of 3.16 ± 0.03. Differences between species were not significant ($p > 0.81$, permutation test). In addition we compared numerous additional statistics of the pinwheel distribution such as the count variance as a function of sampling area, or the charged and uncharged next neighbor distance distributions. None of these quantities indicated a systematic interspecies difference in pattern layout. These observations justify obtaining a more precise estimate of the universal mean pinwheel density by pooling the data from the three species. The grand average of the pinwheel density thus obtained is 3.14 ± 0.03. This value is statistically indistinguishable from the fundamental mathematical constant π. To be more precise, it is expected to deviate from it by less than 0.06. It is therefore tempting to conjecture that a mathematical structure guides visual cortex development and forms the origin of the observed universal statistics.

The long-range self-organization hypothesis

We used a dynamical model of Swift-Hohenberg type [1] to investigate whether self-organization of cortical circuits unfolding under the influence of long-ranging interactions might explain the observed universal pinwheel statistics. In models from this class (1) pinwheel statistics can be studied analytically using known closed form expressions for approximate solutions; (2) the parameter dependence of the emerging maps has been com-

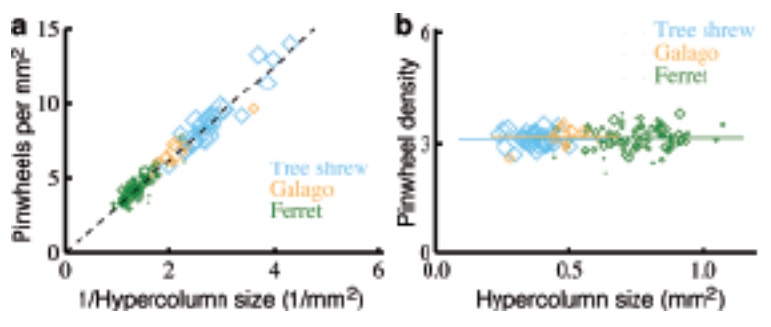

Figure 2: The average pinwheel density is a universal quantity. a, The mean number of pinwheels per *mm^2*, scales with the inverse of hypercolumn size in individuals from three different species. b, Dimensionless pinwheel densities as function of hypercolumn size. Solid lines represent the average pinwheel density for each species (tree shrew, 3.12 ± 0.04; galago, 3.18 ± 0.09; ferret, 3.16 ± 0.03). Hypercolumn size calculated as in [4,5].

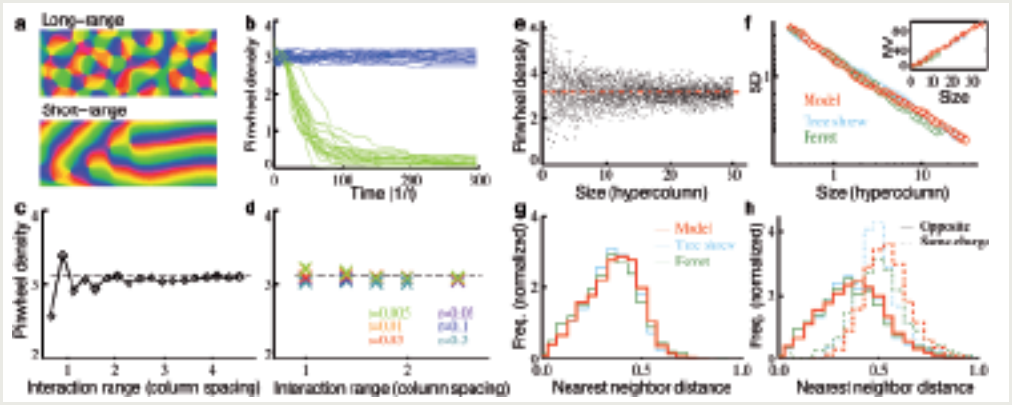

Figure 3
Self-organization dominated by long-ranging interactions can quantitatively explain universal pinwheel statistics. a, Near stationary solutions of the model [1] are either pinwheel rich (upper map) or pinwheel sparse (lower map). b, In the absence of long-range interactions, pinwheel densities decay to zero (green traces, different random initial conditions) whereas in the presence of strong long-range interactions, realistic pinwheel densities are robustly selected (blue traces). c, Average pinwheel densities of closed form solutions valid near criticality. The average is close to the observed value for finite interaction range and converges to π in the large interaction range limit [6]. d, Average densities numerically obtained for different values of the instability parameter. e-h, Spatial organization of pinwheels agrees quantitatively with experiment.

prehensively characterized and (3) numerical simulations of systems approaching the size of the entire primary visual cortex can be performed efficiently and accurately.

The statistics of pinwheel arrangements in maps obtained by extensive numerical simulations of model areas comprising more than 400 orientation hypercolumns and covering timescales larger than the time required for cortical circuits to express mature levels of orientation selectivity are represented in Fig. 3. Results from representative simulations in the presence and absence of long-ranging interactions are shown in Fig. 3a,b. Numerical solutions closely resembled orientation maps throughout the developmental time course, when long-range interactions were present and dominated the developmental dynamics. When only local interactions were present, simulated maps only initially contained pinwheels in realistic densities. The majority of these initially generated pinwheels was lost during the subsequent developmental time course through pairwise annihilation of pinwheels of opposite topological charge reproducing the typical behavior of models dominated by local interactions [2,3]. In the parameter regime of sufficiently wide and strong long-range interactions, a substantial density of pinwheels was preserved at all times. The emergence of average pinwheel densities close to π appears to be a very robust feature of the formation of orientation maps in the long-range interaction dominated regime. It is relatively insensitive to the absolute range of long-ranging interactions and to the distance from the bifurcation point. In the long-range regime, the model also reproduced all other observed universal statistical properties of visual cortical orientation maps (Fig. 3e–h).

These results reveal a striking quantitative invariance of pinwheel organization across animals and species that strongly contrasts the huge interindividual and interspecies variability exhibited by other aspects of visual cortical architecture. It would be surprising, if this invariance was preserved over 50 million years of divergent evolution without a substantial functional benefit. We thus anticipate, that the quantitative laws of pinwheel organization described here will not only help to identify the developmental determinants of pinwheel organization but also provide a useful guidance for resolving the currently elusive functional significance of pinwheels.

[1] F. Wolf, *Phys. Rev. Lett.* **95:**208701 (2005)
[2] F. Wolf, T. Geisel, *Nature* **395:**73 (1998)
[3] M. Schnabel, M. Kaschube, S. Löwel, F. Wolf, *EPJ* **145:**137 (2007)
[4] M. Kaschube, F. Wolf, T. Geisel, S. Löwel, *J. Neurosci.* **22:**7206 (2002).
[5] M. Kaschube, F. Wolf, M. Puhlmann, S. Rathjen, K.F. Schmidt, T. Geisel, S. Löwel, *Eur. J. Neurosci.* **22,** 7206 (2003)
[6] M. Kaschube, M. Schnabel, F. Wolf, *New J Phys.* (in press).

Cooperative Sodium Channel Activation and Neuronal Action Potential Encoding

A. Neef, F. Wolf
M. Huang, W. Wei, B. Naundorf, M. Kreissl, T. Geisel, T. Moser (U Göttingen), S. Löwel (U Jena),
M. Volgushev (U Bochum), I. Fleidervish, M. Gutnick (Hebrew University, Israel)

In all neurons of the cerebral cortex, the results of single neuron computations are encoded into action potential sequences. The dynamics of cortical action potential generators thus determines how much and which information is transmitted to other cells in the brain and conversely which aspects of intracellular activity are not communicated to the receiving neuron. The reduction of information by action potential encoding in neocortical neurons is in fact tremendous. It was recently shown that of the 1000 bits per second that are contained in the ongoing membrane potential fluctuations of a typical cortical neuron only roughly 30 bits are encoded into its output sequence of action potentials [1]. In our research on action potential initiation dynamics in cortical neurons, we are using an approach integrating biophysical modelling, dynamical systems theory, *in vivo* recording of the behaviour of action potential initiation in the intact brain, and neurophysiological and biophysical *in vitro* experiments to unravel the computational rules and biophysical mechanisms of this key step of neuronal computation.

Anomalous action potential dynamics in cortical neurons

Although actively studied for more than three decades by biological and medical researchers, the precise laws of that determine generation of action potential by neurons of the mammalian brain surprisingly are neither well characterized nor mechanistically understood. For instance, it is widely assumed that the initiation of action potentials can be modelled as a threshold crossing process: When the membrane potential of a neuron is driven beyond a fixed threshold voltage, value sodium channels are activated that mediate a strongly depolarizing current that causes the membrane potential to rapidly increase. Surprisingly, we recently found that during the operation of cortical neurons in the intact brain there is no fixed threshold potential underlying the initiation of action potential [2]. Instead, action potentials are obviously initiated over a very wide range of potentials and most importantly even the largest AP initiation potentials can be reached without inducing action potential firing (Fig.1a,b). In addition, the rapidness of action potential ini-

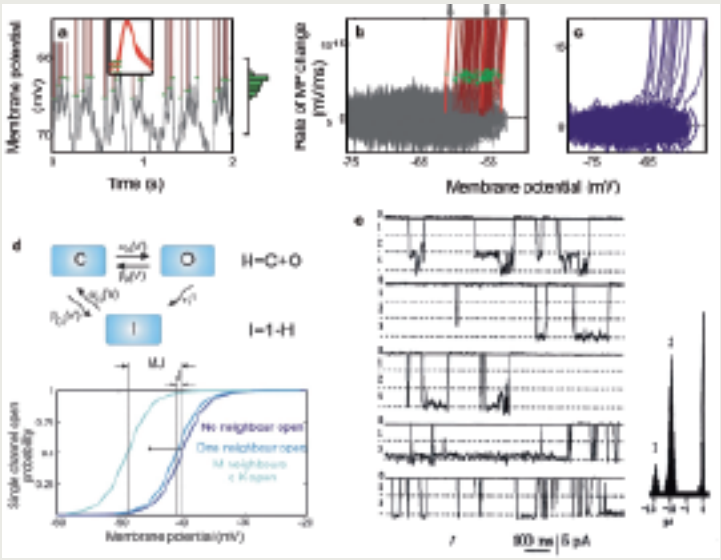

Figure 1: **a** Membrane potential dynamics recorded in a cortical neuron in visual cortex of the intact cat brain. Green bars: AP onset potentials, Histogram to the right distribution of onset potentials. Three APs are shown in high temporal resolution. **b** Pseudo phase plot obtained from the record in **a**. **c** Pseudo phase plot obtained from a simulation based on the cooperative sodium activation kinetics depicted in **d**. **d** state transition scheme for single channel gating (upper panel, *C* closed, *O* Open, *I* inactivated). Voltage dependent transition rates are indicated. Lower panel: hypothetical shift of the activation curve dependent on the number of neigbors in the open state (M). **e** Direct demonstration of cooperative gating of sodium channels. Individual traces represent inward currents recorded in the cell attached configuration from caridiomyocytes. Dashed lines indicate integer multiples of single channel currents. Note the simultaneous opening and closing of pairs and triples of channels. Right: current histogram of the entire record.

tiation, the inverse voltage range over which high rates of membrane potential change are reached during the initial phase of an AP, is much higher than predicted by the universally accepted Hodgkin-Huxley theory. Based on these findings, we suggested that cortical action potential generators might be tailored beyond the range that can be successfully described by the canonical Hodgkin-Huxley theory, indicating that fundamental aspects of the biophysics of action potential initiation in cortical neurons remain unidentified. These results initiated a lively debate on and an ongoing re-evaluation of the universal validity of the classical Hodgkin-Huxley theory of action potential initiation (see e.g. [3-7]).

The cooperative sodium channel activation hypothesis

The abrupt increase of depolarization speed during the initial phase of cortical action potentials that we described suggests that many sodium channels in the neuronal membrane are synchronously activated. This may indicate that the assumption of statistically independence of sodium channel activation that is a basic ingredient of the Hodgkin-Huxley theory is violated in neuronal membranes. We thus considered the hypothesis that neuronal sodium channels may undergo cooperative activation such that activation of one channel can directly induce neighbouring channels to also activate. Intriguingly, quantitative models of membrane potential dynamics based on such a cooperative sodium channel activation kinetics, can faithfully reproduce all key features of action potential initiation as observed in cortical neurons in the intact brain (Fig.1c,d)[2].

Further support for the cooperative sodium channel activation hypothesis comes from *in vitro* experiments which tested one of its key predictions. If inter-channel interactions are assumed distance-dependent in neuronal membranes, then the cooperative sodium channel activation hypothesis predicts that reducing the effective density of channels should weaken cooperativity, and eventually lead to a action potentials onset dynamics conforming with the assumption of statistically independent gating and Hodgkin-Huxley theory. We tested this prediction in vitro, recording action potentials while reducing the density of available sodium channels by the application of tetrodotoxin (TTX). As predicted, TTX application in fact led to substantial reduction in the onset rapidness of action potentials in all tested cortical neurons [2]. Subsequent experiments revealed that a similar transformation of action potential waveform can also be achieved by reducing the extracellular sodium concentration suggesting that sodium ions might be the mediators of inter-channel interactions (Wolf et al. in prep.).

Direct evidence for cooperative ion channel activation

Although prominent neurophysiologists consider the hypothesis of cooperative ion channel activation “exotic” [5,7], the ability of ion channels to exhibit cooperative activation, that we theoretically predicted, was immediately confirmed by an independent experimental study that appeared less than three months after publication of our initial report [8]. In this study, Molina et al. described the activation kinetics of KcsA channels, a minimal model ion channel isolated from bacteria. Their single channel resolution recordings directly demonstrated that channels may either gate statistically independently as conventionally assumed or in a highly cooperative fashion. In addition, ensemble of channels showed transitions between statistically independent and cooperative gating modes that apparently dependent on the degree of channel clustering in the membrane. While it is currently unknown whether neuronal sodium channels do exhibit a similar degree of inter-channel cooperativity, the closely related sodium channels underlying action potential generation and propagation in the heart, have

also been shown to be capable of highly synchronized gating (Fig.1e) [9]. Efforts are under way to further characterize sodium channel cooperativity and the underlying molecular mechanisms in cardiomyocytes in collaboration with the groups of Bodenschatz and Luther, and to probe for this phenomenon in cortical neurons in collaboration with Fleidervish and Gutnick at the Hebrew University of Jerusalem [10].

Functional consequences of rapid onset action potential initiation

Our previous theoretical analyses predict that the very rapid onset of action potentials enhances the ability of neurons to lock the firing times of their action potentials to high frequency components of their synaptic inputs (Fig.2a). We are currently testing this important functional consequence in *in vitro* neurophysiological experiments. In these experiments the intense synaptic bombardment that a cortical neuron experiences *in vivo* is emulated by the injection of a randomly fluctuating dynamical current superimposed with a weak periodic test signal (Fig.2b). Quantifying the amplitude of spike frequency modulation observed in such experiments, as a function of test stimulus frequency, we find that cortical neurons indeed exhibit very high cut-off frequencies on the order of 200 Hz, even when firing at average impulse rates below 10 Hz. In contradistinction, previous theoretical studies consistently found that Hodgkin-Huxley type action potential generators typically exhibit cut off frequencies on the order of their mean firing rate [11,12]. Confirming our theoretical predictions [6,12], these preliminary results indeed suggest that the cut-off frequencies of cortical action potential generators are more than one order of magnitude higher than predicted by the classical Hodgkin-Huxley theory. To further corroborate these results our current efforts are concentrating on developing efficient and quantitatively controlled methods for the estimation of frequency response functions and cut off frequencies from neuronal noise injection experiments.

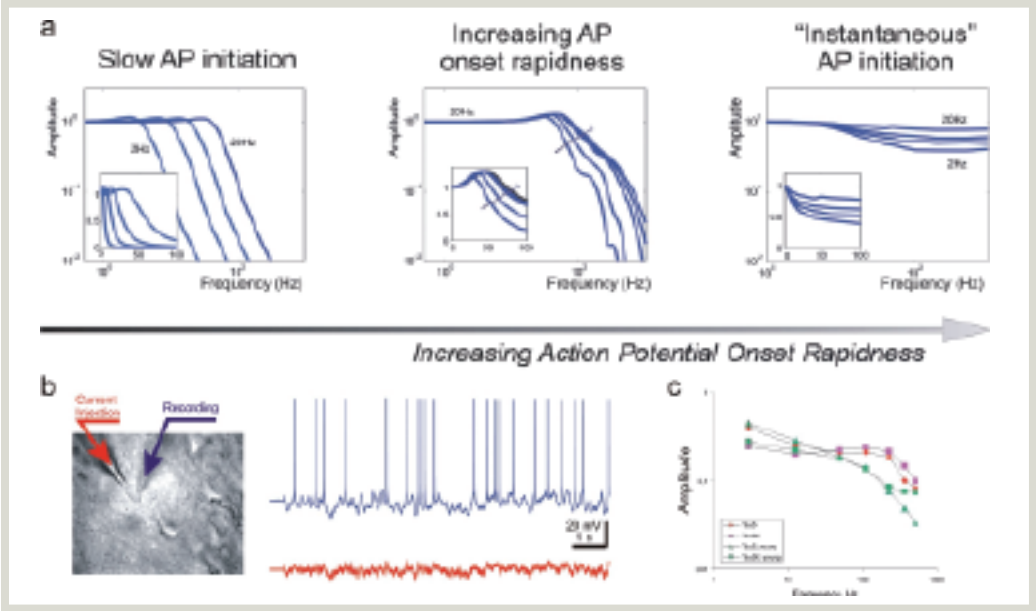

Figure 2: a Amplitude of phase locking of spike times to a weak external stimulus of variable frequency for AP generators of increasing action potential onset rapidness. Curves are marked for different firing rates. **b** Recording configuration for measuring frequency dependent phase locking amplitude in a cortical pyramidal neuron. **c** Transmission functions obtained from a mature and a immature cortical pyramidal neuron, for different correlation times of stochastic input currents.

[1] G. de Polavieja, et al. *J Neurosci* **25**, 5657 (2005).
[2] B. Naundorf, F. Wolf, M. Volgushev, *Nature* **440:1060** (2006)
[3] B. Gutkin, G.B. Ermentrout *Nature* **440:999** (2006)
[4] A.V.M. Herz, T. Gollisch, C.K. Machens CK, *Science* **314:80** (2006)
[5] D.A. McCormick, Y.S. Shu, Y.G. Yu, *Nature* **445:E1** (2007)
[6] B. Naundorf, F. Wolf, M. Volgushev, *Nature* **445:E2** (2007)
[7] B.P. Bean *Nature Rev. Neurosci.* **8** (6): 451 (2007)
[8] M.L. Molina, et al. *J. Biol. Chem.* **281:18837** (2006)
[9] AI. Undrovinas, I.A. Fleidervish, J.C. Makielski, *Circ Res* **71:1231** (1992).
[10] N. Astman, M. J. Gutnick, F. Wolf, I.A. Fleidervish, *Sfn abst.* **466.29** (2007).
[11] N. Fourcaud-Trocme, D. Hansel, C. van Vreeswijk, N. Brunel, *J Neurosci.* **23:11628** (2003)
[12] B. Naundorf, T. Geisel, F. Wolf, *J Comput. Neurosci.* **18:297** (2005)

Time-periodic Patterns in the Actin Cortex

C. Beta
C. Westendorf, E. Bodenschatz
H.C. Ishikawa-Ankerhold, T. Bretschneider and G. Gerisch (MPI for Biochemistry, Martinsried),
A. Müller-Taubenberger (LMU München), R.H. Insall (University of Birmingham, UK)

The dynamical properties of the actin cytoskeleton provide the basis for motility, phagocytosis, and division of eukaryotic cells [1]. A key player in the formation of a dense cortical actin network is the seven-subunit Arp2/3 complex [2] that initiates the nucleation of branches on existing filaments. Its activity is controlled by SCAR/WAVE proteins of the WASp (Wiscott-Aldrich Syndrome protein) family that are downstream effectors of receptor-mediated signaling pathways [3].

In our recent work, we provide evidence for an oscillatory instability in the cortex of mutant cells lacking members of the pentameric SCAR complex [4]. We observed that SCAR-deficient *Dictyostelium* cells exhibit self-sustained, cell-autonomous oscillations in cortical actin density with periods of about 20 seconds, while a steady state with only slight fluctuations is observed in wild-type cells, see Fig.1. Phase-shifts in response to chemoattractant stimuli indicate that the oscillatory system is linked to the chemosensory pathway, *i.e.*, receptor signals are transmitted to the actin machinery, even if SCAR is missing. As chemotaxis is strongly impaired in SCAR-null mutants [5], our results suggest that suppression of oscillations by SCAR is required for efficient directional responses in chemotactic cells. The transition from a steady state in wild-type cells to periodic changes in the density of cortical actin in the SCAR-deficient mutants implies a bifurcation to limit cycle oscillations and highlight the actin machinery as a self-organizing system that can be described by the concepts of non-equilibrium dynamics.

By exposing *Dictyostelium* wild type cells, as well as various cytoskeletal mutant strains, to periodic chemoattractant stimuli we are extending this work. (For the generation of well-controlled, complex chemoattractant stimuli, see our report on *Single cell stimulation in microfluidic environments*). The response behavior of the cellular system to an external periodic force will allow us to characterize intrinsic time scales of the cytoskeleton. In particular, the response of knockout

strains that are deficient in different cytoskeletal proteins will characterize the role of these components in the dynamics of actin-based cell motility.

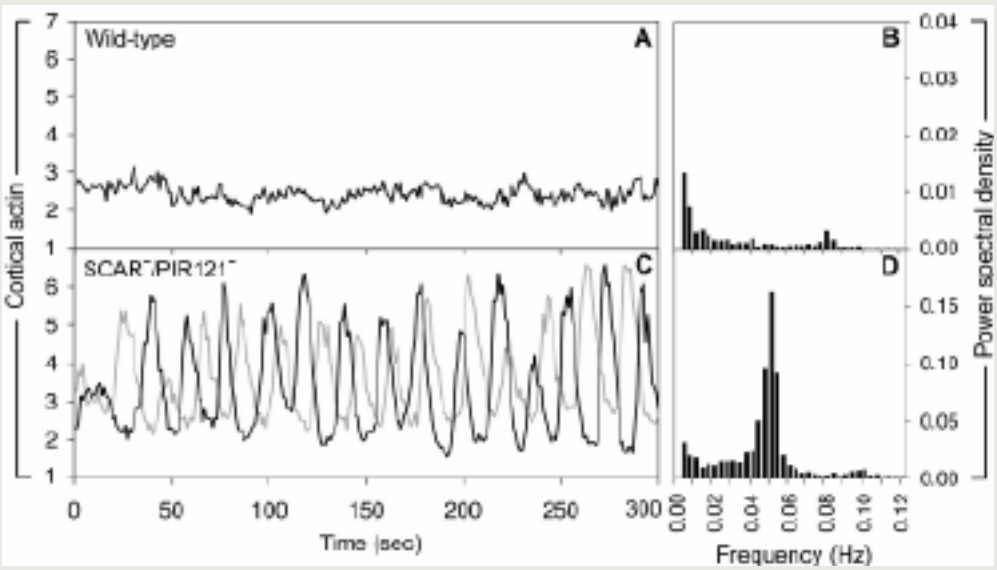

Figure 1: Time series and frequency spectra of cortical actin density in wild-type and mutant cells.
Left panels. Examples of (A) non-periodic fluctuations in a wild-type cell and (C) free-running oscillations in SCAR/PIR121 double-null mutant cells. Independent oscillations in two cells of the SCAR/PIR121 double mutant were recorded at the same time (dark and light curves).
Right panels. Frequency spectra summarizing periodic activities in populations of (B) wild-type cells (D) SCAR/PIR121-double null mutants. The frequency distributions of (B) 27 wild-type and (D) 24 SCAR/PIR121-double null mutants were averaged.

[1] T. D. Pollard and G. G. Borisy, *Cell* **112** (2003) 453.
[2] M. D. Welch, et al., *Journal of Cell Biology* **138** (1997) 375.
[3] L. G. Smith and R. Li, *Current Biology* **14** (2004) R109.
[4] H. C. Ishikawa-Ankerhold, et al. (2007) submitted.
[5] J. E. Bear, J. F. Rawls, and C. L. Saxe, *Journal of Cell Biology* **142** (1998) 1325.

Termination of Fibrillation Using Low-Energy Far-Field Pacing

Stefan Luther, Gisa Luther, Eberhard Bodenschatz
Amgad Squires
R. Gilmour (Cornell, USA), Valentin Krinsky (Nice, France),
G. Hasenfuss und L. Maier (University of Göttingen)

Fibrillation is a state of irregular electrophysiological turbulence of cardiac tissue – and its control and termination is a major clinical challenge. Nucleation of reentrant spiral waves and their subsequent fractionation may result in life-threatening electromechanical malfunction of the heart [1-3]. Spiral waves occur in several systems that all share with the heart the functional properties of excitability and refractoriness. In cardiac tissue, this transition into defect mediated turbulence can be fatal if it originates in the ventricles – the heart's main pumping chambers. Roughly half of the deaths caused by cardiovascular disease are sudden. The majority of those sudden deaths – an estimated 300.000 per year in the U.S. alone – are associated with ventricular fibrillation (VF). If the disorder originates in the atria, it is usually not immediately life threatening. With an estimated 5.5 million patients worldwide, however, sustained atrial fibrillation (AF) is the most common arrhythmia. It is not immediately life threatening, but chronic AF increases the risk of atrial electrical remodeling, stroke and thromboembolism due to clot formation. The control of these dynamical patterns and prevention of fatal arrhythmias is desirable, but it remains a major clinical challenge [4]. Our research focuses on mechanisms that induce, sustain, and eventually terminate cardiac arrhythmias.

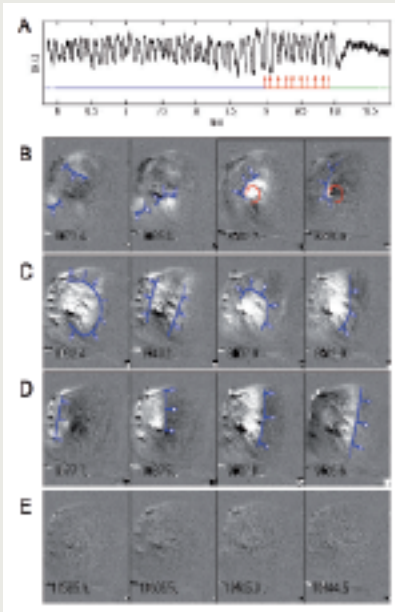

Figure 1
Termination of cardiac fibrillation using far-field pacing. (A) Cardiac action potentials measured optically on the surface of the tissue preparation showing sustained ventricular fibrillation (VF), far-field pacing and capture, and termination. (B) Irregular wave fronts obtained during VF. The grayscale indicates the membrane potential (white = activated, gray = resting). (C) Onset of far-field pacing. (D) Entrainment of cardiac pacing. (E) Quiescent tissue.

At present, the most effective therapy for treating fibrillation is an implantable defibrillator that administers a strong electric shock to reset the entire heart to normal rhythm. Despite recent substantial progress in cardioversion/defibrillation techniques and its to date unsurpassed efficacy, there are intrinsic complications. Cardioversion is a global control method that requires high-energy shocks, which are painful for the patient and often cause tissue damage due to high electric field strengths. Typical shock energies are 10 Joules for implantable cardioverters/defrifibrillators (ICD) and hundreds of Joules for external transthoracic shocks. Negative side effects due to high shock energy highlight the need for new therapeutic approaches focusing on low-energy techniques.

The specific aim of this project is the development of a novel low-energy method to terminate cardiac fibrillation. So far, our experiments have provided ample evidence that fibrillation can be terminated using a minimally invasive, low-energy pulsed electrical *far-field* [5-7] (see Fig.2). Atrial fibrillation is electrically induced by fast pacing from an external electrode. During artificially induced atrial fibrillation in vitro, an electric field is applied by two platinum electrodes providing pulsed far-field stimulation of the tissue. In

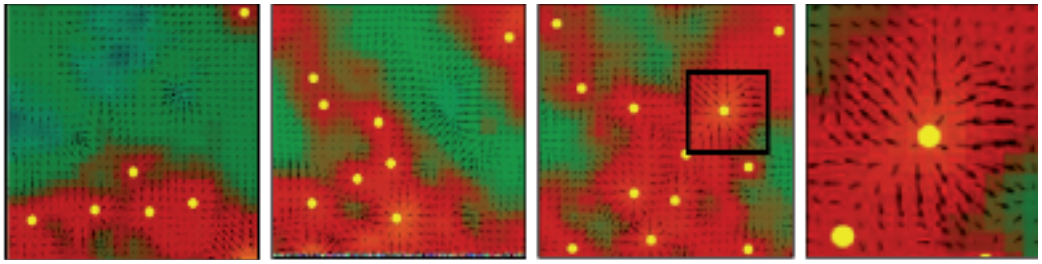

Figure 2: The effect of an electrical field on quiescent cardiac tissue. An electrical field can modify the resting potential in regions adjacent to tissue heterogeneities (e.g. blood vessels) and even lead to wave emission. The number of these wave sources depends on the size of the heterogeneity and the electrical field strength. The formation of so-called virtual electrodes occurs in the tissue bulk but can be observed on the surface: the three panels show an increasing number of wave sources with increasing field strength. The color code indicates the membrane potential (green=resting, red = activated). Multi-site pacing from virtual electrodes is a potential mechanism for the termination of fibrillation using low-energy far-field pulses [5].

the example shown in Fig. 1, an electrical field strength of 1.4 V/cm is sufficient to suppress fibrillation (5 pulses, 5 ms pulse duration, constant pacing interval 85 ms). For sustained atrial fibrillation (4 tissue preparations), we obtain a success rate of 80% (30/36 defibrillation attempts) with electric field strengths ranging from 1.2–1.4 V/cm and 66% (30/35 defibrillation attempts) for 0.8–1.2 V/cm.

Our results have immediate application for the development of defibrillation technology. Low-energy far-field pacing is not meant to replace, but to complement, cardioversion, which remains the ultima ratio for defibrillation. However, chronic cardiac arrhythmias such as atrial fibrillation require frequent treatment and negative effects of cardioversion may become a severe limitation of conventional methods. Pulsed far-field stimulation has the potential to provide a minimally

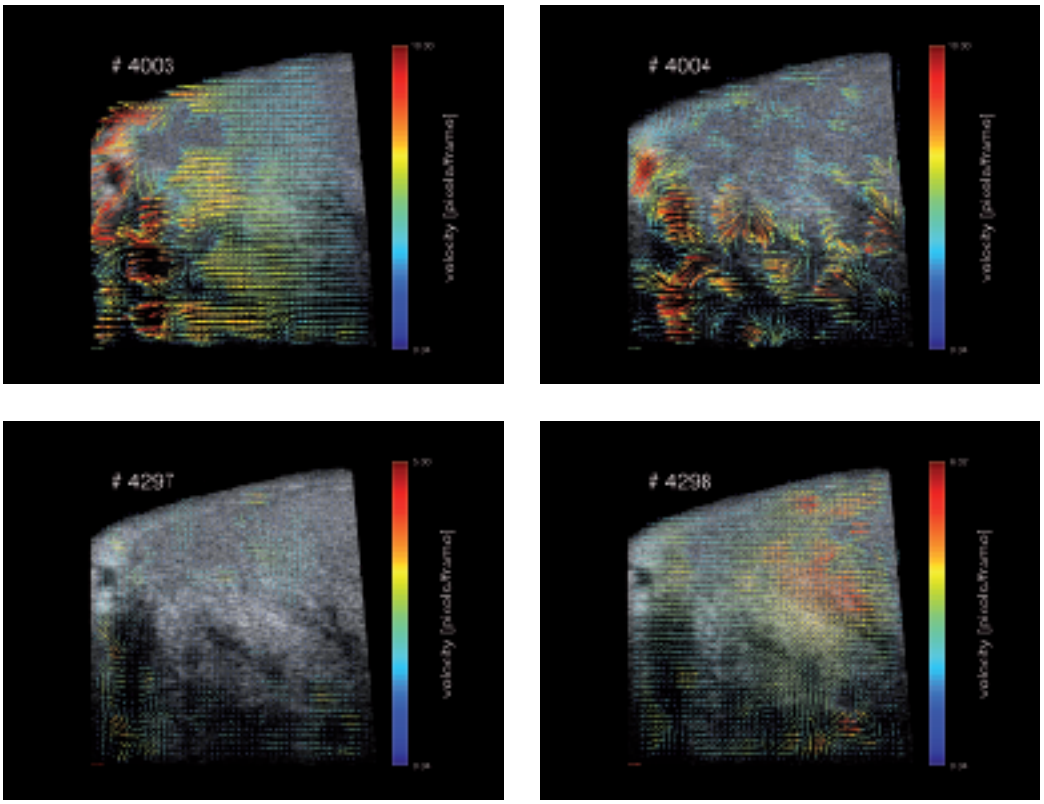

Figure 3
Contractile motion of cardiac tissue obtained from high-resolution cardiac ultrasound imaging. **(Top row)** Displacement vector field of tissue during periodic pacing. The wave propagates from left to right. **(Bottom row)** Displacement vector field during fibrillation.

invasive, low-energy and tissue-preserving therapy to tame cardiac arrhythmias.

The main focus of our research is to elucidate fundamental mechanisms underlying cardiac defibrillation. Progress in this field will depend on the development of new experimental and diagnostic tools. In this project, we are developing optical and acoustic techniques to visualize complex cardiac electrical activity and mechanical motion in vitro and in vivo [8] (see Fig.3). We collaborate with G.Hasenfuss und L.Maier (University Hospital, Göttingen) to explore potential clinical applications.

[1] R.A. Gray, A.M. Pertsov and J. Jalife, *Nature* **392** (1998) 75.
[2] J.M. Davidenko et al., *Nature* **355** (1992) 349.
[3] F.X. Witkowski et al., *Nature* **392** (1998) 78.
[4] A. Karma and R.F. Gilmour, *Physics Today* **60** (2007) 51.
[5] A. Pumir et al., *Phys. Rev. Lett.* **99** (2007) 208101.
[6] S. Luther et al. (submitted to *PNAS*) (2007).
[7] F. Fenton et al. (submitted to *PNAS*) (2007).
[8] G. Luther et al. (submitted to *NJP*) (2007).

Dynamics and Control of Phase Singularities and Spatio-temporal Chaos in Excitable Media

A. Ahlborn, Stefan Luther
Claudia Richter, Amgad Squires
Ulrich Parlitz (University of Göttingen)

Many spatially extended, nonlinear systems exhibit spatio-temporal chaos in terms of irregular wave fronts or turbulent spiral dynamics [1]. Examples can be found in systems as diverse as Rayleigh-Bénard convection, liquid crystals and excitable media. An example for the latter is cardiac tissue. Here, spiral and scroll waves correspond to an electro-mechanical malfunction of the heart. Cardiac arrhythmias occur due to the complex interplay of mechanical and electrical properties on multiple spatial and temporal scales including cellular, tissue, and organ levels. However, the detailed mechanisms of electro-mechanical instabilities leading to arrhythmias remain unknown.

The scientific scope of this project is the development of experimental and numerical methods to characterize, predict, and eventually control spatio-temporal cardiac dynamics. In order to reveal the underlying mechanisms of this complex dynamical system experimentally, we will focus on two-dimensional cardiomyocyte cultures, which allow the study of waves in a simplified and well-defined environment. An example of complex wave motion obtained in a cell culture is shown in Fig.1. Phase singularities are the organizing centers of complex wave motion. The instabilities leading to their creation, interaction, and annihilation are key to the understanding and characterization of cardiac arrhythmias.

This project will focus on taming spatio-temporal chaos using feedback control. Multiple Delay Feedback Control (MDFC) was first introduced by Ahlborn and Parlitz for stabilizing chaotic dynamical systems [2,3]. Recently, the same authors demonstrated that MDFC can

also be used to (locally) stabilize and manipulate spatio-temporal chaos [4]. Fig. 2 shows an example of a spiral defect chaos solution of the complex Ginzburg-Landau equation. To stabilize the dynamic activity feedback signals are applied to a small number of sparsely distributed external control electrodes. The feedback signals are obtained by a weighted average of the local activity of the control cells taken at different, previous times. Fig. 2 shows the transient dynamics of the controlled dynamics after the activation of the feedback. For suitably chosen weight factors (also called gains) and time delays used for implementing the feedback signals, the spiral defect chaos undergoes a transition to planar waves. In a different configuration spirals can be trapped. This mechanism could be used to annihilate counter-rotating spirals or to drive them into a boundary. Similar numerical results were obtained for the Fitzhugh-Nagumo equation, a simplified model of cardiac tissue. In order to quantify the efficacy of the proposed control methods, appropriate methods are required to quantify spatio-temporal dynamics of cardiac tissue [5]. In order to implement the control strategy experimentally, we have established and maintained cell cultures from primary cells (embryonic chickens, neonatal rats) and cell lines (HL-1 [6]). Membrane potential and calcium concentration are measured simultaneously using an optical mapping system and fluorescent dyes (di-4-anneps, Fluo-3). The multi-scale real-time imaging system comprises both a macroscope (upright, Olympus MVX-10) and an inverted microscope (Olympus IX-71) allowing for the simultaneous imaging of events on cellular and tissue levels. The experimental set-up is shown in Fig. 3. The development of a custom-made real-time multi-electrode array for applying the feedback control signals is currently underway.

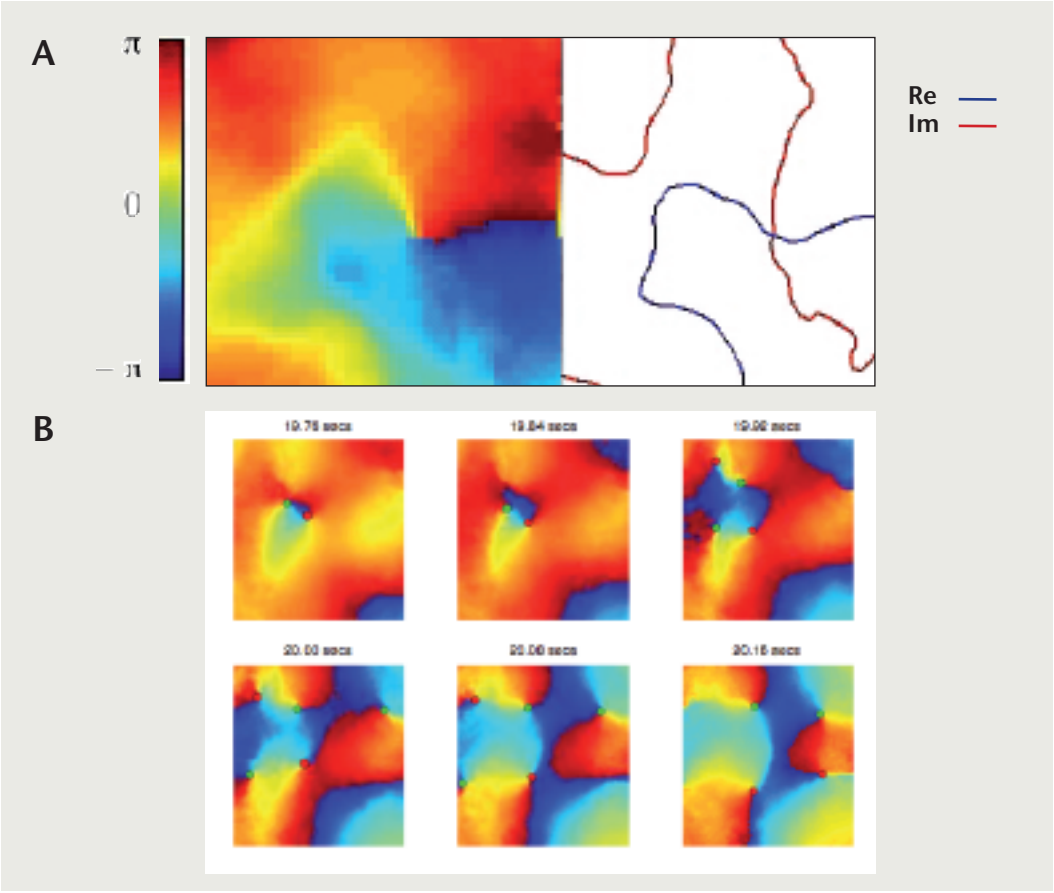

Figure 1
Phase singularities in two-dimensional cardiac myocyte culture. **(A)** Phase of a spiral wave. The position of the phase singularity is obtained from intersections of the zero contour lines of real and imaginary part of the complex signal. **(B)** Temporal sequence of spiral waves. Green and red circles indicate the topological charge ±1 corresponding to clockwise and counter clockwise rotation. Conservation of topological charges requires pair-wise creation and annihilation of phase singularities.

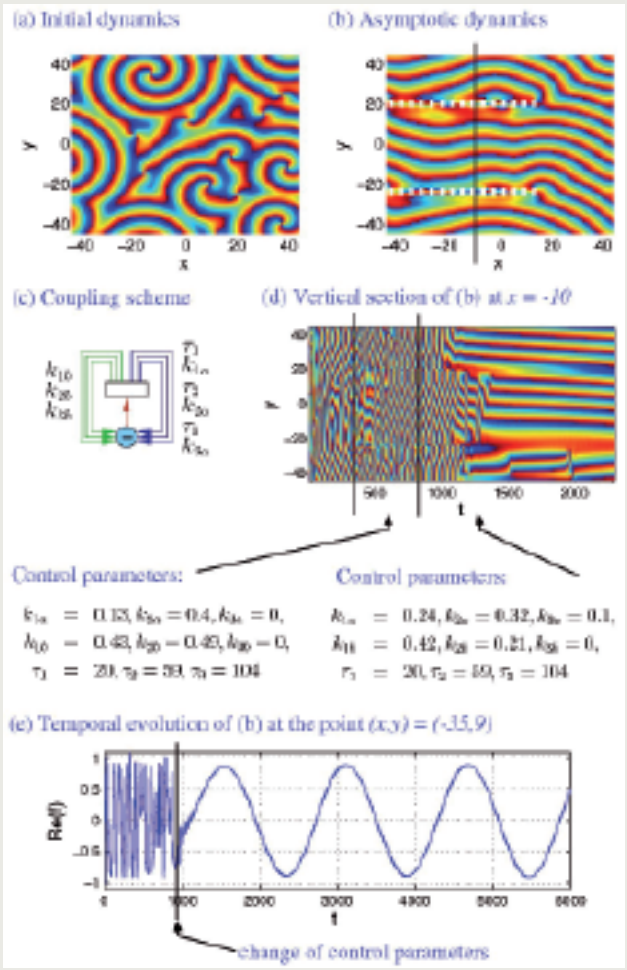

Figure 2
Analysis of the complex Ginzburg-Landau Equation as a prototype for spiral behaviour. (a) Free running system, (b) controlled system. MDFC is applied at the control cells marked white using the coupling scheme given in (c). (d) Vertical section of (b) showing plane waves traveling with different velocities that depend on the chosen control parameters.

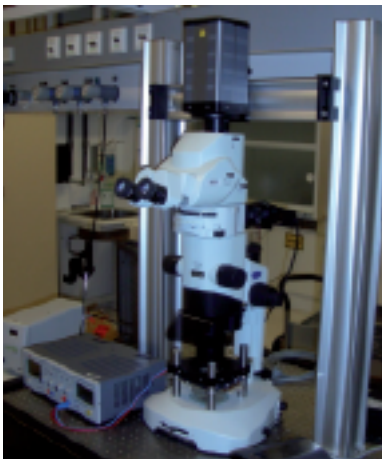

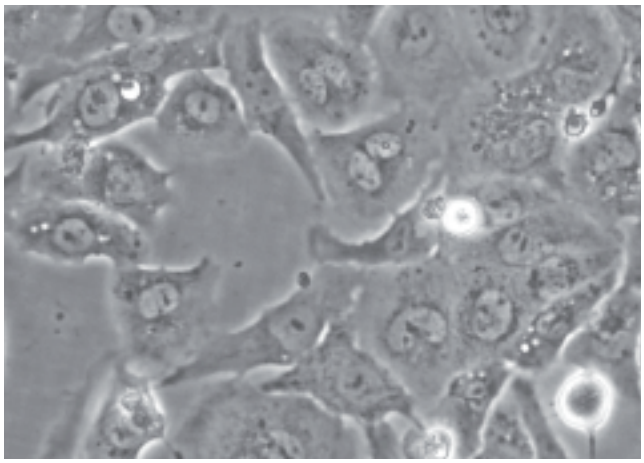

Figure 3
Left: Fluorescence imaging system. Olympus MVX-10 and IX-71.
Right: HL-1 cell culture after 96 hours.

[1] M.C. Cross and P.C. Hohenberg, *Rev. Mod. Phys*. **65** (1993) 851.
[2] A. Ahlborn and U. Parlitz, *Phys. Rev. Lett*. **93** (2004) 264101.
[3] A. Ahlborn and U. Parlitz, *Phys. Rev. E* **75** (2007) 065202.
[4] A. Ahlborn and U. Parlitz, Mulitiple Delay feedback Control, in: Handbook of Chaos Control, Eds. E. Schöll and H.G. Schuster, VCH-Wiley 2007.
[5] A. Squires et al., (submitted to PNAS) (2007).
[6] W.C. Claycomb et al., *PNAS*, **95** (1998) 2979.

Integrable Systems and Soliton Interaction Patterns

F. Müller-Hoissen
A. Dimakis (Chios, Greece)

INTEGRABLE SYSTEMS frequently appear as approximations or limiting cases in physical models. Classical integrable systems with an infinite number of degrees of freedom are given by nonlinear partial differential (or difference) equations (PDEs) for which there is a – not necessarily easy to apply – method to solve them in an *exact* way, which often reveals unexpected features. Among integrable systems are many that exhibit solitons or soliton-like structures. An important example in two spatial dimensions is the Kadomtsev-Petviashvili (KP) equation, which e.g. approximates certain fluid surface waves. In particular, it describes network patterns formed by line wave segments on a shallow water surface (see [1,2,3] for photographs). The constituents are "line solitons", which are closely related to Korteweg-deVries solitons. If surface tension dominates gravity, the KP equation, then referred to as KP-I, admits so-called *lump* solutions. They are localized in both spatial dimensions and show trivial [4] as well as non-trivial [5,6] interactions. Apparently they have not yet been observed in nature and it remains to be seen whether they are within the validity of the KP approximation to the respective real system.

SIMPLE SOLUTION TECHNIQUES

The most powerful method to solve an integrable equation is, if applicable, "inverse scattering". But a quick way to exact solutions is based on the following observations [7-11]. Given a PDE for a function ϕ, we can generalize it to a PDE for an $M \times N$ matrix Φ, choosing a suitable ordering of nonlinear terms, modifying the product in the latter by introducing a constant $N \times M$ matrix Q, and perhaps adding terms that drop out in the scalar case. If Q has rank one, hence $Q = VU^T$ with constant vectors U and V, then $\phi = U^T \Phi V$ solves the original PDE. In this way simple solutions of the matrix PDE can generate complicated solutions (depending on parameters contributed by U and V) of the scalar PDE. But we need to find a solution of an apparently more complicated matrix PDE. An *integrable* scalar PDE, however, typically possesses a generalization to an *integrable* matrix version [12,13]. In the KP case one can apply a finite-dimensional version of Sato theory [14]: a set of matrix Riccati equations, which in turn can be reduced to a linear system, implies the (Q-modified) matrix KP equation. With suitable restrictions imposed on Q, explicit solutions are obtained. Imposing further the rank one condition on Q, one recovers in particular the (multi-) line-soliton and lump solutions of the *scalar* KP equation. But *matrix* KP solutions are also of interest in their own right.

UNIVERSAL LUMP INTERACTION PATTERNS?

A very different integrable equation in $2+1$ dimensions, the Ward equation [15] (modified chiral model, a gauge-fixed hyperbolic (Yang-Mills-Higgs-) Bogomolny equation) possesses lump solutions (see e.g. [16]) with similar behaviour as compared with those of KP-I. Both admit e.g. n-lump configurations with "anomalous" π/n scattering (Fig.1 shows such a solution of a related equation, see below). At first sight these equations have nothing in common besides integrability. In particular,

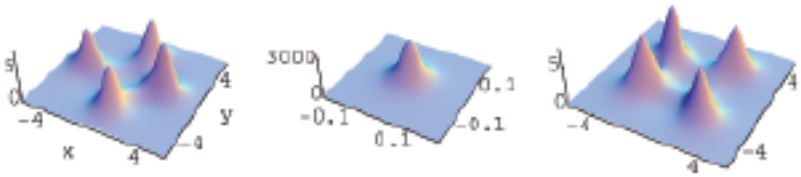

Figure 1: A π/4 scattering process (time increases from left to right) for a 4-lump configuration of the *su*(2) pdCM model, with a large and narrow "freak lump" at collision time [17]. These are plots of a non-negative conserved density.

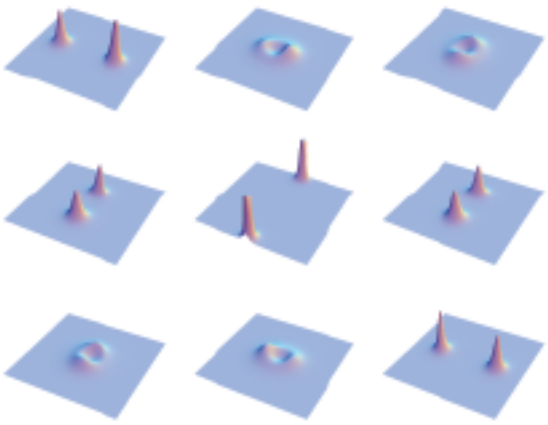

Figure 2: An example of a 2-lump interaction of the *su(2)* pdCM [17]. This is asymptotically a trivial scattering process.

for KP the dependent variable is a real function, for the Ward model it is an *SU(2)* matrix. However, as mentioned above, solutions of the (scalar) KP arise from solutions of the *matrix* (*Q*-modified) KP equation. Moreover, it turned out [17] that an integrability preserving (dispersionless) multi-scaling limit of the latter yields the so-called pseudo-dual chiral model (pdCM). Restricting its dependent variable to take values in the Lie algebra *su(2)*, the latter is closely related ("pseudo-dual") to the Ward model. This indeed establishes a relation between KP and Ward equation, via the pdCM equation, though not a closer link between their solutions. But it allows us to carry solution techniques from KP to pdCM [17]. In particular, this gives access to surprising lump interaction patterns. Examples are displayed in Figs.1 and 2. Also the process in Fig.2 has a KP-I analogue [18]. The pdCM (as well as the Ward model) exhibits further interesting interaction patterns, involving exchange processes of lumps, so that it turns out to be a rich toy model. We note that π/n scattering has also been found, numerically or in a slow-motion approximation, e.g. for lumps of the 2 + 1-dimensional chiral model, monopoles and vortices [19]. These are governed by *non*-integrable equations, though they have structural elements in common with the Ward equation.

Our methods to construct solutions of KP and pdCM equations (and their hierarchies) admit a generalization that also applies to other equations, including the self-dual Yang-Mills equation, of which pdCM and Ward model are reductions. We hope that corresponding explorations will provide easier access to soliton interactions in more complicated systems and reveal common features. Our recent research contributes moreover to various other mathematical aspects of integrable systems [7-11,20-22].

[1] Infeld, E. and Rowlands, G., Nonlinear Waves, Solitons and Chaos, Cambridge Univ. Press (2000).
[2] T. Soomere and J. Engelbrecht, *Eur. J. Mech. B/Fluids* **25** (2006) 636.
[3] http://www.amath.washington.edu/ ~ bernard/kp.html (B. Deconinck: The KP page).
[4] S.V. Manakov et al., *Phys. Lett.* A**63** (1977) 205.
[5] K.A. Gorshkov, D.E. Pelinovsky and Yu.A. Stepanyants, *JETP* **77** (1993) 237.
[6] M.J. Ablowitz et al., *Phys. Lett.* A**267** (2000) 132.
[7] A. Dimakis and F. Müller-Hoissen, *Czech. J. Phys.* **56** (2006) 1123.
[8] A. Dimakis and F. Müller-Hoissen, *Theor. Math. Phys.* **152** (2007) 933.
[9] A. Dimakis and F. Müller-Hoissen, arXiv:nlin.SI/0701010, to appear in Proc. AGMF conference, Lund 2006.
[10] A. Dimakis and F. Müller-Hoissen, *J. Phys. A: Math. Theor.* **40** (2007) F321.
[11] A. Dimakis and F. Müller-Hoissen, *J. Phys. A: Math. Theor.* **40** (2007) 7573.
[12] V.A. Marchenko, Nonlinear Equations and Operator Algebras, Reidel, Dordrecht (1988).
[13] B. Carl and C. Schiebold, *Jber. Dt. Math.-Verein.* **102** (2000) 102.
[14] K. Takasaki, *Rev. Math. Phys.* **1** (1989) 1.
[15] R.S. Ward, *J. Math. Phys.* **29** (1988) 386.
[16] B. Dai and C.-L. Terng, *J. Diff. Geom.* **75** (2007) 57.
[17] A. Dimakis and F. Müller-Hoissen, arXiv:0706.1373.
[18] Z. Lu, E.M. Tian and R. Grimshaw, *Wave Motion* **40** (2004) 123.
[19] N. Manton and P. Sutcliffe, Topological Solitons, Cambridge Univ. Press (2004).
[20] A. Dimakis and F. Müller-Hoissen, arXiv:nlin/0601001.
[21] A. Dimakis and F. Müller-Hoissen, *J. Phys. A: Math. Gen.* **39** (2006) 9169.
[22] A. Dimakis and F. Müller-Hoissen, *J. Phys. A: Math. Gen.* **39** (2006) 14015.

Many-Particle Systems with Complex Equilibria: Statistical Physics and Symbolic Computation

M. Timme
D. Fliegner, F. van Bussel
D. Kozen (Cornell University, USA), S. Stolzenberg (Cornell University, USA),
S. Großkinsky (Warwick Mathematics Institute, USA), C. Ehrlich (University of Dresden)

In systems of statistical physics a few macroscopic quantities specify thermodynamic states (macrostates) which are realized by an ensemble of microscopic states (microstates), defined by the values of all degrees of freedom of all particles. Whereas some specific microstates are essentially irrelevant because they are extremely rare in number and thus highly improbable, a huge number of microstates are typical in the sense that each microstate individually represents the macrostate in a faithful way. For simple systems the relevance of microscopic states is well understood. For instance, for an equilibrium ideal gas in a finite box, by the assumption of the thermodynamics of microcanonical ensembles, each microscopic state is equally probable such that the probability of the gas being in a small part of the box is much smaller than it being distributed over the entire box. In this sense a microstate of the gas that is distributed over the available volume may be a faithful representation of macroscopic variables whereas the microstate of the gas localized in a small part of the box is essentially not relevant for the macrostate.

For many-particle systems with more complicated interactions than those assumed for the ideal gas, however, it is not well understood how microstates contribute to complex macroscopic ground states and other equilibria. Furthermore, for many systems of physical relevance the partition function or its equivalent, even for the ground state, cannot be computed such that these systems are poorly understood [1]. In the current project we study two different paradigmatic systems where we develop the theory and computation of complex macrostates. First, we consider the dynamics and equilibria of reorganization processes of particle aggregates on surfaces. Here we theoretically unified and explained several previous model-specific works and used the new theoretical insights to develop alternative, efficient algorithms to study properties of the equilibria. Second, we consider the anti-ferromagnetic Potts model, a paradigmatic system to study phase transitions in statistical physics; here we use an equivalence between the partition function of Potts models and representation-invariant polynomials in graph theory to compute these polynomials and thus all main observables. In particular, these results contribute towards understanding systems exhibiting positive ground state entropy, an exception to the third law of thermodynamics.

Statistical Physics of Reorganization

Self-organizing many-particle systems – ranging from interacting atoms in clusters to co-acting individuals in flocks of birds – constitute fundamental cornerstones for understanding universal features of complex systems. The physics of particle reorganization on surfaces [2] exhibits dominantly stochastic dynamics where the macroscopic equilibrium, if it exists, consists of many different coexisting microscopic states but is typically characterized by statistical large scale measures (e.g., average thickness, average height fluctuations, fractal dimension, total spatial extent). For instance, a mono-layered connected aggregate of a fixed number of particles is continuously rearranging and assuming a huge number of different aggregates of complicated structure, often of self-similar geometry. The equilibrium of such systems is character-

ized by 'typical' microscopic aggregates that already individually satisfy mean field theory and rearrange into each other: whereas a straight line of single particles constitute one particular connected aggregate that is a possible microscopic realization, aggregates of this maximal length occur extremely rarely and are thus atypical. Many previous works in detail studied several models of specific reorganization mechanisms (e.g., ordinary diffusion, Levy flights or surface diffusion) but it was not well understood how their results depended on the model details. In particular, it was unclear in all of these specific models what a 'typical' aggregate was. This lead to the core question for such reorganizing systems: Which typical microscopic states characterize the macroscopic observables?

In a work together with Stefan Großkinsky (now Warwick Mathematics Institute, UK) and Björn Naundorf we studied a general class of reversible aggregate-reorganization processes [3]. Using the broad mathematical perspective of general Markov processes rather than focusing on specific models for the reorganization mechanism, we found that these processes exhibit globally attracting equilibrium distributions that are universal, i.e. identical for large classes of models. As the equilibrium distribution was obtained analytically, it also became clear which microscopic states significantly contribute to the macroscopic one and are thus 'typical'. As a particular application, our results explain and unify several previous works (e.g., from [4] to [5]) and predict the fractal dimension of the aggregates.

The unified analysis furthermore suggests a new computational approach for studying reorganization phenomena: To obtain equilibrium properties of any such process, computationally expensive reorganization dynamics such as random walks, surface diffusion or Levy flights can be replaced by more efficient yet simpler methods.

Efficient Computation of Partition Functions and Graph-Invariant Polynomials

The Tutte polynomial (TP) of a graph, being closely related to different kinds of enumeration problems, arises independently in statistical physics and graph theory. In physics, it equals the partition function of the Potts model, a paradigmatic lattice spin model, and is as such crucial to a theoretical understanding of phase transitions. In graph theory, the TP is a universal chromatic invariant of a graph and yields many other invariants directly relevant to important graph features such as its communication capabilities, which in turn are of interest, e.g., in computer science. How to efficiently compute the TP (and other related functions of graphs) thus is an important issue in graph theory, of practical relevance in computer science, and an outstanding problem in theoretical statistical physics [6]. However, finding the TP is a computationally hard problem: the time to find it generally increases exponentially with the number of edges in a graph. Conventionally, algorithms for its computation were developed with the aim to cover every possible graph, thus including worst case instances. As a result, their actual performance can often be low on specific types of graphs of interest such that solutions to specific problems become restricted to small graph examples [7] or even practically impossible.

In this project we are developing a new class of computational methods to find the TP and solve related enumeration problems on classes of graphs [8] that are of immediate practical interest in applications. We take this physics perspective [9-11] and develop methods that efficiently exploit the specific properties of large classes of graphs but would loose their advantages if applied to ‚worst-case' instances. The new idea is based on the above-mentioned link of the TP of graph theory to partition functions in physics that are termed as simple summations. We interpret the sum-

mations as symbolic operators and the expressions occurring during evaluation as elements of an abstract ring that satisfies the ring axioms along with further identification rules. Very recently, we worked out the link between the ring representation and conventional summation over variables that occurs in the partition function using methods from mathematical algebra [12].

Using these results from abstract algebra and the physics perspective mentioned above, we are developing graph theoretical algorithms that are based on symbolic summations. The methods are designed such that a resulting algorithm first analyzes and exploits the specific structure of the graph and accordingly represent it in a (close-to) optimal way before performing the actual calculation of the TP.

As a first study on chromatic polynomials (special cases of TPs) suggests, such new methods may drastically outperform existing ones on many graphs of practical interest. For instance, although the Potts model has originally been invented in the 1960s to describe phenomena in physically relevant three-dimensional lattices, three-dimensions could not be accessed so far, neither analytically nor computationally. Using our new method, we now computed antiferromagnetic Potts ground state partition functions of lattices in three dimensions and of disordered versions thereof. Generalization of our current results to full TPs may also have immediate applications to other systems. For instance, one could compute exact partition functions of various ordered and disordered lattices of relevance in physics and possibly access the communication capabilities of complex real-world networks via applied graph theory. In summary, taking into account the structure of the specific graphs of interest, usually ignored by conventional methods, and using a symbolic method of computation based on abstract algebra, yields promising results on moderate and large scale enumeration problems, that in part could not be accessed until today.

[1] A.K. Hartmann and M. Weigt, Phase Transitions in Combinatorial Optimization Problems, Wiley-VCH (Berlin, 2005).
[2] P. Meakin, *Fractals, Scaling and Growth Far from Equilibrium*, Cambridge University Press (Cambridge, UK, 1998).
[3] S. Großkinsky, M. Timme, and B. Naundorf, *Phys. Rev. Lett.* **88** (2002) 245501.
[4] R. Botet and R. Jullien, *Phys. Rev. Lett.* **55** (1985) 1943.
[5] M. Filoche and B. Sapoval, *Phys. Rev. Lett.* **85** (2000) 5118.
[6] A. Sokal, The multivariate Tutte polynomial (alias Potts model) for graphs and matroids, in: "Surveys in Combinatorics 2005", Cambrige University Press (Cambridge, UK, 2005).
[7] P.H. Lundow and K. Markstrom, Research Report 3, Dept. Mathematics, Umea University, Sweden (2002).
[8] A. Andrzejak, *Discr. Math.***190** (1998) 39; D. Noble, *Combin. Prob. Comput.* **7** (1998) 307.
[9] M. Mezard et al., *Science* **297** (2002) 812.
[10] M. Weigt and A. Hartmann, *Phys. Rev. Lett.* **84** (2000) 6118.
[11] M. Mezard, T. Mora, and R. Zecchina, *Phys. Rev. Lett.* **94** (2005) 197205.
[12] D. Kozen and M. Timme, Technical Report, Cornell University, http://hdl.handle.net/1813/8352 (2007)

Hidden Structures in Non-equilibrium Steady States

S. Herminghaus, J. Vollmer, M. Timme

It is one of the major open questions of physics whether there exists a general principle according to which systems far from thermal equilibrium find their stationary states. While equilibrium systems simply seek the minimum of the free energy, the quest for an analogous functional governing non-equilibrium steady states (NESS) in general has so far been unsuccessful. The well-known major obstacle is the absence of detailed balance i.e., the presence of non-trivial probability currents in the steady state. Quite recently, we have introduced a procedure which allows to represent a system by the set of all possible closed loops of probability flux in configuration space [1]. Surprisingly, detailed balance holds in this latter space, thus providing a possible link between equilibrium statistical physics and the dynamics of systems far from thermal equilibrium. This method is inspired by the well-known Poincaré section, which images, for example, a stable limit cycle onto a single point. If there is some noise in the system, the limit cycle will become 'fuzzy', but the overall topology is retained, which is characterized by a strong loop current along the cycle, thereby manifestly breaking detailed balance. In the Poincaré plane, however, one will only see the point representing the cycle to diffuse around; this is obviously much closer to detailed balance than the limit cycle dynamics.

A very general and often used way to represent a non-equilibrium system is by a graph structure. The vertices correspond to the different configurations of the system. The transitions are represented by arrows going from one vertex to another, with rate constants assigned to them. Each such graph, with a finite number of vertices, has a finite number of distinct self-avoiding loops (closed paths), and it can be shown that any steady state flux distribution in the graph can be represented as a superposition of fluxes along these closed loops. If one now defines a new graph in which each vertex symbolizes a loop in the original graph, and computes the transition rates between the loop fluxes (as the arrows in the new graph) from the dynamics in the original graph, it turns out that detailed balance holds in the transformed graph [1]. As a consequence, it is possible to write down a general expression for an entropy as well as a free energy, which attains a minimum in the NESS. Moreover, it can be shown that any non-equilibrium system which may be described by a Markov process on a finite set of states can be mapped onto a classical statistical system with a finite set of energy levels, each of which has a certain well-defined degeneracy [1]. This may open up the possibility to tackle a wide class of systems far from thermal equilibrium with the tools of standard statistical mechanics.

It is the main goal of the present project to explore these possibilities with the help of simple paradigm systems. A first candidate is the frequently studied simple exclusion process [2], in which particles diffuse on a one-dimensional lattice, with double-occupancies forbidden. There are numerous papers in which important quantities like large-deviation functionals have been derived, and it will be of great interest to see whether and how these may be expressed in term of the pseudo-energies emanating from the loop-transform procedure we have proposed. Another simple system is the single-row Mexican Wave (see Fig. 1), inspired by a collective phenomenon of that name sometimes observed in sports stadiums: spectators rise and sit down again in a soliton-wave-like manner [3]. The model system consists of a one-dimensional string of actors, each of which can be in one of three

Figure1
The Mexican Wave, or 'La Ola'. At a certain level of overall excitement of the spectators, solitary-wave-like excitations as the one seen here can be triggered, sometimes spontaneously, but most of the time on purpose by small groups. They may propagate all around the stadium, the typical speed is 12 m/sec [3].

states: sensitive (1), active (2), or refractory (3). An actor in state 1 can be triggered to go into state 2 by a neighbor being already in state 2. The only way out of state 2 is the spontaneous decay into state 3, and from there back to 1. The behavior of each actor is thus cyclic: there can be a probability flux along the loop 1-2-3, but not backwards: it violates detailed balance. If initially all actors are set in state 1, a localized fluctuation may trigger two 'Mexican Waves' going out to the left and right.

Now if there are N actors, the system has 3^N configurations. The number of distinct loops in a graph with V vertices scales roughly as $(V-1)!\, e$, where e is Euler's constant. If $V = 3^N$, this is a formidable number, and the transformed graph will be unmanageably large. However, if we treat each actor separately, we arrive at very simple expressions for the 'level energies' in the individual transformed graphs. These energies depend upon the states of the neighboring actors, such that we can reformulate the system in a way very similar to a 1D Ising system. It will be interesting to compare (or possibly identify) the Mexican Wave with a low lying excited state of the system. On a larger perspective, it will be explored whether other solitary wave phenomena can be successfully described by the same technique.

Another interesting aspect of a general representation of the probablitity distribution functions in a NESS is that it admits to discuss temporal fluctuations of global and local averages. Evaluating the former will allow us to revisit the question under which conditions and for which quantities one can expect to find fluctuation theorems (cf. [4]). The analysis of local averages in Markov systems with a well-defined notion of physical space will give insight in local fluctuations. Similar to the explicitly solvable dynamical system models of transport, this will allow us to explore local fluctuation theorems [5], as well as constraints on the possibility to describe the temporal evolution by macroscopic transport equations [6].

A further path to pursue is the generalization to continuous systems. On the one hand, the number of configurations is even much larger here, but on the other hand, the possible transition rates may be non-zero only for very few transitions. It will be explored whether the theory elaborated for Markov processes can be transformed to a continuous theory, e.g. with the help of path integrals. An important goal is then to find a procedure which transforms non-integrable Fokker-Planck equations into integrable ones, thus yielding a global potential for the stationary flow field.

[1] S. Herminghaus, "Tackling Master Equations with a Flux Loop Transform", arXiv:0710.4913v2, submitted to *Phys. Rev. Lett.*
[2] B. Derrida, J. L. Lebowitz, *Phys. Rev. Lett.* **80** (1998) 209.
[3] I. Farkas, D. Helbing, T. Vicsek, *Nature* **419** (2002) 131
[4] J.L. Lebowitz & H. Spohn, J. Stat. Phys. **95** (1999) 333-365.
[5] L. Rondoni, T. Tél, & J. Vollmer, Phys. Rev. E, **61** (2000) R4679-R4682.
[6] J. Vollmer, *Phys. Rep.* **372** (2002) 131-267.

Phase Transitions far from Equilibrium in Wet Granular Matter

S. Herminghaus, M. Brinkmann, J. Vollmer
K. Huang, Z. Khan, A. Fingerle, K. Roeller, M. Scheel, H. Ebrahimnezhad

Collective phenomena in systems consisting of a large number of coupled similar sub-systems are at the same time ubiquitous and of great fundamental interest. In particular, there is growing interest in cases where the sub-systems are active entities, such as in social systems, biological tissue, or large computer networks. A characteristic feature of active systems is that they break detailed balance, as it is explicitly seen with the actors of a 'Mexican Wave' in a sports stadium (see previous project). An example from condensed matter science with microscopically broken detailed balance are the capillary bridges in wet granular materials. The hysteresis loops constituted by their formation and rupture processes can be traversed only in one direction, such that the dynamical steady states of wet granular matter are characterized by non-trivial probability fluxes currents even on the microscopic scale. We investigate dynamical properties, phase transitions, and critical phenomena in wet granular matter by means of experiments, simulations, and by analytic theory.

While the common granular materials found in everyday life are enormously complex systems, it is of great interest to seek the least complex system which has just enough structure to represent the main features commonly associated with wet granular matter. This is indispensable if one sets out to discover the relevant collective mechanisms leading to the striking properties of these systems. Quite surprisingly, we have found that for many purposes, it is sufficient to consider the grains as spherical, and to assume that the only relevant interaction force (aside from the hard-core repulsion between the grains themselves) is the capillary force [1]. This strongly recommends our model systems not only for understanding the material properties of wet granulates, but also for studying fundamental aspects of collective systems as mentioned above, with detailed balance being intrinsically broken on the microscopic scale. Furthermore, the well-defined energy loss associated with the rupture of a capillary bridge bestows an energy scale to the system. As a result, a pile of, e.g. small glass spheres, wetted by a certain amount of liquid, shows a rich phase transition behavior which is well accessible to experimental investigation and to simulation.

To get into the matter, we have investigated the collective dynamics of wet granular systems by simulation in one dimension and without external drive. Similar studies of 'free cooling' are common in the field of sticky gases, which are studied as simple models

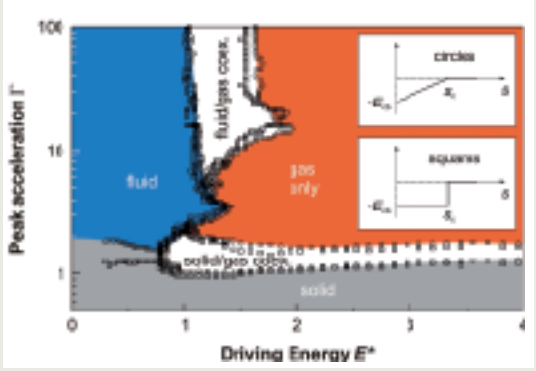

Figure1: The phase diagram for wet granular matter under vertical exitation, as revealed by dynamical simulations with two strongly different hysteretic interaction potentials (insets). Clearly, the shape of the potential is almost irrelevant for the location of the phase boundaries.

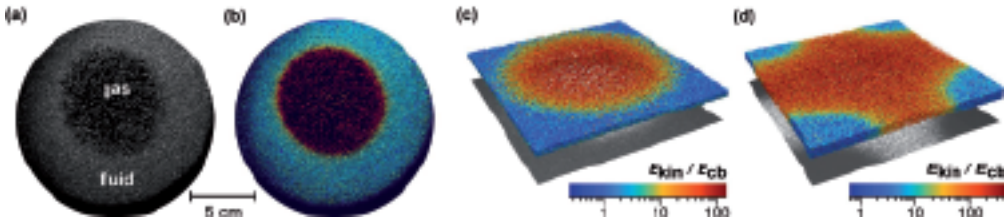

Figure 2
(a) Top view of closed Petri dish containing glass beads (bright dots) wetted by water, under vertical agitation. (b) Same as (a), but colored according to the granular temperature. (c) Event-driven simulation of the experiment with a minimal model. (d) Same as (c), after the 'bubble' has reached the boundary and rearranged to minimize the fluid/gas interface.

for structure formation in accretion disks and planet formation. It could be shown that the presence of a phase transition depends not only on the energy dissipated at each collision, but that the finite extension length of the capillary bridges makes an essential difference [2,3,4]. To reach a deeper understanding of the system, the influence of the liquid on the Kolmogorov-Sinai entropy has been investigated [5,6]. Most importantly, we have set up the equation of state of wet granular matter, assuming spherical particles, and an interaction by hysteretic capillary bridges alone [7]. A crucial step here is the evaluation of the number of capillary bridges per sphere. Excellent agreement between the analytic theory and computer simulations was obtained in the full relevant range of packing densities and rupture distances.

Based on these results, we have investigated in detail the expected phase behavior of vertically agitated wet granular matter in a wide range of solid volume fraction and liquid content (i.e., rupture distance of capillary bridges). Both simulations and analytical calculations predict a first-order-like phase transition from a liquid to a gaseous state. At liquid/gas coexistence, the temperature of the gaseous (dilute) phase is about two times higher than that of the liquid (dense) phase, which clearly shows that this is an intrinsically non-equilibrium state [8]. Simulations with different interaction potentials showed that the structure of the phase diagram is quite universal (Fig.1).These predictions were clearly corroborated by our experiments (Fig. 2). The structure of the phase diagram as well as the corresponding mean-field theory suggest that this phase transition is solely driven by energy, while the usual fluidization observed at lower agitation amplitudes is driven by force [1]. Quite interestingly, the simulations show that the liquid/gas phase boundary seems to exhibit a surface tension, which suggests an excess 'free energy' (Fig. 2c and d). It is of great interest to investigate these quantities using the techniques developed in the previous project.

Several experimental projects are under way to test the predictions made by the theoretical and simulational treatments of the model systems. Among others, we could verify the existence of a liquid/gas critical point in wet granular matter as predicted by analytical theory [7]. Transport processes like convection and diffusion are investigated with tracer techniques in x-ray tomography experiments at a synchrotron beam-line of the ESRF in Grenoble. Furthermore, it was shown that the velocity distribution in a strongly agitated granular medium can be successfully determined by means of Mössbauer absorption spectroscopy.

[1] S. Herminghaus, *Adv. Phys.* **54** (2005) 221.
[2] V. Yu. Zaburdaev, M. Brinkmann, S. Herminghaus, *Phys. Rev. Lett.* **97** (2006) 018001.
[3] A. Fingerle, S. Herminghaus, *Phys. Rev. Lett.* **97** (2006) 078001.
[4] V. Yu. Zaburdaev, S. Herminghaus, *Phys. Rev. E* **75** (2007) 031304.
[5] A. Fingerle, S. Herminghaus, V. Yu. Zaburdaev, *Phys. Rev. Lett.* **95** (2005) 198001.
[6] A. Fingerle, S. Herminghaus, V. Yu. Zaburdaev, *Phys. Rev. E* **75** (2007) 061301.
[7] A. Fingerle, S. Herminghaus, *Phys. Rev. E* **75** (2007) in press.

Experiments on Thermal Convection

B. Hof, G. Seiden, E. Bodenschatz
S. Weiss
J. MacCoy (Cornell), W. Pesch (Bayreuth)

Fluid motion driven by thermal gradients (thermal convection) is a common and most important phenomenon in nature. Convection not only governs the dynamics of the oceans, the atmosphere, and the interior of stars and planets, but it is also important in many industrial processes. For many years, the quest for the understanding of convective flows has motivated many experimental and theoretical studies. Convection usually occurs when a sufficiently steep temperature gradient is applied across a fluid layer. The convection structures appear often in regular arrangement, which we call a pattern. It is the investigation of such convection patterns that is at the center of this project. Pattern formation is common also in many other non-equilibrium situations in physics, chemistry, or biology. The observed patterns are often of striking similarity and indeed their understanding in terms of general, unifying concepts continues to be a main direction of research.

Many fundamental aspects of patterns and their instabilities have been studied intensively over the past 30 years in the context of Rayleigh-Bénard convection (RBC) [1]. In a traditional RBC experiment a horizontal fluid layer of height d is confined between two thermally well conducting, parallel plates. When the temperature difference between the bottom plate and the top plate exceeds a certain critical value the conductive motionless state is unstable and convection sets in.

In the ideal case of an infinitely large fluid layer perfectly straight convection rolls with a wavelength of $\sim 2d$ are formed. In layers of relatively small size substantially different convection patterns are observed (see following page). In the less well-known case of Inclined Layer Convection (ILC) the standard Rayleigh-Bénard cell is inclined at an angle with respect to the horizontal, resulting in a basic state which is characterized not only by heat conduction, but also by a plane parallel shear-flow with cubic velocity profile. This shear-flow not only breaks the isotropy in the plane of the layer, but also, at large angles and when inclined and heated from above, causes a transition from a thermal to hydrodynamic shear-flow instability. For ILC we observed an intricate phase space, filled with nonlinear, spatiotemporally chaotic states [2].

Figure 1: (a) Schematic of the convection cell with micromachined bottom plate (to scale). The fluid height is typically 0.5 mm. (b) microscope image of fabricated polymer stripes on bottom plate.

Spatial forcing in thermal convection experiments

In our experimental investigations we use a pressurized gas cell to study forcing and control of thermal convection in horizontal and inclined fluid layers. As explained in detail in [1], compressed gases have the advantage over other fluids in that they enable an experimental realization of large aspect-ratio samples with short relaxation times (< 2sec). In addition, the Prandtl number can be tuned from 0.17 to 150. The Prandtl number gives the relative importance of the nonlinearities in the heat conduction equation and the Navier-Stokes equation. Our current investigations are restricted to Prandtl numbers < 1.5, where non-relaxational, spatiotemporally chaotic behavior can be observed very close to the onset

of convection. We use spatially periodic and spatiotemporal forcing schemes of various geometries to investigate the influence of modulations on pattern formation. Two types of forcing schemes are applied – one uses micromachined surfaces, as shown schematically in Fig.1, and the other uses a thermal imprinting technique that is improved but similar to the one pioneered by Busse and Whitehead [3]; we illuminate the cell with a 10.6 micron infrared beam emitted by a CO_2 laser, which is absorbed by the main spectral band of an SF_6 gas. A considerable body of literature on time periodic forcing of hydrodynamic patterns, particularly convective patterns, has accumulated. Spatially periodic forcing, on the other hand, has received far less attention.

Surface modulation of the bottom plate in the context of RBC enables us to investigate the affect of forcing on the bifurcation character at onset and on the stabilization of spatiotemporal chaos. In addition, an intriguing long-lived state of localized patterns has been observed (Fig. 2a). When used in the ILC configuration, surface modulation allows for the exploration of novel patterns [4] (Fig. 2b) which emerge as a result of the interplay between the two imposed preferred orientations – the inherent preferred orientation parallel to the gravity component in the inclined plane and the direction along the fabricated stripes.

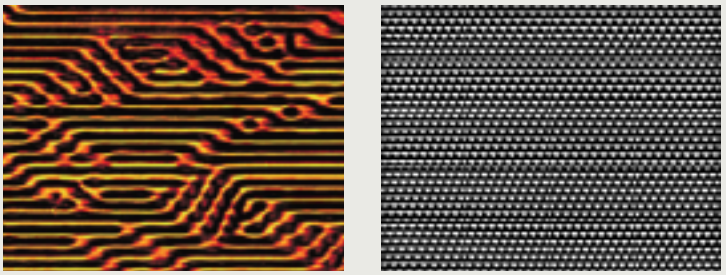

Figure 2: (a) False color image of localized long-lived coherent structures observed for spatial forcing in RBC. (b) Stationary "hexaroll" pattern observed for spatial forcing in ILC. In this case the gravity component in the inclined plane is orthogonal to the surface modulation orientation.

Multiple flow-states in small aspect ratio convection

While most studies in Rayleigh Bénard convection are concerned with flows in cells of large spatial extend or at temperatures far above the onset of convection this project focuses on convection in cells of small aspect ratio and close to onset. Here the number of spatial degrees of freedom is limited which enables an in depth study of the dynamics and the increase in complexity as the temperature difference is increased. Even for a cell with an aspect ratio (diameter/depth) of only four a surprisingly large variety of patterns is found (see Fig. 3) [5]. Which of these flow-states is encountered at a given temperature difference depends on the initial conditions. Our investigation is concerned with the contribution of these multiple flow-states to the complex chaotic dynamics that are encountered at higher parameter values. Preliminary studies show that at slightly higher temperature differences a variety of periodic and chaotic states are observed and again the selection of the state depends on initial conditions. It is currently not clear if these different chaotic attractors remain distinct or begin to merge as the temperature difference is increased and in how far the dynamics at much larger Rayleigh numbers still depend on initial conditions. A particular advantage of the moderate parameter values chosen here is that this enables a direct comparison between experiments and direct numerical simulations. Indeed most of the steady states observed experimentally (and various additional states) have been calculated by L. Tuckerman at LIMSI [6]. We hope that the combination of experiments and fully resolved DNS will enable us to gain new insights into the origin and formation of complex dynamics in RB convection.

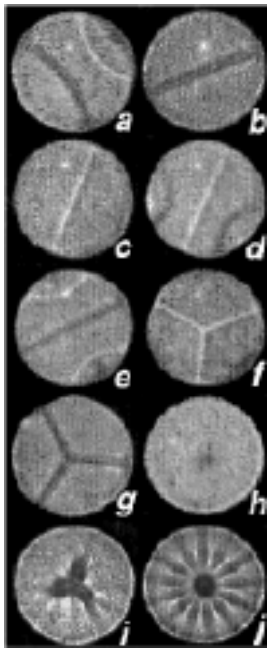

Figure 3: Shadowgraph images of convection patterns viewed from above. Regions of hot/cold fluid rising/falling appear dark/light. The patterns (a)-(h) are steady patterns at Rayleigh number 14000. Examples of time dependent rotating and pulsating states are shown in (i) and (j).

[1] E. Bodenschatz, W. Pesch, and G. Ahlers, A. Rev. Fluid Mech. 32 (2000) 709.
[2] K.E. Daniels and E. Bodenschatz, Phys. Rev. Lett. 88 (2002) 4501.
[3] F.H. Busse and J.A. Whitehead, J. Fluid Mech. 47(1971) 305.
[4] G. Seiden, S. Weiss, J. McCoy, W. Pesch and E. Bodenschatz (Submitted).
[5] B. Hof, P.G.J. Lucas and T. Mullin, *Phys. Fluids* **11**, (1999) 2815
[6] K. Boronska and L.S. Tuckerman J. Fluid Mech. **559** (2006) 279

Phase Separation Induced by a Temperature Ramp

J. Vollmer
G.K. Auernhammer, D. Vollmer (MPI Polymer Research, Mainz)

Intense studies on the experimental and theoretical aspects of the kinetics of phase separation have been carried out over the last decades [1,2]. Most of these studies considered the behavior of systems quenched (cooled rapidly) from the isotropic phase into the biphasic region. In contrast, in many industrial and natural processes the temperature changes are gradual and slow rather than being quenches. Prominent examples are the formation of rain droplets in orographic rainfall or the fabrication of plain bearings, where a liquid binary melt is cooled according to a temperature protocol tailored to arrive at an alloy with a domain structure designed to minimize friction.

In these slowly cooled systems the phase-separation kinetics is quite different from quench experiments. When temperature is ramped diffusion is not fast enough to keep the system close to equilibrium. In the absence of catalyzers of phase separation [1] there will eventually be a massive wave of nucleation producing a large number of tiny droplets in the bulk. Immediately after this nucleation the diffusion can act on length scales of typical droplet distances of less than 100 nm, such that it relaxes supersaturation by orders of magnitude faster than it is generated by the temperature ramping. However, due to coagulation of droplets the rates of the two processes become comparable again after a while. Consequently, a theoretical treatment of systems subjected to a temperature ramp must explicitly deal with the change of the equilibrium composition due to the temperature ramp, with nucleation and with coagulation of droplets.

The common approach to study liquid-liquid phase separation avoids this complication by addressing the situation after a rapid quench of the control parameter (temperature or pressure), which is subsequently carefully kept constant in order not to perturb the phase separation. Often these studies concentrate on the coarsening of the domain structure, during which the typical domain size L grows like a power law [2]. In contrast, an oscillatory evolution of L is observed when samples are taken through a temperature ramp [3-7] where the temperature is slowly varying in time but kept spatially uniform. Early attempts to model these oscillations addressed specific materials such as microemulsions [3] or liquid Ga-Pb mixtures [4]. In contrast, the focus of the present project is the uncovering of generic features of phase separation in systems subjected to a temperature ramp.

To this end we discussed the arising of oscillations in the ϕ^4 model for phase separation

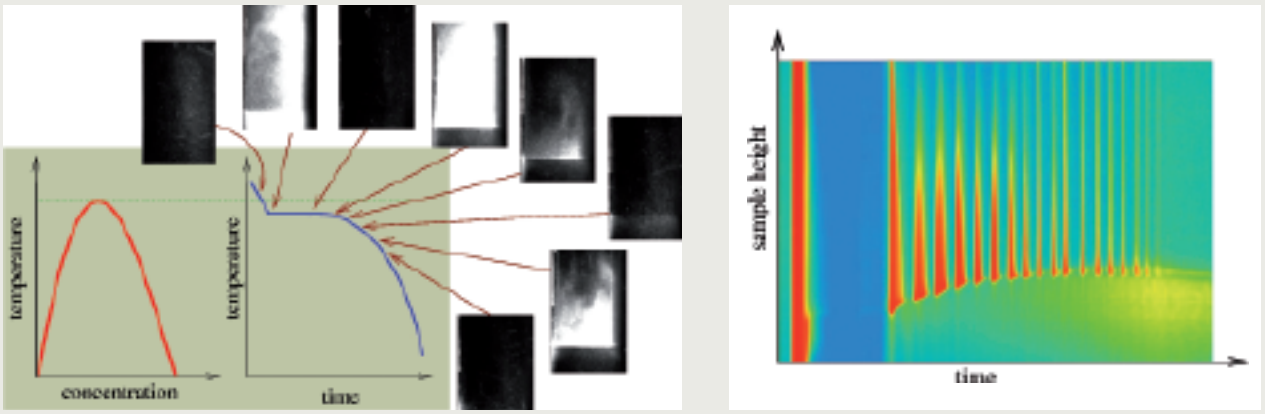

Figure 1: The left graph shows the phase diagram and the temperature protocol for cooling of a methanol/hexane mixture ($\phi_{methanol}$ = 30%), which is monitored by video microscopy. A few snapshots from the video are arranged around plot of the temperature protocol. They show repeated waves of nucleation of droplets, coarsening and sedimentation. This dynamics is conveniently followed in a space-time plot, where the average turbidity in horizontal direction is determined for each picture of the video, and the resulting vertical lines of pixels are combined to a new picture (right panel). To emphasize the changes in turbidity we introduced false colours, where blue refers to a transparent sample, shades of green to yellow increasing turbidity, and red marks a system where vast amounts of large droplets completely block the vision (like in milk). The blue part in the beginning of the experiment represents the waiting time until the system is fully phase separated. The right edges of subsequent vertical red features mark successive waves of sedimentation of droplets, which result in a clearing up of the sample.

in binary mixtures [4,6,7]. This allowed us to identify temperature protocols maximizing the number of observed oscillations, and to establish a minimal model for the appearance of oscillations. The oscillations can best be followed [6] when first waiting until the system is fully phase separated, and then tailoring the temperature ramp in order to fix the dimensionless control parameter N for the rate of change of the concentration. Surprisingly, oscillations are generically observed when the mass density of the coexisting phases is not specifically tailored to be very similar, and when N»1 [7]. The predictions have been compared to recent experimental findings (Fig.1).

The next step in this direction will be to inspect the role of turbulence and convection on the coarsening, and the resulting scaling predictions for the dependence of the oscillation frequency on the dimensionless control parameters.

Another part of the project addresses the initial instabilities of diffusive demixing with respect to nucleation and the onset of convection (Fig.2). Suppressing terms required to deal with surface tension allowed us to estimate the critical dimensionless heating rate N, where the concentration profile becomes unstable to nucleation. However, in order to discuss the mode selection for the diffusion problem one has to take into account the surface tension. To this end the coupled equations for concentration and momentum transport have been discussed in a Galerkin expansion. Our preliminary results are sketched in the right panel of Fig.2. They must carefully be cross-checked, however, due to convergence problems of the Galerkin expansion.

Once this problem is settled we plan to address the demixing in systems with confined geometries, where we expect to find new instabilities and interesting engineering applications.

[1] R. Doremus, *Rates of Phase Transformations* (Academic Press, Orlando, 1985).
[2] A. Onuki, *Phase Transition Dynamics* (Cambridge, Cambridge, 2002).
[3] J. Vollmer and D. Vollmer, *Faraday Discuss.* **112** (1999) 51.
[4] M. Cates, J. Vollmer, A. Wagner, and D. Vollmer, *Phil. Trans. R. Soc. A* **361** (2003) 793.
[5] A. Turchanin, R. Tsekov, and W. Freyland, *J. Chem. Phys.* **120** (2004) 11171.
[6] G. K. Auernhammer, D. Vollmer, and J. Vollmer, *J. Chem. Phys.* **123** (2005) 134511.
[7] J. Vollmer G. K. Auernhammer, and D. Vollmer, *Phys. Rev. Lett.* **98** (2007) 115701.

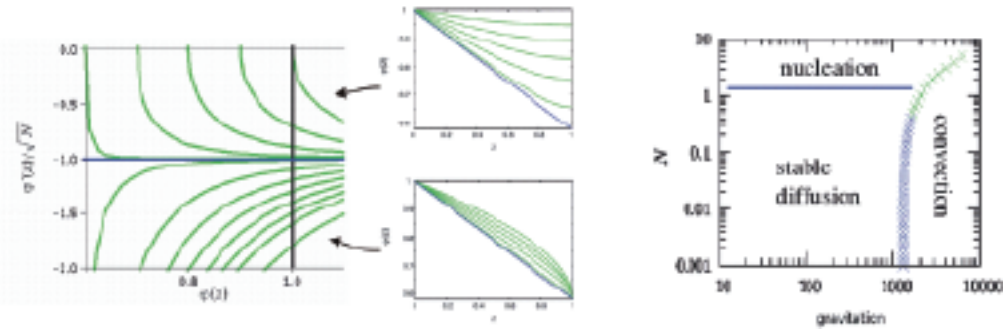

Figure 2: Composition profiles $\varphi(z)$ for the ϕ^4 model in dimensionless units where the height z ranges from 0 at the meniscus to 1 at the far end of the system, and $\varphi(z)$ takes the values ±1 for the two coexisting equilibrium compositions. For each dimensionless control parameter N there is a stable (centre top) and an unstable concentration profile (centre bottom), which can conveniently be summarized in a phase flow graph of the diffusion equation governing the transport in vertical direction shown in the left panel. For $N=(3^{1/2}-1)^2$ the stable and the unstable solution merge in a saddle node bifurcation, and subsequently macroscopic concentration profiles are always unstable with respect to nucleation. Even before nucleation set in, the concentration profile $\varphi(z)$ can become unstable to convection, since it shows a density inversion. The phase diagram to the right shows the threshold for the arising of nucleation together with first estimates for the border to convection.

Anchoring-induced Pattern Formation in Smectic Films

C. Bahr
W. Guo, Y. Iwashita

The characteristic structural length scales in liquid-crystal phases range from few nanometers (smectic density wave) to hundreds of micrometers (cholesteric helix) and can be influenced in many ways, e.g., by external fields, spatial confinement, anchoring on substrates, etc. In recent years, the concept has emerged to use structural features of liquid-crystal phases as matrices or templates to control the self-assembly of micro- and nanosystems. For instance, the distortion of the director field in a nematic phase by small water droplets or solid particles leads to novel long-distance interactions between these particles which may be used for the design of new colloidal systems [1]. Whereas most studies are concerned with nematic liquid crystals, the present project focusses on defect structures in smectic liquid-crystal phases, so-called focal conic domains (FCDs). We explore experimental methods for the targeted generation of FCDs, for controlling their size, for the self-organized arrangement in regular or arbitrary patterns, and for using them as matrices for self-assembling systems.

The formation of FCDs is the answer of a smectic liquid-crystal film to antagonistic boundary or anchoring conditions at its interfaces. FCDs are systems of curved equidistant layers wrapped around two defect lines, an ellipse and a hyperbola passing through each others focal point. In thin films on a solid substrate, these lines degenerate into a circle and a straight line. As shown in Fig.1a, FCDs reconcile between a random planar anchoring (substrate interface) and a homeotropic anchoring (air interface).

On a substrate with random planar anchor-

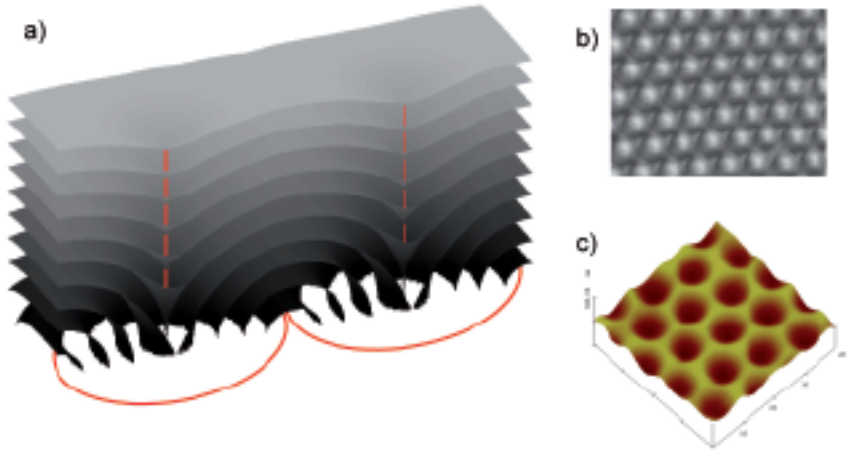

Figure 1: a) Schematic of the smectic layer structure in a cross section through two FDCs in a smectic film on a solid substrate. On the substrate surface, the liquid-crystal molecules align parallel to the substrate plane without a preferred in-plane direction (random planar anchoring); at the air interface, they align perpendicular to the interface plane (homeotropic anchoring); in each layer, they are aligned along the local layer normal. In a FCD, the layers are wrapped around two defect lines (marked in red) possessing the shape of a straight line (running from the substrate to the air interface) and a circle (on the substrate surface). Each FCD causes a depression in the air interface of the film. b) Optical micrograph of a 2D hexagonal pattern formed by FCDs in a smectic liquid-crystal film. The diameter of a single domain is approximately 10 µm. c) AFM image of the surface of the same film. The depth of the surface depressions is approximately 100 nm.

ing conditions, which does not possess any additional structures, FCDs arrange in a 2D hexagonal lattice (cf. Fig. 1b) resulting in a hexagonal pattern of surface depressions that can be studied by AFM (cf. Fig. 1c) [2,3]. The diameter of the FCDs is determined by the thickness of the smectic liquid-crystal film, for thicknesses larger than a few µm, the diameter increases linearly with the film thickness [3].

We are developing methods for controlling arrangement and dimensions of FCDs. One approach is to modify the substrate surface in a way that regions with different anchoring conditions, planar or perpendicular, coexist. This planar/perpendicular anchoring pattern will then translate into a presence/absence pattern of FCDs. Experimentally, this can be achieved by evaporating a thin gold layer, in the presence of a suitable mask, on a substrate with planar anchoring conditions. Since the gold surface induces a perpendicular anchoring (the same as at the air interface), a homogeneous film with uncurved, plane-parallel layers exists on the gold-coated regions, whereas FCDs form on the masked uncoated regions. Fig. 2a shows an AFM image of a smectic film on a substrate possessing square-like gold-coated regions separated by 15 µm wide lines of uncoated surface regions. It is obvious that the FCDs arrange in linear arrays following the anchoring pattern of the substrate surface. The dimensions of the uncoated substrate regions determine also an upper limit for the diameter of the FCDs. Fig. 2b shows linear arrays of FCDs on a 20 µm wide domain-inducing linear substrate area. With increasing

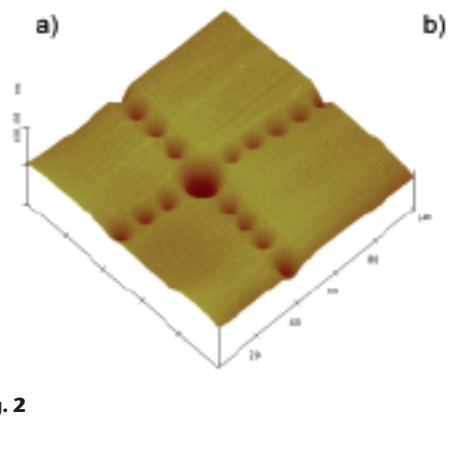

Fig. 2

Figure 2
a) AFM image of a crossing of two linear arrays of FCDs. b) AFM images of linear arrays of FCDs. The images are obtained from smectic films possessing a different thickness (top:3µm middle:5µm bottom:15µm) on a substrate with 20 µm wide lines on which the formation of FCDs is induced. In the thin film, the diameter of a single domain allows for three rows of domains. When the diameter is increased (by increasing the film thickness), the arrangement changes first to two rows and finally to a single row. Note the small satellite domains filling free space between the regular domains.

film thickness (and thus increasing domain diameter), the arrangement changes from a 3-row over a 2-row to a single row array; further increasing the film thickness leaves the diameter of the FCDs unchanged.

Besides linearly structured masks (e.g. TEM grids), we also use monolayers of polystyrene microbeads as masks, resulting in circularly patterned substrates. The diameter of the microbeads (= the diameter of the masked substrate regions) then determines the upper limit for the diameter of FCDs formed on such substrates; the domains retain their diameter even in films with a thickness of several hundred µm [4].

We also study pattern formation in smectic films on substrates which impose an unidirectional planar anchoring (instead of a random planar anchoring). On such substrates, e.g. cleaved layered crystals like mica or MoS_2, the molecules align parallel to the substrate plane and additionally along a certain in-plane direction. In thin smectic films, the layers then form a system of hemicylinders, resulting in a linear depression pattern in the air interface of the film (cf. Fig. 3a). The circular defect lines of the random planar case are now replaced by equidistant straight defect lines on the substrates. Adjacent hemicylinders are separated by defect walls standing perpendicular on the substrate. Because of their much larger energy cost compared to defect lines, these defect walls are expected to become unstable with increasing film thickness. Indeed, we observe in thicker films that the linear depression pattern in the air interface, indicating straight hemicylinders, is replaced by a corrugated surface pattern indicating a more complex arrangement of the smectic layers. We are currently conducting polarized fluorescence confocal microscope studies (cf. Fig. 3c) in order to clarify these structures.

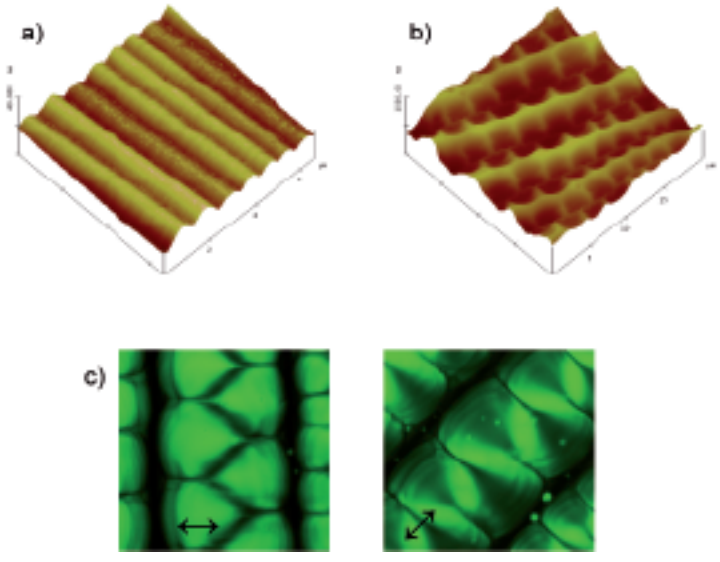

Figure 3: a) AFM image of a smectic film (thickness ≈ 1 µm) on a substrate with unidirectional planar anchoring conditions. The smectic layers form hemicylinders lying on the substrate. **b)** AFM image of a thicker film (≈ 10 µm) on the same substrate. The linear pattern of a) is now decorated by additional features. **c)** Polarized fluorescence confocal micrographs of a film as shown in b). The confocal plane is close to the substrate plane. Arrows are indicating the polarizer position. The liquid crystal is doped with rod-like fluorescent molecules; a high fluorescence intensity indicates that the dye molecules, and thus the liquid-crystal molecules, are aligned along the plane of polarization.

[1] M. Zapotocky et al., *Science* **283**, 209 (1999); S. P. Meeker et al., *Phys. Rev. E* **61**, R6083 (2000); I. Musevic et al., *Science* **313**, 954 (2006).
[2] M. C. Choi et al., *PNAS* **101**, 17340 (2004).
[3] V. Designolle et al., *Langmuir* **22**, 363 (2006).
[4] W. Guo, S. Herminghaus, and Ch. Bahr, *Langmuir*, submitted.

Topical Group

Fluid Dynamics and Fluid Systems

Fluid dynamics and fluid systems span across a wide range of length scales, from the motion of interstellar gas to the formation of clouds and rain in the atmosphere, from mixing milk and coffee on our breakfast tables to the functioning of a single living cell. Despite long-lasting intensive research, complete understanding of the behavior of the fluid systems at both extreme scales is still elusive. In large-scale systems, the flow is usually turbulent, which features irregular flow fields with intense fluctuations and a large range of length and time scales involved. A successful theory of turbulence must therefore describe the nonlinear interactions among the multitude of relevant scales. In small, micro-scale systems, the flow is usually regular and smooth, but boundary effects are crucial for these systems due to the increased surface-volume ratio at small scales. It is therefore imperative to understand the rich physical and chemical phenomena at the interfaces, which extend the current research beyond the traditional fluid dynamics.

On small scales, the continuum picture of fluid flow appears to work amazingly well down to molecular length scales. However, there is no satisfactory theory yet for the friction of a liquid with the wall of the container. The appropriate boundary condition for liquid flow at the molecular scale is not known. The so-called extrapolation length, which quantifies the friction, may vary over many orders of magnitude, even for comparably simple fluid systems. When mobile interfaces are present, such as a free liquid surface, the dynamics of fluid interfaces and three-phase contact at a fluid/solid boundary may become important, which poses additional problems lacking a satisfactory solution so far. Progress in this problems is of great importance for almost all soft matter systems, since fluid interfaces and the pertinent interfacial forces are ubiquitous in biological matter as well as in most complex fluids. It is therefore necessary to investigate the dynamics of fluids with variable internal complexity on different length scales. In particular, is it of great interest to study the interplay of intrinsic length scales of a complex fluid with the geometry of the container boundary. Results from these investigations will have far reaching consequences to, for example, the flow dynamics in blood vessels, microfluidic devices, or within living cells.

The study of large scale systems focuses on fluid turbulence. It ranges from the transition to turbulence in shear flows (pipe, Couette and Taylor-Couette flows), to thermally driven turbulent flows in Rayleigh-Benard systems, to kinematically driven, fully developed turbulence. In addition to turbulence in simple fluids, turbulence in complex fluids shows intriguing properties. For example, a small amount of long-chain polymers added into the flow gives rise to dramatic drag reduction in wall-bounded turbulent flows and to elastic turbulence at very small Reynolds numbers. In addition, our research extends to particle-turbulence interactions, in which a Lagrangian description is natural. The development of measurement techniques also focuses on obtaining Lagrangian information of the turbulence itself or of the particles carried by the flow. The experimental facilities give access to controlled, repeatable laboratory turbulent flows with Reynolds number up to the range of atmospheric turbulence. A unique feature of the facilities is the construction of the high-pressure vessel (the U-Boot). When used with SF_6, the U-Boot provides a low-viscosity environment in which an ordinary turbulent generating device can produce much higher Reynolds numbers compared with in air at normal pressure. Through the International Collaboration for Turbulence Research, the experimental facilities are open to researchers outside the institute.

Discrete Microfluidics

R. Seemann, C. Bahr, M. Brinkmann, T. Pfohl, S. Herminghaus
Y. Iwashita, A. Steinberger, H. Evans, C. Priest, E. Surenjav, S. Thutupalli, V. Chokkalingam,
W. F. Maier (Saarbrücken, Germany), M. Mayor (Basel, Switzerland), P. Schwille (Dresden, Germany)

Monodisperse emulsions with a low volume fraction of the continuous phase (gel emulsions) provide an alternative to conventional microfluidic approaches, where single phase liquids are transported through micro-channels [1]. The well defined geometry of a gel emulsion is comparable to the structure of foam and is governed by the relative droplet size and the geometry of the microfluidic channel. Targeted geometrical rearrangements of droplets enable a plethora of new possibilities including combinatorial chemistry.

For a precise control of the droplet volume we developed a one-step method for the *in situ* production of mono-disperse gel emulsions, suitable for microfluidic processing [2], which can be easily fabricated in a single photolithographic exposure step [3]. This technique uses the destabilization of a quasi 2D liquid jet being transferred into a 3D geometry at a topographic step. It allows to produce emulsions with a monodispersity better than 1.5 % at dispersed phase volume fractions up to 96 %. The production frequency can be varied between a few tens to several hundred droplets per second.

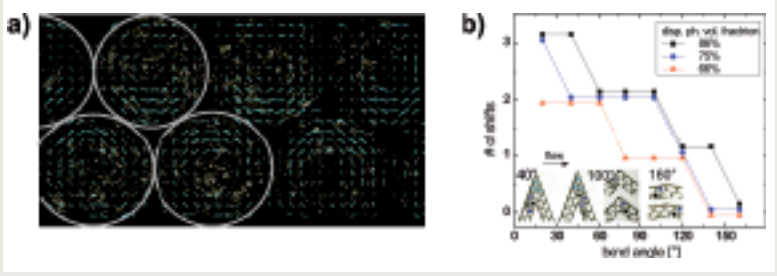

Figure 1: a) Flow pattern within droplets in a zigzag arrangement flowing from right to left. The droplets are indicated by grey circles. b) Number of droplet shifts when a gel emulsion in a zigzag arrangement flows through a bend. The encircled numbers are the dispersed phase volume fraction. Inset: three examples of emulsion arrangements before and after the bend. To illustrate the phase shift, pairs of droplets are marked with red and black dots. In case of acute bends some droplets get trapped at the tip of the bend (marked with yellow dots)

The motion of a gel emulsion in a solid channel system is mainly governed by two physical aspects of the system. One is the dynamics of thin liquid films and three-phase contacts at solid surfaces, which has been investigated in many studies in the recent years [4,5]. The other aspect concerns the mechanical properties of a gel emulsion itself. It is well known that rather dry foams, which correspond to small continuous phase volume fractions in our case, move within pipes by plug flow. This is due to the finite threshold stress required to deform the foam network (e.g., the finite energy required for a T1-transition). Due to this finite threshold, the rearrangement is highly hysteretic and depends on the volume fraction of the dispersed phase. We explore the equilibrium arrangements as a function of droplet size, channel geometry, and volume fraction. Furthermore, we explore the passive manipulation of the droplet arrangements by the channel geometry, the active manipulation by externally applied magnetic fields using ferrofluids as continuous phase, and the motion within the droplets, induced by the friction of the emulsion lamellae, for a controlled manipulation of the emulsion droplets in order to position, sort, exchange, compile and redistribute liquid compartments [6,7,8].

In contrast to conventional microfluidics where the reactants are always exposed to the surrounding channel walls, the individual droplets of our discrete microfluidics are separated from the surrounding matrix once they are formed. Hence in combination with a

method to merge individual droplets, discrete microfluidics allows to study (bio-)chemical reactions and processes, which would clog a conventional microfluidic device.

We found that the coalescence of single lamellae between individual droplets can be targeted using the destabilizing effect of an electric field [9] on emulsion lamellae [10] (electro-coalescence). This technique is very effective for small lamellae thicknesses, where a short pulse (few volts) is sufficient to combine droplets containing even delicate biological reactants.

As an example, we applied electro-coalescence to produce small silica particles [3]: Two droplet fabrication units were synchronized to produce alternating droplets containing tetramethoxysilane (TMOS) and an ammonia solution, respectively. The droplets were coalesced, mixed, and gelled within a few seconds. A perspective of this fabrication technique is to produce a large number of different ceramic particles with various chemical compositions for catalytic purposes.

In a similar approach we study the evolution of a fibrinogen network as a function of the thrombin concentration by mixing an aqueous solution of fibrinogen monomers and the enzyme thrombin. The mechanical properties of the fibrinogen network which has formed in the droplets can be measured through its response when flowing through appropriately shaped constrictions in the microfluidic channels. Experiments in the presence of vascular smooth muscle cells in the (developing) fibrinogen network will show how cells respond on the changing environment.

Aside from using the individual droplets as reaction containers, we also exploit the fact that regular arrangements of droplets provide as well regular arrangements of surfactant bilayers. These can be used to align hydrophobic molecules with hydrophilic end groups across the lamellae in a well organized fashion. Exposing the emulsion to certain channel network geometries, we can control the orientation of the molecules inserting into the lamellae. Using molecules with an asymmetric voltage-current characteristics, it should be possible to construct molecular electronic circuits based on the controlled (re-)manipulation of the droplet arrangements.

Furthermore, the bi-concave shape of foam lamellae is suited to focus X-rays (compound refractive lens, CRL). Due to the small refractive index of the organic foam lamellae, several ten to hundred lamellae (typically 50–200) are needed to achieve a desired focal length in the range of 20–200 cm. A dynamic CRL is achieved by a continuously renewing linear train of droplets produced by step emulsification [2]. Due to the continuous refreshing of the droplets radiation damage is negligible and the dynamic CRL should be ideal for usage in high intense X-ray beams (e.g. X-FEL). The focal length of the CRL can be continuously tuned forming a zoom lens by varying the volume of the bubbles. As refractive materials we use alkanes and liquid crystals, which have desirable X-ray absorption properties and which can be effectively stabilized using the surface freezing effect [11,12]

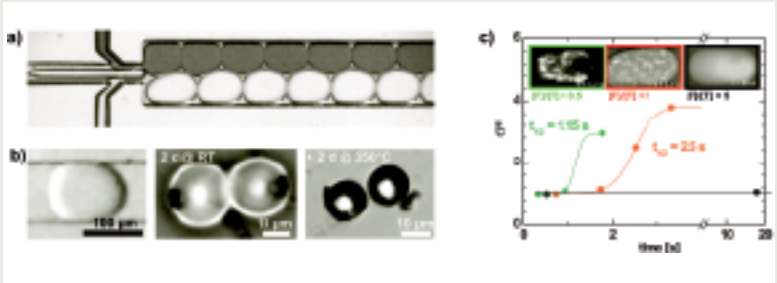

Figure 2: a) Pairs of droplets (indicated by a dye) produced with a double step-emulsification. The alternating droplet production self-synchronizes via pressure cross-talk. b) *left*:. gel droplet in a microfluidic channel right after coalescing a pair of droplets containing TMOS and ammonia, respectively. *middle* and *right*: subsequent processing of the gel particle outside the microfluidic device. After drying at room temperature (*middle*) and baking at 350°C (*right*) the droplets shrink from about 100 μm to about 10 μm. c) Extend of fibrinogen network formation normalized by the standard deviation of the image intensity σ* as function of time for various enzyme concentrations [F/T]. *Inset*: fluorescence micrographs of the fibrinogen network inside droplets.

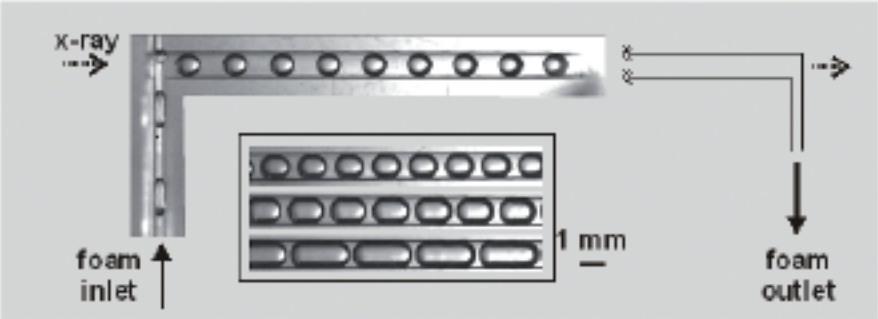

Figure 3: Micrograph of the inlet part of an emulsion – CRL micro machined into PMMA. To realize different focal lengths, the number of curved interfaces can be varied as shown in the inset.

[1] K. Jacobs, R. Seemann, and H. Kuhlmann, *Nachrichten aus der Chemie* **53** (2005) 302.
[2] C. Priest, S. Herminghaus, and R. Seemann, *Appl. Phys. Lett.* **88** (2006) 024106.
[3] V. Chokkalingam, et al., *The Proceedings of the µTAS 2007*, Eds. J.-L. Viovy, P. Tabeling, S. Descroix, L. Lalaquin, ISBN 978-0-9798064-0-7
[4] J. Becker, et al., *Nature Materials* **2** (2003) 59.
[5] R. Seemann, et al., *J. Phys.: Condens. Matter* **17** (2005) S267.
[6] C. Priest, et al., *Proceedings of the 4th world congress on emulsions* (2006).
[7] C. Priest, et al., *The Proceedings of the µTAS 2007*, Eds. J.-L. Viovy, P. Tabeling, S. Descroix, L. Lalaquin, ISBN 978-0-9798064-0-7
[8] E. Surenjav, et al., *The Proceedings of the µTAS 2007*, Eds. J.-L. Viovy, P. Tabeling, S. Descroix, L. Lalaquin, ISBN 978-0-9798064-0-7
[9] S. Herminghaus, *Phys. Rev. Lett.* **83** (1999) 2359.
[10] C. Priest, S. Herminghaus, and R. Seemann, *Appl. Phys. Lett.* **89** (2006) 134101.
[11] R. Lucht, Ch. Bahr, and G. Heppke, *J. Phys. Chem. B* **102** (1998) 6861.
[12] Ch. Bahr, *Phys. Rev. Lett.* **99** (2007) 057801.

Single Cell Stimulation in Microfluidic Environments

C. Beta, E. Bodenschatz
D. Wyatt, T. Fröhlich, H.U. Bödecker, M. Theves
W.-J. Rappel (UC San Diego, USA)

Quantitative studies of cellular systems require experimental techniques that can expose single cells to well-controlled chemical signals with high spatiotemporal resolution. A prime example for the need of quantitative stimulation experiments is the study of eukaryotic chemotaxis, which is of fundamental importance for many biomedical phenomena. The initial steps of the chemotactic signaling cascade take place within only a few seconds [1]. Progress in unraveling the dynamics of such intracellular pathways thus relies on experimental techniques that provide quantitative control of chemical stimuli on the length scale of individual cells, with a temporal resolution higher than the time scales of intracellular signaling events.

In our Research Report 2006, we have shown preliminary data on the use of caged compounds in micro-flow systems. We have now developed this approach into a well- established flow photolysis technique to generate tailored stimuli on the length scale of individual cells with sub-second switching times

[2]. In a flow photolysis experiment, cells are placed in a microfluidic channel under a continuous fluid flow that carries the caged, *i.e.*, inert form of a signaling agent. The latter can be activated by photo-chemically splitting off the cage through exposure to short wavelength irradiation. By illuminating a region in the flow immediately upstream of the cell, the uncaged signaling substance is carried across the cell by the fluid flow. Changing the shape of the light source and thus the residence time of the caged substance under the UV-light can generate concentration profiles of arbitrary shape. This is demonstrated in Fig. 1 by the release of a caged fluorescent dye. We have applied this flexible approach to study chemoattractant-induced intracellular responses in *Dictyostelium* cells. Here, both cytoskeletal dynamics and membrane translocation of fluorescent fusion proteins have been considered (see our reports on *Directional sensing in eukaryotic cells* and *Time-periodic patterns in the actin cortex*).

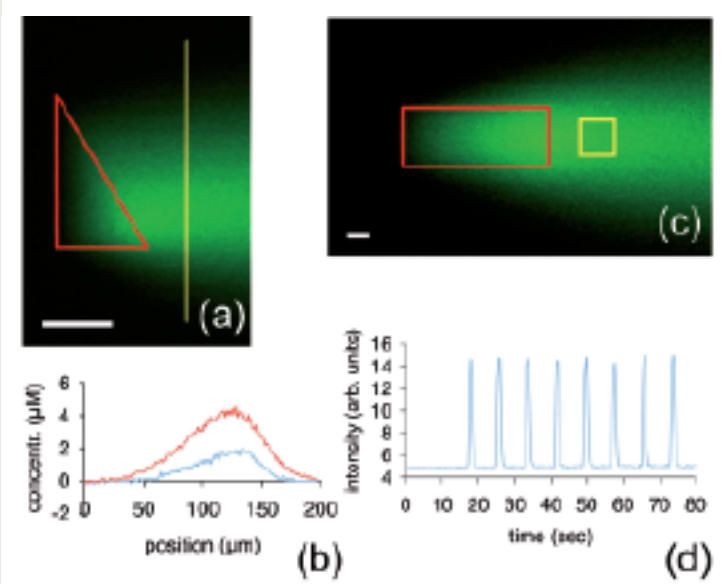

Figure 1: (a) Photo-release of DMNB-caged fluorescein in a triangular uncaging region (red), scale bar 50µm. (b) Fluorescence intensity along the yellow line in (a) for a mean flow speed of 67 m/sec (red) and 133 m/sec (blue). (c) Release of caged fluorescein inside a rectangular uncaging region (red), scale bar 10µm. (d) Fluorescence intensity averaged inside the 15x15µm yellow region in (c) for a pulsed uncaging light source. Fluid flow from left to right.

Besides flow photolysis, also conventional microfluidic techniques are used in our group for live cell experiments. In particular, the use of a microfluidic gradient mixer, that has been successfully employed in *Dictyostelium* wild-type migration studies (Research Report 2006 and Ref. [3]), is currently extended to characterize the chemotactic behavior of *Dictyostelium* cell lines with deficiencies in cytoskeletal regulators. We will focus on mutant strains that are, at the same time, studied at the level of their intracellular dynamics (see our report on *Time-periodic patterns in the actin cortex*).

Another focus of our work has been the numerical investigation of flow effects that arise from the interplay of fluid velocity, diffusive transport, and cell geometry [4]. Microfluidic setups for live cell experiments generally operate under continuous flow conditions and rely on diffusive mixing and fluid flow to produce a well-defined, temporally stable concentration profile. In most cases, such devices are characterized for operating conditions where fluid runs through smooth micro-channels. However, biological cells are three-dimensional, impermeable objects that extend into the channel and perturb the flow field in their vicinity. If a non-uniform distribution of chemicals, *e.g.*, a gradient, is carried along with the fluid, these distortions can have a profound influence on the actual concentration across the surface of the cell. This is schematically illustrated in Fig. 2(a). We have performed three-dimensional finite element simulations to study the influence of flow speed and geometry on the distribution of chemicals across the surface of a cell in a microfluidic channel. The effect of cell height, elongation, and orientation to the flow has been systematically investigated. In Fig. 2(b), an example is shown that demonstrates deviations in the surface concentration of a passive scalar depending on the orientation of an elongated cell with respect to the flow.

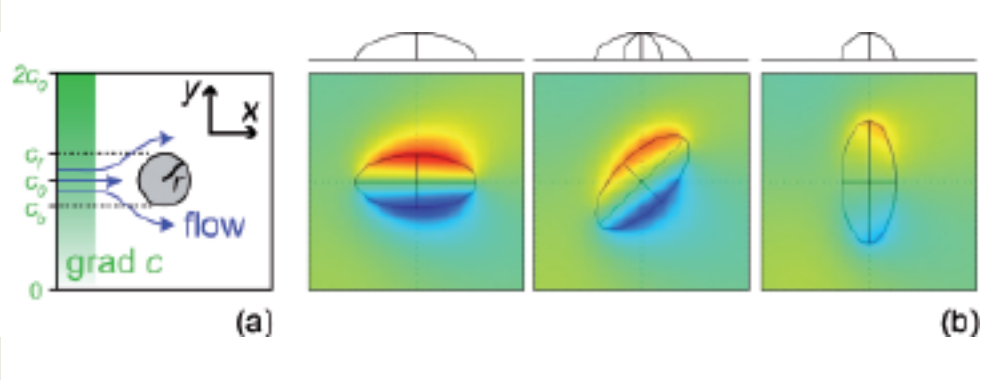

Figure 2: (a) Illustration of flow-induced "shielding": at high flow speeds, the concentration gradient across the cell is reduced as compared to the imposed gradient upstream. (b) Gradient exposure of a cell under flow conditions. Fluid flow runs from left to right, a linear concentration gradient is imposed perpendicular to the flow. The deviation in concentration on the surface of an elongated cell is shown for different orientations with respect to the flow.

[1] C. A. Parent and P. N. Devreotes, *Science* **284** (1999) 765.
[2] C. Beta, et al., *Analytical Chemistry* **79** (2007) 3940.
[3] L. Song, et al., *European Journal of Cell Biology* **85** (2006) 981.
[4] C. Beta, et al. (2007) submitted.

Soft Biological Objects in Microflow

T. Pfohl
H.M. Evans, D. Steinhauser, E. Stellamanns
M. Engstler (TU Darmstadt), H. Stark (TU Berlin), R. Winkler, G. Gompper (FZ Jülich), S. Herminghaus

The dynamic behavior of soft biological objects is ideally probed using microflow environments [1,2]. In the case of single celled organisms, flow allows us to better approximate biological conditions such as those in blood vasculature. In addition, the flow profile can predictably alter the drag force on the cells. On smaller scales, single filaments reveal distinct behaviors depending on the details of their flow environment. In addition to simple flow profiles, the incorporation of complex geometries will enable us to probe the mechanical properties of soft objects.

The unicellular parasite *Trypanosoma brucei* has long been known to cause African sleeping sickness, but the defense of these trypanosomes against the hosts' immune system remained a mystery. New research we have performed in collaboration with M. Engstler (Darmstadt) indicates that hydrodynamic shear flow is responsible for the performance of trypanosomes [3]. The cell membrane contains the glycoprotein VSG which serves as a physical barrier to components of the immune system, but also binds to and cycles antibodies laterally along the membrane. Time lapse experiments showed that Immunoglobulin G antibody-VSG complexes (IgG-VSG) were

driven toward the posterior cell pole by hydrodynamic drag and were subsequently engulfed and degraded by the trypanosome cell machinery (see Fig.1). The movement of IgG-VSG in the cell membrane is dependent on the directional motility of the trypanosomes. In order to better isolate the effects of flow and confinement on trypanosomes, we utilize microfluidic devices. The dynamic motility of trypanosomes is monitored in well controlled flow profiles of small microchannels (~2μm–15μm). Stroboscopic illumination enables multiple snapshots per camera exposure, thereby allowing us to accurately track the cells, shown in Fig.2. Detailed analysis of the protein cycling within the trypanosome membranes as they travel in flow fields and in more complex geometries (and, consequently, quantitatively different surface drag forces) will tremendously aid the current understanding of these cells' vitality. Periodic expanding elements in the channel designs will also allow us to determine the visco-elastic recovery of soft objects in flow. Red blood cells serve as an ideal starting system for these studies, because their basic properties are known from other techniques and they are not self-propagating, as trypanosomes. These experiments show great potential in biotechnical applications in addition to their worth as fundamental studies, since individual organisms or objects may be sorted based on their mechanical properties.

Scaling down from single organisms, we also investigate the behavior of the protein actin in flow. Actin filaments, aside from their biological roles in cellular motility and mechanical stability, are also ideal semi-flexible polymers. Our previous studies quantified the effect of microscale confinement on actin [4-6]. Novel experiments characterize the stochastic and deterministic motion of actin in hydrodynamic flow [7]. Actin filaments flow inside symmetric microchannels (on the same length scale as the filaments' persistence and contour length) with a Poiseuille velocity profile. Stroboscopic imaging is used to capture the motion of the same filament as it flows through the channel (see Fig.3b), and the focus plane is approximately at the channel center (Fig.3a). We find qualitatively distinct behaviors, shown in Fig.3b. Filaments flowing directly in the center of the channel exhibit a U-profile which mimics the flow field. The x-y profiles of these filaments overlay well with an analytical model using the hydrodynamic beam equation of an elastic rod, as shown in Fig.3d. In regions outside of the center, the filaments tend to be either extended or tumbling. We attribute the tumbling of filaments to an instability that occurs when the filament is caught in the parabolic profile with its leading end in higher shear. A striking phenomenon is revealed through a detailed analysis of the center-of-mass probability distribution of the filaments: with increasing flow velocity, we find a maximum in the distribution at one- and three-quarter width from the channel wall (see Fig.3c). That is, we find a migration away from the channel center as well as from

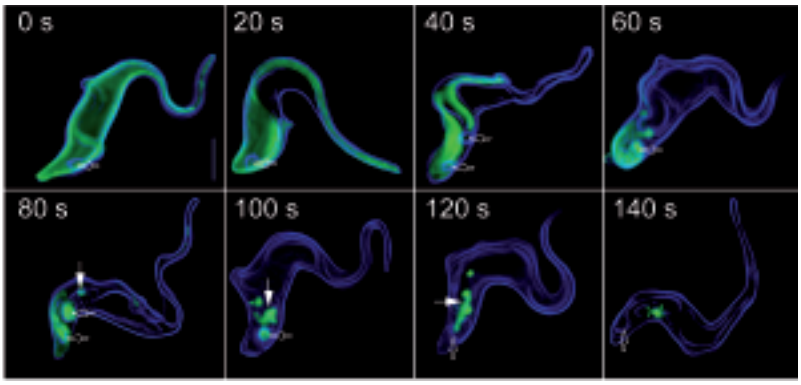

Figure 1: Visualization of Immunoglobulin G antibody removal from the cell surface of the bloodstream stage *Trypanosoma brucei*. Scale bar: 3 μm.

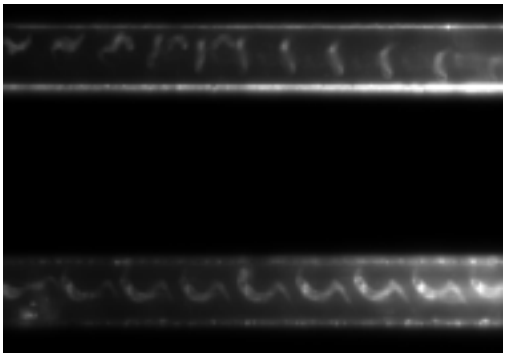

Figure 2: Stroboscopic imaging of trypanosomes in microchannels (width: 15μm; depth: 3.5μm; flow velocity: 1.6mm/s).

the channel walls. This cross-streamline migration has been predicted in simulations for flexible polymers and rigid rods. However, the evidence of cross-streamline migration until now was sparse, and surprisingly we find a stronger effect in our experiments than that predicted. The origin of this migration is the hydrodynamic interactions of the filaments with the walls and the different cross-streamline motilities of the filaments depending on their extension. Due to the linear shear rate increase from the channel center outward toward the walls, the filaments are more extended away from the center. Because extended filaments have smaller cross-streamline diffusivity than relaxed ones, there is a net migration of the polymers away from the center in a velocity dependent manner. On closer inspection, we have found that individual filaments may experience different diffusivities along their length, requiring more detailed analysis of images to completely understand the cross-streamline migration process.

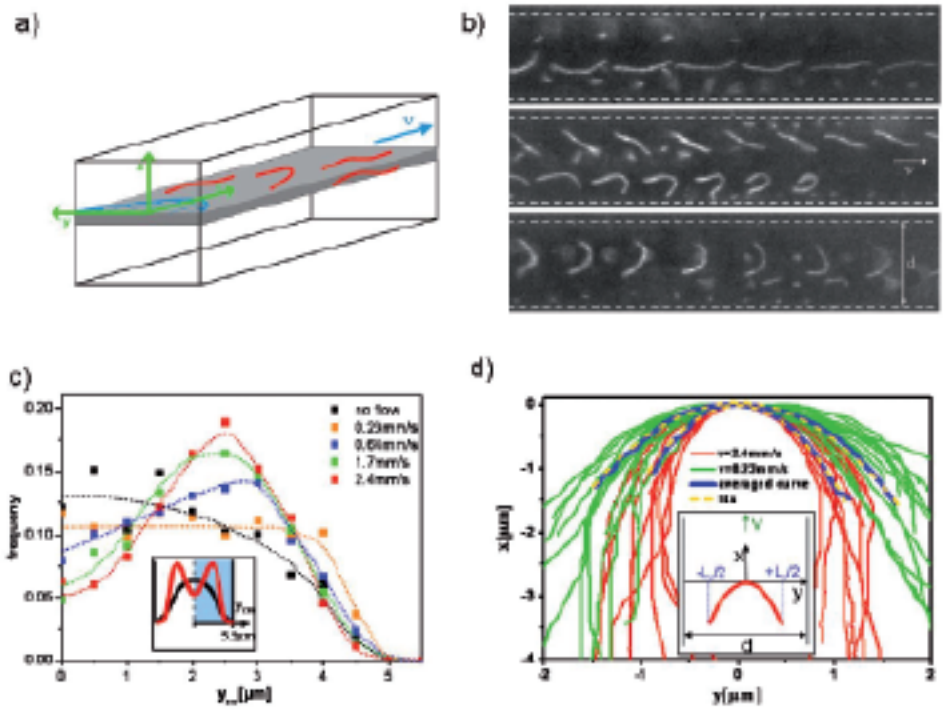

Figure 3: Semiflexible actin filaments in microchannels (10µm x 10µm) are shown schematically in (a). Typical images of actin in flow (b) show different profiles. The center-of-mass probability distribution of filaments (c) and the x-y profiles of bent filaments in the channel center (d) show behaviors that we aim to understand quantitatively.

[1] T. Pfohl, F. Mugele, R. Seemann, S. Herminghaus, *ChemPhysChem* **4** (2003) 1291.
[2] A. Otten, S. Köster, B. Struth, A. Snigirev, T. Pfohl, *Journal Of Synchrotron Radiation* **12** (2005) 745.
[3] M. Engstler, T. Pfohl, S. Herminghaus, M. Boshart, G. Wiegertjes, N. Heddergott, P Overath, *Cell* **131** (2007) 505.
[4] S. Köster, D. Steinhauser, T. Pfohl, *Journal of Physics: Condensed Matter* **17** (2005) S4091.
[5] S. Köster, H. Stark, T. Pfohl, J. Kierfeld, *Biophysical Reviews and Letters* **2** (2007) 155.
[6] S. Köster, J. Kierfeld, T. Pfohl, submitted
[7] D. Steinhauser, S. Köster, H. Stark, T. Pfohl, submitted.

Surface Ordering in Complex Fluids

C. Bahr, R. Seemann, S. Herminghaus
Y. Iwashita, E. Kadivar
H. Stark (TU Berlin)

Understanding the behaviour of soft matter at interfaces is essential for numerous topics in fields like nanotechnology, biophysics, colloidal systems, etc. We study heterogeneous fluid systems, in particular ordering phenomena at liquid/liquid or liquid/gas interfaces. The main focus is on liquid-crystal/water interfaces, but liquid-crystal/air, alkane/water, and alkane/air systems are also considered. Besides tackling fundamental questions in areas such as wetting or surface phase transitions, we aim at the development of new application-oriented systems, e.g. a dynamic microfluidics-based lens for x-rays.

In continuation of our first experiments [1], we have conducted a comprehensive experimental and theoretical study of the interface between aqueous surfactant solutions and liquid crystals in the vicinity of the nematic- isotropic transition. In the temperature range above the nematic-isotropic transition temperature of the bulk liquid crystal, T_{NI}, different ordering behaviours at the interface are observed which are crucially influenced by the amount of surfactant adsorbed at the interface. For high surfactant concentrations, a pronounced surface-enhanced order is observed: a nematic surface phase is present several degrees above T_{NI} the thickness of which diverges as T_{NI} is approached from above (cf. Fig.1a). With decreasing surfactant content, the behaviour changes to surface-decreased order: then, a less ordered, nearly isotropic surface phase exists below T_{NI}, and the thickness of this less-ordered surface phase grows as T_{NI} is approached from below (cf. Fig.1b).

The crossover in the interface-induced ordering behaviour is interpreted within the framework of a Landau-de Gennes model in which the influence of the interface is described by two quantities, anchoring strength γ and preferred nematic surface order parameter S_0 [2]. The model yields order parameter profiles which, after being translated to refractive index profiles, completely account for all experimental data obtained by ellipsometry. Figs. 1c and 1d show theoretical wetting diagrams in the γ-S_0 plane together with the experimental γ-S_0 data pairs determined for five systems with different surfactant concentrations. As to be expected, the preferred surface order parameter S_0 decreases with decreasing surfactant concentrations to a value close to zero in the system with the lowest surfactant content. The second surface parameter, the anchoring strength γ, also decreases first with decreasing surfactant concentration but surprisingly increases again in the system with the lowest surfactant content. This is probably due to interactions stemming from the bare water interface: whereas at a surfactant-laden liquid-crystal/water interface the anchoring of the liquid-crystal is perpendicular, a bare water interface imposes a strong random planar anchoring upon the liquid crystal.

We have also studied liquid-crystal/water interfaces in the vicinity of smectic-A-isotropic transitions [3]. Again, we observe at high surfactant concentrations a pronounced surface-enhanced order. In contrast to the nematic-isotropic case, the ordered surface phase grows stepwise in a layer-by-layer fashion as the bulk transition temperature T_{AI} is approached from above (cf.Fig.2a). At higher surfactant concentrations, each step in the ellipsometric data corresponds to the formation of a single smectic layer at the interface; the ordered surface phase thus consists of an integral number of smectic layers (cf. Fig.2b). With decreasing surfactant concentration, the temperatures of the layering transitions

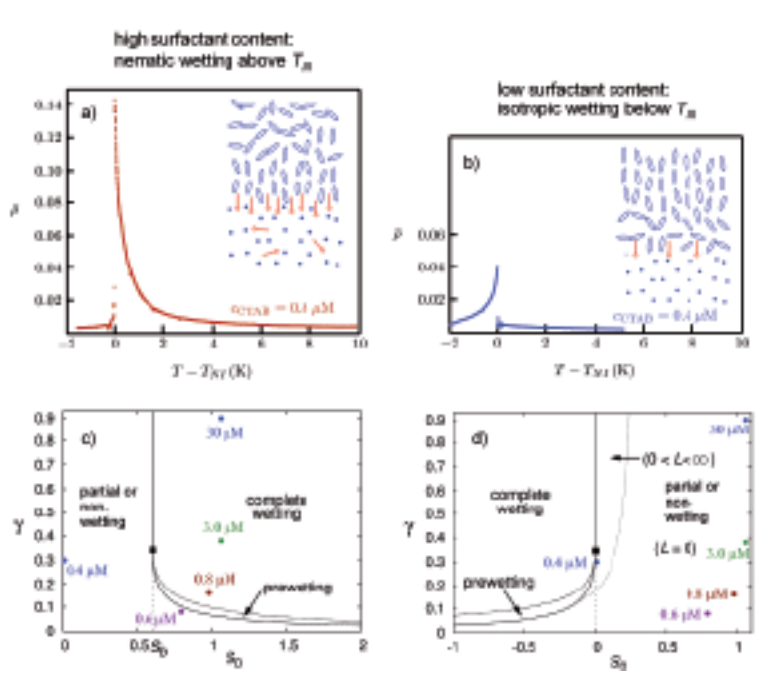

Figure 1: a) and **b)** Temperature dependence of the ellipticity coefficient ρ at the interface between the liquid crystal 8CB and aqueous surfactant solutions of the surfactant CTAB; T_{NI} designates the nematic-isotropic bulk transition temperature, the CTAB concentration in the aqueous volume phase amounts to 0.8 μM (a) and 0.4 μM (b). The magnitude of ρ is linearly related to the thickness of an interface phase that differs in its optical properties from the two semi-infinite volume phases; the data in a) reflect the growth of a nematic surface phase above T_{NI} whereas the data in b) indicate the growth of a less-ordered, nearly isotropic surface phase below T_{NI}. Included are also schematic drawings of the interface structure for high surfactant content and $T>T_{NI}$ (a) and low surfactant content and $T<T_{NI}$ (b); liquid-crystal molecules are drawn as blue ellipses, surfactant molecules are symbolized in red and the aqueous phase is symbolized by blue dots. **c)** and **d)** Theoretical diagrams of the wetting behaviour as function of anchoring strength γ and preferred surface order parameter S_0. The diagrams describe the nematic wetting as T_{NI} is approached from above (c) and the isotropic wetting as T_{NI} is approached from below (d). The colored dots indicate the γ-S_0 data pairs that could fit the experimental behaviour of five systems with different surfactant concentrations between 0.4 μM and 30 μM.

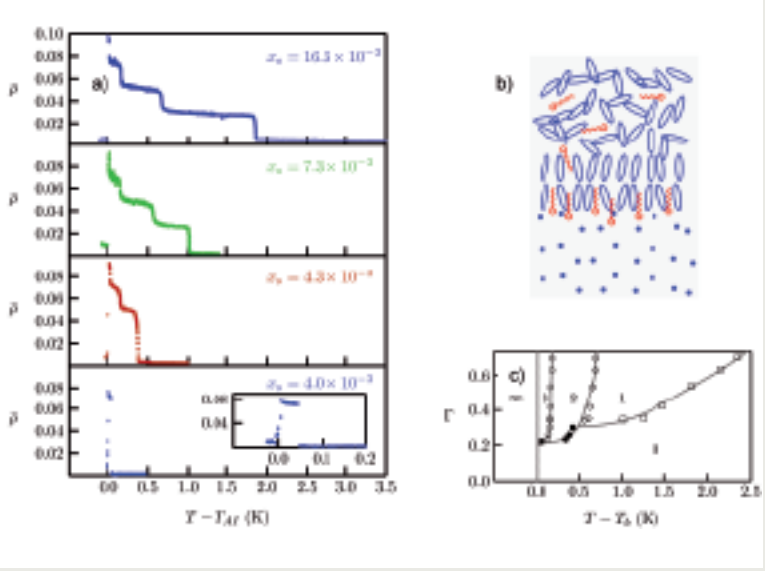

Figure 2: a) Temperature dependence of the ellipticity coefficient ρ at the interface between the liquid crystal 12CB and water for four different concentrations of the surfactant monoolein in the liquid-crystal phase (given by the mole fraction values x_s in the figure); T_{AI} designates the smectic-A-isotropic bulk transition temperature. The stepwise increase of ρ reflects the layer-by-layer growth of the smectic surface phase as T_{AI} is approached from above. **b)** Schematic drawing of the interface structure at $T>T_{AI}$ with a two-layer smectic surface phase; liquid-crystal molecules are drawn as blue ellipses, surfactant molecules are symbolized in red and the aqueous phase is symbolized by blue dots. **c)** Surface phase diagram as function of surfactant coverage Γ and temperature difference to the bulk transition temperature T_b (=T_{AI}). The numbers 0 to 3 indicate how many smectic layers are present in the ordered surface phase.

shift downward to T_{AI} and single-layer transitions merge to multiple-layer transitions. The resulting surface phase diagram (Fig. 2c), in which single-layer transition lines merge at triple points to multiple-layer transition lines, is the first experimental confirmation of long lasting theoretical predicitions [4] about smectic surface transitions.

Because of the enhanced surface order in the isotropic temperature range, smectic liquid crystals are promising systems for applications in discrete microfluidics. In discrete microfluidic systems, droplets of a dispersed phase (e.g. water or aqueous solutions) are separated by thin membranes of a continuous phase (e.g. oil or organic liquids) and are

transported through microchannels. Using isotropic liquid crystals in the temperature range of smectic surface ordering as continuous phase should enable the control of structure and stability of the organic membranes that separate the aqueous droplets in discrete microfluidic systems. Fig. 3a shows a microchannel with water droplets dispersed in the isotropic, surfactant containing phase of a smectic liquid crystal a few degrees above the bulk transition to the smectic phase. Preliminary results indicate changes of the behaviour of this system at the upper temperature limit of surface ordering and at the transition temperature to the smetic bulk phase. Smectic surface order is also observed at bare isotropic liquid-crystal/air interfaces [5]. Fig. 3b shows air bubbles dispersed in the isotropic phase of a smectic liquid crystal; the highly monodisperse bubbles were generated in a microchannel [6] and are stabilized by smectic surface order without the use of a surfactant. A row of such bubbles in a microchannel could be the starting point for the development of a microfluidics-based dynamic lense for x-rays.

A similar kind of suface ordering, surface freezing, is observed at bare alkane/air and at surfactant-laden alkane/water interfaces [7]. We will extend the present studies to these systems in order to explore their suitability for the above described applications.

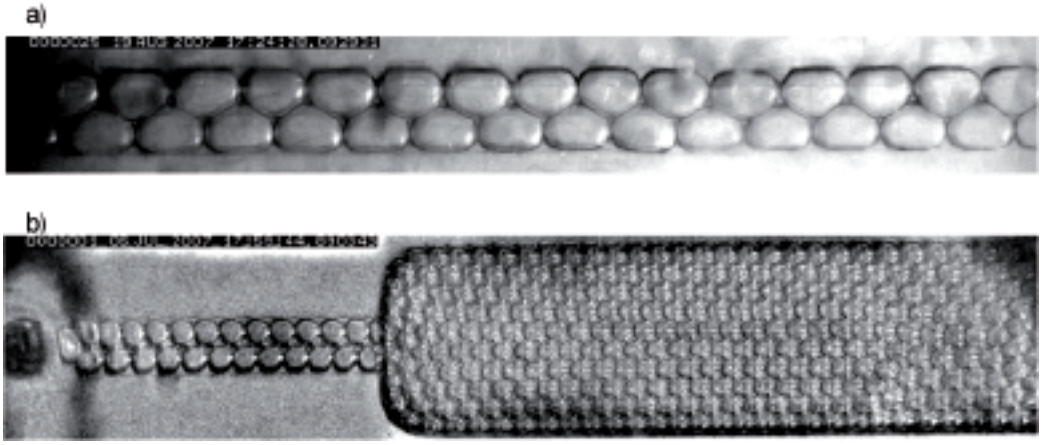

Figure 3: a) A microchannel with water droplets separated by thin lamellae of the liquid crystal 12CB containing a small amount of the surfactant monoolein. The temperature is a few degrees above the smectic-A-isotropic transition of 12CB, i.e., the volume phase of 12CB is isotropic but at the interface to the water droplets a small number of smectic layers exist. The stability of the emulsion changes at higher temperatures where the surface-enhanced order disappears. **b)** Generation of monodisperse air bubbles in the isotropic phase of the liquid crystal 12CB. At bare liquid-crystal/air interfaces, a similar surface order is observed as at surfactant-laden liquid-crystal/water interfaces; thus, a foam can be generated without using a surfactant. Present studies explore the suitability of the system shown above for a dynamic, microfluidics-based lens for x-rays.

[1] Ch. Bahr, *Phys. Rev. E* **73**, 030702(R) (2006).
[2] E. Kadivar, Ch. Bahr, and H. Stark, *Phys. Rev. E* **75**, 061711 (2007).
[3] Ch. Bahr, *Phys. Rev. Lett.* **99**, 057801 (2007).
[4] Z. Pawlowska et al., *Phys. Rev. A* **38**, 5342 (1988); A.M. Somoza, L. Mederos, and D.E. Sullivan, *Phys. Rev. E* **52**, 5017 (1995).
[5] B.M. Ocko et al., *Phys. Rev. Lett.* **57**, 94 (1986); R. Lucht, Ch. Bahr, and G. Heppke, *J. Phys. Chem. B* **102**, 6861 (1998).
[6] C. Priest, S. Herminghaus, and R. Seemann, *Appl. Phys. Lett.* **88**, 024106 (2006).
[7] B.M. Ocko et al., *Phys. Rev. E* **55**, 3164 (1997); Q. Lei and C.D. Bain, *Phys. Rev. Lett.* **92**, 176103 (2004).

Wetting of Topographic Substrates

R. Seemann, M. Brinkmann, S. Herminghaus
Krishnacharya Khare, Konstantina Kostourou,
B. M. Law (Kansas, USA), J.-C. Baret (Strasbourg, France),
M. M. Decré (Eindhoven, The Netherlands), B. Wagner (Berlin),
K. Jacobs (Saarbrücken), A. Münch (Nottingham, UK),
A. Phela, T. M. Jovin (Göttingen)

Appropriate surface topographies can be used to confine liquid to certain regions of a substrate and, in combination with an active control of wettability and geometry, to transport it along prefabricated connection lines. In this approach, one takes advantage of the fact that the affinity of a wetting liquid to steps [1] and corners differs from planar surfaces. In order to explore the stability boundaries of certain liquid morphologies in terms of surface wettability we started to consider a spectrum of groove geometries including triangular, rectangular and trapezoidal cross sections. The static wetting morphologies consist of short chain polystyrene deposited via the gas phase [2,3,4,5,6].

Depending on control parameters such as the contact angle, the liquid volume, and the geometry of the grooves, a large variety of liquid morphologies can be found [7,8,9,10,11].

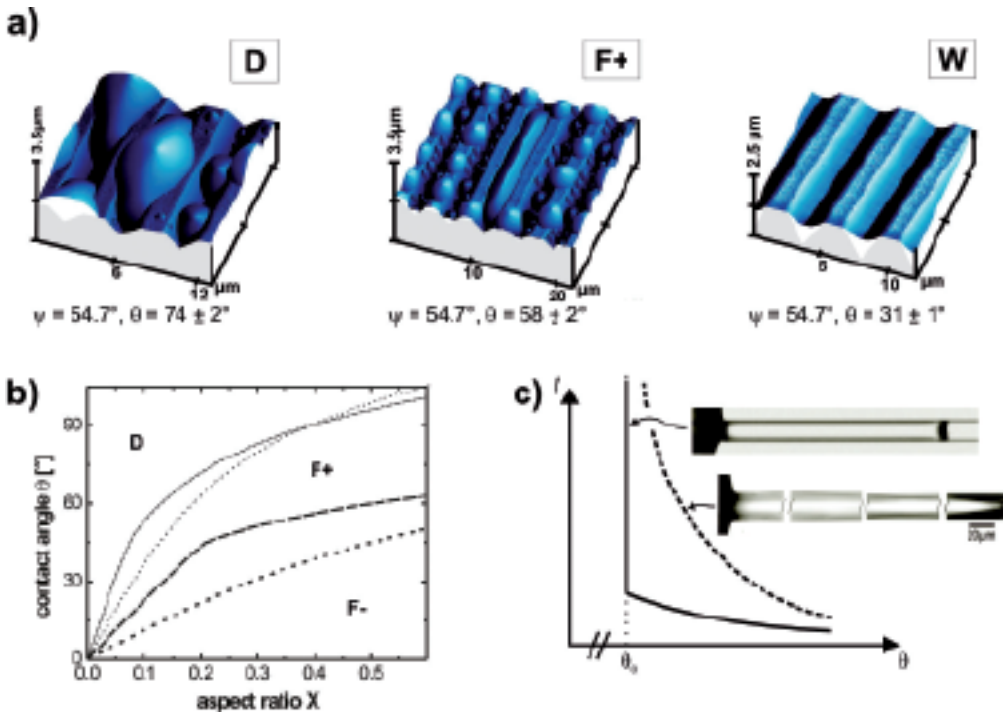

Figure 1: a) Scanning force micrographs (AFM) of polystyrene droplets wetting triangular grooves. Droplet morphologies (D), liquid filaments, (F+), with positive Laplace pressure, $P_L > 0$, and liquid wedges, (W), with $P_L < 0$. b) Direct comparison of the morphology diagrams for triangular (dotted line) and rectangular grooves (dashed line). The groove geometries are described by a function $y = h\,|2x/w|^{\nu}$. The rectangular groove then corresponds to the limit $\nu \to \infty$, while the triangular groove is described by $\nu = 1$ and $X = {}^1/_2 \tan\psi$. The fine lines indicate the transition from droplets (D) to filaments with positive Laplace pressure (F+), while the bold lines indicate the transition from positive to negative Laplace pressure filaments (F-). c) Schematic representation of the total length of the liquid filament, *l*, as a function of the contact angle, as found for rectangular (solid line) and triangular (dashed line) grooves. The optical micrographs show liquid filaments in a rectangular and a triangular groove, respectively.

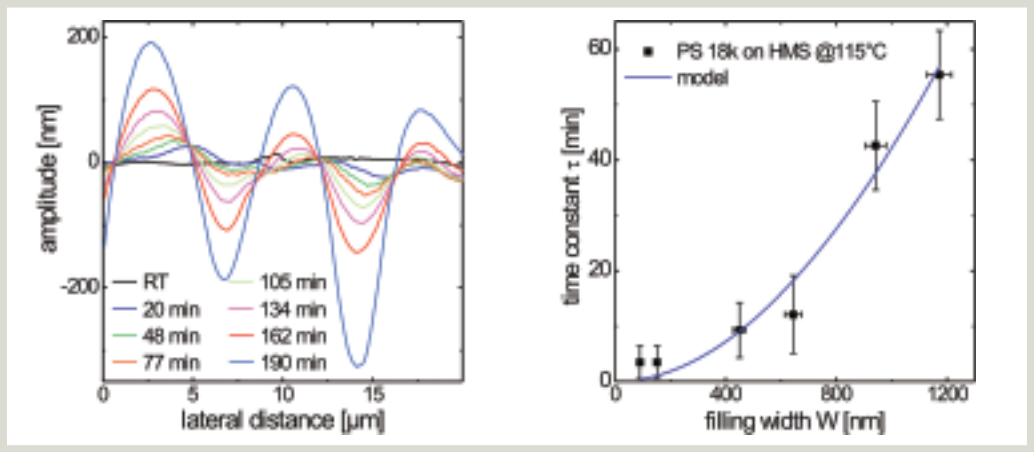

Figure 2
left: Time series of AFM scan lines showing the growth of the fastest growing instability mode. right: Time constant, τ, for different filament widths. The solid line displays a fit to the data assuming partial slip properties. The shown fit gives a slip length of 480 ± 50 nm.

All experimentally found morphologies in grooves with triangular [10,11] and rectangular cross section [8,9,11] are in excellent agreement with theoretical predictions. The basic liquid morphologies found in triangular and in rectangular grooves are very similar but differ in some characteristic details with a large impact to possible applications.

By applying an AC-voltage between a conducting aqueous solution and a substrate we can modify the wettability (electrowetting), and thus can switch between different liquid morphologies [11,12]. The transition between a drop-like morphology and an extended liquid filament can be used to transport liquid along prefabricated grooves. For rectangular grooves we find a filling threshold and liquid filaments with constant cross section whose contact line is pinned to the upper edges of the grooves. The contact angle at the filling threshold is in quantitative agreement with the stability boundaries of the static wetting morphologies [9,11,12]. The length of the resulting filaments is finite and can be described quantitatively by a voltage drop along the filament assuming a transmission line model [9,11,12]. In case of triangular grooves, however, we find a continuous filling transition with locally varying cross section along the filament. A fine liquid tip advances into the grooves, whose tip angle decreases as the filling angle is approached [9,11].

As a direct consequence of the filling behavior, groove filling in rectangular grooves is fully reversible [9,11,12,13]. The observed dynamics is in agreement with calculated mobility parameter for the respective geometry [13]. Whereas the drainage is simply given by the Washburn behavior (length of the filament $l \sim t^{0.5}$), one has to account for the decreasing voltage at the tip of the filaments as its length increases [12]. In triangular grooves, a continuously advancing filament has free contact lines located at the sidewalls of the grooves. Whenever the contact angle is larger than the wedge angle (e.g. by reducing the applied voltage), the filaments will have a positive mean curvature. These filaments are unstable and decay into chains of isolated droplets with a preferred distance, driven by the locally varying Laplace pressure with the filament width. The preferred wavelength and the time scale of the decay can be described by a linear stability analysis[10].

Imaging this dewetting process by AFM *in situ*, allows to record the dynamics of the instability[10] and to determine its characteristic time constant, τ. Since the mobility does not only depend on the geometry but also depends on the hydrodynamic boundary conditions at the substrate, we can determine the slip length in our system when analyzing τ as a function of filling width, *W*.

Besides changing the apparent contact angle

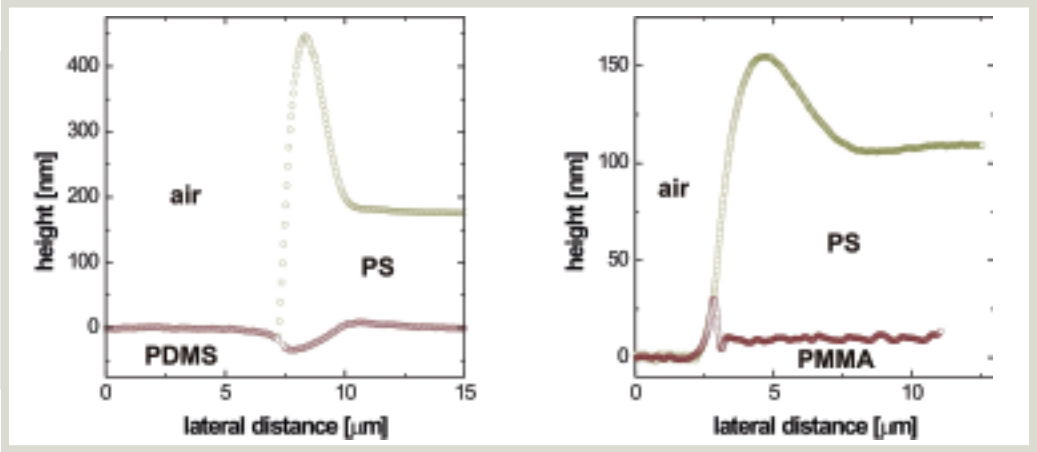

Figure 3
Rim profiles of polystyrene dewetting from a rubber elastic PDMS substrate (left) and a liquid PMMA substrate (right).

of the liquid, we explore the possibility to switch between different wetting morphologies by varying the geometry of the grooves using rubber elastic substrates. The filling and de-filling dynamics is slowed down by about 20 times compared to solid substrates [14]. To get deeper insight into this phenomenon, the dewetting dynamics of thin films on plane visco-elastic substrates is studied. We find characteristic deformations for various visco-elastic substrates. For decreasing elastic modulus the depth of the deformation increases and the dewetting velocity decreases indicating an energy dissipation process that is inverse proportional to the bulk elastic modulus.

[1] M. Brinkmann and R. Blossey, *Eur. Phys. J. E* **14** (2004) 79.
[2] R. Seemann, et al., *J. Phys.: Condens. Matter* **17** (2005) S267.
[3] R. Seemann et al., *J. Polymer Sci. B* **44** (2006) 2968.
[4] S. Peter et al., *J. Phys.: Condens.* Matter **19** (2007) 205119.
[5] R. Fetzer et al., *Phys. Rev. Lett* **99** (2007) 114503.
[6] R. Seemann, S. Herminghaus, K. Jacobs, in CISM Courses and Lectures No. 490, Spinger Wien New York, ISBN 978-3-211-69807-5 (2007).
[7] R. Seemann, E. J. Kramer, and F. F. Lange, *New J. Phys.* **6** (2004) 111.
[8] R. Seemann, et al., *Proc. Natl. Acad. Sci.* **102** (2005) 1848.
[9] M. Brinkmann, K. Khare, and R. Seemann, in Microfluidic Technologies for Miniaturized Analysis Systems, Springer Wien New York, ISBN 978-0-387-28597-9 (2007).
[10] K. Khare et al., *Langmuir* **23** (2007) 12138.
[11] K. Khare et al., *Langmuir* **23** (2007) 12997.
[12] J.-C. Baret, et al. *Langmuir* **21** (2005) 12218.
[13] J.-C. Baret, et al. *Langmuir* **23** (2007) 5200.
[14] A. Phela, R. Seemann, and T. M. Jovin, *J. Am. Chem. Soc.* **129** (2007) 468.

Spectroscopy at the Aqueous Surface

M. Faubel
B. Winter (MBI, Berlin), E.F. Aziz (BESSY, Berlin)
J. Hemminger (Irvine, USA), P. Jungwirth (Praha, CZ)

Photoelectron spectroscopy at the liquid surface allows investigations of molecular structures and of the molecular forces in a liquid at the atomic level [1]. With recent improvements of this technique we succeeded in observing the photoelectron signature of solvated protons in the micron-size water jet-target apparatus which was developed in Göttingen and is jointly operated with the Max-Born-Institut in Berlin on a soft X-ray beamline of the BESSY facility [2]. In a subsequent experiment we show that the pH-value controlled protonation/deprotanation of a solvated amino acid is directly visible in photoelectron spectra and compares reasonably well with state of the art theory of electronic quantum structure of organic molecular ions in liquids [3]. The PE-measurement of chemical shifts may open up the way for a complementary method to NMR chemical shift studies by laser pump- x-ray probe liquid experiments with femtosecond time resolution.

The liquid target photoelectron experiment uses a water jet with 12 µm diameter in a working vacuum of 10^{-5} mbar. According to Knudsen conditions for the 8.1 mbar vapor pressure of a water surface cooled to 4°C, the vapor blanket of the liquid microjet is transparent for photoelectrons and for Extreme-UV and soft X-rays. Tunable Synchrotron radiation is focussed to a spot size of 12 x 23 µm on the liquid jet with typical intensity of 10^{12} photons /s and with energy resolution better than 0.3 eV at 500 eV. Photoelectrons escape unperturbed into the vacuum from a liquid surface layer with 0.3 nm to 20 nm thickness (depending on the photoelectron kinetic energy) and are recorded with an electron energy analyser as photoelectron spectra, shown in Fig.1 and in Fig.2.

One most important chemical property of liquid water is its ability to dissociate spontaneously into protons and OH^--ions with a product concentration of 10^{-7} for neat water with pH 7. In order to making the solvated proton or H_3O^+ visible in a photoelectron spectrum we compare a 3m solution of HCl and a 4m solution of nitric acid HNO_3 [2] with the previously analysed valence shell spectrum of pure liquid water [1]. Both acid spectra, in Fig.1, show an additional weak peak feature at a binding energy of 20 eV, which is not present in reference spectra taken for NaCl solution and for NaOH solution. Clearly identifiable, also, are the Cl^- and OH^- peaks, for the respective solvated anions. With numerical methods, tested earlier on simpler alkali-halide salt solutions, the different solutions were modelled in Molecular Dynamics calculations and individual valence shell (adiabatic) electron binding energy distributions were computed with quantum chemical methods by sampling over 20 selected MD-configurations. The theoretical results, shown in Fig.1, for all ions agree qualitatively with the experiment. For the solvated proton a (H_3O^+)-hydrate structure is assumed and the calculated binding energies are represented as vertical bars, one of which is coinciding with the observed 20 eV structure. A second theoretical peak with the lower binding energy of 9.5 eV is obscured in a region with strong experimental background of the neutral water valence structure. The $H_5O_2^+$ model ion solvation structure was also calculated in this theory and yields binding energies which are shifted by 2 eV with respect to the observed 20 eV peak. Thus, the frequently discussed Zundel vs. Eigen protonation structure is in favour of the Eigen (H_3O^+) hydrated proton structure at

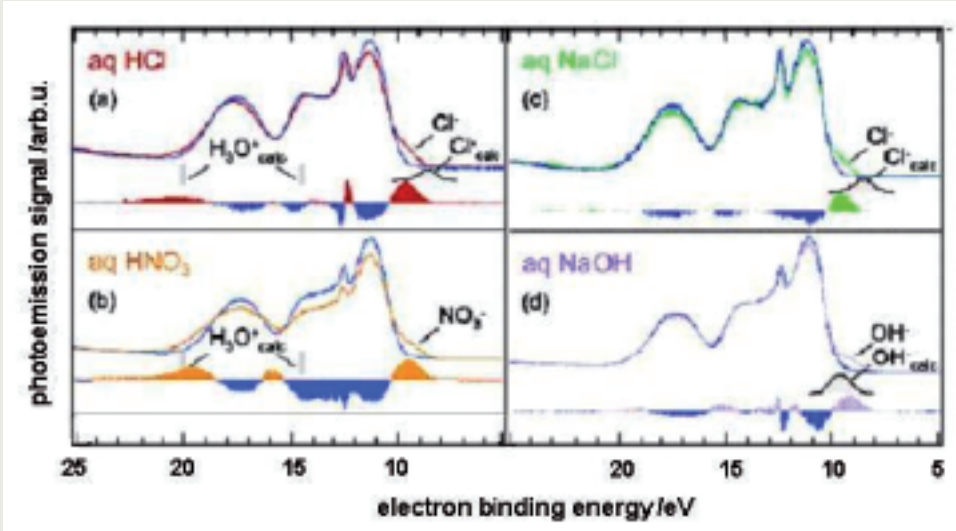

Figure 1
Photoemission spectra of aqueous solutions of 3 m HCl, 4 m HNO_3, 3 m NaCl, and 2 m NaOH. For comparison, the pure water PE spectra and the differential spectra are also shown. Gray shaded features indicate the calculated ionization energies of H_3O^+, and calculated PE bands of Cl^- and of OH^-.

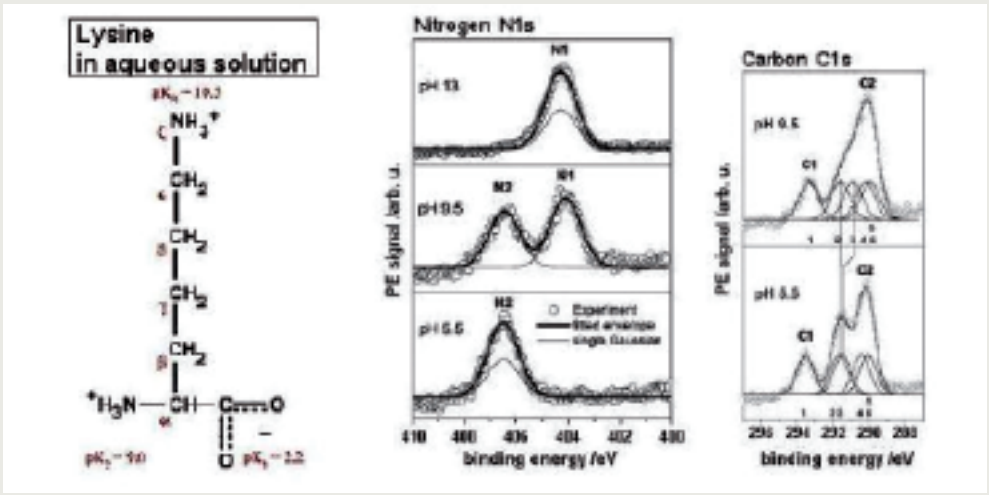

Figure 2
Lysine structure and its Nitrogen 1s and Carbon 1s photoemission spectra for different pH values in 0.5 m aqueous solution. At pH 13 both amino groups are neutral and have identical N1s core level BE of 404.3 eV (peak "N1"). At pH 5.5 both amino sites are protonated, with a single N1s peak at the shifted BE =406.5 eV. For the intermediate pH=9.5 one amino group remains neutral, and two peaks are observed, The C1s PE spectra show one constant peak "C1", associated with the COO^- group. Five separate Gaussian peaks can be fitted into the more complicated C1s photoelectron spectrum. The two carbon atoms next to an amino group show significant BE shifts of 0.4 eV upon protonation of their adjacent amino group.

the high proton concentrations of the present experiment.

The protonation of amino groups in biological molecules can be monitored also by photoelectron spectroscopy in aqueous solutions. Changes of the acidity in a protein solution can change the amino group charge and can induce changes of the molecular geometry and reactivity. This we investigate in a first model study of the pH dependence of the core level electron spectra of the amino acid Lysine, shown in Fig. 2. Changing the pH of an (0.5m) aqueous solution of Lysine from basic to acidic results in nitrogen 1s and carbon 1s chemical shifts to higher binding energies. These shifts are associated with the sequential protonation of the two amino groups, which affects both charge state and hydrogen bonding to the surrounding water molecules. The N1s chemical shift is 2.2 eV, and for carbon atoms directly neighboring a nitrogen the shift for C1s is ~0.4 eV [3]. The experimental binding energies agree reasonably with calculated energies of Lysine(aq) for different pH values which were obtained with a modified cavity Density Functional Theory, using commercial software (Gaussian 03).

[1] B. Winter, M. Faubel, *Chemical Reviews* **106** (2006) 1176.
[2] B. Winter et al., *Journal of the American Chemical Society* **128** (2006) 3864.
[3] D. Nolting et al., *J. Am. Chem. Soc.* 129 (2007) 14068.

Transition to Turbulence in Shear Flows

B.Hof, A. deLozar, J. Vollmer

Despite the relevance of turbulence to a multitude of processes throughout nature our conceptual understanding of the turbulent state is very limited. While many studies of turbulence deal with the dynamics and scaling behaviour at very large Reynolds numbers, our approach is different: we are aiming to understand the dynamics in parameter regimes where turbulence first occurs. We anticipate that here the dynamics are sufficiently low dimensional to to enable us to gain insights into the make up of the turbulent state. The equations governing the motion of fluids have been known for a long time. In the vast majority of cases however we are unable to determine analytical solutions describing the often extremely complex motion observed in praxis. The difficulty in finding an adequate expression describing the fluid motion stems from the nonlinear nature of the governing equations.

In recent years progress in tackling this problem has been made by applying ideas from nonlinear systems theory [1,2]. Here it has been suggested that turbulence evolves around unstable solutions of the governing equations which arise already at fairly low Reynolds numbers. Due to their instability, individual solutions can not persist in practical flows. However, given a large enough number of such unstable states a complex entity (i.e., a turbulent saddle or attractor) can form through further bifurcations and entanglement, which gives rise to chaotic motion persisting over macroscopic time scales.

Indeed such unstable solutions have been found numerically for a variety of flows including that of a fluid down a straight pipe[3,4]. Our experiments [5] (Fig.1 top row) have given a first indication that these unstable states can be observed transiently in a turbulent flow and therefore that they are indeed relevant to fluid turbulence.

Further experimental studies concerned with the relevance of such states are carried out in two different geometries, pipe flow and plane Couette flow (a fluid layer sheared between two moving walls). In both studies state of the art high speed velocity measurements (Tomographic Particle Image Velocimetry) are carried out to identify unstable states. By measuring typical observation times, rate

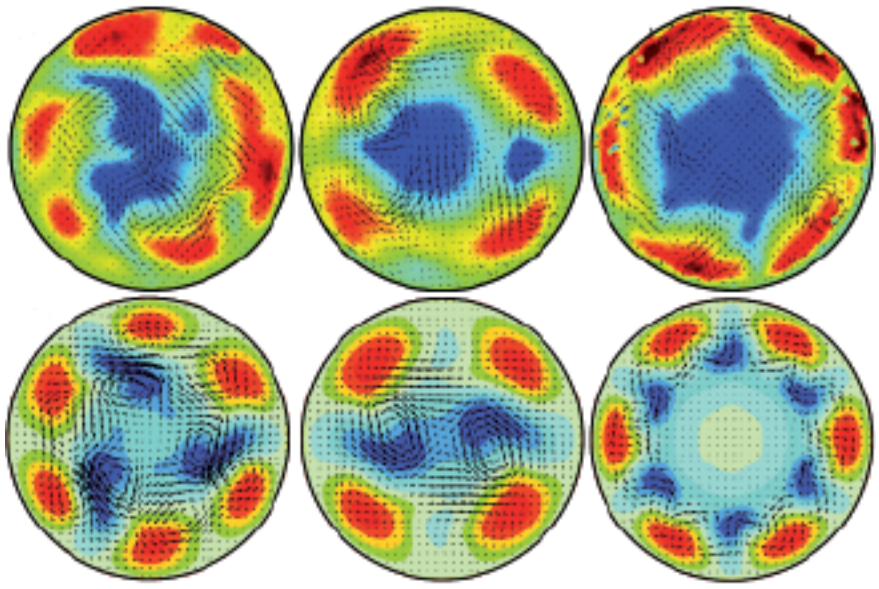

Figure 1
Cross sectional view of velocity fields in a pipe. High/low streamwise velocities are shown in red/blue(the laminar parabolic velocity field has been subtracted. top row: Experimental observations of travelling wave transients in a turbulent flow. Bottom row: Numerical calculations of exact unstable travelling wave solutions.

of recurrence and sequence of these states we try to gain further insights into their relevance. Using volume resolved velocity fields we hope to ultimately be able to reconstruct the dynamical and topological connections between unstable states transiently appearing in the turbulent flow. New methods and better statistics may allow considerable progress beyond the first steps taken into this direction [6], which were based on the analysis of numerical data.

A related project evolves around the question if turbulence in pipe and Couette flow is a sustained state or if it only has a finite lifetime [7]. While the conventional view is that turbulence is a transient at low Reynolds numbers but becomes sustained at a critical point, our lifetime measurements question this standpoint. Generally the lifetime of the turbulent transients increases very rapidly as the Reynolds number increases. Furthermore (similar to nuclear decay) the lifetime distributions are exponential which is the typical scaling known for escape rates from chaotic saddles. The unresolved question is if at some critical point the chaotic saddle turns into an attractor and lifetimes become infinite or if they remain finite. Some of our recent measurements are shown in Fig. 2, where inverse lifetimes are plotted as a function of Reynolds number Re. The exponential scaling suggests that inverse lifetimes only approach zero in the asymptotic limit. In other word, for any finite Reynolds number, turbulence will eventually decay in these systems. These observations have the important consequence, that at least in principle even at very high Reynolds numbers, where for all practical purposes turbulence is sustained, it should be possible to relaminarize the flow with minimal energy input. In any case the exponential lifetime measurements confirm the relevance of the nonlinear dynamics concepts to fluid turbulence.

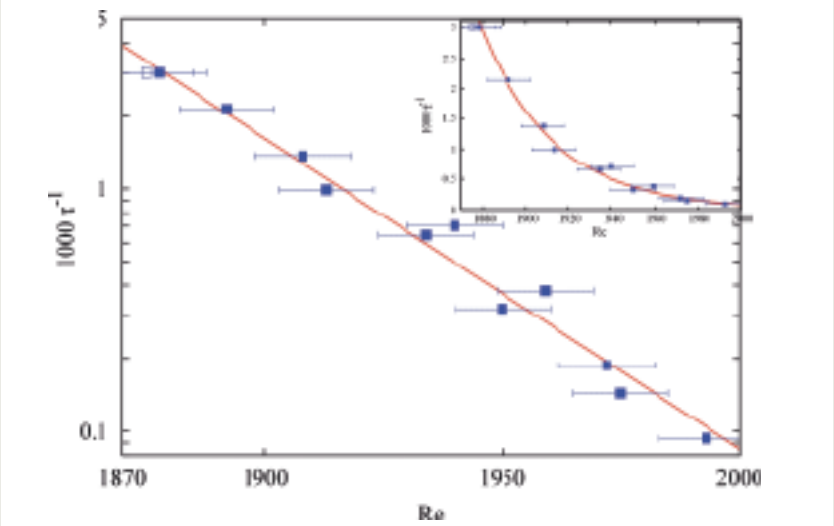

Figure 2
Exponential scaling of inverse lifetimes measured in a pipe experiment.

[1] B. Eckhardt, et al. *Annu. Rev. Fluid Mech.*, **39**, 447-468 (2007).
[2] J. Vollmer, T. Schneider & B. Eckhardt, (submitted, 2007).
[3] H. Faisst & B. Eckhardt, *Phys. Rev. Lett.* **91**, 224502 (2003).
[4] H. Wedin & R. R. Kerswell, *J. Fluid Mech.* **508**, 333–371 (2004).
[5] B.Hof, et al.*Science*, **305**, Issue90, pp 1594-1598, (2004).
[6] T. M. Schneider, B. Eckhardt, & J. Vollmer, Phys. Rev. E **75**, 066313 (2007).
[7] B.Hof, et al. *Nature*, **443**, 05089, pp 59-62. (2006).

Rayleigh-Benard Turbulence

E. Bodenschatz
G. Ahlers (UC Santa Barbara, USA), D. Fünfschilling (ENSIC Nancy, France)

The achievement of ultra-high Rayleigh numbers Ra in the study of turbulent convection is a major goal at the forefront of turbulence research. The reason for this is the need for exploring the ultimate parameter range where the system is no longer controlled by boundary layers adjacent to the top and bottom plates. Understanding this regime, first predicted by Kraichnan, is important because many geo-physical and astro-physical systems involve values of Ra in the 10^{20} range and higher which is not accessible explicitly in the laboratory. Two experiments using helium gas at cryogenic temperatures, one by the Grenoble/Lyon (GL) and the other by the Oregon/Trieste (OT) group, have achieved ultra-high values of Ra, but unfortunately disagree with each other. The GL experiment claims to have found the ultimate regime for $Ra > 10^{11}$; the OG experiment, even though it reached unprecedented values of $Ra \sim 10^{17}$, did not.

The Turbulent Convection Facility (TCF) will utilize the U-Boot of Goettingen. The sample will have a height of 2.2 m and a diameter of 1.1 m. At a mean temperature of 40 deg C, a pressure of 15 bar, and a temperature difference of 40 K Ra will be 7×10^{14} at a Prandtl number of 0.84. The small deviations from the Boussinesq approximation that will prevail are now well understood on the basis of measurements at Santa Barbara at similar temperature differences.

The TCF will be used as well for the study of the large-scale circulation (LSC) in the turbulent fluid. The dependence of its Reynolds number Re on Ra will be studied in a heretofore-unexplored range of Ra. An important qualitative question is whether the LSC will survive in the highly fluctuating environment at very large Ra. Lagrangian particle tracking measurements of the turbulent flow in the sample interior are envisioned for the future. For this purpose all the measurement equipment (three cameras, computer, lamps, etc.) will be inside of the U-Boot.

The TCF will also be used as a facility for a small visitor program. In this respect the guesthouses of the MPIDS will be very important.

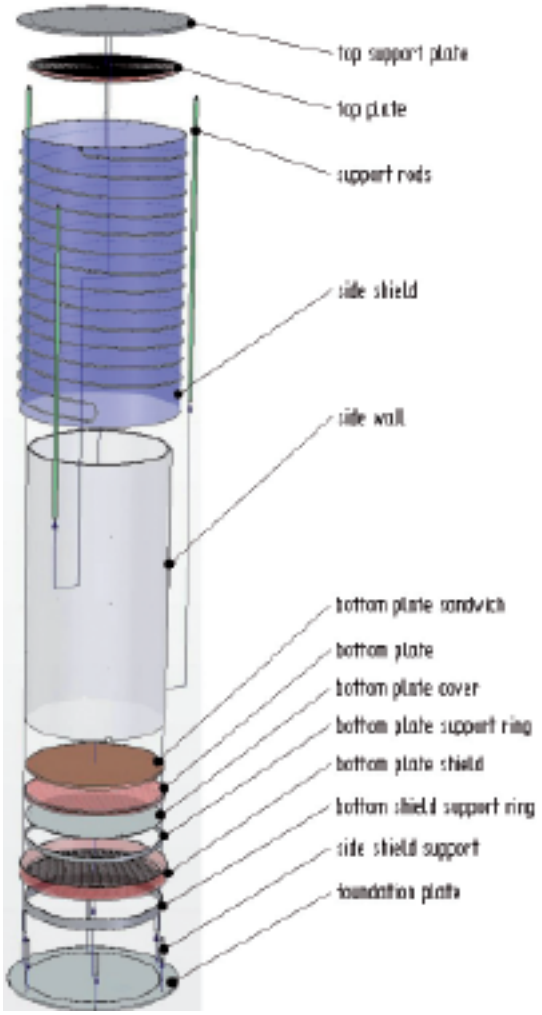

Figure 1
Schematic drawing of the design of the convection cell. It has a diameter of 1.1m and a height of 2.2m. The bottomplate design allows accurate heat transport measurement. The plexiglas cylinder is isolated by a thermal shield.

Particles in Turbulence

G. Bewley, M. Gibert, H. Xu., Eberhard Bodenschatz
K. Chang, R. Zimmermann.
M. Bourgoin (CNRS-Grenoble, France), L. Collins (Cornell, USA), J.-F. Pinton (CNRS-Lyon, France),
F. Schmitt (CNRS-Wimereux, France), R. Shaw (IfT, Germany), H. Siebert (IfT, Germany),
Z. Warhaft (Cornell, USA)

The interaction between particles and fluid flow is prevalent in many turbulent flows. For example, it is thought that turbulence mediates the formation of rain, the dispersion of pollutants, the development of sand storms, and sedimentation in bodies of water. Even zooplanktons in oceans can be regarded as 'active' particles in a turbulent flow. In addition, tracer particles are routinely used in basic scientific research to study the behavior of the fluid itself, using techniques in the laboratory such as particle image velocimetry, particle tracking, and laser Doppler velocimetry, and in studies of environmental flows using balloons and floaters. In these applications, scientists would like to know the conditions under which a particle can be considered to be moving as the fluid it displaces. The prediction of particle behavior in turbulent flows and of the feedback from particles to the turbulence itself is thus not only an important practical problem, but an intriguing scientific challenge.

The complexity of the problem can be appreciated by considering the number of dimensionless parameters that describe a system of particles in turbulence. The Reynolds number, $\mathrm{Re} = UL/\nu$, characterizes the turbulence, where U and L are measures of the velocity fluctuations and the length scales of the flow and ν is the kinematic viscosity of the fluid. The particle Reynolds number Re_p, characterizes the local flow around a single particle. The Stokes number, $\mathrm{St} = \tau_p/\tau_f$, compares the response time of a particle to the time characteristic of the small scales of turbulence, and the Froude number $\mathrm{Fr} = u_p/u_f$, compares the settling velocity of a particle to the velocity characteristic of the small scales of turbulence. Here, $\tau_p = \rho_p d^2/18\mu$, and $u_p = \Delta\rho d^2 g/18\mu$, where μ is the dynamic viscosity of the fluid, g is the acceleration of gravity, and $\Delta\rho$ is the density difference between particle and fluid. In addition, the ratio of the particle diameter to the length characteristic of the small scales of turbulence, d/η, and mass density ratio between particle and fluid, ρ_p/ρ_f, may also independently describe the dynamics of the system, although these can be expressed as combinations of the other dimensionless numbers in special cases. Finally, the volume fraction ϕ (or equivalently, the mass loading) of the particles is an indicator of the importance of particle interactions, and of the global modification of the turbulence by the presence of the particles. In general, other dimensionless numbers should be considered when other forces or interactions exist, such as surface tension and electrostatics.

When the particle Reynolds number, Stokes number, and the Froude number are small ($\mathrm{Re}_p \ll 1$, $\mathrm{St} \ll 1$, and $\mathrm{Fr} \ll 1$), and the volume fraction is low, the seeded particles follow fluid flow faithfully and may be regarded as passive tracer particles. We have investigated the Lagrangian properties of turbulence by

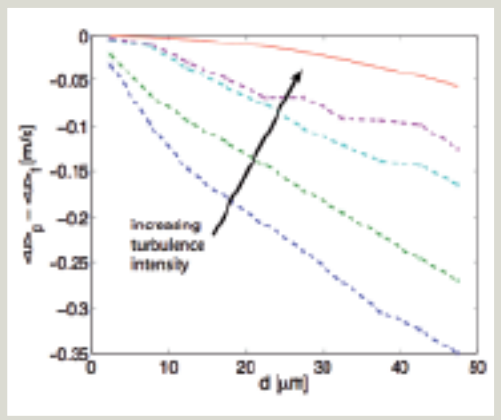

Figure 1
The settling rate of particles. The figure shows the data for the mean velocity of particles binned by the size of the particles for a series of turbulence intensities. Under each of the conditions explored, the particles fall much faster than predicted for a particle in a quiescent fluid, indicated here by a red line. Numerical integration of the equations of motion for a particle falling through a linear vertical gradient in the vertical velocity of the fluid shows a qualitatively similar enhancement of the local settling velocity.

optically tracking the motion of these tracer particles in intense turbulent water flows using a three-dimensional particle tracking system developed in our group [1]. The experimental results show interesting single- and multi-particle Lagrangian statistics of fluid turbulence [2-4] (details on p.111–114 of this report).

For particles with size much smaller than the Kolmogorov scale of the flow, but density much larger than fluid density, the Stokes number can approach one or be even larger. The inertia of these particles cannot be neglected. An important problem related to the interaction between inertial particles and turbulence is cloud dynamics and rain formation [5]. Aimed at studying such an interaction, we have investigated the sedimentation of water droplets with a distribution of diameters between 5 and 50 microns in the turbulence generated by an array of randomly actuated jets of air. Preliminary results from laser Doppler measurements indicate that the settling rate of particles through the fluid is sensitive to non-uniformities of long-time average of the background turbulence, or the mean flow. As shown in Fig.1, we find that over a broad range of sizes, particles fall faster than the calculated settling velocity of the particles through a quiescent fluid. Furthermore, the magnitude of the settling velocity enhancement decreases as the turbulence intensity increases. This result is counterintuitive, since the measured settling velocity of the particles approaches the one predicted for no turbulence only in the limit of intense turbulence. However, the trend can be recovered by considering a simple model that incorporates vertical variation of a background mean fluid flow. Although previous experiments and numerical simulations have shown a comparatively subtle enhancement of the settling velocity of particles by uniform turbulence [6,7], our result may be of more practical importance, since most real flows exhibit a degree of non-uniformity.

Figure 2
A picture of a copepod. Copepods live in a wide range of aqueous environments. Because they are small, their motion is strongly influenced by the movements of the surrounding fluid. However, they are also capable of propelling themselves at speeds of up to several centimeters per second for short times.

While heavy inertial particles are thought to be excluded from regions of high vorticity, being centrifuged out to regions of high strain, lightweight particles tend to be drawn toward the centers of vortices. Because of this, one can consider that the different types of particles sample different parts of a turbulent velocity field, the regions of high strain and the regions of high vorticity. This feature makes it possible to study separately the properties of the flow in these separate regions by observing the different types of particles, and we anticipate exploring this theme in the future by introducing air bubbles into the turbulent water flows in our apparatuses.

As scientists generate flows with larger and larger Reynolds numbers on the laboratory scale, using novel forcing techniques and fluids, the smallest scales of turbulent motion become correspondingly smaller and smaller. It is sometimes impossible to use particles smaller than the Kolmogorov scale as tracers due to technique limitations. In addition, in many systems of interest, such as the planktons in water (see e.g, [8] for a recent work), the particle sizes are larger than the Kolmogorov scale of the flow. It is therefore important to understand the effect of particle size on the behavior of the particle, particularly as the size of the particle becomes larger than the Kolmogorov scale of the flow. Our preliminary results show that unlike small but heavy particles, the large but neutrally buoyant particles are not biased against the high-vorticity regions and hence still sample the entire flow

field. This is consistent with previous work in our group [9] and with a very recent experimental measurement [10]. Further investigation in this direction is another of our missions in the coming years.

Copepods are shrimp-like animals (Fig. 2) that live in many bodies of water, providing a substantial fraction of the protein available to predators in these waters. The existence of copepods is therefore important to the overall health of these ecosystems, and their behavior is sensitive to the conditions of the water in which they live. Through our collaboration with the Coastal and Littoral Ecosystems Wimereux CNRS Laboratory in France, we have just started to investigate the behavior of these animals using our particle tracking system. Fig. 3 shows the measured velocity distribution functions of copepods in still water. The distributions feature flat tails and differ strongly from the velocity distribution in turbulence that is approximately Gaussian. The highly intermittent nature of copepod motion can be seen from the auto-correlation of their acceleration. A typical propelling cycle lasts only about 20ms with peak acceleration up to a few g. We will continue this line of work to discover how their behavior depends on the environmental turbulence.

In summary, by exploiting the measurement techniques that we have developed for studying turbulent flows, we are able to venture into a fertile and perhaps more general field: the study of particles in turbulence. Currently, our focus is to study the turbulent flow itself using small tracer particles. We have just started to investigate the sedimentation of water droplets in air, the motion of particles larger than Kolmogorov scale, and the interesting behavior of copepods. We are looking forward to uncovering further mysteries in the dynamics of such a widely applicable field.

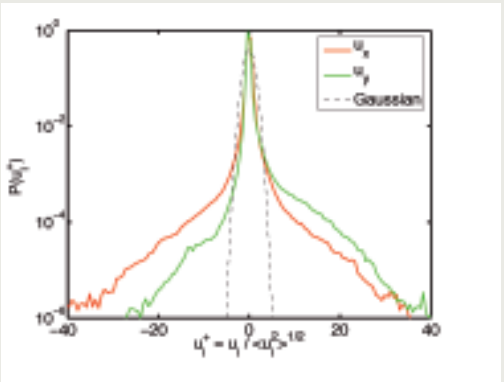

Figure 3:
(a) The probability density function (PDF) of copepod velocity components in still water. The x-coordinate is horizontal and the y-coordinate points upwards in the vertical direction. It was observed during the measurement that copepods were attracted towards the illuminating lights, which were arranged above the water surface. **(b)** Auto-correlations of copepod acceleration components.

[1] N. T. Ouellette, H. Xu, E. Bodenschatz, *Exp. Fluids* **40** (2006) 301.
[2] M. Bourgoin et al, *Science* **311** (2006) 835.
[3] H. Xu et al, *Phys. Rev. Lett.* **99** (2007) 204501
[4] H. Xu, N. T. Ouellette, E. Bodenschatz, *New. J. Phys.* (2007) in press.
[5] R. A. Shaw, *Annu. Rev. Fluid Mech.* **35** (2002) 183.
[6] T. Bosse, L. Kleiser, E. Meiburg, E. *Phys. Fluids* **18** (2006) 027102.
[7] T. S. Yang, S. S. Shy, *J. Fluid Mech.* **526** (2005) 171.
[8] J. Mann et al, *J. Plankton Res.* **28** (2006) 509.
[9] G. Voth et al, *J. Fluid Mech.* **469** (2002) 121.
[10] N. M. Qureshi et al, *Phys. Rev. Lett.* **99** (2007) 184502.

Turbulence in Polymer Solutions

M. Torralba Cuello, H. Xu, E. Bodenschatz
L. Collins (Cornell, USA), J. Schumacher (TU-Ilmenau),
A. Pumir, D. Vincenzi (CNRS-Nice, France)

THE PRESENCE of minute long-chain polymers in a flow may strongly change the flow. At very low Reynolds numbers, it gives rise to the interesting behavior of elastic turbulence [1] and may enhance mixing [2]. At high Reynolds numbers, introducing polymers into wall-bounded flows can lead to the fascinating drag reduction phenomenon, which is a subject of intense current interest(see [3] for a recent review).

Using three-dimensional particle tracking, we are currently studying the effect of polymers on bulk turbulence at high Reynolds numbers, far away from the boundary. The turbulence is generated by a von Kármán swirling water flow between counter-rotating baffled disks. We are planning to carry out experiments also in the Lagrangian Exploration Module (LEM), where the turbulence is expected to be more homogeneous and isotropic. The LEM is currently under construction (see p. 88–90 of this report).

For Newtonian turbulence, most of our understanding comes from the Richardson-Kolmogorov energy cascade hypothesis [4] which states that the energy injected at large length scales is transferred to smaller length scales until it is dissipated at the smallest length scales, where viscosity acts. This classical picture is not valid at the presence of polymeric additives. When stretched by the flow, polymer chains are able to store energy and can release it into the flow when stretching forces become smaller. There will also be losses of kinetic energy during this stretching-recoiling process. Thus, polymer chains introduce new energy transfer and energy dissipation mechanisms into the flow that can be very important even in a very dilute regime. Using three-dimensional particle tracking technique, we studied the modification of turbulence energy cascade by polymer additives. From the Eulerian structure functions, we measured the energy transfer rate ε_T in the inertial range and the viscous energy dissipation rate ε_D in the dissipation range at different polymer concentrations (Fig.1), all in the dilute regime (much lower than the so-called overlap concentration). We observed that while the energy dissipation rate is reduced by any presence of polymers, the energy transfer rate shows a transition at a certain concentration, below which ε_T is not affected [5].

The effect of the polymers is also noticeable in Lagrangian measurements of the auto-correlation of fluid acceleration (Fig.2). At concentrations below the transition concentration, the auto-

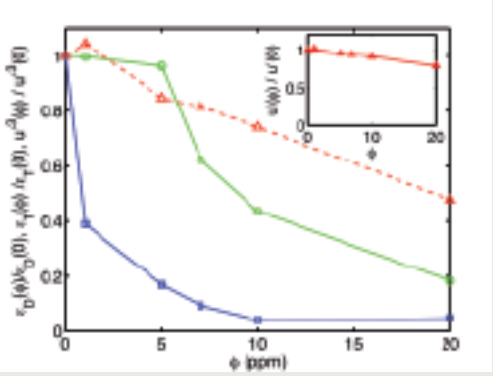

Figure 1: Effect of polymer concentration ϕ on different length scale dynamics: small scales energy dissipation rate ε_D (blue squares) is strongly modified at all polymer concentrations whereas energy transfer rate ε_T (green circles) is almost unaffected for concentrations up to 5 ppm. The large length scale quantity u'^3 (red triangles) related to energy injection rate is the less affected by polymer concentration. Inset: the velocity fluctuations decrease slowly with polymer concentration. All the data were extracted from Eulerian quantities at R_λ=350 and Wi=6.0.

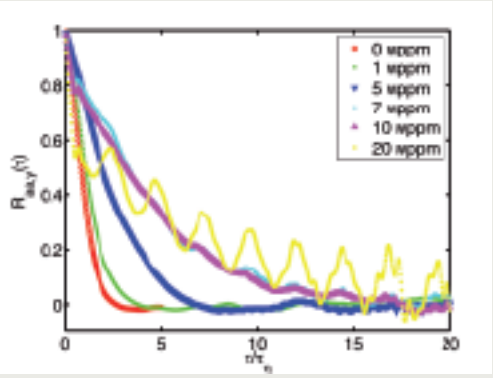

Figure 2: Lagrangian auto-correlation function of fluid acceleration at different concentrations. The curves correspond to measurements in the radial direction for R_λ=350 and Wi=τ_p/τ_η=6.0 (τ_p is polymer relaxation time and τ_η is the Kolmogorov time scale determined from the water experiments). Notice that the oscillations in the auto-correlation function appear only for concentrations for which energy transfer rate is affected by polymer concentration (Fig.1).

correlations are very similar to that in Newtonian flow, except that the time scales are slowed down by polymers. At concentrations above the transition, however, there appear oscillations in the auto-correlations. The frequency of such oscillations is independent of polymer concentration, but the magnitude increases with concentration.

Our previous measurements showed that the turbulence generated from a von Kármán flow is far from being isotropic (see p. 88–90 for further details). At the presence of polymers in the turbulence, the degree of anisotropy increases with polymer concentration [6] (Fig. 3). This increase is due to the coupling between the anisotropy and inhomogeneity of the flow and the anisotropic response of the polymers, as it has been shown that the elongational properties of polymer solutions can be strongly different from the properties of the same solutions in pure shear flows even at very low concentrations [7] when the elongation rates are much faster than the polymer relaxation time. The anisotropy is also detected in the auto-correlation of fluid acceleration. Both radial and axial auto-correlations display oscillations above the transition concentration, but the frequency of the oscillations in the axial direction is roughly two times the frequency of the oscillations in the radial direction.

To determine the importance of the elasticity, we are planning to use different polymers and to change fluid properties by adding other agents. To understand the mechanism of the transition and the asymmetry of the auto-correlation, we also intend to carry out micro scale measurements to characterize the alignment and the elongation of fluorescently dyed polymers in the turbulent flow. The characterization of pure elongational flows of the dilute polymeric solutions used in our experiments may be helpful in the understanding of the anisotropy in the acceleration auto-correlation and will be performed for the polymeric solutions used in the experiments.

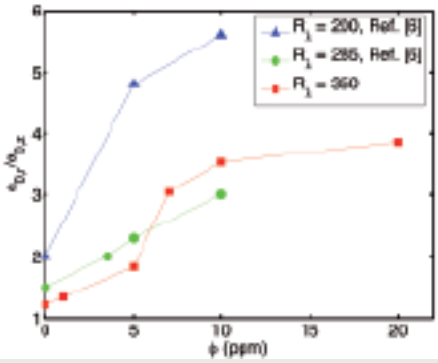

Figure 3: Degree of anisotropy of acceleration variance as a function of polymer concentration at R_λ=200, Wi=1.2 (triangles); R_λ = 285, Wi=3.5 (circles); and R_λ = 350, Wi=6.0 (squares). All experiments are carried out in the same von Kármán swirling water flow. The R_λ = 200 and R_λ = 285 data are from Ref. [6] and are measured with silicon-strip detectors. The R_λ = 350 data are measured with high-speed CMOS cameras.

[1] A. Groisman and V. Steinberg, *Nature* **405** (2000) 53.
[2] A. Groisman and V. Steinberg, *Nature* **410** (2001) 905.
[3] I. Procaccia, V. L'vov, R. Benzi, *Rev. Mod. Phys.* (2007) *accepted*.
[4] A.N. Kolmogorov, *Dokl. Akad. Nauk SSSR*, **30** (1941) 301.
[5] N.T. Ouellette, H. Xu and E. Bodenschatz, submitted to Phys. Rev. Lett. (2007).
[6] A. Crawford, PhD dissertation, Cornell University, (2004).
[7] V. Tirtaatmadja, G.H. McKinlay and J.J. Cooper-White, *Phys of Fluids* **18** (2006) 043101.

Measurement Techniques

M. Gibert, H. Nobach, H. Xu, E. Bodenschatz
R. Zimmermann
J.-F. Pinton (ENS-Lyon, France), N. Mordant (ENS-Paris, France),
C. Tropea, M. Kinzel (TU Darmstadt, Germany)

Experimental investigations of fluid dynamics and the verification of statistical turbulence models require measurement techniques that allow access to the fundamental flow equations. Beside pressure tubes and hot-wire probes we extensively use modern optical, tracer based measurement techniques like Laser Doppler Velocimetry or Particle Image Velocimetry, allowing access to the flow quantities without disturbing the flow field. However, these techniques are restricted to measurement at fixed points in space (Eulerian measurements). Much closer to the driving forces of flow motion are the Lagrangian statistics of material transport. To measure Lagrangian statistics, individual particle tracks must be followed in time and space simultaneously. This requires the development of new measurement techniques, optimized to directly measure the Lagrangian quantities.

Lagrangian Particle Tracking (LPT)

After successfully adapting the silicon strip detectors used in high-energy physics experiments to highspeed Lagrangian particle tracking in fully developed turbulence that provided single-particle measurement with high accuracy [1,2,3], our group developed a three-dimensional Lagrangian particle tracking system using off-the-shelf high-speed digital cameras [4]. The system can simultaneously follow hundreds of seeded particles in turbulent flows with Taylor microscale Reynolds number $R_\lambda \sim 10^3$. The multi-particle statistics in three-dimensional intense turbulence obtained from such a system revealed rich physics that was not accessible in previous experiments or simulations [5,6]. The extremely fast frame rates needed to resolve the smallest time scales in intense turbulence set stringent requirements on the optical recording system. Images of some particles might disappear from observation and reappear again later due to hardware limitations, e.g., the fluctuations of illumination intensity, the existence of light-insensitive circuit on the CMOS sensor array, and thermal and electronic noises. As a result, the measured particle trajectories usually consist of segments separated by the 'lost periods'. A recent development of the LPT technique is to connect those trajectory segments by exploiting the continuity in both position and velocity space [7]. As shown in Fig.1, the connected trajectories provide statistics over much longer time lags, particularly for multi-particle statistics such as relative dispersion and evolution of Lagrangian tetrahedra [8] (see also Fig.2, p.112).

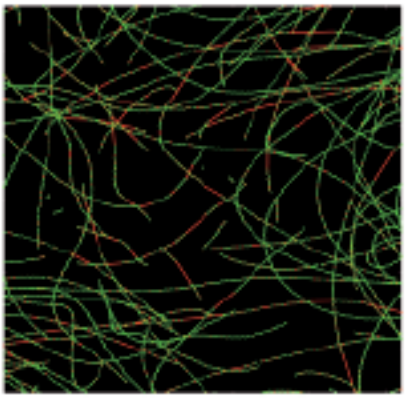

Figure 1: Connected particle trajectories. The trajectory segments from original data are shown in green. The interpolated positions determined from the connecting algorithm are shown in red. The average trajectory length (measured as number of frames observed) increased by a factor of 5.

Vorticity Optical Probe (VOP)

Because of the importance of vorticity dynamics in turbulence energy cascade, it has long being a desire to measure vorticity accurately in intense turbulent flows. Currently, vorticity can be measured using spatially designed multi-hotwires [9], or calculated from PIV [10] or Particle Tracking Velocimetry (PTV) [11] data. In all these indirect measurements, fluid velocities at close vicinities must be resolved and the vortocities are obtained from velocity differences. This requirement, combined with the finite spatial resolution of the techniques, severely limited either the range of Reynolds number applicable, or the access to Lagrangian statistics, or both. The pioneer work by Webb & co-workers [12] demonstrated the feasibility to measure vorticity directly

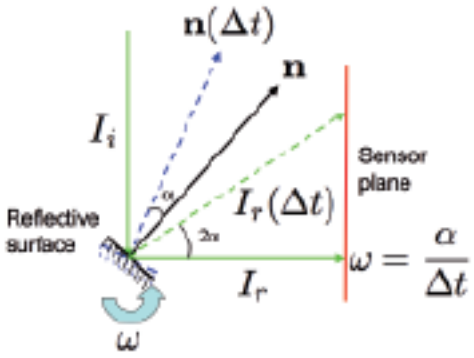

Figure 2: The principle of the Vorticity Optical Probe (VOP). The incident light beam is reflected from the mirror rotating at anangular velocity equal to half of the vorticity. The sweeping of the reflected beam is detected on the sensor in a high speed camera, from which the instantaneous vorticity can be measured.

by tracing the light beam reflected from a rotating mini-mirror seeded into the flow (Fig. 2). Currently, we have in the lab acrylamide gel coated hexagonal lead carbonate crystals that serve as mirrors. As the size of these VOP particles is $25\mu m$ and the density is matched to water, they will follow the fluid faithfully, in both translation and rotation, in our von Kármán water flow up to $R_\lambda \sim 10^3$. The trajectories of the reflected light beam will be recorded using the high-speed Phantom cameras to achieve sub-Kolmogorov time resolution. With our experiences in 3D-LPT, it is possible to follow simultaneously hundreds of these particles in the flow and measure their vortocities. The challenge, as well as a long-term goal of this project, is to simultaneously measure both the vorticities and the positions of multiple such particles, which would then give us access to spatial correlations of vorticities in high-Reynolds number flows, a key step toward experimental studies of intense vortex structures in fully developed turbulence [13,14].

Extended Laser Doppler Measurements

The small measurement volume of the laser Doppler technique (Fig. 3) allows a denser seeding of the flow field compared to the Lagrangian Particle Tracking and therefore a higher temporal and spatial resolution. Consequently, the Laser Doppler system is a much-needed alternative for flows with very small scales as the Goettingen High Pressure Turbulence Facilities. The point-wise measurement of the Laser Doppler technique normally restricts the derived statistics to Eulerian quantities. However, two extensions of the techniques allow access to Lagrangian quantities.

From the change of frequency within the laser Doppler burst signal, the velocity gradient can be estimated. Since the observed signal comes from single particles, this velocity gradient is the Lagrangian particle acceleration. In collaboration with the TU Darmstadt, we were able to successfully use a commercial LDV system to measure both, particle velocity and

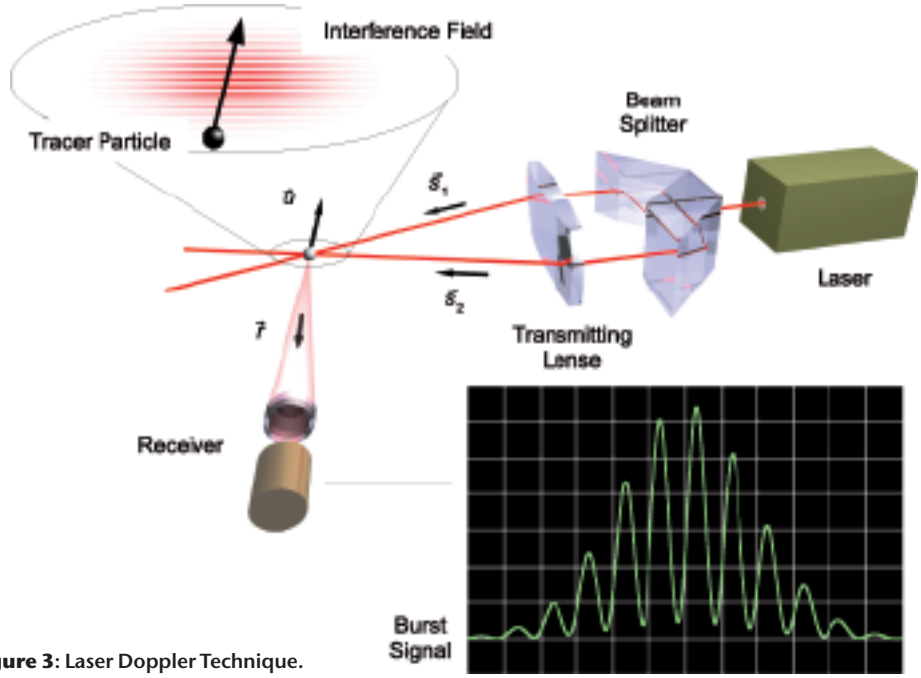

Figure 3: Laser Doppler Technique.

acceleration in backward scatter [15,16,17]. Because of the small measurement volume of an LDV system, the alignment procedures and the signal processing require the highest possible accuracies. Only this allows acceleration measurements with sufficient resolution. To resolve probability density functions of acceleration, the fringes pattern in the measurement volume must realize an accuracy of the fringes distances of the order of 0.01 %. We developed test facilities and routines to improve the alignment procedure and to verify the accuracy of the instrument. With a wire freely falling through the measurement volume, we were able to resolve the gravity constant and to determine systematic and stochastic errors which could limit the instrument resolution.

The Extended Laser Doppler Velocimetry (ELDV, [18]) with an expanded measurement volume will allow us to recover particle velocity trace of about 20 times the Kolmogorov time scale (τ_η) with a very high sampling rate. This measurements apparatus stands on various experimental challenges: first it will naturally reduce the systematic error due to the imperfect interference pattern in the standard local LDV/LDA system but in the mean time it will also reduce the signal to noise ratio. The other challenge is about the data analysis, which involve a non-trivial time/frequency analysis. This work will be of high interest in the Goettingen Turbulence Tunnel where the particle spatial density will be low compared to usual systems (mixers) where the standard LDV/LDA method has already demonstrated its accuracy. Moreover, the ELDV system will give us access to the acceleration correlation function (which LDV/LDA cannot provide) and acceleration probability density function, which are suitable to study the behavior of inertial particle in turbulent flows. The dynamics of such inertial particles is relevant for many natural and engineering applications (transport, mixing, dispersion) and has already triggered numerous works in the past few years (e.g. [19]): numerical and experimental for relatively high Reynolds number (and in most of the cases with very heavy particles). Those studies enlighten a very rich dynamic with respect to the Stokes number associated to the particle/flow couple, but also show some inconsistencies in between numerical and experimental measurement. A very high Reynolds number measurement would be of great interest to investigate the asymptotic regime and at even a higher-level of interest we will get closer to geophysics applications (such as rain initiation, pollution dispersion, or sediments transport in rivers).

Particle Image Velocimetry (PIV) & Tomographic PIV

Particle Image Velocimetry (PIV) has become the prime choice for processing image-based flow measurements in fluid dynamics experiments. Advanced image processing algorithms use techniques like direct correlation (with a special normalization [20]) to reduce the influence of particle images truncated at the edges of the interrogation areas, iterative shift and deformation of image subspaces [21] or the iterative deformation of the entire images including weighting of the image subspaces to be correlated [22] to improve both, the accuracy and the spatial resolution. In numerical simulations, of the image processing an accuracy better than 0.01 pixels displacements between the two consecutive images has been found. In contrast, the application to real images from experiments shows less

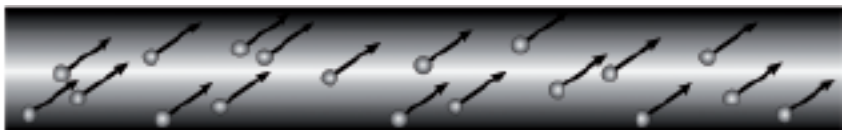

Figure 4: Individual particle intensity variations.

optimistic results, where the usually observed limit is of order 0.1 pixel. Only under special conditions, like in two-dimentional flows with carefully aligned light sheets, a better accuracy has been achieved. As a possible reason for the different achievable accuracy in simulations and experiments we found that in experiments, particles usually change their position within the light sheet (Fig.4) [23]. As a consequence, each particle individually changes its intensity between two exposures. Usually, this effect is not taken into account in most simulations of the measurement process. However, it causes deviations of the displacement estimates. Even if it strongly limits the achievable accuracy of the PIV technique based on the cross-correlation of two consecutive images (Fig.5), it is not a fundamental limitation of the PIV technique itself. The required information is available and can be extracted with appropriate model fits. However, the model estimation is very costly and not the appropriate tool to be used in an experimental environment. Therefore, we investigate the possibility of using special image filters which are robust again this influence.

To extend the PIV principle to the Lagrangian framework we also develop a three-dimensional time-resolved measurement system, namely a time-resolved tomographic PIV system in collaboration with an industrial partner. The advantage of the system compared to Lagrangian Particle Tracking will be the higher seeding density giving more detailed access to the flow gradients.

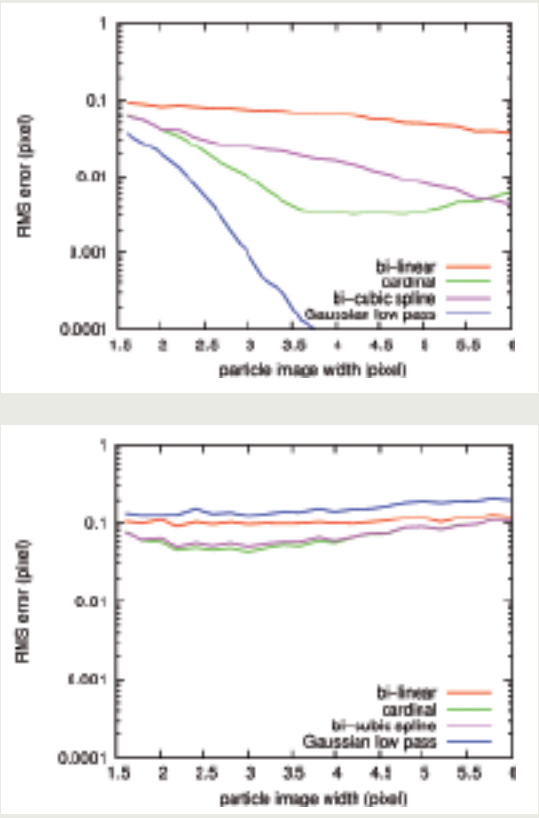

Figure 5: RMS errors of the PIV image processing (a) without and (b) with individual particle intensity variation.

[1] A. La Porta et al., *Nature* **409** (2001) 1017.
[2] G.A. Voth et al., *Rev. Sci. Instru.* **12** (2001) 4348.
[3] G.A. Voth et al., *J. Fluid Mech.* **469** (2002) 121.
[4] N. T. Ouellette, H. Xu, and E. Bodenschatz, *Exp. Fluids* **40** (2006) 301.
[5] M. Bourgoin et al., *Science* **311** (2006) 835.
[6] N. T. Ouellette et al., *New J. Phys.* **8** (2006) 109.
[7] H. Xu. (2007) under review.
[8] H. Xu, N. T. Ouellette, and E. Bodenschatz. New J. Phys. (2007) in press.
[9] M. Kholmyansky, A. Tsinober, and S. Yorish, *Phys. Fluids* **13** (2001) 311.
[10] J.M. Wallace and J. F. Foss, *Annu. Rev. Fluid Mech.* **27** (1995) 469.
[11] B. Lüthi, A. Tsinober, and W. Kinzelbach, *J. Fluid Mech.* **528** (2005) 87.
[12] M.B. Frish and W.W. Webb, *J. Fluid Mech.* **107** (1981) 173.
[13] S. Douady, Y. Couder, and M. E. Brachet, *Phys. Rev. Lett.* **67** (1991) 983.
[14] J. Jiménez et al., *J. Fluid Mech.* **255** (1993) 65.
[15] H. Nobach, M. Kinzel and C. Tropea, Optical Methods of Flow Investigation, *Proc. of SPIE* **6262** (2006) 1.
[16] M. Kinzel et al., Proc. of the 13th International Symposium on Applications of Laser Techniques to Fluid Mechanics, June 26-28 (2006), Lisbon, Portugal.
[17] M. Kinzel et al., Lasermethoden in der Stroemungsmesstechnik, September 5-7 (2006), Braunschweig, Germany.
[18] R. Volk et al. arXiv:0708.3350v1 [physics.u-dyn], accepted in PRL (2007).
[19] R. Volk et al. arXiv:0710.3257v1 [nlin.CD] (2007) submitted.
[20] J. Nogueira, A. Lecuona and P.A. Rodriguez, *Exp. in Fluids* **30** (2001) 309.
[21] H.T. Huang, H.E. Fiedler and J.J. Wang, *Exp. in Fluids* **15** (1993) 263.
[22] J. Nogueira, A. Lecuona and P.A. Rodriguez, *Exp. in Fluids* **27** (1999) 107.
[23] H. Nobach and E. Bodenschatz, Proc. 7th International Symposium on Particle Image Velocimetry, September 11-14 (2007), Rome, Italy.

Turbulence Generation and Manipulation

G. Bewley, M. Gibert, H. Xu, E. Bodenschatz
K. Chang, R. Zimmermann
J.-F. Pinton (ENS-Lyon, France), M. Bourgoin (LEGI-Grenoble, France),
Z. Warhaft (Cornell, USA), J.C. Vassilicos (Imperial College London, UK)

For nearly 100 years, the paradigm flow used for the experimental investigation of turbulence has been the one generated by a regular grid moving relative to the fluid. Scientists have studied grid turbulence extensively because a properly designed grid generates turbulence that is nearly homogeneous and isotropic, and this is the idealized model assumed in most turbulence theory. However, grid turbulence is often coupled with a large background mean flow. Our aim in developing new ways of generating turbulence is to create flows with a small mean component, and to be able to control the degree of anisotropy and inhomogeneity of the turbulence. We discuss the reasons for this and our work in exploring such flows in this section.

An important technical reason for the attractiveness of grid turbulence is that it is often coupled with a large mean flow, particularly in a wind tunnel. This mean flow makes Eulerian measurements possible using a single probe fixed in the laboratory frame in combination with Taylor's frozen turbulence hypothesis. However, in the past decades the rise of interest in the Lagrangian statistics of turbulence has promoted the rapid development of Lagrangian measurement techniques, and these techniques are difficult to implement in a wind tunnel. This is because the techniques almost exclusively rely on tracking the motions of tracer particles, and the large mean flow in a wind tunnel sweeps particles out of a fixed measurement volume in a short time, unless external mechanisms are implemented to move the measurement volume along with the mean flow [1,2]. For this reason, most Lagrangian data available today are obtained from systems in which one can observe individual particles for longer times.

The effort to find new ways to generate and manipulate turbulence is also inspired by the persistent need to understand flows characterized by large values of the Reynolds number, and to explore the influence of large-scale non-uniformities of the flow on turbulence. Not only are flows with these properties seen in industrial and geophysical settings, but also they are fundamentally interesting because it is thought that certain statistics of the flow are only predictable in the limit of large Reynolds numbers.

Aside from wind tunnels, the von Kármán flow between counter-rotating disks is one of the mostly widely studied turbulent flows [3,4,5,6] and it is also one of the flows studied in our group. The turbulence in the von Kármán flow can reach a very high Reynolds number, but it is neither homogeneous nor isotropic. While studying this flow, we were intrigued by two experimental findings that might also bear theoretical importance, and we discuss each of these below.

The first finding concerns the return to isotropy at high Reynolds numbers. Kolmogorov [7] hypothesized that when the Reynolds number is very large, turbulence will have the same properties regardless of how it was generated. We have measured three quantities representing velocity increments at different time scales in the flow. At scales larger than the integral scale, it is thought that the velocity increments are related to the velocity fluctuations, υ'. At dissipative scales, the velocity increments are proportional to the Lagrangian acceleration. In between the two, the Lagrangian structure function is a direct measure of the velocity increments. As shown in Fig.1, the degree of anisotropy in these three quantities is very different at a given

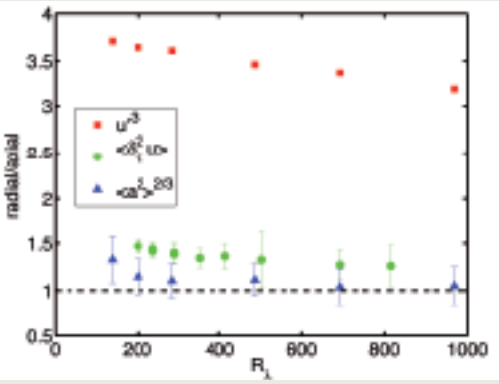

Figure1: The degree of anisotropy at different scales in the von Kármán flow as a function of the Reynolds number. The plot shows the ratio of the radial components to the axial components of various quantities. The large scale quantity is v'^3 (data from [5]); the inertial range scale quantity is $\langle \delta_r v \rangle$ with $r_L \approx r \approx r_T$ (data [11]); the small scale quantity is $\langle a^2 \rangle^{2/3}$ (data from [5]). The exponents of these quantities are chosen such that they have the same dependence on the energy dissipation rate ε.

Reynolds number, with the large scale being the most anisotropic. This result is consistent with the Kolmogorov hypothesis. While it is true that the degree of anisotropy decreases with the Reynolds number for all three quantities, the observed return to isotropy is very slow for the inertial and large scales. If these trends hold in turbulence generated in other ways, then almost all engineering flows must also be anisotropic, even at small scales, since they are usually generated by anisotropic forcing and at moderate Reynolds numbers.

The second striking experimental observation concerns anisotropy in the Eulerian frame. We observe that even though the flow is anisotropic, the relations derived for isotropic turbulence still hold for spatial averaged statistics. Fig. 2 shows the transverse structure function $D_{NN}(\boldsymbol{r})$ and the longitudinal structure function $D_{LL}(\boldsymbol{r})$ measured in the von Kármán flow. For any given direction of the separation vector $\boldsymbol{r}$, the isotropic relation $D_{NN}(\boldsymbol{r}) = (4/3)D_{LL}(\boldsymbol{r})$ is not satisfied. However, if all the directions of $\boldsymbol{r}$ are taken into an average, the relation holds well for the average. The question that follows is then whether this result holds for all anisotropic turbulence, or if it is simply fortuitous for von Kármán flows.

To answer such questions, one would like to be able to generate turbulence at unprecedented Reynolds numbers and to be able to control the degree of homogeneity and isotropy of the turbulence. It has been shown that an approximately homogeneous and isotropic flow with a low mean component can be achieved by using multiple loudspeaker driven jets to force the fluid from different angles [8]. Inspired by this work, we are con-

Figure 2: The ratio of the Eulerian second order structure functions $(3/4)D_{NN}(\boldsymbol{r})/D_{LL}(\boldsymbol{r})$. In isotropic flows, this ratio should be 1, independent of the choice of the separation vector $\boldsymbol{r}$. The symbols show the result when the angle of $\boldsymbol{r}$ is conditioned to be within a range $\theta \pm \pi/12$ relative to the rotation axis. The effect of large-scale anisotropy is clearly seen, although there may be a hint of return to isotropy at small spatial scales. On the other hand, the ratio of the spatially averaged structure functions is very close to 1 over a wide range of scales (black curve).

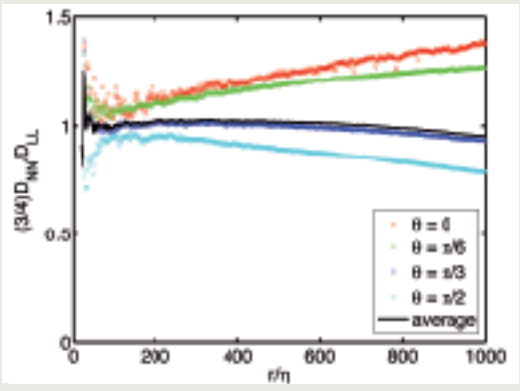

structing several apparatuses. Our apparatuses include a device named the Lagrangian Exploration Module (LEM), whose boundary has the shape of an icosahedron, with propellers at the 12 vertices (Fig.3). We are building the LEM together with collaborators at ENS-Lyon, France. In addition, we are building jet driven flows in containers with cubic and soccer ball-like geometries. In these containers, air jets generated separately by 32 loudspeakers drive the turbulence. In each of these apparatuses, we anticipate that it will be possible to regulate the degree of isotropy by individually modulating the amplitude of the motions of each propeller or loudspeaker. Using pressurized sulfur-hexafluoride (SF_6) as a working fluid, turbulence at $R_\lambda \sim 3000$ can be achieved with Kolmogorov time and length scales resolvable by existing measurement techniques.

Finally, we also have a high-pressure SF_6 turbulence tunnel scheduled for completion in Feb. 2008 (see next Section). It is designed to generate flows with Reynolds numbers, based on the Taylor scale, of up to 10^4, whereas current laboratory apparatuses are limited to values of the Reynolds number of up to about 10^3. Turbulence in the tunnel can be generated by active grids [9] or by fractal grids [10]. These novel grids are under development by various groups, including those of Z. Warhaft at Cornell University and J.C. Vassilicos at Imperial College London, with whom we are collaborating on the design of the grids. The tunnel allows investigation of the turbulence with both stationary probes and a sled capable of moving along the tunnel with the mean flow. The sled makes it possible to study Lagrangian dynamics over long particle trajectories using particle tracking.

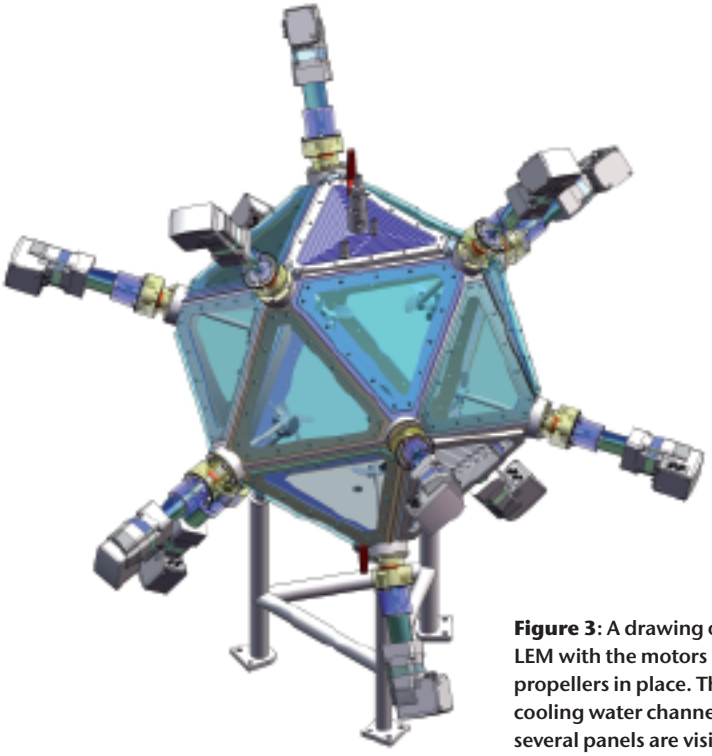

Figure 3: A drawing of the LEM with the motors and propellers in place. The cooling water channels on several panels are visible, which will be used to take away the heat generated by the turbulent flow inside.

[1] Y. Sato and K. Yamamoto, *J. Fluid Mech.*, **175** (1987) 183.
[2] S. Ayyalasomayajula et al., *Phys. Rev. Lett.*, **97** (2006) 144507.
[3] A. La Porta et al., *Nature*, **409** (2001) 1017.
[4] N. Mordant et al., *Phys. Rev. Lett.*, **87** (2001) 214501.
[5] G. A. Voth et al., *J. Fluid Mech.*, **469** (2002) 121.
[6] M. Bourgoin et al., *Science*, **311** (2006) 835.
[7] A.N. Kolmogorov, *Proc. Roy. Soc. A*, **434** (1991) 9.
[8] W.Hwang and J. K. Eaton, *Exp. Fluids*, **36** (2004) 444.
[9] L. Mydlarski and Z. Warhaft, *J.Fluid Mech.*, **320** (1996) 331.
[10] D. Hurst and J. C. Vassilicos. *Phys. Fluids*, **19** (2007) 035103.
[11] N. T. Ouellette et al., *New J. Phys.*, **8** (2006) 102.

Göttingen High Pressure Turbulence Facility (GTF)

H. Nobach, H. Xu, E. Bodenschatz
D. Fünfschilling (ENSIC Nancy, France),
Z. Warhaft (Cornell University, USA), A. Tsinober (Imperial College, GB),
Researchers from ICTR (International Collaboration for Turbulence Research – www.ictr.eu)

Investigations of the fundamental properties of turbulence require flows with high Reynolds numbers under well-controlled conditions. The flow properties need to be resolvable by modern measurement technology from the largest to the smallest spatial and temporal scales. On Earth the highest turbulence levels (Reynolds numbers $\sim 10^7$) are found in the atmospheric boundary layer. Even the most violent flows on Earth, such as plinian volcanic eruptions, have similar turbulence levels. The observations of natural flows are difficult, as the conditions are rarely stationary and the scales of the flow are very large and make detailed measurements utmost difficult. For example, when considering the turbulent motion of clouds in the atmospheric boundary layer, the largest scales of the flow are typically 100m, while the smallest scales are fractions of millimeters. Another complication is that clouds are carried by a mean wind. With current measurement technology it is very difficult, if not impossible, to resolve all scales of the dynamics of turbulent clouds. In addition, the turbulence generation mechanisms in nature are multifold and it is difficult to investigate how the turbulence depends on its generation mechanisms. In the foreseeable future computational fluid dynamics can substitute experiments only for moderate Reynolds numbers at idealized flow conditions. Therefore, experimental facilities generating turbulent flow fields at high Reynolds numbers are essential for the research. The properties of turbulence can either be measured from the spatial (Eulerian) perspective or from the perspective of particles carried by the flow, the so-called Lagrangian perspective. While Eulerian measurements, have traditionally been conducted in wind tunnels with hot wire anemometry, only recently it has become possible to conduct Lagrangian measurements with high accuracy at high Reynolds number thanks to the advance in imaging technology.

High Reynolds-numbers at manageable temporal and spatial scales under well-controlled conditions can be realized by employing the principle of physical self-similarity. The turbulence Reynolds number scales as $\mathrm{Re} = \rho v L/\eta$, where ρ is the density of the fluid, v is the fluctuating velocity, L is the energy injection scale and η is the molecular dynamical viscosity. One-way to achieve high Reynolds numbers is to use cryogenic He gas. In this case very high Reynolds numbers can be achieved, however, with very small spatial and temporal scales that currently cannot be fully resolved by measurement technology. In addition, many methods well tested at room temperature are difficult to use at cryogenic temperatures. An alternative way is to increase the density by pressurizing the gas. This increases the Reynolds numbers, as the molecular dynamical viscosity is approximately independent of pressure. In addition, by using a heavy gas, like sulfur hexafluoride (SF_6) it is possible to reach high Reynolds numbers already at moderate pressures of only 10-20 bar.

In Göttingen we have decided to go the second path. We have installed two facilities that use pressurized SF_6 gas at up to 19 bar. The institute installed a gas handling and liquefaction system that handles and stores 12 tons of SF_6. The gas is used in two facilities – the **Göttingen Turbulence Tunnel** and the **Göttingen U-Boot**. While the first is a wind tunnel with an extra long measurements section to allow particle tracking in the decaying turbulence behind a passive or active grid, the lat-

ter is used for the investigations in Lagrangian mixers and of turbulent thermal convection. In addition to serving the in-house experimentalists, the **GTF** provides visitors with the possibility to study phenomena in turbulent flows under very well controlled conditions at high Reynolds and Rayleigh numbers.

The Building: Both facilities are housed in a newly constructed building that has been optimized for vibration isolation and high temperature stability. It has been equipped with control systems allowing the safe use of the pressurized gases and of lasers. High bandwidth fiber optics links the facilities to a 80 processor data analysis cluster. A 36m^2 class 1000 clean room is available for micro fabrication of sensors, like the hotwire probes needed for the Eulerian measurements in the Turbulence Tunnel.

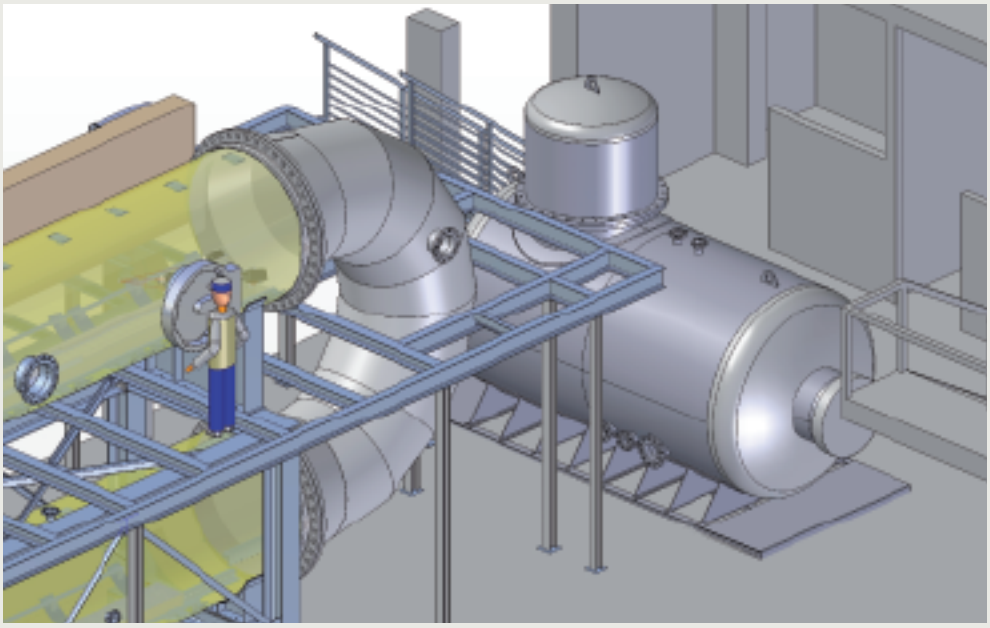

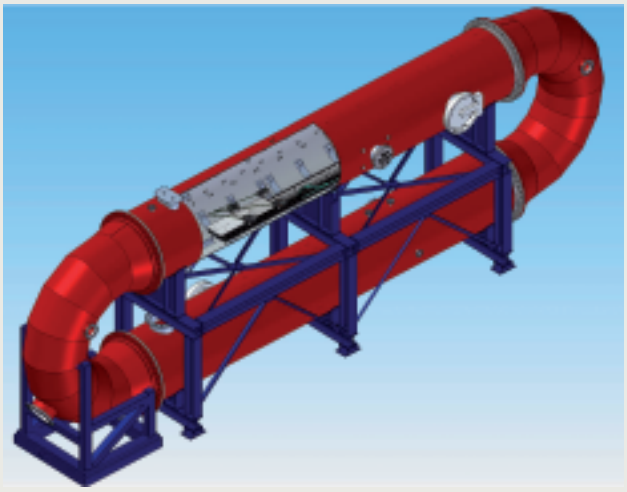

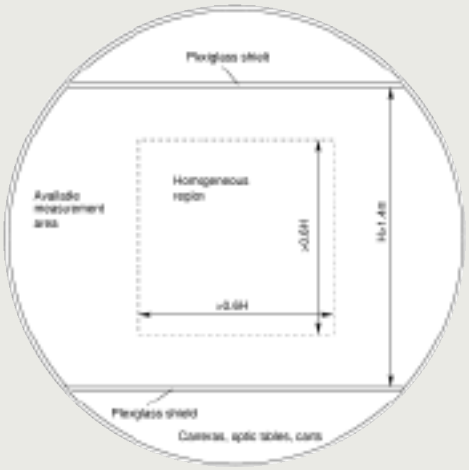

The Turbulence Tunnel: Reynolds numbers of up to Re~10^7 are possible in this recirculation tunnel when filled with SF_6 at 15bar. The tunnel is upright and consists of two measurement sections with a cross-sectional area of 1.9m^2 and lengths of 9m and 7m, respectively. Passive or active grids that are mounted at the entrance of each measurement section generate the turbulence. Two sleds, driven by linear motors, are installed that allow measurement devices (e.g. cameras and optics) to be moved with the mean velocity (up to 5m/s) of the circulating gas. The tunnel is pressure and temperature controlled, and has optical and electrical access. The circulating gas can be filtered to <1μm in order to provide a clean gas. Equipment can be installed either on the sleds or all along the measurement sections. Measurement equipments to be used in the tunnel are high-speed cameras, LDV/PDA system, and hot wires.

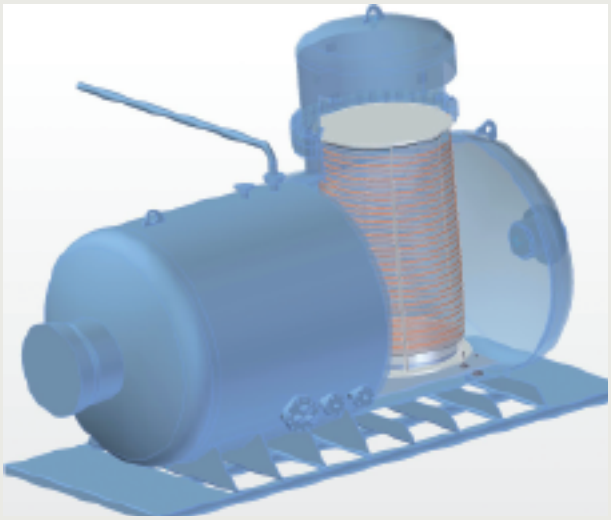

The U-Boot: This is a general-purpose pressure vessel. It has been designed to house different experiments. Similarly to the turbulence tunnel, all equipment can be used inside the vessel for measurements from heat transport and PIV to 3D-Langrangian Particle Tracking (LPT). Experimental inserts available include a von Kármán type mixer with R_λ~3,500 and a turbulent cylindrical Rayleigh-Benard experiment of 1.1m diameter and 2.2m height that will reach Rayleigh numbers as large as Ra~10^{15}.

The Specifications:
Tunnel: length 18m, height 6m, inner diameter 1.8m, pressure 1mbar-15bar, temperature: 20-35°C, mech. power 210kW, cooling power 280kW, kin. visc. SF_6 (15bar) 1.5x$10^{-7}$$m^2$/s. Expected properties: $\langle u \rangle_{max}$=5m/s, $u_{rms,max}$=1m/s, L_{max}=0.45m, $R_{\lambda,max}$~10^4, ε_{max}=1.4W/kg, η >8μm, τ_η>0.4msec.
U-Boot: length 5.3m, max. height 4.0m, outer diameter 2.5m, straight cylinder length 4m, dome 1.5m high and 1.2m in diameter, pressure 1mbar-20bar, temperature: 20-35°C, cooling power <50kW. Expected properties: Ra_{max} = 7x10^{14} at high Ra only weakly non Boussinesq.
Gas Handling System: 4 tanks, 2.8m^3 each, height 4m, diameter 1m, oper. pressure 1mbar-15bar, evacuation of tunnel air (1bar -> 1mbar)2.5h, pressurizing SF6 1mbar-> 15bar 8h, depressurizing SF6 15bar -> 1mbar 22h, filling with air (1mbar->15bar) 1h.
Measurement Systems: 3D-LPT (36kHz), TOMO-PIV, LDV, PDPA, hotwires, lasers, optics, data analysis and storage cluster.

Topical Group

Fluctuations, Disorder and Transport

What makes the grain silo fail and the computer bit flip? In a wide range of physical research, fluctuations and disorder have shifted out of the peripheral vision into the focus of attention. Complex systems often show large scale fluctuations of relevant quantities like the huge pressure fluctuations in large grain piles that can let silos collapse. And mesoscopic systems may be too small for fluctuations to be washed out by large ensembles and too big for microscopic events to prevail, so that electronic signals are dominated by complex fluctuations. In those kinds of systems it is imperative to gain a deep understanding of the mechanisms of the fluctuations and the effects induced by large scale, i.e. correlated, disorder.

This topical group is not joined by the similarity of the physical systems studied in the individual projects, but rather by similar phenomenology observed and similar methods needed for the description. Avalanches well known from granular matter – but still not fully understood – are predicted in the dynamics of ultra cold atoms (a Bose-Einstein-condensate) leaking out of optical lattices with an apparently new mechanism creating them. And scale free behavior is found in spinglasses and mesoscopic conductance. Anomalous random walks in complex environments are linking social studies, polymer physics, light propagation in random lasers and the dynamics of chemical reactions.

In the following we give an overview of the current activities of this topical group. They are mostly concerned with transport phenomena, where disorder and fluctuations play the leading role. Starting with the dynamics of dry and wet granular matter and spinglasses, the trail leads on to the elasticity of polymeric materials. Random walks and anomalous diffusion are studied by fractional calculus and numerical methods in physical, biological and social systems. Studies on single and many particle mesoscopic physics, the dynamics of chemical reactions and on fundamental aspects of turbulence form the conclusion of this section.

Different projects use different approaches for similar phenomena and different phenomena are studied by similar methods. We are therefore confident that an exchange of expertise and a combination of methods and ideas from the different research areas will benefit all projects and stimulate interesting new collaborations that may help to tackle some of the open problems in understanding the effects created by correlated disorder and the nature of complex fluctuations.

Correlations and Transport in Granular Fluids

T. Aspelmeier, A. Zippelius
A. Fiege, W.T. Kranz
E. Ben-Naim (Los Alamos, USA), T. Pöschl (Bayreuth), N.V. Brilliantov (Potsdam)

The Boltzmann equation for inelastically colliding particles has been a rather successful tool to account for cooling and transport in granular gases. However most previous work has considered grains with translational degrees of freedom only which is correct for perfectly smooth particles. If there is some surface roughness, the collisions between the particles give rise to an exchange of translational and rotational energy in addition to energy dissipation.

We have shown that in a granular gas of rough particles the axis of rotation is correlated with the translational velocity of the particles [1]. The average relative orientation of angular and linear velocities depends on the parameters which characterize the dissipative nature of the collision. We model the dissipation by a constant coefficient of normal restitution ε_n and the roughness by a corresponding coefficient of tangential restitution ε_t. We then quantify the orientational correlation via

$$\langle \cos^2\theta \rangle = \frac{1}{N} \sum \frac{(\vec{v}_i \cdot \vec{\omega}_i)^2}{\vec{v}_i^2 \vec{\omega}_i^2} .$$

A theory for these correlations has been derived and validated with numerical simulations for a wide range of coefficients of normal and tangential restitution. The limit of smooth spheres is shown to be singular: even an arbitrarily small roughness of the particles gives rise to orientational correlations.

The kinetic theory of driven and undriven granular gases, taking into account both translational and rotational degrees of freedom, allows for a calculation of the high-energy tail of the stationary bivariate energy distribution, depending on the total energy E and the ratio $\chi = \sqrt{E_w / E}$ of rotational energy E_w to total energy [2]. Extremely energetic particles have a unique and well-defined distribution $f(\chi)$ which has several remarkable features: χ is not uniformly distributed as in molecular gases; $f(\chi)$ is not smooth but has multiple singularities. The latter behavior is sensitive to material properties such as the collision parameters, the moment of inertia and the collision rate. Interestingly, there are preferred ratios of rotational-to-total energy. In general, $f(\chi)$ is strongly correlated with energy and the

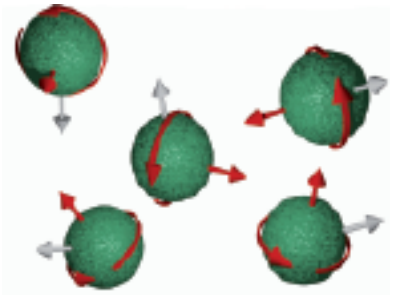

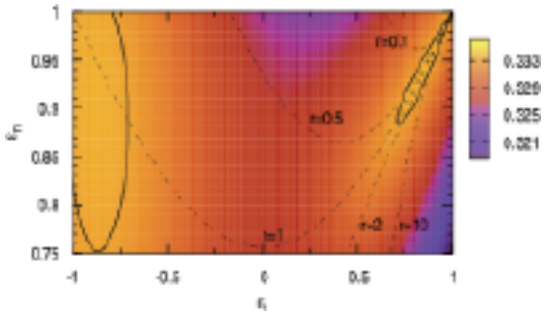

Figure 1: a) The angular (red) and linear (grey) velocities of rough spheres can a priori have arbitrary relative orientation. We roughly distinguish between a cannon ball like behaviour where the axes are approximately aligned and a tennis ball like behaviour where the axes form a right angle.

b) Shown is the color coded stationary value of $\langle \cos^2 \theta \rangle$, a measure for the orientational correlation, as a function of the coefficients of normal (ε_n) and tangential (ε_t) restitution. The solid line marks vanishing correlations. Yellow colour indicates cannon ball behaviour while red & blue hues indicate tennis ball like orientations.

deviations from a uniform distribution grow with energy.

Driven granular matter is inherently out of equilibrium and its static and dynamic properties are highly nontrivial [3, 4]. Structure formation in driven granular matter is investigated using the simplest possible driving mechanism, i.e. driving each particle i via a random force $\vec{\zeta}_i\,(\langle\zeta_i^a\zeta_j^b\rangle \sim \delta_{ij}\,\delta_{ab})$. While this is not the situation usually found in experiments, it allows for analytical progress which is not possible for more realistic driving methods (e.g. shaking, fluidizing by air, etc.). Structure and dynamics of such a system depend crucially on whether the driving satisfies momentum conservation, and on the length scale on which momentum is conserved. A hydrodynamic analysis shows that granular matter driven in this fashion does not exhibit clustering instabilities but develops to a steady state [6] which displays unexpected spatial correlations in the density and velocity fields. The static and dynamic structure factors obtained from this analysis are used as input for a mode-coupling calculation [5] of the velocity autocorrelation function $\psi(t) = \langle \vec{v}(0)\cdot\vec{v}(t)\rangle$ in the driven steady state. Both the velocity autocorrelation function and the diffusion constants derived from it can then be compared to simulations.

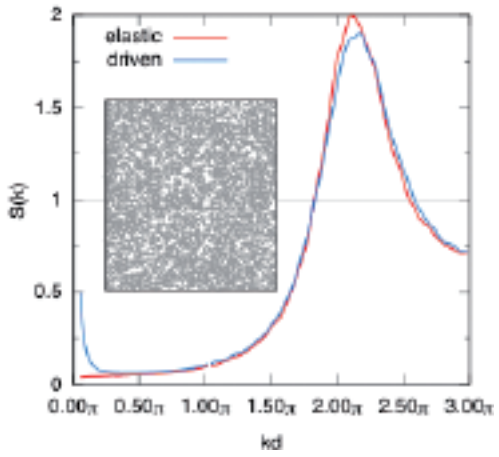

Figure 2: The static structure factor $S(k)$ of a system of hard spheres for perfectly elastic interactions and for a driven inelastic system where the driving fulfills momentum conservation only on the largest length scales. Both curves show data from large scale event driven simulations. Note the diverging structure factor in the driven case for small wave numbers k. The inset shows a small part of a representative driven system.

[1] N.V. Brilliantov, T. Pöschel, W.T. Kranz and A. Zippelius, *Phys. Rev. Lett.* **98** (2007) 128001.
[2] E. Ben-Naim and A. Zippelius, *J. Stat. Phys.* **129** (2007) 677.
[3] A. Zippelius, *Physica A* **369** (2006) 143.
[4] I. Goldhirsch, *Annu. Rev. Fluid. Mech.* **35** (2003) 267.
[5] J. Bosse, W. Götze and M. Lücke, *Phys. Rev. A* **17** (1978) 434.
[6] T. P. C. van Noije, M. H. Ernst, E. Trizac and I. Pagonabarraga, *Phys. Rev. E* **59** (1999) 4326.

Statics and Dynamics of Wet Granulates

M. Brinkmann, R. Seemann, J. Vollmer, S. Herminghaus
J. Sarkar, Z. Khan, J.O. Claussen,
H. Ebrahimnazhad Rhabari, M. Scheel, D. Hornung
M. DiMichiel (Grenoble, France), A. Sheppard (Canberra Australia)

When mixed with a wetting liquid, a pile of sand grains turns into a moldable material. The mechanical stability is a consequence of the air-water interfaces spanning between adjacent sand grains. Quite surprisingly the mechanical stability of a wet granulate does not depend on the amount of liquid over a wide range. Only for a high liquid content close to saturation, the cohesion weakens and the granular pile looses its stability [1,2]. This decrease of capillary cohesion can lead to a sudden fluidization of the granulate under external loads, in particular in response to shear stress [3] (when a landslide is induced by heavy rainfall [4]). A thorough understanding of the complex dynamic behavior of wet granular piles has to address several physical aspects ranging from the geometry of random packings, via capillarity and wetting of complex geometries, to the fluid dynamics and mechanics of cohesive granulates.

First, we have studied the equilibrium shapes of wetting liquids in static granular assemblies. Owing to their high symmetry and well defined geometry, we started our investigation with random piles of spherical beads. High resolution x-ray micro-tomography [1,5] and the application of efficient segmentation algorithms [6] allowed us to resolve the packing geometry of grains, and the shape of the liquid structures in three dimensions with a micrometer resolution (Fig.1). The experimentally detected liquid shapes could be directly compared to the results of numerical minimizations of the interfacial energy employing a finite element representation of the liquid-air interface in the respective bead geometries [1] (see Fig. 2). The experimentally observed distribution of angular distances between neighboring contact points exhibits a sharp peak at 60°. Consequently, the opening angle of a capillary bridge in the pile is limited by 30°. The coalescence of neighboring capillary bridges leads to open liquid structures with a large liquid-air interface with constant Laplace pressure (Fig.3a).

Rather than being spherical, the grains in 'real' granulates are irregularly shaped. In order to reduce the symmetry of the grains we consider random assemblies of cylinders, and liquid structures between irregular granules. Time resolved imaging of the liquid structures by ultrafast x-ray tomography [1] revealed that liquid is exchanged between individual liquid structures on a typical timescale of several minutes, see inset of Fig.3a. The transport of the wetting liquid in the granular pile is driven by differences in Laplace pressure and may proceed via the vapor phase or within a wetting film. The interplay of the diffusive exchange between the individual water domains and the sudden changes in the Laplace pressure caused by coalescence events sets the growth law for the coarsening of the liquid structures. Percolation phenomena and the distribution of volume and Laplace pressure will be studied in a minimal model, and compared to detailed Lattice Boltzmann simulations of the two phase fluid in the pile.

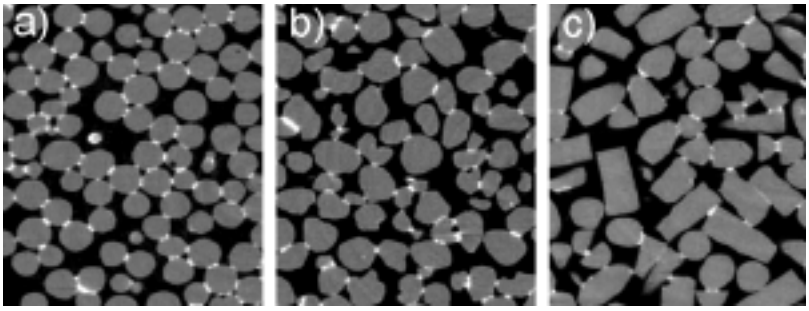

Fig 1: Compilation of x-ray micro-tomographies of different types of wet grains: **a)** spherical beads, **b)** rounded sand grains, and **c)** cylindrical segments.

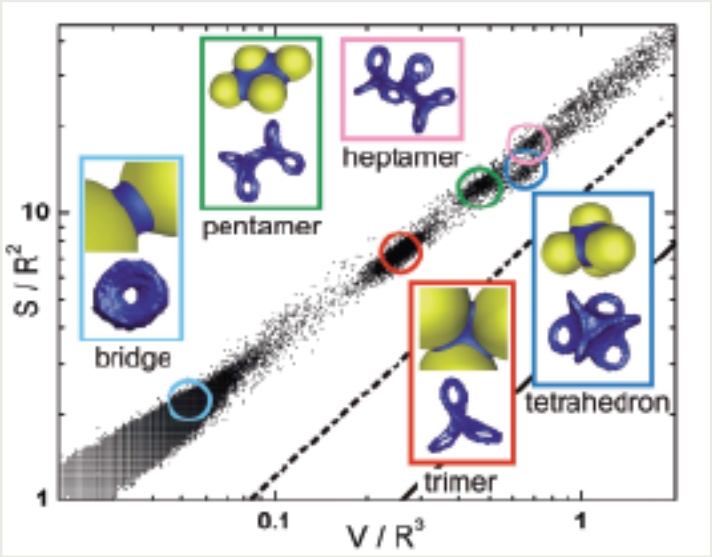

Figure 2 Surface to volume plot of liquid structures found by X-ray micro-tomography in a wet pile of spherical beads (average bead radius R = 240 μm). The distinct groups of data points correspond to a certain class of liquid morphologies. Insets: liquid morphologies as found by X-ray micro-tomography in comparison to numerical minimizations. The dashed line indicates the surface to volume ratio of the largest cluster at W = 0.17; the solid line corresponds to complete filling of the voids, which lies at least three times below the experimentally found values.

The insensitivity of the mechanical stability with respect to the liquid content was demonstrated for spherical beads and sand grains in a variety of mechanical tests including fluidization by vertical agitation [7], tensile stress measurements using a centrifuge, and in shear cell experiments [1,2], cf. also Fig. 3b. Fluidization of a dense granulate under shear forces in the regime of individual liquid bridges is presently studied in a molecular dynamics simulation with hysteretic interparticle forces. One of the objectives of this study is to explore which aspects of the transport in these systems can faithfully be described by macroscopic transport equations for momentum and energy.

[1] M. Scheel et al., Morphological clues to the stability of wet granular piles, *Nature Materials*, in press

[2] S. Herminghaus, Dynamics of wet granular matter. *Advances in Physics* **54**, 221 (2005)

[3] P. Tegzes, T. Vicsek, P. Schiffer, Avalanche Dynamics in wet granular material. *Phys. Rev. Lett.* **89**, 094301 (2002)

[4] N. Lu, B. Wu, C.P. Tan, Tensile strength characteristics of unsaturated sands. *Geotech. Geoenviron. Eng.* **133**, 144-154 (2007)

[5] M. Di Michiel et al. Fast microtomography using high energy synchrotron radiation. *Rev. Sci. Instr.* **76**, 043702 (2005)

[6] A. P. Sheppard, R. M. Sok, H. Averdunk, Techniques for image enhancement and segmentation of tomographic images of porous materials. *Physica A* **339**, 145–151 (2004).

[7] Z. Fournier et al., Mechanical properties of wet granular materials, *J. Phys. Condens. Matter* **17,** 2140 (2004)

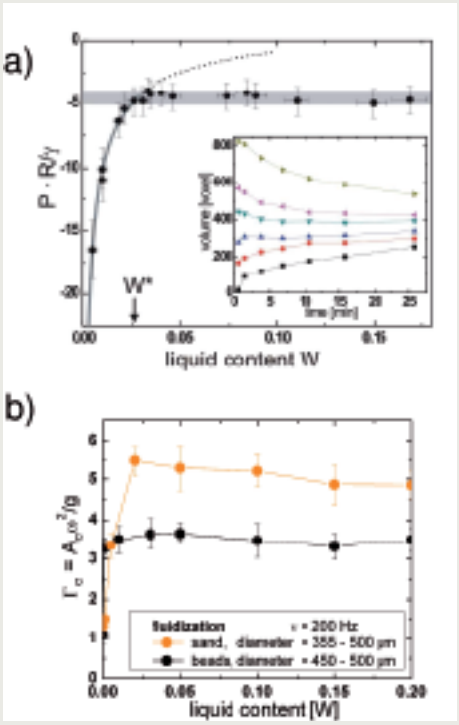

Figure 3: a) Laplace pressure of capillary water bridges in an assembly of spherical glass beads as a function of the liquid content, W. The pressure, P has been rescaled by the surface tension, γ, and bead radius, R. We find a clear plateau for W>W*=0.025. The inset shows the volume of individual capillary bridges as a function of time after sample preparation. **b)** Fluidization amplitude, Γ_c, of wet glass beads and sand as function of liquid content, W. Except for very small liquid contents, Γ_c is virtually independent of W.

Free Energy Fluctuations and Domain Wall Energies in Spin Glasses

T. Aspelmeier
A. Braun (University of Göttingen), M.A. Moore (Manchester, UK),
A. Billoire (Saclay, France), E. Marinari (Rome, Italy)

The effects of disorder in low dimensions are in general poorly understood. Spin glasses offer a unique way to investigate these effects since they are the 'simplest' disordered systems and since the recent development of powerful new methods has made analytical and numerical progress possible.

One of the central and unsolved problems in spin glass physics are domain wall energies. Unlike in ferromagnets, the free energy of a low energy excitation is very difficult to estimate because a region of spins which is flipped relative to the ground state (a droplet) can make use of the disorder inherent in the sample. By choosing a surface which predominantly crosses weak bonds the droplet of linear size L can minimize its energy which is then proportional to L^{θ} with $\theta \leq \frac{d-1}{2}$, while its surface becomes a fractal object with dimension d_s. In [1] we found a very surprising correspondence between the domain wall free energy (in dimensions $d \geq 6$) and the sample-to-sample fluctuations of the free energy ΔF in the mean-field Sherrington-Kirkpatrick model. This model corresponds to $d = \infty$ and has no spatial structure at all. The question of finding the domain wall energy is therefore equivalent to finding ΔF. However, this quantity is also very difficult to calculate. Numerical estimates have only been carried out at zero temperature and lead to $\Delta F \sim N^{\mu}$ with $\mu \approx 0.25$, where N is the system size. The correspondence between ΔF and the domain wall energies leads to the prediction $\theta = d\mu$.

In order to calculate ΔF analytically, we have developed a new method based on interpolating Hamiltonians [2,3]. Interpolating Hamiltonians have been introduced in the literature to prove, among other things, the correctness of the Parisi free energy for the Sherrington-Kirkpatrick model and are a very powerful tool to obtain rigorous results. Our new method leads to an unexpected exact relation between ΔF and spin glass chaos. Chaos refers to the property of spin glasses that an arbitrarily small change in e.g. the temperature or the couplings leads to a totally uncorrelated equilibrium state (in the thermodynamic limit). This correspondence between fluctuations and chaos is extremely powerful because it allows, for the first time, an analytical calculation of the fluctuations by calculating chaos (which is possible by replica methods), and it suggests new algorithms to obtain the fluctuations numerically at nonzero temperature. So far we have obtained the "rigorous" upper bound $\mu \leq \frac{1}{4}$ and expect to be able to calculate μ exactly in the future.

While we do not yet have the precise answer for μ, its most likely value is $\frac{1}{6}$. This is the result of heuristic arguments and simulations [4]. The main idea behind these arguments is that the infinite hierarchy of replica symmetry breaking in the Sherrington-Kirkpatrick model is stabilized at a finite value in a finite system due to self-energy terms. An estimate of the self-energy leads to an estimate for the number of symmetry breaking steps $K \sim N^{1/6}$. Many quantities can be calculated for a finite value of K from the Parisi scheme and thus their finite size corrections can be inferred from the relation between K and N. We obtain for example the values $-\frac{2}{3}$ for the shift exponent (the exponent which governs the difference between the free energy per spin and its thermodynamic limit as a function of system size), the same value for the corresponding exponent for the internal energy, $\mu = \frac{1}{6}$ and

various other finite size correction exponents. All of these predictions agree well with extensive numerical simulations.

Although μ is a quantity which stems from the mean-field model, the value $\mu=\frac{1}{6}$ has far-reaching consequences for the physics of finite dimensional spin glasses. The prediction $\theta=d\mu$, which applies only above the upper critical dimension of *6* and only if replica field theory is valid, can be tested numerically [5]. Good agreement is observed. This constitutes a very strong test for replica field theory. In low dimensions $d<6$, however, the calculation in [1] indicates that the domain wall energy is dominated by a different term if indeed μ were equal to $\frac{1}{6}$. This suggests a changeover from the replica symmetry breaking field theory in high dimensions to a droplet-like theory in low dimensions.

We plan to extend our approach of using interpolating Hamiltonians to finite dimensional spin glasses. Again we expect an exact relationship between fluctuations and chaos. In contrast to the mean-field case, the fluctuations in finite dimensions are known while chaos is hard to calculate. Our approach will allow us to obtain information about chaos from the known fluctuations.

In order to further illuminate the question whether and how a change in spin glass physics occurs at the upper critical dimension, we have investigated a different model, the m-component spin glass on the Bethe lattice [6]. In conjunction with the cavity method, which we have extended to m-component spins, the low-temperature phase of a vector spin glass has been analyzed in great detail. When the number of spin components is infinite, the system is replica symmetric for all connectivities. We have derived zero temperature scaling laws which connect exponents for finite-N, infinite-m systems with those of infinite-N, finite-m ones, allowing us to make predictions for a finite number of components. The drawback of this method is that it implicitly assumes replica symmetry. As an alternative, we can access finite-m systems sytematically using a $\frac{1}{m}$-expansion. In numerical simulations, the latter approach shows a first phase transition to a replica symmetric low temperature phase, followed by a second phase transition to a state with broken replica symmetry. This second phase transition will offer us the opportunity to investigate the reasons for symmetry breaking as a function of temperature, connectivity and number of spin components in detail in the future.

[1] T. Aspelmeier, M. A. Moore, and A. P. Young, *Phys. Rev. Lett.* **90** (2003) 127202.
[2] M. Goethe and T. Aspelmeier, cond-mat/0610228, submitted to *Phys. Rev. B.*
[3] T. Aspelmeier, *in preparation*.
[4] T. Aspelmeier, A. Billoire, E. Marinari and M.A. Moore, arXiv:0711.3445v1, submitted to *J. Phys. A*.
[5] S. Boettcher, *Europhys. Lett.* **67** (2004), 453.
[6] A. Braun and T. Aspelmeier, *Phys. Rev. B* **74** (2006) 144205.

Anisotropic Random Networks and Nematic Elastomers

A. Zippelius
M. Kiems
P. Benetatos (University of Göttingen), P.M. Goldbart (Urbana-Champain, USA)

The classical theory of rubber elasticity [1] has been remarkably successful in describing the behavior of elastomeric systems in which there is no long-ranged nematic order. A blend of phenomenology and molecular-level reasoning, it is based on a few simple assumptions and bears great predictive and descriptive power. It models rubbery materials (i.e. elastomers) as incompressible networks of entropic Gaussian polymer chains and, further, assumes that the cross-links (i.e. the junctions of the polymer network) are fixed in space (for any given macroscopic deformation) but nevertheless deform affinely under macroscopic deformation. The classical theory gives their elastic free energy density f as $f=\frac{\mu}{2}\,Tr\Lambda^T\Lambda$, for a spatially uniform deformation $r\rightarrow\Lambda\cdot r$ that conserves the volume (i.e. obeys $det\,\Lambda=1$). For most rubbery materials the assumption of volume conservation (i.e. incompressibility) is well satisfied. The shear modulus μ is given by $n_c k_B T$, where T is the temperature and k_B is Boltzmann's constant. The parameter n_c is usually referred to as "the density of effective chains in the network." The classical theory explains many essential features of rubbery materials, such as their stress-strain curves (at least for deformations that are not too large), and the striking temperature-dependence of their shear moduli, as well as their strain-induced birefringence (i.e. the stress-optical effect).

Recently, an elegant anisotropic generalization of the classical model [2], known as the neo-classical model, was constructed to describe the highly unusual elasticity of nematically ordered elastomers, i.e. rubbery materials having (spontaneously) broken rotational symmetry, and has done so with considerable success. According to the neo-classical model, in the presence of nematic order the elastic free energy of a nematic elastomer under a deformation Λ is given by $f=\frac{\mu}{2}\,Trl_0\Lambda^T l^{-1}\Lambda$, where l_0 and l are the (in general, anisotropic) step-length tensors in the initial (i.e. $\Lambda=1$) and the deformed (i.e. $\Lambda\neq1$) states that characterize the conformations of the polymer chains. The step length tensors l_0 and l have the symmetry of the nematic order parameters in the initial state and in the deformed state, respectively. A remarkable feature of Eq. (2) is that in the nematic phase, for which l_0 and l are both anisotropic and differ only by a rotation, there exists a continuous manifold of deformations that cost zero elastic free energy.

We have constructed a Landau theory for the gelation transition in cross-linked polymer systems possessing spontaneous nematic ordering, based on symmetry principles and the concept of an order parameter for the amorphous solid state [3]. This theory has been derived from a simple microscopic model of cross-linked dimers. Minimization of the Landau free energy in the presence of nematic order yields the neo-classical theory of the elasticity of nematic elastomers and, in the isotropic limit, the classical theory of isotropic elasticity. These phenomenological theories of elasticity are thereby derived from a microscopic model, and it is furthermore demonstrated that they are universal mean-field descriptions of the elasticity for all chemical gels and vulcanized media.

Motivated by the organization of cross-linked cytoskeletal biopolymers, we have developed a semimicroscopic replica field theory for the formation of anisotropic random networks of semiflexible polymers [4]. The networks are formed by introducing random permanent cross-links which fix the orientations of the corresponding polymer segments to align with one another. Upon increasing the cross-

link density, we obtain a continuous gelation transition from a fluid phase to a gel where a finite fraction of the system gets localized at random positions. For sufficiently stiff polymers, this positional localization is accompanied by a *continuous* isotropic-to-nematic (IN) transition occuring at the same cross-link density. As the polymer stiffness decreases, the IN transition becomes first order, shifts to a higher cross-link density and is preceded by an orientational glass (statistically isotropic amorphous solid) where the average polymer orientations freeze in random directions.

We are currently extending these studies to polar systems as well as two-dimensional networks of semiflexible chains which are cross-linked under a prescribed angle. The aim is to investigate the appearance of orientational order in the solid phase depending on the cross-linking geometry and the bending stiffness of the polymers. Another direction of future research are crosslinked directed polymers, a simple model system with built-in anisotropy. Crosslinking directed polymers will give rise to an anisotropic gel which in addition to a tilt stiffness will be characterized by a finite in-plane shear modulus. This would be a novel cross-link-induced amorphous solidification transition – besides the thermodynamic transition of a flux-line liquid to the Abrikosov lattice.

[1] L. R. G. Treloar, *The Physics of Rubber Elasticity* (Clarendon Press, Oxford, 1975).
[2] M. Warner and E. M. Terentjev, *Prog. Polym. Sci.* **21** (1996) 853.
[3] X. Xing et al. *preprint* (2007).
[4] P. Benetatos and A. Zippelius, *Phys. Rev. Lett.* **99** (2007) 198301.
[5] X. Mao et al., *Europhys. Lett.* **80** (2007) 26004.

Anomalous and Nonlinear Diffusion in Physics and Biology

D. Brockmann, M. Timme, V. Zaburdaev, T. Geisel, S. Herminghaus
V. V. Belik, V. David, B. Schwenker,
L. Hufnagel (EMBL, Heidelberg),

Complex dynamical systems in physics, biology and ecology exhibit the interplay of spatial structure, nonlinear interactions of dynamical entities, fluctuations due to internal stochasticity and anomalous transport of interacting agents. The key goal of the projects outlined below is to discern qualitative and characteristic features of classes of complex dynamical effects when various combinations of these factors interact.

In a first project [2] we show that spatial inhomogeneities can speed up stochastic dispersal if the dispersal is anomalous, unlike ordinary diffusion which is typically slowed down in spatially structured environments. In a second project we show that mean field models for wave propagation into an unstable region are structurally unstable if the dispersal of particles in superdiffusive [3], i.e. arbitrarily small perturbations to the system entail qualitatively different dynamics.

Accelerating random walks by disorder

A particle performing ordinary diffusion is typically characterized by a spatiotemporal scaling relation $|X(t)| \sim t^{1/2}$. An increasing

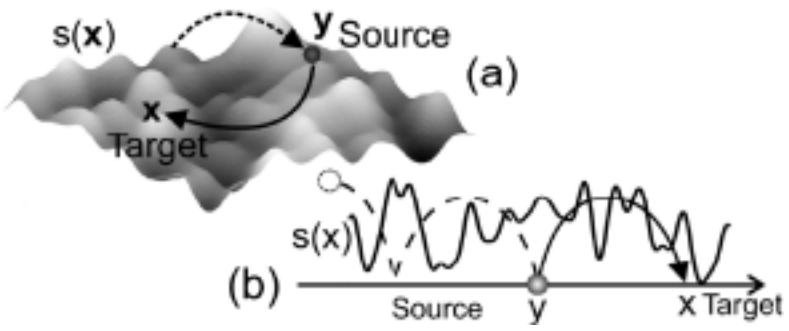

Figure 1: Random walk processes in inhomogeneous salience fields *s(x)* in two (a) and one (b) dimensions. Source and target locations of a random jump are denoted by *y* and *x*, respectively.

number of physical and biological systems are in conflict with this relation and exhibit anomalous diffusion. Whenever the spatio-temporal scaling relation $|X(t)| \sim t^{1/\mu}$ with an exponent $0 < \mu < 2$ is observed a system is said to exhibit superdiffusive behavior. Theoretically, superdiffusion is often accounted for by scale free random walks [4] which have become known as Lévy flights. They can be described macroscopically by a fractional diffusion equation,

$$\partial_t p(x,t) = D_\mu \Delta^{\mu/2} p(x,t)$$

in which the ordinary Laplacian is replaced by a fractional operator. A generalization of this equation suitable for spatially structured systems is given by

$$\partial_t p = s^c \Delta^{\mu/2} s^{c-1} p - p s^{c-1} \Delta^{\mu/2} s^c$$

in which the spatial heterogeneity is modeled by a salience field $s(x) > 0$ and the key parameter $0 \le c \le 1$ which governs the impact of origin and destination locations on the transition rate (Fig.1). Our analysis reveals that unlike ordinary random walks, non-local superdiffusive processes show distinct regimes of attenuation and acceleration (Fig.2). Consequently, spatial inhomogeneities can facilitate the spread of superdiffusive processes, in contrast to the common belief that external disorder generally slows down stochastic processes.

Figure 2: The impact of source and target location on the asymtotics of random walk processes. The quantity $G_{\mu,c}(0)$ describes the impact of the heterogeneity on the asymptotic dispersal magnitude. Positive or negative values of this quantity indicate that the process is slowed or sped up, respectively. Only Lévy flights can exhibit facilitated dispersal speed.

Wavepropagation in Reaction-Superdiffusion dynamics

One of the fundamental processes involved in nonequilibrium pattern formation is the spatial propagation of interfaces or fronts. One of the most prominent models that exhibits propagating fronts is the Fisher-Kolmogorov-Petrovsky-Piscounov (FKPP) equation for the spatial concentration $u(x,t)$ of a reacting agent: $\partial_1 u = \lambda u(1-u) + D\Delta u$. The description of physical and biological systems with this type of equation assumes that the number of particles is sufficiently high such that fluctuations can be neglected and that particles disperse diffusively in space. When the assumption on diffusion is relaxed and superdiffusive agents are considered one is tempted to generalize the FKPPE by replacing the diffusion term with the fractional operator introduced above:

$$\partial_t u = \lambda u(1-u) + D\Delta^{\mu/2} u$$

This equation has been studied in detail [5] and unlike the original FKPPE it does not exhibit constant speed traveling wave front solutions with an exponential front shape. A key result of our study is that fractional reaction-superdiffusion equations of the type above are structurally unstable: As soon as arbitrarily small fluctuation are introduced (i.e. an arbitrarily large but finite number of reacting particles) constant speed front propagation and exponential front shapes are recovered much like in ordinary reaction-diffusion systems.

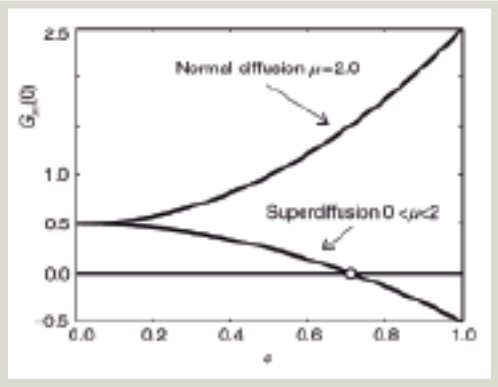

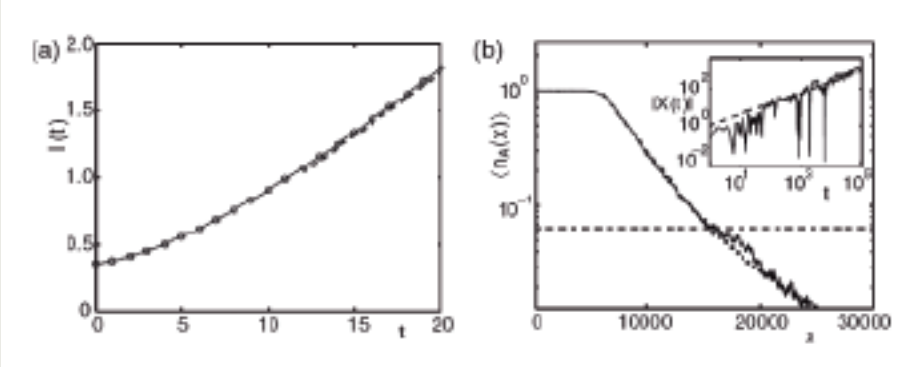

Figure 3: Asymptotic front velocity in the full stochastic model of a paradigmatic two particle reaction kinetic scheme *A+B →2A*. (a) The solid line depicts the total mass *I(t)* of type A particles as a function of time. A constant front velocity is attained asymptotically (dashed line). (b) Average shape of the wave front of type A particles in the linear regime.

[1] D. J. Watts and S. H. Strogatz, *Nature* **393** (6684), 440 (1998); M. E. J. Newman, *Proceedings of the National Academy of Sciences of the United States of America* **103** (23), 8577 (2006); A. L. Barabasi and R. Albert, *Science* **286** (5439), 509 (1999).
[2] V. Belik and D. Brockmann, *New Journal of Physics* **9**, 54 (2007).
[3] D. Brockmann and L. Hufnagel, *Phys Rev Lett* **98** (17), 178301 (2007).
[4] T. Geisel, J. Nierwetberg, and A. Zacherl, *Phys Rev Lett* **54**, 616 (1985); T. Geisel, A. Zacherl, and G. Radons, *Phys Rev Lett* **59**, 2503 (1987).
[5] D. del-Castillo-Negrete, B. A. Carreras, and V. E. Lynch, *Phys Rev Lett* **91** (1) (2003); R. Mancinelli, D. Vergni, and A. Vulpiani, *Physica D-Nonlinear Phenomena* **185** (3-4), 175 (2003).

Transport and Non-linear Dynamics in Mesoscopic Systems

R. Fleischmann, T. Kottos, H. Schanz (until Spring 2007), T. Geisel
O. Bendix, K. Bröking, H. Hennig, J.A. Mendéz-Bermúdez (now at Puebla, Mexico), J. Metzger
D. Cohen (Ben Gurion Univ., Israel), L. Hufnagel (EMBL Heidelberg),
H.-J Stöckmann (Univ. Marburg), D. Weiss (Univ. Regensburg)

Micro- and nanoscale semiconductor electronic and optical devices are prime examples of mesoscopic systems that inspire our activities in this project. Not only are these interesting from a technological point of view but provide superb models for studying fundamental aspects of mesoscopic wave propagation, Hamiltonian non-linear dynamics, quantum chaotic systems and the transition from ballistic transport to branched flows and localization. In this report we focus on our recent progress in the understanding of mesoscopic conductance fluctuations [1] as an example of our past and ongoing activities stretching from the study of scared wave functions in quantum graphs to the light transmission through the retina [2].

A prominent feature of electronic transport in mesoscopic systems is that the conductance as a function of an external parameter, e.g., a gate voltage or a magnetic field, shows reproducible fluctuations caused by quantum interference [3]. In a disordered mesoscopic conductor – which is smaller than the phase coherence length of the charge carriers but large compared to the average impurity spac-

ing – the transmission is the result of the interference of many different, multiply scattered, and complicated paths through the system. As these paths are typically very long compared to the wavelength of the charge carriers the accumulated phase along a path changes basically randomly when the external parameter is varied. This results in a random interference pattern, i.e., reproducible fluctuations in the conductance of a universal magnitude on the order of $2e^2/h$, the so-called *universal conductance fluctuations* [4]. The role of disorder in providing a distribution of random phases can as well be taken by chaos. Thus ballistic mesoscopic cavities like quantum dots in high-mobility two-dimensional electron gases that form chaotic billiards show the same universal fluctuations. If the average of the phase gain accumulated on the different paths traversing the system exists, the conductance curves are smooth on parameter scales that correspond to a change of the average phase gain on the order of and smaller than the wavelength of the carriers. In systems with mixed phase space, where chaotic and regular motion coexist, this phase gain, however, is typically algebraically distributed, and an average phase gain does not exist (neglecting the finiteness of the coherence length and assuming the semiclassical limit $h_{eff} \to 0$). Therefore the conductance curve of such a system fluctuates on all parameter scales and forms a fractal. The fractal dimension D is connected to the exponent γ of the algebraic distribution of phase gains by $D = 2 - \gamma/2$ [5]. This prediction from semiclassical theory inspired a number of both theoretical and experimental works and such fractal conductance fluctuations (*FCFs*) have since been confirmed in gold nanowires and in mesoscopic semiconductor quantum dots in various experiments [6]. The whole scope of conductance fluctuations is, however, still not understood. Motivated by puzzling experimental results showing a dependence of the fractal dimension on the coherence length [7], we studied the classical limit of transport through quantum dots finding fractal fluctuations. We were able to explain and generalize these findings and have shown that the conductance of purely classical low-dimensional Hamiltonian systems very fundamentally exhibits fractal fluctuations, as long as transport is at least partially conducted by chaotic dynamics. Thus not only mixed phase space systems, but fully chaotic systems as well, generally show FCFs with a fractal dimension determined by fundamental properties of chaotic dynamics [1].

How Hamiltonian chaotic dynamics leads to fractal fluctuations in the conductance, i.e. the transmission, shall be demonstrated in the paradigmatic case of the standard map

$$q_{t+1} = (q_t + p_{t+1}) \bmod 2\pi$$
$$p_{t+1} = p_t + K \sin(q_t),$$

which goes through the whole KAM route to chaos: from integrable ($K = 0$) via a mixed phase space to fully chaotic in dependence of the non-linearity parameter K (for the K values used below the phase space is fully chaotic). One can think of the map taking the role of the *Poincare surface of section* in a billiard model of a quantum dot. We attach *leads* to the map by opening it at $p = \pm\pi n$, i.e. we start trajectories on the line $p = -\pi n$ and follow the dynamics until they are leaving the region of interest ("the system") either at $p = +\pi n$ (transmission) or at $p = -\pi n$ (reflection).

To visualize the phase space structures responsible for the reproducible fluctuations we split the exit set (the phase space part that leaves the system in the next iteration) into a transmission and a reflection part and color code them red and blue. We then iterate the map backwards in time and see that red and blue lobes form in the injection lead, i.e. the phase space below $p = -\pi n$ (Fig. 1 top left; the complete time reversed mapping is visualized in the top right for the 1st and 4th backward iteration). These lobes form by the characteristic stretching-and-folding action of chaotic

dynamics. An important finding is that the thickness w of these lobes is *algebraically distributed*, $n(w) \propto w^{-\alpha}$, even for fully developed chaos (a heuristic argument for this is given in [1] connecting α to the escape-rate γ and the Lyapunov-exponent λ; see Fig.1 bottom center) and not exponentially as one might have expected. The action of small external parameter changes (here the variation of K) is mainly to shift these lobe structures over the starting line $p = -\pi n$ (Fig. 1 center row). Each lobe's contribution to the transmission (red) or the reflection (blue) is given by the length of the segment of the starting line intersecting with the lobe. The variation of this length with K leads to spike like structures in the transmission curve T(K) (Fig.1 top center) with a maximal height $\Delta T_{max} \propto w^{\beta}$ (Fig.1 lower left). We could analytically estimate the fractal dimension of the transmission (i.e. conductance) curve and found

$$D = \alpha - \beta.$$

In conclusion, we could show that transport through chaotic systems due to the typical lobe structure of the phase space in general produces fractal conductance curves, where the fractal dimension reflects the distribution of lobes in the exit and/or entry set. In contrast to the semiclassical effect, the size of the fluctuations is not universal, but depends on specific system parameters. Due to the fractal nature of the classical conductance, however, there is no parameter scale that separates coherent and incoherent fluctuations.

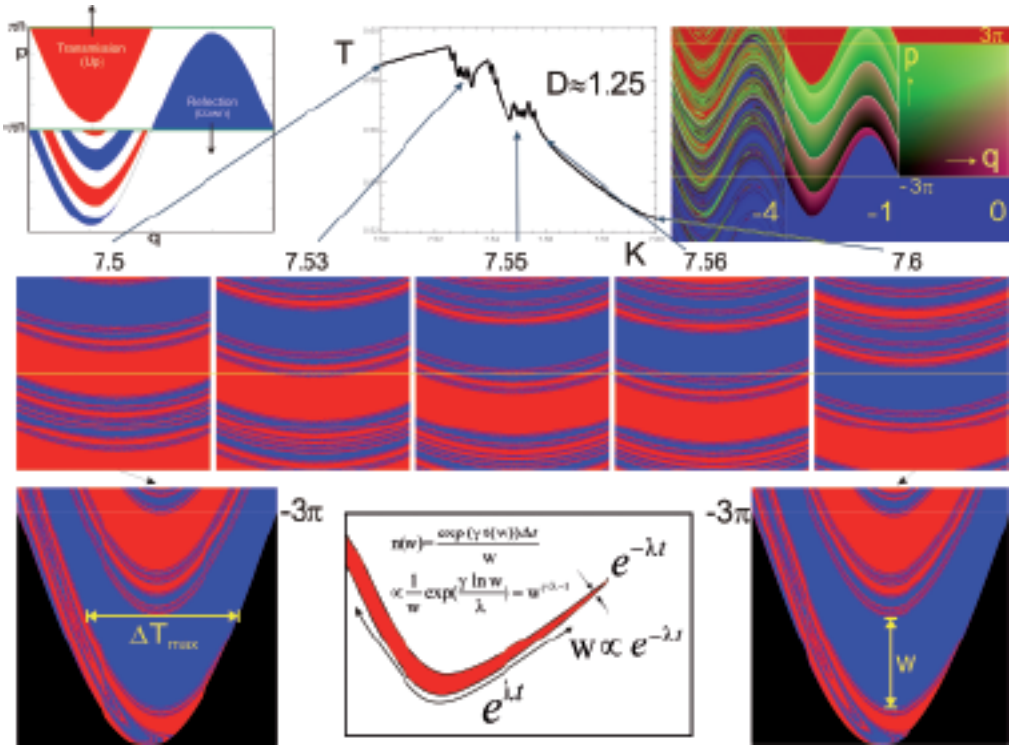

Figure 1
The typical lobe structure of the phase space of chaotic systems leads to fractal transmission fluctuations (n=3)

[1] H. Hennig, R. Fleischmann, L. Hufnagel, and T. Geisel, Phys. Rev. E **76**, 015202 (R) 2007.
[2] e.g. H. Schanz and T. Kottos, *Phys. Rev. Lett.*, 90:234101, 2003; O. Bendix, R. Fleischmann, and J. Metzger, *in preparation (2008)*; D. Cohen, T. Kottos, and H. Schanz, *Journal of Physics A: Math. Gen.*, **39**:11755-11771 (2006); M. Weiss, A. Méndez-Bermúdez, and T. Kottos, *Physical Review B*, **73**:045103 (2006); O. Bendix, J.A. Méndez-Bermúdez, G.A. Luna-Acosta, U. Kuhl, and H.-J. Stöckmann, *Microelectronics Journal*, **36**:285-288, 2005; M. Prusty and H. Schanz, Phys. Rev. Lett., 98:176804 (2007); M. Prusty and H. Schanz, *Phys. Rev. Lett.* **96**:130601 (2006)

[3] C. M. Marcus et al., *Phys. Rev. Lett.* **69**, 506 (1992).
[4] See e.g. *Introduction to Mesoscopic Physics*, edited by Y. Imry, Oxford University Press, Oxford, 2002.
[5] R. Ketzmerick, *Phys. Rev. B* **54**, 10841 (1996); L. Hufnagel, R. Ketzmerick, and M. Weiss, *Europhys. Lett.* **54**, 703 (2001).
[6] H. Hegger et al., *Phys. Rev. Lett.* **77,** 3885 (1996); A. S. Sachrajda et al., Phys. Rev. Lett. **80**, 1948 (1998); A. P. Micolich et al., J. *Phys.: Condens. Matter* **10**, 1339 (1998); Y. Ochiai et al., Semicond. Sci. Technol. **13**, A15 (1998); Y. Takagaki, *Phys. Rev. B* **62**, 10255 (2000).
[7] A. P. Micolich et al., *Phys. Rev. Lett.* **87**, 036802 (2001); A. P. Micolich et al., Physica E **13**, 683 (2002).

Quantum Chaos and Mesoscopic Transport with Interacting Bosons

T. Kottos, R. Fleischmann
T. Geisel, M. Hiller, H. Hennig
D. Cohen (BGU, Israel), A Ossipov (Nottingham, U.K.), J. Bodyfelt, G.S. Ng (Wesleyan, USA)

Considerable progress in cryogenics during the last decades has made it possible to experimentally realize Bose-Einstein-Condensates (BECs), whose macroscopic quantum states have attracted the imagination of physicists for generations. One of the most fascinating experimental achievements was the realization and manipulation of BECs of ultra-cold atoms in optical lattices (OL) and the creation of "atom chips" which are suggested as potential building blocks for quantum information processing while at the same time they allow for novel, concrete applications of quantum mechanics such as atom interferometers and atom lasers. The precise tailoring and manipulation of OL on the other hand have allowed us to investigate complex solid state phenomena, such as the Mott-Insulator to superfluid transition, the Josephson effect, the atom blockade phenomenon in quantum-dot-like potentials, Anderson localization, and Bose-Glass transitions. In fact, it is envisioned that the emerging field of atomtronics (i.e. the atom analogue of electronic materials, devices and circuits) will be able to provide much more powerful devices in comparison with the solid-state ones where device imperfections and decoherence quickly destroy the delicate quantum effects. Finally, interacting bosonic systems, having a well defined classical limit, provide an excellent playground where fundamental issues related to the advancement of classical, semiclassical, and statistical methods can be addressed.

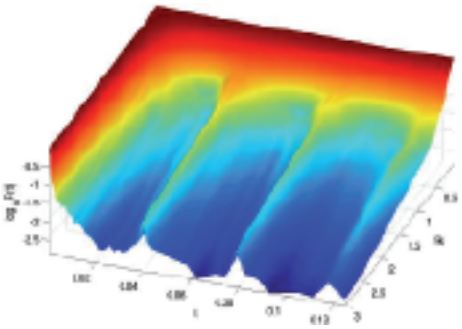

Figure 1
Parametric evolution of the fidelity F(t) for different perturbation strengths δk of the intersite coupling, as a function of time. The fidelity exhibits echoes at multiples of t_{echo} associated with the classical self-trapping effect due to non-linear interactions between bosons.

Among all the exciting issues raised in the framework of interacting bosonic systems, we have chosen to organize our group's research efforts on studying their response to external driving fields (say perturbations of the intersite coupling δk), and on their transport and decay properties from an OL. More specifically, in a series of recent papers [1,2,3] we

have analyzed the parametric evolution of the Local Density of States (sudden limit), wave-packet dynamics scenario (rectangular perturbations) and Fidelity decay (time-reverse perturbations) for the case of bosons loaded in a three site lattice (quantum trimer). Issues like quantum chaos, decoherence and quantum-classical correspondence were in the focus of these investigations. An important outcome of these studies was the identification of pronounced structures in the energy landscape of the perturbation operator which reflect the underlying classical lattice dynamics. The most dramatic consequences were observed in the study of quantum irreversibility. We found the appearance of pronounced echoes (see Fig.1) in the Fidelity, which are associated with the so-called self-trapping mechanism in non-linear lattices. Making use of this effect, we were able to 'engineer' the Fidelity echoes by preparing the initial state at a specific energy [3].

Recently [4] we proposed a BEC stirring device which can be regarded as the incorporation of a quantum pump into a closed circuit: it produces a DC circulating current in response to a cyclic adiabatic change of two control parameters of an optical trap (the on-site potential $v_0 = \varepsilon$ of one well, termed the "shuttle", and the relative coupling $(k_1 - k_2)/(k_1 k_2)$ between the "shuttle" and the other wells of the OL, see Fig.2). Using the Kubo formalism we found that the nature of the transport process depends crucially on the sign and on the strength of the interatomic interactions. We distinguished between four regimes of dynamical behavior: For strong repulsive interaction the particles are transported one-by-one, which we call sequential crossing; For weaker repulsive interaction we observe gradual crossing or coherent mega crossing; Finally, for strong attractive interaction the particles are glued together and behave like a huge classical ball that rolls from trap to trap. We expect the induced circulating atomic current to be extremely accurate,

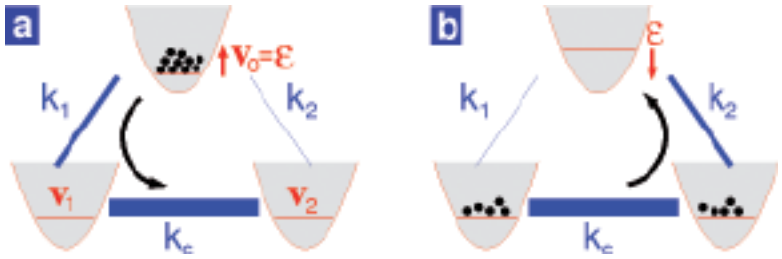

Figure 2: Illustration of the model system. In the first half of the cycle **(a)** the particles are transported from the "shuttle" to the "canal" via the k_1 bond, while in the second half of the cycle **(b)** the particles are transported back from the "canal" to the "shuttle" via the k_2 bond. See the text for further details.

which would open the way to various applications, either as a new metrological standard, or as a component of a new type of quantum information processing device.

We have also addressed the decay properties of Bose-Einstein-Condensates in leaking (open) OLs. In [5] we have analyzed the open Bose-Hubbard model with two sites and we have shown that the inverse lifetimes undergo a cascade of bifurcations. Specifically we showed that the decay process is much more complicated than the one dictated by the standard linear rate equation. Motivated by these findings, we have investigated (in the mean field limit), the outgoing current of BECs loaded in larger OLs [6]. We found that for some critical values of the rescaled (with respect to the lattice size) interatomic interaction strength, the current decays in avalanches that follow a power-law distribution (see Fig.3) indicating the existence of a novel phase transition. This behavior is due to the creation of stable discrete breathers and reflect the complexity of the underlying classical phase-space.

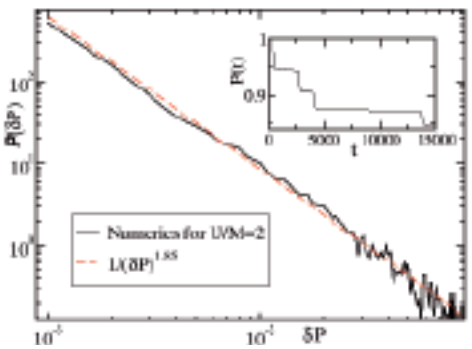

Figure 3
Distribution (over initial conditions) of avalanches P(δP) for an open optical lattice with a rescaled interatomic interaction U/M=2, where M=128 is the sample size, and U is the interatomic interactions (in units of the intra-tunneling rate). A scale free power law distribution is evident. The best linear fit is indicated with the red dashed line. Inset: A representative realization of the decaying BEC population P(t) showing avalanches.

[1] M. Hiller, T. Kottos, and T. Geisel, *Phys. Rev. A* **73**, 061604(R) (2006).
[2] M. Hiller, T. Kottos, and T. Geisel, *in preparation* (2007).
[3] J. D. Bodyfelt, M. Hiller, and T. Kottos, *Europhys. Lett.* **78**, 50003 (2007).
[4] M. Hiller, T. Kottos and D. Cohen, *submitted* (2007); arXiv:0708.4304v1
[5] M. Hiller, T. Kottos, and A. Ossipov, *Phys. Rev. A* **73**, 063625 (2006).
[6] G. S. Ng, H. Hennig, R. Fleischmann, T. Kottos, T. Geisel, *in preparation* (2007).

Photodissociation and Recombination of Molecules with Atmospheric Relevance

R. Schinke, S. Y. Grebenshchikov, M. V. Ivanov

The investigation of elementary reactions in the gas phase (exchange reactions, photodissociation, unimolecular dissociation etc.) is important for understanding the complicated chemistry, for example, in combustion and in the atmosphere. Our theoretical studies aim at reproducing detailed experimental data by *ab initio* methods, explaining measured data on the basis of fundamental equations and making predictions for experiments, which are difficult to perform in the laboratory. The tools are global potential energy surfaces (PESs), calculated in the Born-Oppenheimer approximation by solving the electronic Schrödinger equation, and the solution of the nuclear Schrödinger equation for the intramolecular dynamics of the atoms on these PESs [1,2]. In recent years we concentrated our activities on two molecules, ozone (O_3) and nitrogen dioxide (NO_2), which both are under intense experimental investigations in many laboratories.

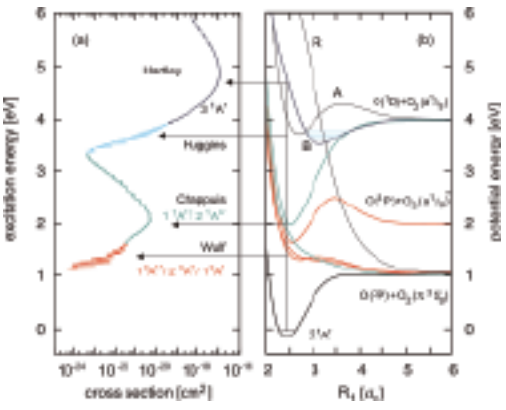

Figure 1
(a) The measured absorption cross section (in cm^2; logarithmic scale) of ozone as function of the excitation energy. **(b)** One-dimensional cuts through the potential energy surfaces relevant for the photodissociation of ozone. R_1 is one of the O–O bond lengths; the other one is fixed at $R_2 = 2.43a_0$ and the bond angle is $\alpha = 117°$. $E = 0$ corresponds to $O_3(X)$ in the ground vibrational state (zero point energy). The horizontal arrows illustrate the electronic assignments of the absorption bands. From Grebenshchikov et al., *Phys. Chem. Chem. Phys.* **9** (2007) 2044.

Our studies of the photodissociation of O_3,

$$O_3 + h\upsilon \rightarrow O + O_2 \quad , \quad (1)$$

are more or less completed and the results have been summarized in Ref. [3]. The photoabsorption cross section of ozone in the wavelength region from the near ir to the near uv shows four different bands: Wulf, Chappuis, Huggins and Hartley [Fig.1(a)]. Each band corresponds to one (or several) particular electronic states which are excited by the photon. Calculations have been performed for all bands. The quantitative description of process (1) requires the calculation of PESs of all electronic states involved, each being a function of the three internal coordinates of O_3. In addition, the non-Born Oppenheimer coupling elements are required if more than one state is involved – and that is indeed the case in all bands. Fig.1(b) shows one-dimensional cuts along the dissociation coordinate of all states of ozone, which take part in the photodissociation. For ten states global PESs have been determined. Quantum mechanical dynamics calculations, i.e., the solutions of either the time-independent or the time-dependent Schrödinger equation, yield the absorption spectrum and the final rotational-vibrational product state distributions. The

comparison of the theoretical results with detailed experimental data is generally very good [3]. In our most recent effort to unravel the photophysics of ozone we considered two additional bands following the Hartley band and extended the calculations up to the vacuum uv wavelength region [4]. In particular, we could unambiguously identify the electronic states excited in the 7 eV band as well as in the 9 eV band. In conclusion, the calculations, performed in Göttingen over the past five years, yielded – for the first time – a quite complete dynamical picture of reaction (1) up to photon energies of ~ 9 eV.

The photodissociation of NO_2 is equally important and challenging. In 2007 we started calculations similar to ozone and calculated PESs of several highly excited states of $^2A'$ symmetry. We concentrated on the second absorption band which in many respects parallels the dissociation of ozone in the Hartley band. First dynamics calculations are in reasonable agreement with experimental data [5]. However, they also raise interesting questions concerning either the limitations of the calculations or the interpretation of the experiments.

The recombination of ozone,

$$O + O_2 + M \rightarrow O_3 + M \quad , \qquad (2)$$

in collisions of O atoms and O_2 molecules is a very complicated process; here, the atom (or molecule) M is necessary to carry away the excess energy. Despite the many experimental and theoretical studies over several decades it is not yet really understood. Questions concern the temperature dependence of the formation rate coefficient, and thus the formation mechanism (energy transfer or chaperon mechanism or both), and its surprisingly strong isotope dependence [6]. The latter effect leads to a non-statistical distribution of isotopomers in the atmosphere as has been first measured in the 1980'ies by means of balloon experiments. Especially the isotope dependence has inspired a great deal of interest among theorists because it seems to reveal a fundamental reaction mechanism. Up to now there is no satisfactory explanation on the basis of real *ab initio* calculations; a status report critically reviews all the dynamical calculations in the last decade to explain this effect [7]. The more realistic calculations (statistical and classical mechanics calculations), each of which however makes some model assumptions, hint at the difference of zero-point energies in the different channels, in which the highly vibrationally excited ozone complexes can dissociate, as the main cause of the isotope effect [8]. In our current work we are building a model which is based on rigorous quantum mechanical calculations for state-specific lifetimes of O_3^* resonances as well as a fully quantum mechanical description of the stabilization of the resonances in collisions with M. Because of the thermal averaging, such calculations are exceedingly complicated and time-consuming.

Because of the non-statistical (i.e., less chaotic) behaviour of ozone, its recombination appears to be a special case for a triatomic molecule. NO_2, on the other hand, is known to be classically chaotic. Its recombination can be much better described by customary methods [9].

[1] R. Schinke. *Photodissociation Dynamics.* Cambridge University Press, Cambridge, (1993).
[2] S. Yu. Grebenshchikov, R. Schinke and W. L. Hase. In *Unimolecular Kinetics*, edited by N. Green. (Elsevier, Amsterdam, 2003).
[3] S. Yu. Grebenshchikov et al., *Phys. Chem. Chem. Phys.* **9** (2007) 2044.
[4] R. Schinke and S. Yu. Grebenshchikov, DOI:10.1016-*J.Chem. Phys.*2007.08.024.
[5] R. Schinke, S. Yu. Grebenshchikov and H. Zhu, submitted.
[6] K. Mauersberger et al., Adv. At. *Mol. Opt. Phys.* **50** (2005) 1.
[7] R. Schinke et al., Annu. *Rev. Phys. Chem.* **57** (2006) 625.
[8] R. Schinke and P. Fleurat-Lessard, *J. Chem. Phys.* **120** (2005) 094317.
[9] M. V. Ivanov, H. Zhu and R. Schinke, *J. Chem. Phys.* **126** (2007) 054304.

Mathematical Aspects and Fundamentals of Turbulence

W. Pauls, H. Xu, E. Bodenschatz
T. Matsumoto (Kyoto, Japan), U. Frisch (Nice, France), J. Bec (Nice, France),
A. Pumir (Nice, France), J. van der Hoeven (Paris, France),
J.-Zh. Zhu, S. Kurien (Los Alamos, USA), R. Pandit, S. S. Ray (Bengaluru, India)

Mathematical aspects of turbulence

Mathematical study of turbulent flows is based on the Navier-Stokes equations, which are standardly used in physics and engineering, the most frequently considered case being that of incompressible flows. Since the main dimensionless parameter, the Reynolds number, is high, we are also lead to consider solutions of the Navier-Stokes equations in the limiting case of vanishing viscosity, which formally corresponds to the Euler equations.

In spite of substantial progress in the mathematical analysis of these two equations (see e.g. [1,2,3]), a number of fundamental problems remain unsolved. For example, it is unknown, for the Euler equations as well as for the Navier-Stokes equations, whether a three-dimensional flow with smooth initial conditions can become singular in a finite time. Actually, the regularity of the solutions of the Navier-Stokes equations is one of the seven Millennium Problems selected by the Clay Mathematical Institute [4].

One of the most prominent dynamic effects in inviscid flows or in flows with small viscosity is depletion, i.e. the tendency of the flow to suppress nonlinearities and to organize itself into structures that are almost stationary. Actually, the failure to prove the global regularity in the three-dimensional case is intimately related to this phenomenon. Depletion can be studied most effectively on the example of the Euler equations where it is not obscured by the presence of the viscous term. In the cases in which the existence and regularity of solutions is assured, such as the two-dimensional Euler and Navier-Stokes equations, it plays an important part in determining the long-time dynamics of the solutions.

To address these issues, in particular the question of existence of finite-time singularities in three dimensions we use the following approach: for real analytic initial conditions solutions of the Euler and the Navier-Stokes equations are analytically continued to complex values of the spatial variables, in which case the hydrodynamic fields also assume complex values. It is known that any real finite-time singularities are necessarily preceded by complex ones. Therefore, numerically one can detect the possible appearance of real finite-time singularities by monitoring the dynamics of the complex singularities. One possibility to study the structure and the temporal behavior of the complex singularities consists in analyzing the Fourier coefficients of the solutions, see [5,6].

In particular, we have studied in detail the analytic properties of the solutions of the two- and threedimensional Euler equations by using formal expansions and ultra high-precision arithmetics [7,6]. We have found that the scaling of the solutions depends on the initial conditions, being thus non-universal. In some cases we were able to determine the scaling exponent with the relative precision of about 10^{-6}. We conjecture that the reason for the observed non-universal behavior of the solutions is the depletion phenomenon. One of the goals for the future is to study more extensively the complex singularities of solutions in three dimensions, in particular with respect to dependence on the initial conditions.

For the Navier-Stokes equations we found that for the initial conditions of the type studied in [5,7,6] we can use the formal expansion of the type introduced by Sinai in [8]. The expansions used for the Euler equations are then recovered in the limit of the vanishing

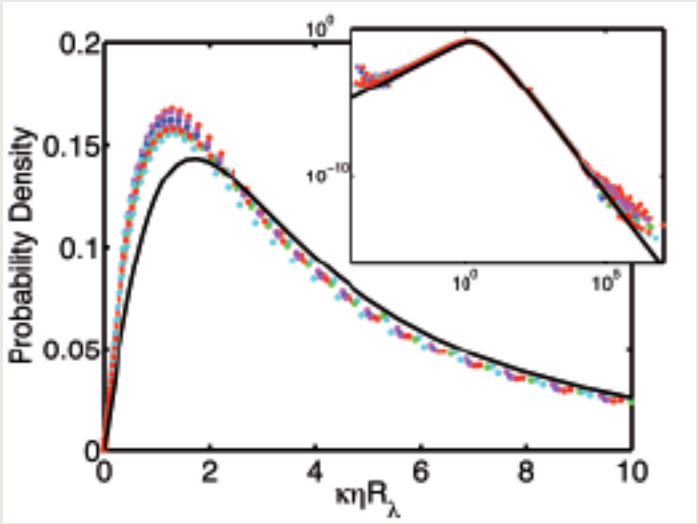

Figure 1: (adapted from Ref. [13]) The PDFs of curvature normalized by the Kolmogorov length scale η and the Reynolds number R_λ, compared with the prediction based on the Gaussian model. The inset shows the data plotted on logarithmic axes. Our theory clearly captures the power-law tails of the PDF. The data collapse for the different Reynolds numbers, but the peak of the model PDF is different from that of the experimental PDFs.

viscosity. It is an important task for the future to perform a careful numerical and analytical analysis of these expansions and to study their extensions to more complicated initial conditions.

Bottleneck phenomenon in fully developed turbulence

It has been found recently that for many equations of hydrodynamical type, including the Navier-Stokes equation, the use of hyperviscosity with a high power of the Laplacian becomes asymptotically – that is when the power of the Laplacian is increased while keeping the effective dissipation threshold constant – equivalent to using a Galerkin truncation with zero dissipation. This observation may have some consequences for numerical simulations of turbulence, since hyperviscosity with high powers of the Laplacian is frequently used in computations to increase the inertial range for a given resolution. Actually, high values of the dissipativity lead to new phenomena which can make the expected benefit illusory but which are of interest by themselves.

Recently, Chichowlas et al. have studied the temporal dynamics of the Galerkin-truncated three-dimensional Euler equations [9]. At intermediate times the system starts thermalizing at the wave-numbers close to the truncation wave-number, with the high-wavenumber energy spectrum k^2 corresponding to the absolute equilibrium. At lower wavenumbers the spectrum exhibits an inertial range comparable to that of the standard fully-developed turbulence with $k^{-5/3}$ spectrum. To improve our understanding of the intermediate-time dynamics of Galerkintruncated system we are currently studying the Galerkin-truncated one-dimensional Burgers equation, in collaboration with S.S. Ray and R. Pandit from the Indian Institute of Science.

We have shown that the bump in the energy spectrum – also called the bottleneck – which is observed in numerical simulations using hyperviscosity (and sometimes in simulations using only the normal viscosity) is actually a counterpart of the energy pile-up close to the truncation wave-number in Galerkin-truncated systems. From this observation follows, for example, that the statistics of the flow in the bottleneck region are close to Gaussian, the intermittency being suppressed.

Lagrangian geometric structures in intense turbulence

The last decade has witnessed a growing interest in the Lagrangian perspectives of turbulence, stimulated by the success of explai-

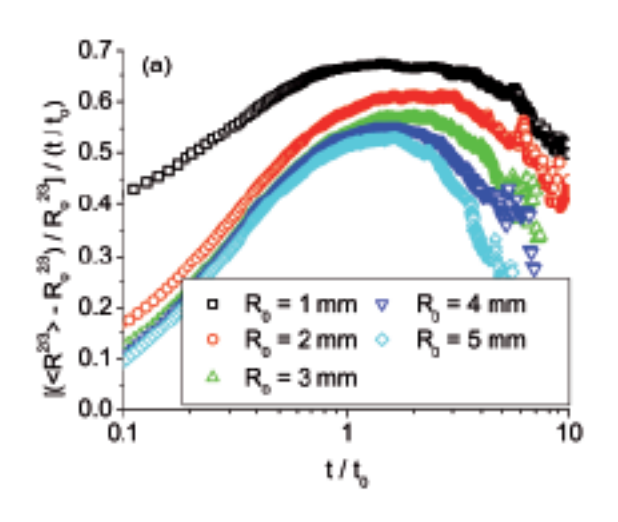

Figure 2
Plot of $(\langle R^{2/3}\rangle - R_0^{2/3})/R_0^{2/3}/(t/t_0)$, which should show a plateau region independent of the initial separation R_0 for times $t_0 << t << T_L$, if there is a Richardson scaling range. The existence of the plateaus are clear, but the values of the plateaus still depend on initial separation at the Reynolds number of the experiment ($R_\lambda = 690$).

ning the anomalous scaling of passive scalars [10,11], which had been a long-time puzzle when studied in Eulerian framework alone. Geometric information along Lagrangian trajectories has been also analyzed and related to the turbulence properties.

It has been found recently from numerical simulations that the probability density function (PDF) of the curvature of Lagrangian trajectories in turbulent flows have pronounced power-law tails [12]. The same power laws are also observed in our particle tracking experiments [13]. It is then tempting to relate the large curvature events to the intense vortex filaments in turbulence. A detailed analysis, however, reveals that the large curvature events are actually resulted from the reversal of the flow and a simple model based on Gaussian statistics captures the tails of the PDFs (Fig.1). On the other hand, if curvatures are averaged over a time interval of the order of Kolmogorov time scale, then the tails are absent and there exists a good correlation between the high accelerations and the large averaged curvature events [13].

The simplest geometric object involving more than one Lagrangian particle is a line segment connecting the two particles. The evolution of the length of the segment, $R(t)$, in a turbulent flow is the long-standing relative dispersion problem. Richardson studied this problem the first time and proposed a model equation, which predicted that the mean square separation should increase with time as t^3 [14], independent of their initial separation R_0. Our experimental data showed that the initial separation actually plays an important role in the relative dispersion problem. As predicted by Batchelor [15], only when the time is larger than a time scale $t_0 = (R_0^2/\varepsilon)^{1/3}$, the separation may become independent of R_0 [16]. Using the recently developed technique to connect interrupted trajectory segments (see p.84–87), we are able to obtain long time statistics which demonstrate the existence of a $\langle R^2\rangle \sim t^3$ range, but the scaling is not universal, i.e., the scaling coefficient still depends on initial separation (Fig. 2). An extrapolation of the current data implies that a truly Richardson region may only be observed if $R_\lambda \sim 10^4$ [17].

For three-dimensional flow, a minimum of 4 points is needed in order to describe the effect of turbulence. Such a "tetrad model" have been proposed before [18] and have been checked in numerical simulations [19,20] and experiments at relative low Reynolds numbers [21]. We observed the same change of the shape of tetrahedra in intense turbulence [17], namely, three-dimensional turbulence in general tends to flatten isotropic objects by

compressing in one direction while expanding in the other two directions. We are currently collaborating with A. Pumir at CNRS-Nice, France, one of the developers of the tetrad model, to investigate the dynamics following these Lagrangian tetrahedra and the preliminary results are exciting.

[1] P. Constantin, in *Mathematics Unlimited-2001 and Beyond*, Springer-Verlag, 2001, 353–360.
[2] A. J. Majda and A. L. Bertozzi, *Vorticity and Incompressible Flows*, Cambridge University Press, 2002.
[3] C. Bardos and E. S. Titi, *Russian Math. Surveys* **62** (2007) 409–451.
[4] http://www.claymath.org/millennium/
[5] T. Matsumoto, J. Bec and U. Frisch, *Fluid Dynamics Research* **36** (2005) 221–237.
[6] W. Pauls, Complex Singularities of Incompressible Inviscid Flows, *PhD thesis*, 2007.
[7] W. Pauls et. al., *Physica D* **219** (2006) 40–59.
[8] Ya. Sinai, Power Series for Solutions of the 3*D*Navier–Stokes System on *R*3, *J. Stat. Phys.* **121** 779–803.
[9] C. Cichowlas et al., *Phys. Rev. Lett.* (2005), 264502.
[10] B. I. Shraiman and E. D. Siggia, *N*ature **405** (2000) 639.
[11] G. Falkovich, K. Gawedzki, M. Vergassola, *Rev. Mod. Phys.* **73** (2001) 913.
[12] W. Braun, F. De Lillo, B. Eckhardt, *J*. Turbul. **7** (2006) 62.
[13] H. Xu, N. T. Ouellette, E. Bodenschatz, *Phys. Rev. Lett.* **98** (2007) 050201.
[14] L. F. Richardson, *Proc. Roy. Soc. Lond. A*, **110** (1926) 709.
[15] G. K. Batchelor, *Q. J. R. Meteorol. Soc.*, **76** (1950) 133.
[16] M. Bourgoin et al., *Science*, **311** (2006) 835.
[17] H. Xu, N. T. Ouellette, E. Bodenschatz, *New. J. Phys. in press*, (2007).
[18] M. Chertkov, A. Pumir, B. I. Shraiman, *Phys. Fluids* **11** (1999) 2394.
[19] A. Pumir, B. I. Shraiman, M. Chertkov, *Phys. Rev. Lett.* **85** (2000) 5324.
[20] L. Biferale et al., *Phys. Fluids* **17** (2005) 111701.
[21] B. Lüthi et al., *J. Turbul.* **8** (2007) 45.

Topical Group

Networks, Signaling and Control

How do viruses spread in pandemics and infect millions of people in short time and how can we prevent this? How do neurons communicate, both on the physico-chemical level at individual synaptic connections and on the level of large and complicated networks that compose our brain? How does structure influence function in cells and their constituents? These are just some fundamental aspects of a broader question we are interested in: What are the principles underlying the transfer, spreading and processing of information and resources in complex systems?

The topical group *Networks, Signaling and Control* conjoins those activities of the Institute in the natural and life sciences that address this common theme. Still, the phenomena studied are found on a large variety of temporal and spatial scales, from global, international distances to cellular and sub-cellular sizes – and from years to milliseconds. Moreover, the recent results presented here contain experimental and theoretical work, partially in joined projects, from fields as distinct as epidemiology, systems neuroscience, and cellular biophysics. Far beyond the discovery and identification of new phenomena, we focus on a deeper understanding of why and how these occur. Consequently, not only experimental methods are developed further. In parallel we explore and consolidate advanced ways of analyzing nonlinear time series from data and the subject often forces new routes in theory and mathematics that are similar across the particular systems studied. This unifies the topical group also from the methodological side: Besides other examples, the theory of stochastic processes is developed and applied in studies of epidemic spreading as well as of the response properties of individual nerve cells; and aspects of mathematical graph theory are used to obtain insights into the heterogeneous connectivity of networks of social contacts, the precise timing of signals in neuronal networks and the impact of structure onto function in sensing and processing in single cells.

On the next pages, we present some of our key results of the past years of research, with contributors from the three departments, the Network Dynamics Group, as well as independent research fellows working at the institute (F. Theis, T. Tzvetanov, A. Neef, D. Bibitchkov). The projects cover novel findings on systems from three major sub-areas that are also defined by both temporal and spatial scales: There is a contribution by D. Brockmann and collaborators that studies dynamic spreading of diseases on geographical and national scales. Several distinct studies discuss different aspects of processing in neural systems, from the control of behaviour (Herrmann, Geisel) and the precise dynamics of neuronal networks (Tzvetanov, Timme) to the fine but important details of synaptic signaling between individual neurons (Bibitchkov, Wolf) and often combining theory and experimentation. Finally, two contributions elaborate on novel insights into the structure of and the information flow in cellular and subcellular processes (Beta, Pfohl).

A recent highlight is the finding by A. Levina, M. Herrmann and T. Geisel that and how neural networks are capable of self-organizing themselves into a critical state using adaptive synaptic connections. This theoretical study provides the first consistent explanation of recent experimental findings that neuronal systems under certain conditions may show electrical activity that is organized in avalanches, i.e. occurs with a size distribution that exhibits power law decay. Similar phenomena are well-known in the physics of phase-transitions, but their experimental evidence in neurobiological systems came as a critical surprise that is now elucidated theoretically.

Emergent Geographical Community Structures: Universalities and National Differences

D. Brockmann, F. Theis
V. David, T. Geisel

GEOGRAPHICAL COMMUNITIES and their boundaries are key determinants of various spatially extended dynamical phenomena. Examples are migration dynamics of species, the spread of infectious diseases, bioinvasive processes, and the spatial evolution of language. The given geopolitical segmentation of geographies into nations, divisions, federal states, regions and counties is typically hierarchical, evolved historically and is primarily determined by cultural differences (e.g. languages, dialects), geological factors (rivers, mountain ranges) and historical events. Independent of this geographical classification into coherent multi-scale regions, human traffic networks have evolved that couple various regions on all length scales. Given the intensity and range or modern travel, it becomes a difficult task to quantify the importance of boundaries between regions, particularly between countries, and to identify similarities between communities based on human traffic. In this project we investigate how multi-scale human transportation networks encode geographical community structures, how they differ from geopolitical classifications and whether they are spatially coherent.

Our analysis is based on a proxy network for human transportation obtained from the geographic circulation of more than 10 million dollar bills in the United States recorded at the bill tracking website *www.wheresgeorge.com*. The data extends that of a previous study on the discovery of scaling laws of human [1] travel by an order of magnitude and permits an approach to multi-scale human transportation from a network perspective. In this approach the nodes of the network are 3109 counties in the United States. The flux of dollar bills between the counties is given by a weight matrix W. Each element W_{nm} counts the number of bills that traveled between counties n and m. The network is roughly symmetric and strongly heterogeneous. The heterogeneity is reflected in the distribution of three quantities: 1.) the weights W_{nm} 2.) the flux of bills per node $F_N = \sum_m W_{nm}$ in and out of a node and 3.) the degree of the node k_n, i.e. the number of other nodes a given node is connected to. All three quanties are broadly distributed (Fig.1).

A number of sophisticated graph-cutting algorithms to identify hidden cluster or community structure in symmetric weighted networks

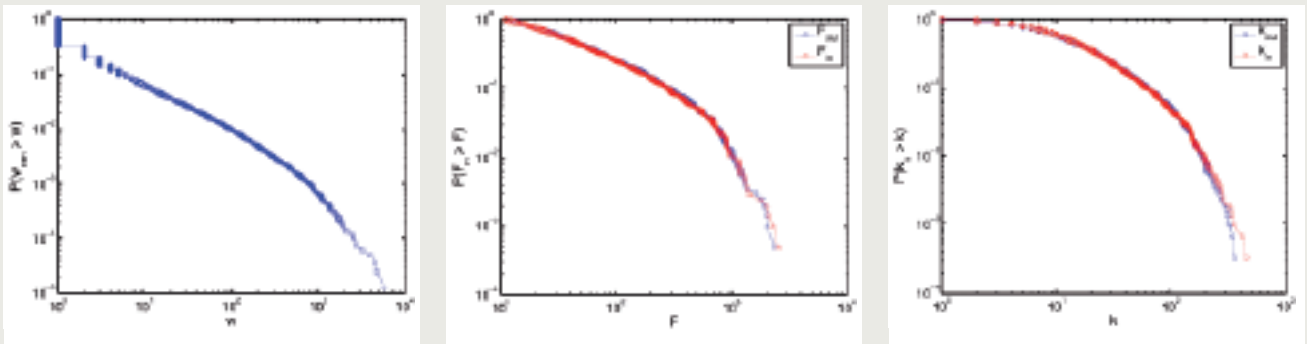

Figure 1: Heterogeneity of multi-scale transportation networks: **Left**: Cummulative probability of weights. **Center**: Cummulative probability of node flux. **Right**: Integrated degree distribution.

Figure 2: Multi-scale human traffic network. Each figure depicts the connectivity of the most connected counties in the United States in terms of most intense traffic flow. The algorithm for community identification is unware of the embedding illustrated on the right. It only knows the connectivity depicted on the left.

have been developed recently [2]. Most of these algorithms try to maximize a quantity known as the modularity of a network partitioning, i.e. a segmentation of the set of nodes into k groups. Qualitatively the modularity of a potential partitioning of a network computes the total link weight within each cluster and compares this to the expected total weight. A high value for the modularity is achieved when the partitioning reflects the internal community structure of the network.

Unlike other complex networks (e.g. gene regulatory networks or author citation networks) transportation network are embedded in a metric space, i.e. the nodes possess positional information and one can exploit this additional information in order to compute traffic based geographical community structure. In our project we do the opposite. We ask: How much community structure is encoded in the transportation network's topology alone, ignoring the spatial information. We thus apply a maximum modularity algorithm that only knows the topological structure as defined by the weight matrix. The main results of our analysis are shown in Fig. 3 and can be summarized as follows: Even though the algorithm has no information on the geographic location of the nodes, it identifies spatially coherent communities. This is a big, big surprise. The United States can be separated in to approx. 11 most independent regions. Although effective boundaries of these regions correlate with federal state boundar-

Figure 3: **Large scale community structure of the United States as encoded in the global transportation network. The map on the right shows a segmentation of the New England States into communities on a finer scale.**

ies, predominantly they do not coincide with political boundaries. If one applies the same algorithm on a finer scale, e.g. starting out with the New England cluster, the algorithm again identifies spatially coherent communities on a finer scale.

Currently we are investigating large scale community structures of Europe given various national and international transportation networks for sixteen European countries, examples of which are depicted in Fig. 4.

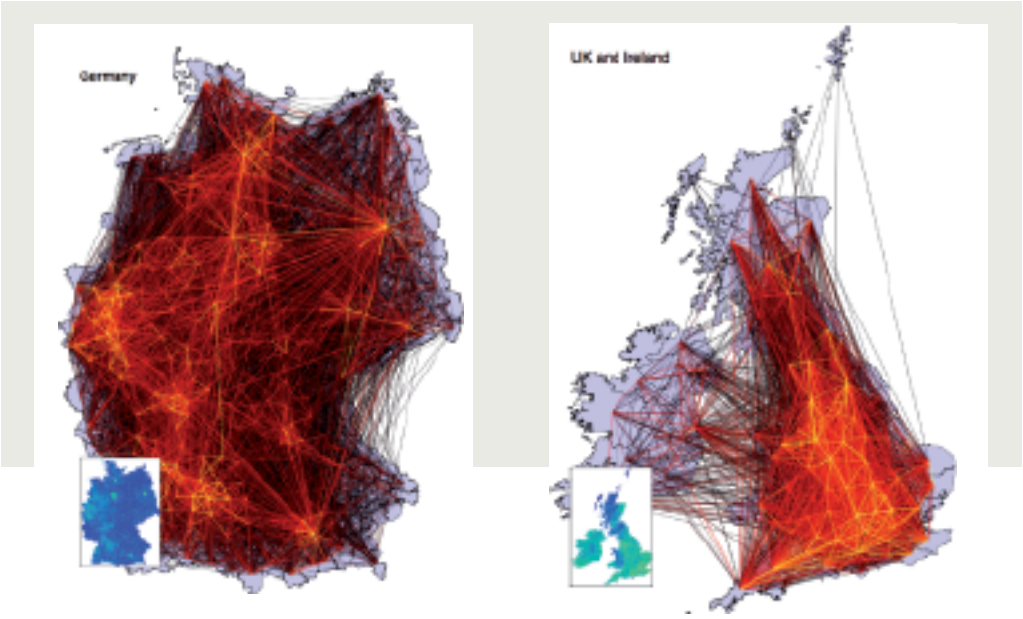

Figure 4: Multi-Scale Transportation networks: Germany (left) and United Kingdom and Ireland (right).

[1] D. Brockmann, L. Hufnagel, and T. Geisel, *Nature* **439** (7075), 462 (2006).
[2] M. E. J. Newman, *Physical Review E* **74** (3) (2006); M. E. J. Newman, Proceedings of the National Academy of Sciences of the United States of America 103 (23), 8577 (2006).

Criticality in the Control of Behavior

J. M. Herrmann, T. Geisel
A. Levina, K. Fiedler, G. Martius, F. Hesse,
F. Theis, T. Pfohl, A. Biess, R. Der

Self-Organized Criticality in the Activity Dynamics of Neural Networks

Neural networks display characteristics of critical dynamics in the neural activities [1]. This theoretical prediction was confirmed by the power-law statistics for the size of avalanches of neural activity in real neurons [2], where the critical behavior is re-approached even after a substantial perturbation of the parameters of the system. These findings provide evidence for the presence of self-organized criticality (SOC) [3], a key concept to describe the emergence of complexity in nature. It is present in a large number of seemingly unrelated phenomena such as piling of granular media, plate tectonics and stick–slip motion. Particularly in neural systems, however, it raises questions concerning the underlying mechanisms of the regulation towards the critical state and the functional role of the phenomenon.

For a globally coupled network of rather simple model neurons *special parameter values* have been identified that give rise to a power-law distribution of the responses to weak external stimulation [1]. More recently, we have provided numerical evidence [4] that a realistic neurotransmitter dynamics at the synapses of the network leads to a phase transition towards a critical regime such that a nearly critical behavior is present even for a *broad range* of the maximum synaptic efficiency (Fig. 2). A breakthrough was the analytical treatment of the interaction between the neural activity and the synaptic transmitter dynamics [5]. In this study it was shown that the self-organized critical behavior is typical due to a self-tuning of system parameters towards critical effective values. It is particularly interesting that biologically realistic synaptic dynamics causes the neuronal avalanches to turn from an exceptional phenomenon into a typical and robust self-organized critical behavior, with the only condition that the total resources of neurotransmitters exceed a certain minimum value.

A suggestive explanation of the functional role of self-organized criticality results from

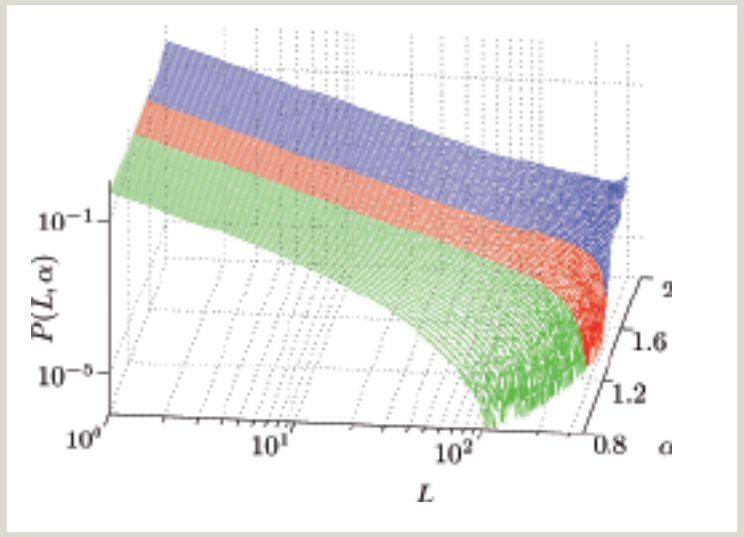

Figure 1: Probability distributions of the avalanche size L in the neural activity of a globally coupled network with dynamical synapses. In a finite system (N=300) we observe different dynamical regimes for an increasing maximal synaptic efficiency α: sub-critical (green), critical (red), and super-critical (blue). With increasing system size the critical regime is enlarged and eventually covers the full range above a certain value of α.

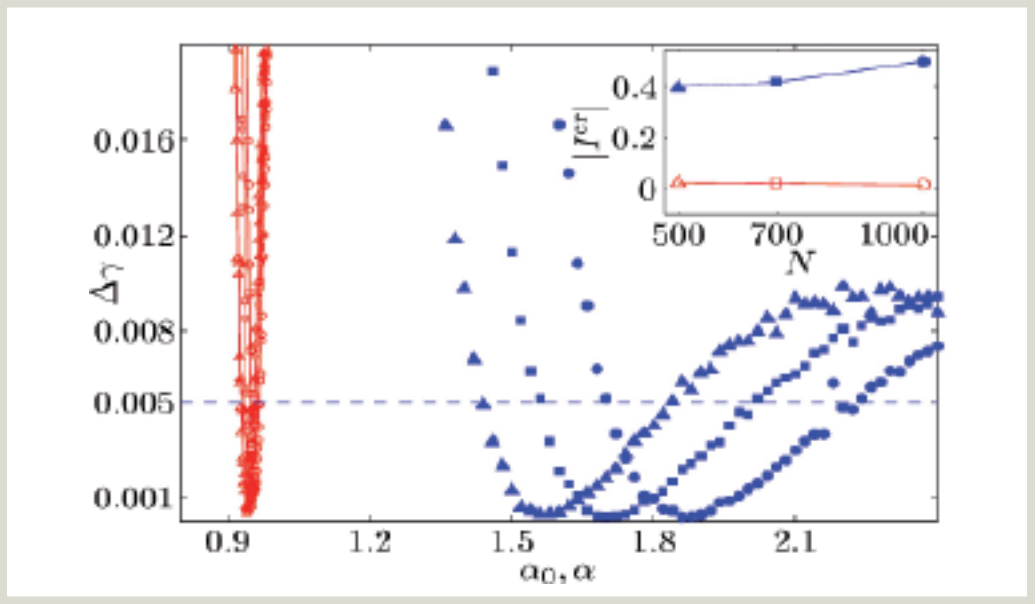

Figure 2: The quality of fit of the power law (see Fig. 1) is shown as a function of the synaptic strength α_0 for static synapses (red) and as a function of the maximal synaptic efficiency α for dynamic synapses (blue). The inset shows the width of the interval where the fitting error is below 0.005. For the dynamic synapses this interval increases for increasing system size and has been shown analytically to diverge.

an effectiveness constraint. If the system adjusts its parameters such that each spike causes on average one of the target neurons to become subsequently active and, on the other hand, the total activity is to remain bounded and stationary, then it can be proved within the framework of branching theory that the resulting activity distribution is indeed critical. Moreover, this consideration allowed us to derive a learning rule from first principles that guides the system towards criticality and resembles biological learning rules [6].

Criticality and Self-organization of Behavior

The biological function of self-organized criticality is much less understood than the physical mechanisms behind this phenomenon. A stereotyped response to external stimuli would be less advantageous than a flexible reaction which may amplify barely noticeable events in the environment based on information which has been accumulated in the internal state of the brain. Critical dynamics thus seems beneficial to living beings and it is known to bring about optimal computational capabilities, optimal transmission and storage of information, and sensitivity to sensory stimuli. It may represent a state where many options are available to the organisms and which is effective in development, fall-back behaviors, and exploration. We are interested in the developmental aspects of motor behavior in animals which we study in biomorphic autonomous robots, see Fig. 3. Here the work on the neural systems needs to be extended to incorporate the interaction with the environment. In simplified examples it can be shown explicitly that criticality is achieved from an objective function that characterizes both the sensitivity of the behavior with respect to sensory inputs and the predictability of the sensory effect while performing a behavior. The question whether such principles are effective also in simple organisms is a topic of cooperation in the MPIDS.

In physically realistic simulations of autonomous robots with various sensory configurations and body shapes we obtain a continuous flow of behaviors that explores the variety of interactions of the robot with its environment. There remains, however, a restriction to self-

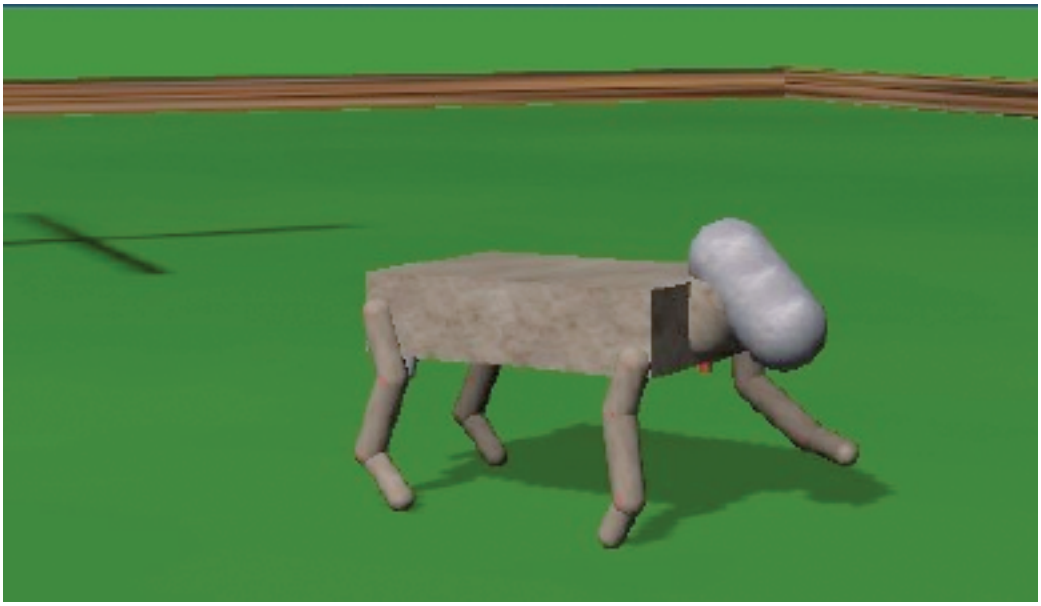

Figure 3: Physically realistic simulation of a four-legged robot. From the objective of simultaneous sensitivity of the behavior with respect to sensory inputs and predictability of sensory effects of the behavior, the quadruped generates autonomously a variety of behaviors that include rising and lowering, coordination of leg movements, and basic locomotory movements.

organized solutions of relatively simple control problems such as the coordination of limb movements. In order to achieve complex and goal-directed behaviors we consider an architecture where the low-level criticalization is complemented by a additional learning mechanisms which evaluate the learning progress of the low-level adaptation in various environmental situations [9] or which use external reward signals to select behaviors which are generated by the self-organizing controller [11]. Presently, the controller is replaced by a multi-agent control system where individual agents engage in the control of the robot if their prediction of the current behavior of the robot is sufficiently reliable, cf. Figs. 4 and 5. This approach revealed a similarity to pattern forming algorithms studied in the visual system [12]. They seem to be relevant also for the development of motor representations, where the competition among agents leads to a specialization of the corresponding behav-

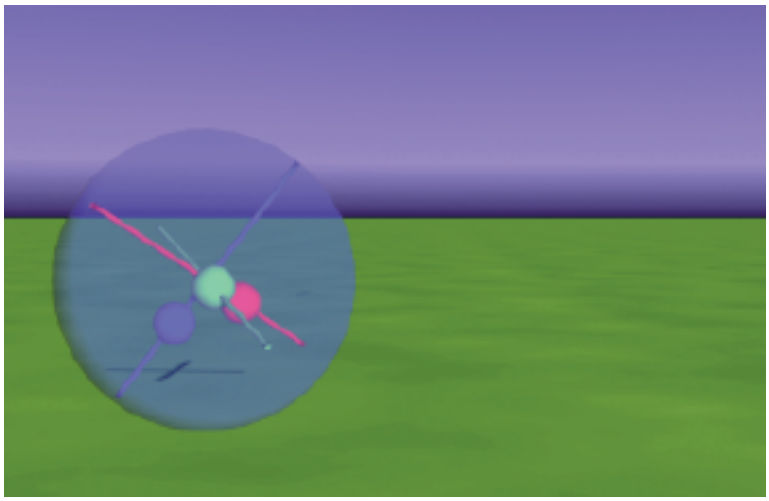

Figure 4: Physically realistic simulation of a spherical robot which is driven by three internally movable masses.

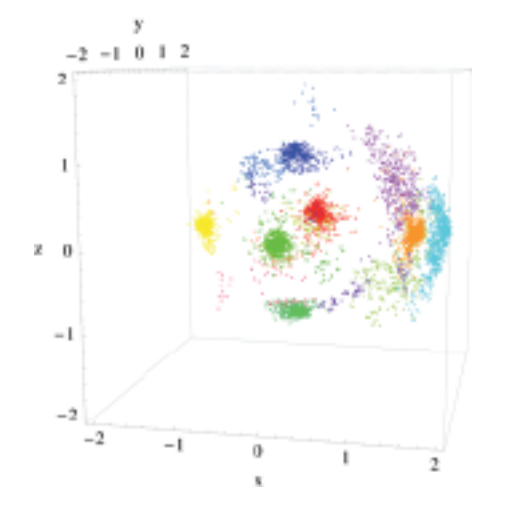

Figure 5: When controlled by a multi-agent system, the spherical robot (Fig. 4) develops representations of a number of natural behaviors where each behavior corresponds to one controlling agent. The thereby emerging elementary behaviors are characterized by one fixed axis and a coordinated movement of the masses along the other two axes.

iors which can be interpreted as elementary behaviors. In order to connect the results of this project more closely to results from biological experiments as well as to evaluate the behaviors emerging in the robots we are studying algorithms for the analysis of complex data, which focus on intrinsic significance measures for the detection of relevant data features [7, 8]. The interaction of the controller with the sensory system and memory is studied in an integrated architecture that was originally developed for attention mechanisms [13], but proved to be generalizable to the control of bio-robots.

[1] C. W. Eurich, J. M. Herrmann, U.Ernst, *Phys. Rev. E* **66** (2002).
[2] J. Beggs and D. Plenz, *J Neurosci.* **23**, 11167 (2003).
[3] P. Bak, C. Tang, K. Wiesenfeld, *Phys. Rev. Lett.* **59,** 381 (1987).
[4] A. Levina, J. M. Herrmann, T. Geisel, *Adv. in Neural Information Proc. Syst.* (2005).
[5] A. Levina, J. M. Herrmann, T. Geisel, Nature Physics, doi:10.1038/nphys758 (2007).
[6] A. Levina, U. Ernst, J. M. Herrmann,. *Neurocomputing*, **70**:1877-1881 (2007).
[7] J. M. Herrmann, F. Theis, In: H. Yin et al. (eds.), *IDEAL 2007*, LNCS **4881**, Springer, 198 (2007).
[8] M. Voultsidou, S. Dodel, J. M. Herrmann.*Comput. & Visualiz. in Science*, **10:2**, 100-110 (2007).
[9] F. Hesse, R. Der, J. M. Herrmann. In: L. Berthouze et al. (eds), *EpiRob*, Cognitive Studies **134**, 37-44 (2007).
[10] K. Doubrovinski J. M. Herrmann. *Neural Computation*, accepted (2008).
[11] G. Martius, J. M. Herrmann, R. Der. In F. Almeida e Costa (ed.), *ECAL 2007*, LNCS **4648**, Springer, 766-775, 2007.
[12] N. M. Mayer, J. M. Herrmann, M. Asada, T. Geisel, *J. Korean Phys. Soc.* **50**, 150-157 (2007).
[13] H. Schrobsdorff, M. Ihrke, B. Kabisch, J. Behrendt, M. Hasselhorn, J. M. Herrmann, *Connection Science* **19**, *203-221* (2007).

Understanding Visual Perception of Orientation and Motion through Local Contextual Interactions

T. Tzvetanov
J.M. Herrmann

The visual system of humans and other primate species is highly efficient in coding and processing visual information together with being strongly influenced by high-level cognitive processes such as visual attention. Human perceptual skills are the consequence of thousands of neuronal activations in visual cortex. These neurons individually contribute to the perception of the environmental input through a still discussed decoding scheme [1]. Our general scientific interests are concerned with understanding human perceptual performances on low-level visual features, e.g. orientation or motion, based on theoretical and computational principles derived from neurophysiological knowledge of the areas coding the features.

Our current main scientific interest concerns the investigation of contextual interactions in perception of orientation and direction of motion and their understanding from the viewpoint of computational neuroscience. The interests in the contextual effects for both domains come from knowledge in all three scientific approaches: theoretical considerations, neurophysiology, and psychophysics. Both theoretical features have circular definition, their neurophysiological coding in areas V1 and MT have strong similarities, and, for the few comparisons available, psychophysics reports hint toward similar contextual effects in both circular domains. Therefore, this project is to simultaneously investigate the contextual effects on perception of orientation and direction of motion when task relevant stimuli are flanked or surrounded with supplementary stimuli, and to propose a common theoretical work for predicting the human perceptual results (Fig. 1). The project is built on the three insights based on theoretical, neurophysiological and psychophysical knowledge.

The features "orientation" and "direction of motion" are defined in circular space, with the former spanning 180 degrees range and the later 360 degrees range. Therefore, they can be normalized to a common circular dimension within a range of -1 and 1, for example.

The way the two features are represented at the earliest cortical stages, area V1 for orientation and area MT for direction of motion, demonstrates strong similarities in the way they are encoded in the neuronal population [7]. Both areas show hypercolumn structures, with neurons representing all possible orientations/directions of motion at a given spatial location, together with a good retinotopic representation of the visual field. This implementation scheme is believed to relate the strong contextual modulations in neurophysiology and psychophysics [2].

The performance of human subjects in detection and perception of orientation or direction of motion of a target stimulus is strongly influenced by surrounding stimuli. Thus, the contextual modulation exerted by task-irrelevant surrounding stimuli on behaviorally relevant central stimuli is demonstrated behaviorally. These contextual modulations are observed with two psychophysics measures: (1) "Contrast" detection changes of the stimulus due to flanking stimuli (orientation [3]; direction of motion [4,2]) repulsion effect on perceived orientation/direction of motion of a target stimulus due to surrounding stimuli (orientation [5]; direction of motion [6]).

This project is built on the above theoretical and practical knowledge and the main track of the project is that the contextual effects in orientation and direction of motion should

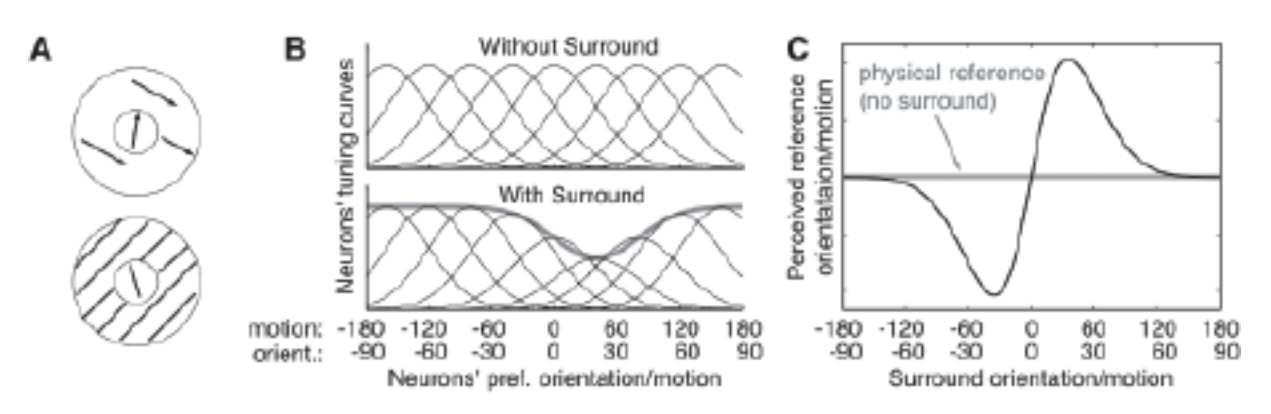

Figure 1: (A) Example of an experimental configuration of center-target stimulus surrounded by an annular task-irrelevant stimulus (top: motion direction; bottom: orientation). (B) Theoretical uniform population of neurons responding to the center stimulus, arranged in hypercolumn representation of the feature (all neurons have identical tuning characteristics: maximal firing rate, tuning width). The graphics represent a subset of neuronal tuning curves with various preferred values (top: no surround is present around the center stimulus; bottom: the presence of the surround at +40/+20 deg. decreases the max. firing rate of a subset of the neuronal population – model following neurophysiological reports). (C) Prediction of perceived reference point as a function of the surround orientation/motion direction for a discrimination task around the reference: E.g. is the stimulus clockwise/counterclockwise from the vertical = 0 deg.

be explained using a common background given the circular feature behavior of both domains. If the final perceptual outcome is based on identical theoretical neuronal structure coding circular feature, then the accumulated experimental and theoretical knowledge should allow a unified explanation of contextual effects in circular space.

The practical work will investigate in multiple psychophysics experiments the perception of human subjects of target stimuli when flanked with surrounding task-irrelevant stimuli. It will allow a full characterization of the interactions and collect behavioral data. The common modeling framework based on neurophysiological knowledge will be tested on the data for predicting the perceptual outcomes (see Fig. 1 for an illustration of repulsion effect). The final aim of this project is to look for theoretical understanding of the computational structure present in the brain that is involved in coding circular features across visual space.

[1] Abbott & Dayan (2001) Theoretical Neuroscience, MIT press
[2] Hubel & Wiesel (1974a) J. Compar. Neurol. **158**, 267–294; Hubel & Wiesel (1974b) *J. Compar. Neurol.* **158**, 295–306; Born & Bradley (2005) *Ann. Rev. Neurosci.* **28**, 157–189.
[3] Polat (1999) *Spatial Vis.* **12**, 143–162; Dresp (1999) *Spatial Vis.* **12**, 129–142; Tzvetanov & Simon (2006) Vis. Res. 46, 1302-1306.
[4] Walker & Powell (1974) *Nature* **252**, 732–733; Nawrot & Sekuler (1990) *Vis. Res.* **30**, 1439–1451; Ido et al. (2000) *Vis. Res.* **40**, 503–516;
[5] Kapadia, Westheimer & Gilbert (2000) *J. Neurophys.* **84**, 2048–2062.
[6] Kim & Wilson (1997) *Vis. Res.* **37**, 991–1005; Tzvetanov et al. (2006) *Vis. Res.* **46**, 3651–3658.
[7] Mayer, Herrmann, Asada & Geisel (2007) *J. Korean Phys. Soc.* **50** (S01), 150-157

Patterns of Precisely Timed Spikes in Strongly Hetergeneous Neural Networks

R.-M. Memmesheimer, M. Timme
S. Jahnke, F. van Bussel. F. Wolf, T. Geisel
M. Denker, S. Grün (RIKEN Brain Science Institute, Japan)

Patterns of precisely timed and spatially distributed spikes have been experimentally observed in different neuronal systems [1,2]. These spike patterns correlate with external stimuli (events) and are thus considered key features of neural computation [3]. Their dynamical origin, however, is unclear. One possible explanation for their occurrence is the existence of excitatorily coupled feed-forward structures, synfire chains [4,5], which are embedded in a network of otherwise random connectivity and receive a large number of random external inputs. In complementary theoretical modeling studies we investigate whether precise spike timing and temporal locking can naturally arise in the nonlinear dynamics of recurrent neural networks that contain no additionally embedded feed-forward structures. In particular, we study how a system simultaneously exhibiting significant interaction delays, a complicated network connectivity, and strong heterogeneities can still coordinate the timing of spikes of different neurons, possibly even if they are not directly linked by a synapse. We have addressed four groups of phenomena:

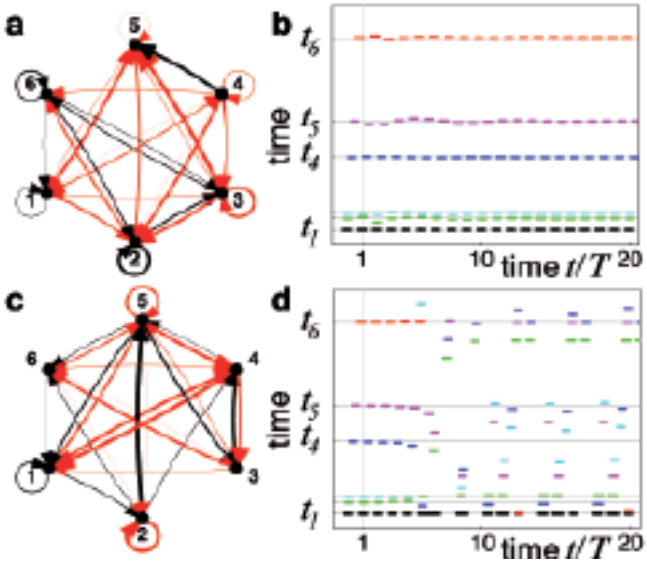

Figure 1: Two different networks (a), (c) realize the same predefined pattern ((b), (d) grey lines). A small random perturbation is applied at the beginning of the second period. The network dynamics (spike times relative to the spikes of neuron 1, color coded for each neuron), shows that in network (a) the pattern is stable and thus regained after a few periods (b); in network (c) it is unstable (d) and eventually another pattern will be assumed.

Speed Limits to Coordinating Spike Times

In large networks of spiking neurons, we uncovered a topology-induced speed limit to coordinating spike times [6] and explained both the speed and its limit via random matrix theory. The mechanism underlying the coordinating barrier points to a cooperative effect of the existence of a minimum time a neuron needs to generate subsequent spikes, the temporally discrete communication between neurons and their complex interaction network [7].

Heterogeneous Networks with Specific Dynamics

Under which conditions can spiking neural networks exhibit certain predefined patterns of precisely timed spikes? For a broad class of model networks (that include, among other features, strong heterogeneities, complicated connectivity and distributed delays) we found analytical restrictions defining the subset of all networks (parameterized by features of single neurons and their interactions) which exhibit an arbitrary predefined pattern [8,9]. This provides a novel method to find potential network structures, for instance by modifying the synaptic interaction strengths that generate a desired, e.g. experimentally observed dynamics. In particular, the method enables us to find stable and unstable patterns (Fig.1), which might both be computationally relevant, cf. [10,11]. In a first application, we

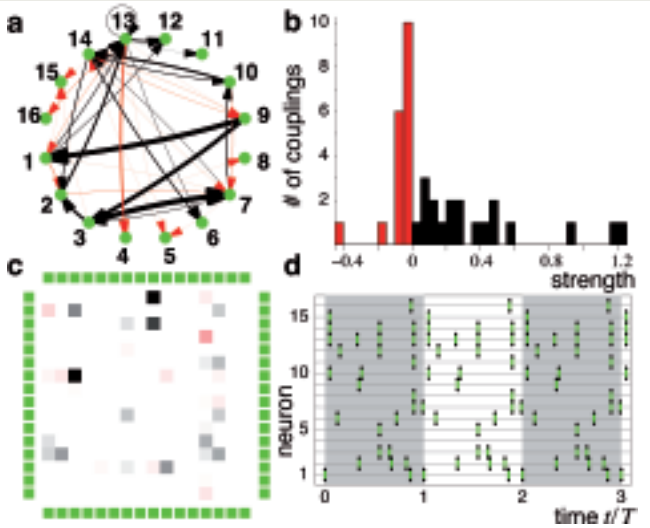

Figure 2: Network exhibiting a predefined dynamics and simultaneously minimizing wiring costs (in L1-norm). The network realizes a minimal number of connections under the dynamical condition that the predefined spike pattern is invariant. (a) Network solution is sparse, with excitatory (black) and inhibitory (red) connections; thickness proportional to coupling strength. (b) Heterogeneous distribution of coupling strengths. (c) Same network in matrix representation also indicates sparseness and heterogeneity. (d) Numerical simulations of spiking dynamics (green bars) shows that the network indeed exactly exhibits the predefined spike patterns (underlying black bars).

combined this network design with additional requirements onto the resulting network, for instance realizing networks with a given type of coupling (e.g., only inhibitory) and a given type of connectivity (e.g., with exponentially distributed number of synapses per neuron) which simultaneously exhibits a desired spike pattern.

In a second application, we exploited the general perspective in order to determine networks that exhibit a predefined pattern, but simultaneously optimize structural features, e.g. minimize wiring costs [12] (Fig.2). Current work proceeds towards further refinement and generalization of the design method as well as on its practical applications.

Recent experimental results [13] obtained by the group of Wolf Singer, Max Planck Institute for Brain Research, Frankfurt, strongly indicate the importance of the precise timing of spikes in unprecedented detail. The experimentally observed second order spike patterns are as yet unexplained. This initiated a further intense investigation of the origin of precise timing in recurrent networks. Furthermore, in collaboration with the Bernstein Center for Computational Neuroscience Berlin and the RIKEN Brain Science Institute, we recently developed a novel method for detecting precise timing dependencies between spiking activity and the coarser signal of local field potentials (LFPs) [M. Denker et al., in preparation]. Application of the method to activity recorded from motor cortex of awake behaving monkeys revealed that during a movement preparation task spikes tend to keep a fixed phase relationship to the LFP, largely independent of the LFP amplitude [14].

Revealing Network Topology From Dynamics

When driving one or more units of a network, how does its collective dynamical response depend on the network topology? Starting with networks of simple model units we found that the dynamical response is characteristic of both the driving signal and the network connectivity [15]. Under weak conditions, measuring the dynamics of a driven network reveals where in the network a given unit is located. This uncovers partial information of the network topology from measuring the dynamics only. Recently, we used this insight to identify the network connectivity from repeated measurements of the precise spatio-temporal response dynamics [16]. It turned out that for sparsely connected networks, the number of experiments required

for faithful reconstruction scales sublinearly with network size, a feature that might be very advantageous when reconstructing real networks. So far, our theoretical analysis was focused on networks of one-dimensional units in relatively simple, e.g. periodic, states. To make the new promising method applicable to real-world networks we currently broaden the theoretical scope of the method to include, e.g., networks of multi-dimensional dynamical units and more complicated collective states.

How Chaotic is the Balanced State?

Highly irregular dynamics is a prominent feature of multi-dimensional complex systems and often attributed to chaos. Sparsely coupled networks of spiking neurons may exhibit very irregular dynamics. For a wide range of conditions, they display a balanced state [17] in which excitatory (positive) and inhibitory (negative) inputs to each neuron balance on average and only the fluctuations create spikes at irregular, seemingly random points in time. Mean field theory shows that such irregular balanced activity occurs in networks with excitatory and inhibitory recurrent feedback as well as in networks that receive external excitatory inputs and exhibit recurrent inhibition only. Going beyond mean field theory, our recent exact studies on the microscopic dynamics of the latter networks reveals that the dynamics is not chaotic but rather dynamically stable [18], a fact that comes as a surprise to many theoreticians, not only in the neurosciences (Fig. 3).

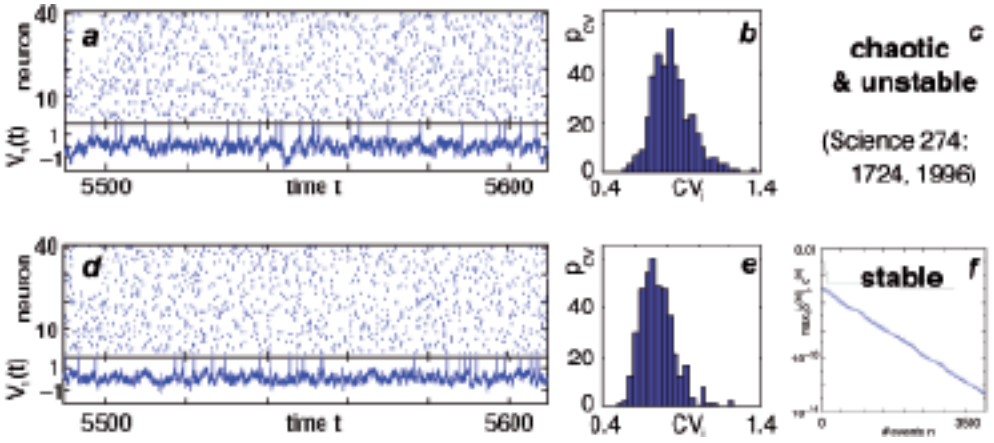

Figure 3: Dynamics of the balanced state in sparsely connected random networks. (a) -(c) For networks with excitatory and inhibitory recurrent connections, the balanced state of highly irregular activity is chaotic [17]. (d)-(f) Unexpectedly, for networks receiving external excitatory currents and recurrent inhibition a very similar irregular balanced state, that is even equivalent in mean field description, is dynamically stable [18]. (a),(d) Spiking dynamics of 40 out of 400 neurons and membrane potential trace of sample neuron 1, (b),(e) Coefficient of variation, (f) Exponential decay of dynamical perturbations indicates stability.

[1] M. Abeles et al., *J. Neurophysiol.* **70** (1993) 1629.
[2] Y. Ikegaya et al., *Science* **304** (2004) 559.
[3] M. Abeles *Science* **304** (2004) 523.
[4] M. Diesmann, M.-O. Gewaltig, and A. Aertsen, *Nature* **402** (1999) 529.
[5] Y. Aviel, C. Mehring, M. Abeles, and D. Horn, *Neural Comput.* **15** (2003) 1321.
[6] M. Timme, F. Wolf, and T. Geisel, *Phys. Rev. Lett.* **92** (2004) 074101.
[7] M. Timme, T. Geisel, and F. Wolf, *Chaos* **16** (2006) 015108.
[8] R.-M. Memmesheimer, M. Timme, and T. Geisel, in: *Verhandl. DPG **(VI)*** **40**, (2/2005), DY 22.6, pg 202.
[9] R.-M. Memmesheimer and M. Timme, *Phys. Rev. Lett.* **97** (2006) 188101.
[10] P. Ashwin and M. Timme, *Nonlinearity* **18** (2005) 2035.

[11] P. Ashwin and M. Timme, *Nature* **436** (2005) 36.
[12] R.-M. Memmesheimer and M. Timme, *Physica D* **224** (2006) 182.
[13] K. Gansel and W. Singer, *Soc. Neurosci. Abstr.* (2005) 276.8.
[14] M. Denker et al., *Neurocomputing* **70** (2007) 2096.
[15] M. Timme, *Europhys. Lett.* **76** (2006) 367.
[16] M. Timme, *Phys. Rev. Lett.* **98** (2007) 224101.
[17] C. van Vreeswijk and H. Sompolinsky, *Science* **274** (1996) 172.
[18] S. Jahnke, R.-M. Memmesheimer, and M. Timme, *Phys. Rev. Lett.* (2007) in press; http://arXiv.org:0705.3214v1

Role of Short Term Synaptic Plasticity in the Efficient Neural Signaling

D. Bibitchkov
M. Timme, H. Kielblock
E. Neher, H. Taschenberger, J. Bao (MPI for Biophysical Chemistry, Göttingen)

NEURONS COMMUNICATE with each other by sending and receiving short electrical pulses via synaptic connections. Precise knowledge of the properties of these signaling devices is crucial for understanding the processing of information in the brain. Such a description is complicated, taking into account that synapses are far from being static. Synapses show dynamic behavior in the transmission of signals from pre- to postsynaptic neuron, even on a short time scale (from milliseconds up to a few seconds). The aim of this study is to formulate a concise model of short-term synaptic plasticity in the calyx of Held, a giant synapse in the auditory brainstem, and to gain a better understanding of the role of the observed dynamics for the processing of sensory information in the auditory pathway.

The modelling is based on electrophysiological data obtained (by our collaborators at the *Max Planck Institute for Biophysical Chemistry*) from the recordings performed in rat brain stem slices. As a particular feature, the synapse shows pronounced short-term depression, a process that originates from the depletion of a pool of readily releasable vesicles during transmission of incoming spikes and leads to a decrease of postsynaptic responses during repeated stimulation. The data indicate that the dynamics of recovery of the vesicle pool from depression cannot be described using a single time scale; the synaptic dynamics can rather be modeled as a process with activity-dependent recovery rate. This type of dynamics leads to an adaptation of the speed of the vesicle replenishment to the frequency of presynaptic stimulation.

The obtained model well fits the experimental data (see fit at Fig.1). Using this model, we study the role of such realistic synaptic dynamics in the transmission of sensory information. Chemical synapses can be seen as devices transmitting information from sender (a presynaptic cell) to receiver (a postsynaptic cell) and transforming singular input events (spikes) into analogue outputs (post synaptic potentials). Therefore, we analyzed the properties of the synapse from

the perspective of information theory which provides an analytical framework to study efficiency of signal transmission through communication channels. Calculating the mutual information between presynaptic spike trains and postsynaptic responses at the synapse we estimate optimal stimulation conditions and synaptic parameters in terms of maximization of information transfer. The results show that activity-dependent recovery, when compared to synapses with fixed recovery rates, extends the frequency range in which the information about the interspike intervals is coded by synaptic responses, see Fig. 2.

Interestingly, the synaptic parameters observed for the calyx of Held are close to the theoretically predicted optimum, i.e. they maximize the amount of transmitted information for the physiologically relevant frequency range [1]. This indicates that short-term synaptic plasticity provides an adaptive mechanism for optimal transmission of relevant features of incoming signals through a synapse.

As a next step, we study how the observed synaptic dynamics could affect the behavior of networks of synaptically coupled cells. With reference to the auditory pathway it is yet unknown how synaptic dynamics affects the network participating in sound localization. Given that the above dynamic features are observed for a broad class of synapses, we will study their effects on the behavior of networks of coupled neuronal oscillators, which have so far only been investigated for fixed connection strengths, see e.g. [2]. These studies are expected to shed new light on how the synaptic dynamics can be utilized in the brain for relevant computations.

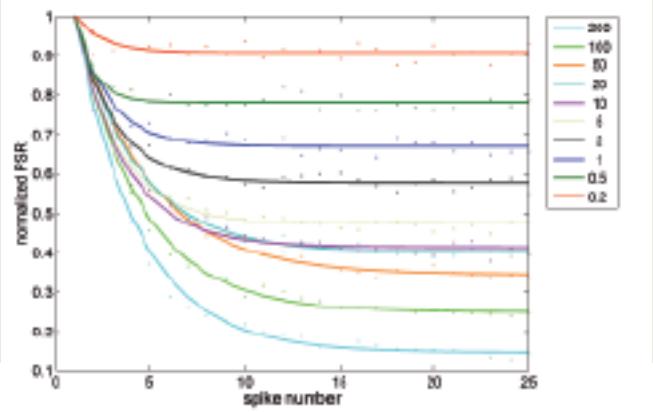

Figure 1: Postsynaptic responses to regular spike trains of various frequencies (from 0.2 to 200 Hz) recorded at the Calyx of Held synapses (dots) and simulated using the model of synaptic depression with frequency-dependent recovery (solid lines).

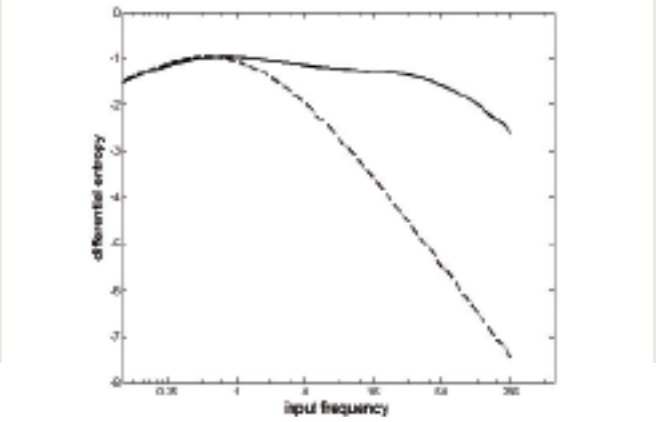

Figure 2: Information contained in postsynaptic responses of a deterministic depressing synapse about the interspike intervals plotted as function of presynaptic firing frequency. Solid line: synapse with activity-dependent recovery rate, broken line: a synapse with a constant recovery time $\tau = 4.7$ s.

[1] D.Bibichkov, J.Bao and E.Neher *BMC Neuroscience* **8** (2007) 90.
[2] R.-M. Memmesheimer and M.Timme *Phys. Rev. Lett.* **97** (2006)188101.

The Synaptic Nanomachine Underlying Auditory Encoding

F. Wolf , A. Neef
T. Moser, A. Brand, N. Chapochnikov, P. Pirih,
D. Khimich (University of Göttingen), D. Riedel (MPIbpC)

The temporal structure of sound impinging on our ears is used by the brain with an astonishingly high degree of temporal resolution on the order of a dozen *micro*seconds. Examples of such high temporal precision of neuronal sound processing range from for binaural sound source localisation to speech recognition [1]. The temporal precision of sound encoding is preserved over many orders of magnitude in sound intensity [1]. Accumulating evidence indicates that the decision to generate an action potential in the auditory nerve relies on the behaviour of a surprisingly small number of molecules. In our current research, we are investigating the dynamics of intracellular signaling that underlies this intriguing example of temporal fidelity using an approach integrating high resolution electrophysiological measurements and biophysical and mathematical modelling.

Sound information is conveyed to the brain by action potential patterns of spiral ganglion neurons in the inner ear and auditory nerve (Fig 1B). Individual action potentials of auditory nerve fibers are triggered by vesicle release at specialized synapses (Fig 1D) of the sensory cells, the inner hair cells. These cells perform several signal transduction steps from liquid movement over membrane voltage transients to ion channel gating, Ca^{2+}-influx and finally release of transmitter filled vesicles. Recently, strong evidence was found that at the hair cell synapse several vesicles can be released in a coordinated, synchronized fashion [2,3]. Furthermore, control of vesicle release by Ca^{2+}-channel gating seems to follow a nano-domain regime i.e. the fusion of a certain vesicle is typically triggered by the Ca^{2+} entering through only one or very few Ca^{2+}-channels adjacent to the vesicle (Fig. 1E;[4,5]). The transmitter content of one vesicle is presumably sufficient to trigger postsynaptic action potential generation. As a consequence, the spike timing in an auditory nerve fiber is determined by the stochastic opening of one or very few Ca^{2+}-channels. Thus the molecular and biophysical organization of the inner hair cell synapse at first sight appears rather vulnerable to molecular noise. In order to understand the mechanistic basis of the temporal fidelity in sound encoding, it is thus important to characterize this intriguing cellular signaling architecture with quantitative precision and to systematically assess how temporal fidelity is achieved by a molecular nanomachine operating in a regime where perceptual decisions are apparently left to single molecule thermal fluctuations.

Coordinated vesicle release

Electrophysiological recordings from auditory nerve fibers in rat and bullfrog detected excitatory postsynaptic currents with widely varying amplitude [2,5,6]. This suggests that a presynaptic release event can involve multiple vesicles – either released in a highly synchronous fashion, or fused with each other before release. To clarify whether the observed postsynaptic variability indeed has a presynaptic cause, we used presynaptic whole cell measurements. Model studies demonstrated that non-stationary fluctuation analysis using non parametric statistical methods of error estimation would be able to estimate the capacitance of an average release event (in the range of 100 aF) on a fluctuating background capacitance of a whole cell (7 fF) and despite the considerable measurement noise (tens of fF peak-to-peak)[3]. Analysing whole cell capacitance measurements obtained

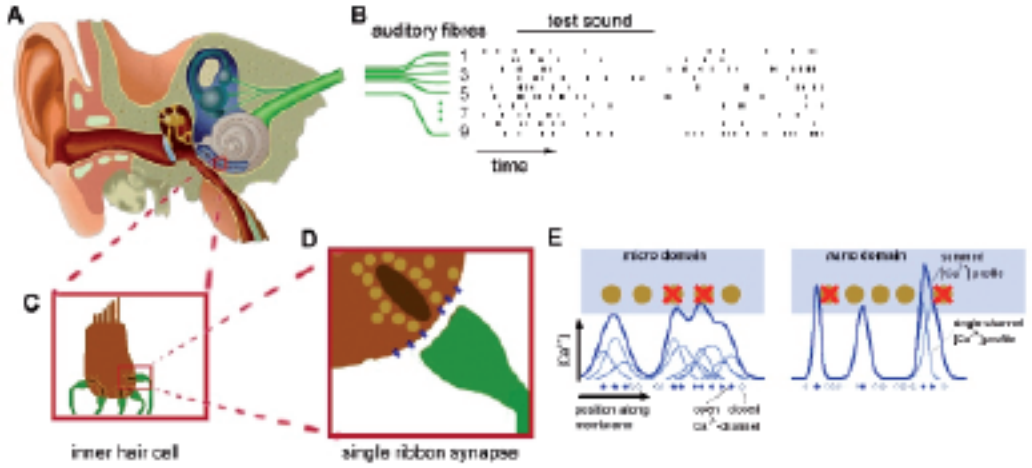

Figure1: **A** Section through a human ear. The VIII nerve, comprising the auditory fibres is drawn in green. **B** Diagram of single auditory fibres and respective sound evoked spike trains. **C** Schematic of a hair cell with 5 ribbon synapses and initial segments of the auditory nerve fibres shown. **D** Enlargement of a single hair cell synapse, showing the ribbon in dark brown, synaptic vesicles in light brown and Ca^{2+}-channels in blue. **E** Diagram of Ca^{2+} channels (diamond symbols) and vesicles (light brown, fusing vesicles crossed out). The range of intracellular $[Ca^{2+}]$ that is sufficient to trigger fusion is schematically represented by the light blue area. Left panel: In a case with high channel open probability but of brief openings the Ca^{2+}-domains around multiple channels merge into a microdomain. Fusion of any vesicle is triggered by Ca^{2+} entering through a number of channels. Right panel: Longer lasting but rare channel openings create strong Ca^{2+}-nano-domains that can trigger fusion, if a vesicle is sufficiently close to the channel.

in the perforated patch configuration using these methods, we found the average release event at the ribbon synapse of mouse inner hair cells indeed comprises more than one vesicle (Fig.2A;[3]). However the extend of coordination in our experiments was smaller than expected from postsynaptic recordings. We conclude that only about half of the fusion events involve more than one vesicle [3]. Currently, we are using a detailed biophysical model of local Ca^{2+}-signals to investigate if such synchronous release events might be a consequence of the nano-domain coupling and how the coordination of release might be computationally exploited by postsynaptic mechanisms to encode sound intensity information.

Achieving single channel-single Vesicle resolution

To directly observe Ca^{2+}-influx – vesicle secretion coupling at an individual synapse we modified existing methods to reach very low noise levels in simultaneous current and capacitance recordings [7]. It is now possible to simultaneously detect Ca^{2+}-channel openings and the fusion of single vesicles. Initial results showed exocytic events (vesicle fusion) ranging from 50 to 600 aF in size (Fig. 2B), supporting the idea of coordinated multivesicular release. Furthermore these measurements can further scrutinize the hypothesis of nano-domain control. However, some experimental problems remain to be solved as the frequency of fusion events observed is extremely low and the time course of individual events is much slower than expected. In the near future, we are starting to combine single channel/single vesicle detection with physiologically motivated i.e. smooth and periodic stimuli rather than square pulses that are usually used to study synaptic transmission. This will allow us to clarify how the temporal structure of auditory stimuli is encoded at the hair cell synapse.

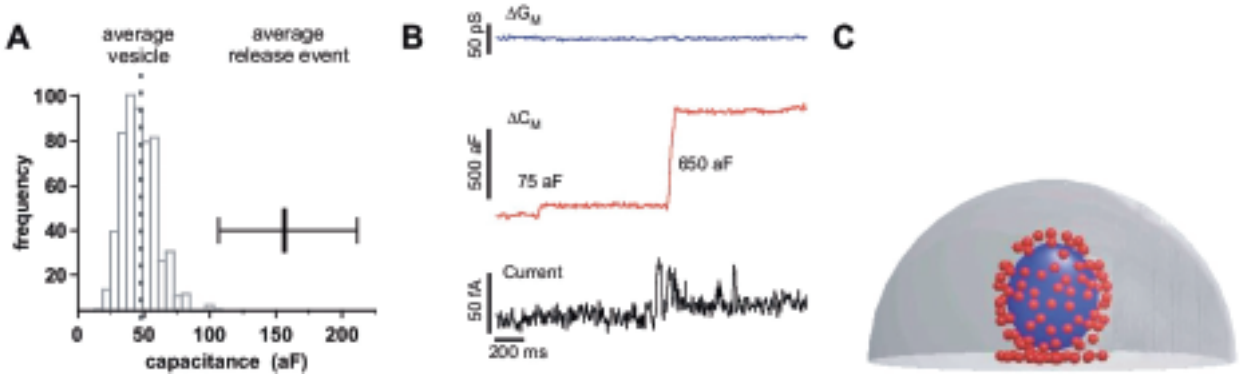

Figure 2: **A** Comparison of estimates of vesicle sizes obtained from electron microscopy and functional estimates of release event sizes (grey: size distribution of ribbon associated vesicles, the vertical bar represents the mean; black: mean and 95% confidence interval of release event size). The disparity between the sizes of individual vesicles and release events indicates coordinated release of multiple vesicles. **B** On-cell recording from a inner hair cells showing patch membrane conductance (blue), capacitance (red) and current (black). Upward deflection in the capacitance trace denote exocytic events, their size is noted. The current trace shows a current increase of about 10 fA during the big fusion event, a behaviour also observed in chromaffin cells. **C** Geometry of the biophysical ribbon synapse model. Space is discretized in tetrahedral simplices, allowing a faithful representation of ribbon and vesicle geometry.

Towards a biophysical model of the ribbon synapse

The complexity of the sound encoding nanomachine makes it desirable to simulate its function to aid understanding and constrain hypotheses. Fortunately, the large amount of electrophysiological and morphological data makes it possible to create a detailed biophysical model of this system. A detailed biophysical model of the ribbon synapse is currently being implemented with a event driven Monte-Carlo simulation system for single molecule based diffusion-reaction systems (Jentsch et al. in preparation). This model comprises stochastic channel gating and Ca^{2+}-influx, buffered Ca^{2+} diffusion and binding to the Ca^{2+} sensors of vesicles that lead to vesicle release. We plan to extend it to the postsynaptic element. Previous simulations with reduced models demonstrated that exocytosis driven by whole cell calcium currents and using experimentally constrained model of the hair cell Ca^{2+}-sensor failed to reproduce the experimentally observed kinetics. This finding is in line with previous evidence indicating that exocytosis operates under nano-domain control and thus presumably is driven by single channel currents. As a consequence the behavior of any realistic biophysical model of the inner hair cell ribbon synapse is expected to sensitively depend on the precise gating kinetics of individual Ca^{2+} channels. As currently available data do not sufficiently constrain the dynamics of nano-domain $[Ca^{2+}]$ signals we are currently systematically scanning the impact of different hypothetical single channel kinetics. In the future, our own *in situ* single Ca^{2+} channel recordings will yield important tests of and constraints on this key determinant of auditory encoding.

[1] T. Moser, A. Neef, D Khimich *J Physiol* **576:**55 (2006)
[2] E.Glowatzki & P. Fuchs *Nat Neurosci.* **5(2):**147 (2002)
[3] A. Neef, P. Pirih, D. Khimich, F. Wolf, T. Moser *J Neurosci* **27**:12933 (2007)
[4] A. Brandt, D. Khimich, T. Moser, *Neurosci* **25**, 11577 (2005)
[5] Goutman & Glowatzki, *Proc Natl Acad Sci U S A.* **104:**16341 (2007)
[6] E.C. Keen & A.J. Hudspeth *Proc Natl Acad Sci U S A.* **103:**5537 (2006)
[7] A. Neef, C. Heinemann, T. Moser, *Pflugers Arch* **454:** 335 (2007)

Directional Sensing in Eukaryotic Cells

C. Beta, E. Bodenschatz
G. Anselem, A. Bae
R. Kree, A. Zippelius (University of Göttingen), W.-J. Rappel (UC San Diego, USA)

Cell motility and chemotaxis are encountered throughout the living world. They are considered a paradigm of complex dynamics in biological matter [1]. While directed locomotion of bacteria is well understood and detailed models of procaryotic chemotaxis are available, less is known about chemotactic signaling in eukaryotic cells. In higher organisms, the pathways that link the membrane receptor input to rearrangements of the cytoskeleton and directed actin polymerization are more complex and only partly known [2]. Eukaryotic cells like neutrophils or the social amoeba *Dictyostelium discoideum* can detect chemoattractant gradients as shallow as a 1% difference in concentration between the front and the back of the cell and exhibit high sensitivity to gradients ranging over several orders of magnitude [3,4]. This can be only achieved, if highly nonlinear interactions govern the early stages of chemotactic signaling, generally referred to as *directional sensing*.

During the first ten seconds after exposure to a chemoattractant gradient, an intracellular symmetry breaking occurs that is reflected in asymmetric spatial distributions of numerous proteins across the cell [5]. These subcellular reorganizations can be experimentally observed by fluorescence microscopy imaging of various GFP-tagged constructs. Among the best-known examples of these redistributing components are pleckstrin homology (PH) domain proteins. Although their precise role in directional sensing is controversially debated [6,7], it is generally assumed that such asymmetric rearrangements of proteins precede the downstream events that lead to actin driven membrane protrusions and, ultimately, cell locomotion.

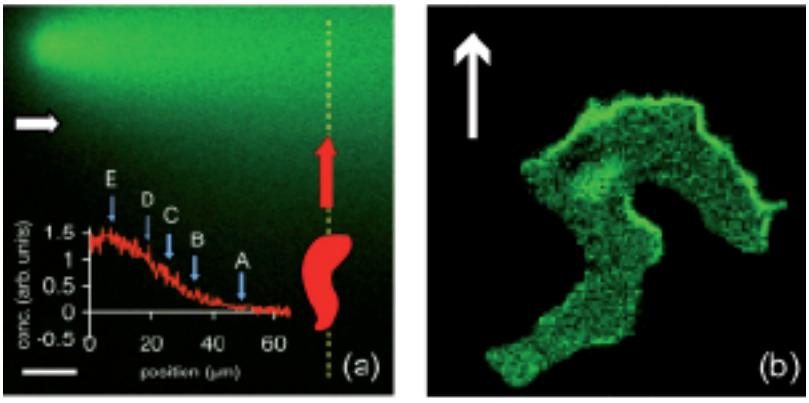

Figure 1: (a) Photorelease of DMNB-caged fluorescein by a laser point source located in the upper left corner; scale bar 10 μm; flow from left to right as indicated by the white arrow. (a, inset) Fluorescence intensity along the dashed yellow line. (b) Directional membrane translocation of CRAC-GFP in a gradient of cAMP (gradient direction as indicated by the white arrow).

Various models have been proposed to describe the initial intracellular symmetry breaking during directional sensing. Since many molecular details of the chemotactic signaling network remain unknown, most of these models consequently focus on phenomenological, low-dimensional descriptions to capture the overall dynamics, see *e.g.* [8]. To assess the quality of such models and to decide between different models with competing predictions, quantitative data on directional sensing is required. In the framework of this project, we take a first step towards systematic mapping of intracellular responses as a function of external directional stimuli.

We performed experiments on a *Dictyostelium* strain that carries a green fluorescent protein (GFP), tagged to the cytosolic regulator of adenylyl cyclase (CRAC), a cytosolic PH-domain protein. Upon stimulation in a gradient of the chemoattractant cyclic adenosine 3',5'-monophosphate (cAMP), membrane translocation of CRAC-GFP in the direction of higher cAMP concentration, accompanied with cytosolic depletion, can be observed by fluorescence microscopy imaging, see Fig. 1(b). We employ

our tools of microfluidic flow photolysis to expose CRAC-GFP cells to well-controlled, systematically changing gradients of cAMP (see also our report on *Single cell stimulation in microfluidic environments*). The chemoattractant is released by a laser point source in the micro-flow and spreads by lateral diffusion as it is carried downstream by the flow. This is illustrated by the release of a caged fluorescent dye in Fig.1(a). The slope of the gradient profile is varied by changing the power of the photo-uncaging laser, so that the cellular response can be mapped as a function of the external gradient.

An example for such a dose/response relation is shown in Fig.2. Here, the cytosolic depletion is shown as a function of the external gradient steepness. While for strong gradients the response is independent of the external signal, a linear dependence can be seen for shallower gradients. Interestingly, the response sets in with a finite amplitude at shallow gradients. Note, however, that the number of cells responding decreases for decreasing gradient steepness, suggesting that the threshold to trigger a response is different from cell to cell.

In addition to our experimental efforts, we proposed a generic model of directional sensing that is based on the simple pattern formation paradigm of bistability [9]. By combining a two-component activator/inhibitor system with a bistable module, the front and back halves of the cell converge to different stable fixed points upon stimulation with an extracellular chemoattractant gradient.

In future projects, our work on directional sensing of chemical cues will be extended to include studies of mechanosensing. It has been shown that external shear stress can trigger similar pathways as the stimulation of chemoattractant receptors [10]. We will use atomic force microscopy to explore the signaling networks of mechanosensing by performing highly localized and well-controlled mechanical stimulation in combination with fluorescence imaging of intracellular reporters.

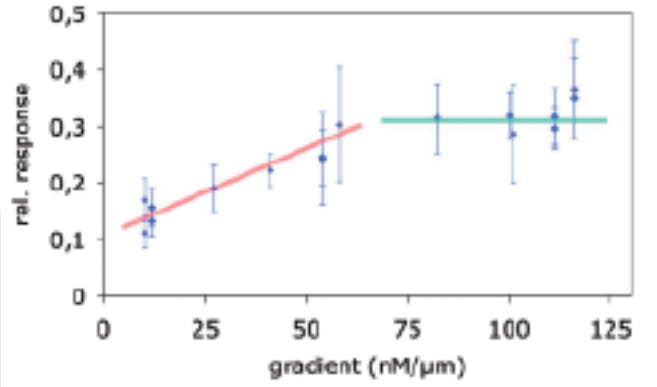

Figure 2
Response in cytosolic depletion as a function of the external cAMP gradient.

[1] A. R. Horwitz and J. T. Parsons, *Science* **286** (1999) 1102.
[2] P. J. M. Van Haastert and P. N. Devreotes, *Nature Reviews Molecular Cell Biology* **5** (2004) 626.
[3] P. R. Fisher, R. Merkl, and G. Gerisch, *Journal of Cell Biology* **108** (1989) 973.
[4] L. Song, et al., *European Journal of Cell Biology* **85** (2006) 981.
[5] C. A. Parent and P. N. Devreotes, *Science* **284** (1999) 765.
[6] K. Takeda, et al., *Journal of Biological Chemistry* **282** (2007) 11874.
[7] O. Hoeller and R. R. Kay, *Current Biology* **17** (2007) 813.
[8] H. Levine, D. A. Kessler, and W. J. Rappel, *Proceedings of the National Academy of Sciences of the United States of America* **103** (2006) 9761.
[9] C. Beta, G. Amselem, and E. Bodenschatz (2007) submitted.
[10] J. Dalous, et al., *Biophysical Journal* (2007) in press.

Structure and Dynamics of Cellular and Extracellular Networks

T. Pfohl, R. Seemann, A. Gholami, E. Bodenschatz, S. Herminghaus
H.M. Evans, G. Anselem, C. Beta, R. Dootz, E. Surenjav, S. Uppaluri
J. Wong (Boston, USA), S. Struth, G. Grübel (Hamburg),
J. Kierfeld (Dortmund), M. Falcke (Berlin), T. Pompe (Dresden)

The self-assembly of biological materials is often induced by conditions that are mimicked exceptionally well using microfluidics, such as pH changes or the incorporation of additional proteins. Also, dimensions and flow fields can be tuned to confine and orient networks and assemblies [1]. We utilize the advantages of microenvironments to study a variety of biomolecules, ranging from extracellular collagen and fibrin to materials found inside the cell, such as DNA and actin.

Building on our previous design in spark-eroded steel [2], new microflow foils enable in situ investigations with many different techniques (e.g. x-ray, fluorescence microscopy, FTIR) in an essentially limitless set of flow and channel topologies [3].These new foils, made from the elastomer PDMS and kapton films, are incredibly flexible yet able to withstand the pumping of very viscous materials (see Fig.1). X-ray microdiffraction is used to investigate the structure of DNA alone or with small positively charged dendrimers in microflow [4,5]. The non-equilibrium assembly of these oppositely charged materials also relates to the compaction of DNA in chromosomes. In some cases, mixing in the devices enables phase formation that is unattainable using conventional methods. For example, a coexistence of DNA-dendrimer mesophases oriented transverse, as well as parallel, to the flow direction is seen in maximum shear flow.

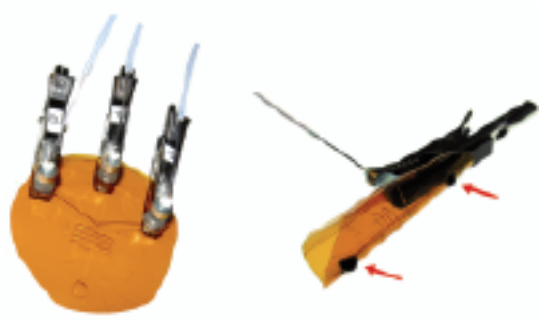

Figure 1: Flexible microfoil flow cells are compatible with x-ray studies (colored liquid flows from inlet to outlet, marked with arrows).

Among their many roles, collagen fibers contribute to the mechanical properties of soft tissue and bone, and influence cell morphology and migration. However, the hierarchy of collagen assembly is still unresolved. Using a hydrodynamic focusing flow device, we create a pH gradient between (high pH) NaOH and (low pH) collagen solution [6,7]. We find that the fibrillization of collagen, accompanied by a marked increase in viscosity, occurs at around pH 7. Using numerical expressions and finite element modeling, predictions of collagen gelation at neutral pH are in good agreement with experiments (see Fig. 2a). Interestingly, x-ray microdiffraction studies in flow reveal an alignment of pentameric collagen subunits that cannot be measured in bulk samples (see Fig. 2b). We attribute this finding to the unambiguous chemical environment created in diffusion-limited mixing scenarios. Additionally, a network of collagen fibers can be used as an elastic matrix for self-propelling particles, such as the parasite *Trypanosoma Brucei* (see p.65–67) [8]. Properties of the network can be extracted with appropriate analysis of the parasites' motility.

Protein meshes can also serve as elegant models for the study of visco-elastic networks. We explore dynamic phenomena of the protein, fibrin, which is a primary component of blood clots. In the presence of the enzyme thrombin, fibrinogen molecules evolve into a 3D fibrin network. To develop and manipulate this robust network, we produce fibrin in nanodroplets (see project 2.2.1) [9]. This prohibits sticky surface interactions between the protein and device walls, since the droplets are formed within an oily continuous phase.

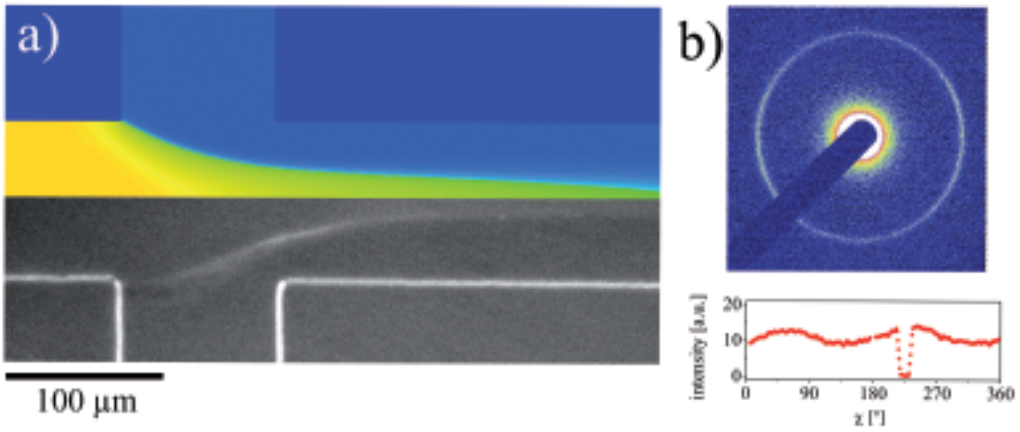

Figure 2
a) Collagen fibers form in a pH gradient (simulated, top, and phase contrast micrograph, bottom). **b)** SAXS 2D image shows diffraction peak with alignment (lower, azimuthal scan) for feature having 4.3 nm spacing.

Furthermore, the incorporation of geometric structures enables the controlled deformation of individual droplets, as shown in Fig.3. High resolution fluorescence microscopy is used to analyze the elastic recovery of these networks through several cycles of mechanical deformation.

An oil-water interface can also be used as an artificial system to mimic the leading edges of a crawling cell, known as lamellipodia, filopodia, or microspikes according to their shapes. Lamellipodial actin filaments (a key cytoskeleton protein) form a highly cross-linked and polarized network with a broad sheet-like structure. The dynamic polymerization of actin filaments near the cell membrane is thought to generate the motile force responsible for cellular protrusions and is essential for cell locomotion and cell-cell adhesions. Previous studies have quantified the confining effects of microenvironments on single actin filaments of a finite length [10]. We aim to study actin related proteins 2/3 (Arp2/3) complex-dependent actin dynamics by looking at the instabilities of oil-water interfaces in the presence of several proteins that regulate actin assembly. Thus, we mirror lamellipodial protrusion in well defined conditions, in order to learn how the details of actin polymerization and regulation work together in a spatially distributed manner to generate and regulate the cell front.

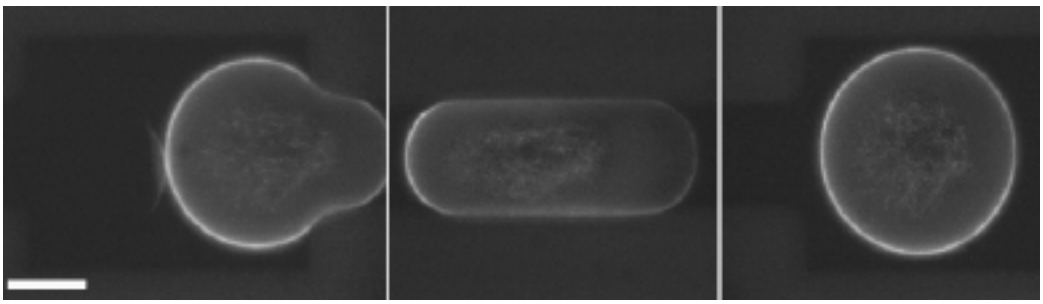

Figure 3: A single fibrin droplet responds to deformation in snapshots (images collected from left to right, scalebar 80 µm).

[1] H. M. Evans, R. Dootz, S. Köster, B. Struth, T. Pfohl, *Bull. Pol. Acad. Sci.: Technical Sciences* **2** (2007) 217.
[2] A. Otten, S. Köster, B. Struth, A. Snigirev, T. Pfohl, *Journal Of Synchrotron Radiation* **12** (2005) 745.
[3] R. Dootz, H. M. Evans, S. Köster, T. Pfohl, *Small* **3** (2007) 96-100.
[4] R. Dootz, A. Otten, S. Köster, B. Struth, T. Pfohl, *J. Phys.: Condens. Matter* **18** (2006) S639.
[5] T. Pfohl, A. Otten, S. Köster, R. Dootz, B. Struth, H. M. Evans, *Biomacromolecules* **8** (2007) 2167.
[6] S. Köster, H. M. Evans, J. Y. Wong, T. Pfohl, *Biomacromolecules*, in press, (2007) bm700973t.
[7] S. Köster J. B. Leach, B. Struth, T. Pfohl, J. Y. Wong, *Langmuir* **23** (2006) 357.
[8] M. Engstler, T. Pfohl, S. Herminghaus, M. Boshart, G. Wiegertjes, P. Overath, *Cell* **131** (2007) 505.
[9] E. Surenjav, H. M. Evans, T. Pfohl, C. Priest, S. Herminghaus, R. Seemann, *The Proceedings of the µTAS 2007*, Eds. J.-L. Viovy, P. Tabeling, S. Descroix, L. Lalaquin, ISBN 978-0-9798064-0-7
[10] S. Köster, H. Stark, T. Pfohl, J. Kierfeld, *Biophysical Reviews and Letters* **2** (2007) 155.

Publications

Department of Nonlinear Dynamics

2003

G. Berkolaiko, H. Schanz, and R. S. Whitney, "Form Factor for a Family of Quantum Graphs", *J. of Physics A* **36** (2003) 8373.

D. Brockmann, "Superdiffussion in Inhomogeneous Scale-free Enviroments", George-August Universität, Göttingen (2003).

D. Brockmann, and T. Geisel, "Particle Dispersion on Rapidly Folding Random Hetero-Polymers", *Phys. Rev. Lett.* **91** (2003) 048303.

D. Brockmann, and T. Geisel, "Lévy Flights in Inhomogeneous Media", *Phys. Rev. Lett.* **90** (2003) 170601.

D. Cohen, and T. Kottos, "Non-perturbative response: Chaos versus Disorder", *J. of Phys. A: Math. and General* **36** (2003) 10151.

S. Gruen, A. Riehle, and M. Diesmann, "Effect of cross-trial nonstationarity on joint-spike events", *Biological Cybernetics* **88** (2003) 335.

M. Kaschube et al., "Localizing the ticklish spots of cortical orientation maps", in 2nd Symposium of the Volkswagen Stiftung "Dynamics and Adaptivity of Neuronal Systems - Integrative Approaches to Analyzing Cognitive Functions" (2003).

M. Kaschube et al., "The Pattern of Ocular Dominance Columns in Cat Primary Visual Cortex: Intra- and Interindividual Variability of Column Spacing and its Dependence on Genetic Background", *European Journal of Neuroscience* **18** (2003) 3251.

T. Kottos, and D. Cohen, "Quantum irreversibility of energy spreading", *Europhys. Lett.* **61** (2003) 431.

T. Kottos, A. Ossipov, and T. Kottos, "Signatures of Classical Diffusion in Quantum Fluctuations of 2D Chaotic Systems", *Phys. Rev. E* **68** (2003) 066215.

T. Kottos, and U. Smilansky, "Quantum Graphs: A Simple Model for Chaotic Scattering", *Journal of Physics A: Mathematical and General* **36** (2003) 3501.

N. Mayer, J. M. Herrmann, and T. Geisel, "Shaping of Receptive Fields in Visual Cortex During Retinal Maturation", *Journal of Computational Neuroscience* **15** (2003) 307.

C. Mehring et al., "Activity dynamics and propagation of synchronous spiking in locally connected random networks", *Biological Cybernetics* **88** (2003) 395.

A. Ossipov, T. Kottos, and T. Geisel, "Fingerprints of classical diffusion in open 2D mesoscopic systems in the metallic regime", *Europhys. Lett.* **62** (2003) 719.

T. Prager, B. Naundorf, and L. Schimansky-Geier, "Coupled three-state oscillators", *Physica A* **325** (2003) 176.

H. Schanz, "Reaction Matrix for Dirichlet Billiards with Attatched Waveguides", *Physica E* **18** (2003) 429.

H. Schanz, and T. Kottos, "Scars on Quantum Networks Ignore the Lyapunov Exponent", *Phys. Rev. Lett.* **90** (2003) 234101.

H. Schanz, M. Puhlmann, and T.Geisel, "Shot noise in Chaotic Cavities from Action Correlations", *Phys. Rev. Lett.* **91** (2003) 134101.

T. Tetzlaff et al., "The spread of rate and correlation in stationary cortical networks", *Neurocomputing* **52-54** (2003) 949.

M. Timme, F. Wolf, and T. Geisel, "Unstable attractors induce perpetual synchronization and desynchronization", *Chaos* **13** (2003) 377.

M. Weiss, L. Hufnagel, and R. Ketzmerick, "Can simple renormalization theories describe the trapping of chaotic trajectories in mixed systems?" *Phys. Rev. E* **67** (2003) 046209.

F. Wolf, and T. Geisel, "Universality in Visual Cortical Pattern Formation", *Journal of Physiology - Paris* **97** (2003) 253.

2004

D. Cohen, and T. Kottos, "Quantum dissipation due to the interaction with chaos", *Phys. Rev. E* **69** (2004) 055201.

M. Denker et al., "Breaking Synchrony by Heterogeneity in Complex Networks", *Phys. Rev. Lett.* **92** (2004) 074103.

J. M. Herrmann, M. Holicki, and R. Der, "On Ashby's homeostat: A formal model of adaptive regulation", in *From animals to animates* **8** (2004), 324.

J. Hass, J. M. Herrmann, and T. Geisel, "Evolutionary design of an adaptive dynamic walker", in *Proc. Workshop on Climbing and Walking Robots* 2004.

K. Pawelzik, B. Si, and J. M.Herrmann, "Robot exploration by subjectively maximizing objective information gain", in *Proc. IEEE International Conference on Robotics and Biomimetics*, 2004.

J. Hass, J. M. Herrmann, and T. Geisel, "Evolutionary design of an adaptive dynamic walker", in *Proceedings of 7th International Conference CLAWAR* (2004) 765.

M. C. Geisler et al., "Detection of a Landau Band-Coupling-Induced Rearrangement of the Hofstadter Butterfly", *Phys. Rev. Lett.* **92** (2004) 256801.

M. Hiller et al., "Quantum Reversibility: Is there an Echo", *Phys. Rev. Lett.* **92** (2004) 010402.

L. Hufnagel, D. Brockmann, and T. Geisel, "Forecast and Control of epidemics in a globalized world", *PNAS* **101** (2004) 15124.

R.-M. Memmesheimer, A. Gopakumar, and G. Schäfer, "Third post-newtonian accurate generalized quasi-keplerian parametrization for compact binaries in eccentric orbits", *Phys. Rev. D* **70** (2004) 104011.

N. Mayer, A. A. Forough-Nassiraei, M. Browne, J. M. Herrmann, and T. Christaller, "An asymmetric 2-d passive dynamic walker", in *The Ninth International Symposium on Artificial Life and Robotics*, number 23-7 in GS, 2004.

T. Kottos, and H. Schanz, "Statistical Properties of Resonance Width for Open Quantum Systems", *Waves in Random Media* **14** (2004) S91.

T. Kottos, and M. Weiss, "Current Relaxation in Nonlinear Random Media", *Phys. Rev. Lett.* **93** (2004) 190604.

A. Ossipov, and T. Kottos, "Superconductor-poximity effect in hybrid structures: Fractality versus Chaos", *Phys. Rev. Lett.* **92** (2004) 017004.

M. Timme, F. Wolf, and T. Geisel, "Topological Speed Limits to Network Synchronization", *Phys. Rev. Lett.* **92** (2004) 074101.

A. Zumdieck et al., "Long Chaotic Transients in Complex Networks", *Phys. Rev. Lett.* **93** (2004) 244103.

2005

P. Ashwin, and M. Timme, "When instability makes sense", *Nature* **436** (2005) 36.

P. Ashwin, and M. Timme, "Unstable attractors: existence and robustness in networks of oscillators with delayed pulse coupling", *Nonlinearity* **18** (2005) 2035.

D. Brockmann, L. Hufnagel, and T. Geisel, "Dynamics of Modern Epidemics", in *SARS: A Case Study in Emerging Infections* (R. Weiss ed.), Oxford University Press (2005).

D. Cohen, T. Kottos, and H. Schanz, "Quantum pumping: The charge transported due to a translation of a scatterer", *Phys. Rev.* E **71** (2005) 035202.

J. M. Herrmann, H. Schrobsdorff, and T. Geisel, "Localized activations in a simple neural field model", *Neurocomputing* **65-66** (2005) 679.

M. Kaschube et al., "Predicting sensitive spots in visual cortical orientation preference maps." in *11th Magdeburg International Neurobiological Symposium "Learning and Memory: cellular and Systematic Views"* (2005).

A. Levina, J. M. Herrmann, and T. Geisel, "Dynamical Synapses Give Rise to a Power-Law Distribution of Neuronal Avalanches", in *NIPS** 2005 (2005).

A. Méndez-Bermúdez, T. Kottos, and D. Cohen, "Parametric evolution of eigenstates: Beyond perturbation theory and semiclassics", *Physical Review E* **72** (2005) 027201.

A. Méndez-Bermúdez, and T. Kottos, "Probing the eigenfunction fractality using Wigner delay times", *Physical Review B* **72** (2005) 064108.

A. Méndez-Bermúdez et al., "Trends in Electro-Optics Research", Nova Science Publishers, (2005) 231.

B. Naundorf, T. Geisel, and F. Wolf, "Action potential onset dynamics and the response speed of neuronal populations", *Journal of Computational Neuroscience* **18** (2005) 297.

B. Naundorf, T. Geisel, and F. Wolf, "Dynamical response properties of a canonical model for type-I membranes", *Neurocomputing* **65** (2005) 421.

T. Kottos, "Statistics of resonances and delay times in random media: beyond ransom matrix theory", *Journal of Physics A: Math. Gen.* **38** (2005) 10761.

S. Dodel, J. M. Herrmann, T. Geisel, and J.-B. Poline, "Network structure of functional connectivity from frmi", in Proc. 9th HBM *Neuroimage* **19:2** (2005)

J. Hass, J. M. Herrmann, and T. Geisel, "Biomechanics and low-level control of bipedal locomotion", in *Neuroforum*, Supplement 75B, **1** (2005).

R.-M. Memmesheimer, and G. Schäfer, "Third post-newtonian constrained canonical dynamics for binary point masses in harmonic coordinates", *Phys. Rev. D* **71** (2005) 044021.

O. Bendix, and J. A. Méndez-Bermúdez, "Design of switches and beam splitters by use of chaotic cavities", *Optics Letters* **30** (2005) 1396.

O. Bendix, J. A. Méndez-Bermúdez, G. A. Luna-Acosta, U. Kuhl, and H.-J. Stöckmann, "Design of beam splitters and microlasers using chaotic waveguides", *Microelectronics Journal* **36** (2005) 285.

H. Hennig, J. Breidbach, and L. S. Cederbaum, "Electron Correlation as the Driving Force for Charge Transfer: Charge Migration Following Ionization in N-Methyl Acetamide", *Journal of Physical Chemistry A* **109(3)** (2005) 409.

H. Hennig, J. Breidbach, and L. S. Cederbaum, "Charge transfer driven by electron correlation: A non-Dyson propagator approach", *The Journal of Chemical Physics* 122(13) (2005) 134104.

M. Puhlmann et al., "Quantum decay of an open chaotic system: A semiclassical approach", *Europhysics Letters* **69** (2005) 313.

H. Schanz, "Phase-Space Correlations of Chaotic Eigenstates", *Phys. Rev. Lett.* **94** (2005) 134101.

H. Schanz, T. Dittrich, and R. Ketzmerick, "Directed chaotic transport in Hamiltonian ratchets", *Phys. Rev. E* **71** (2005) 026228.

H. Schanz, and M. Prusty, "Directed chaos in a billiard chain with transversal magnetic field", *Journal of Physics A: Mathematical and General* **38** (2005) 10085.

K. F. Schmidt et al., "Adult plasticity: Activity-dependent short- and long-term changes of functional maps in cat visual cortex", in *11th Magdeburg International Neurobiological Symposium "Learning and Memory: cellular and Systematic Views"* (2005).

M. Voultsidou, S. Dodel, and J. M. Herrmann, "Neural Networks Approach to Clustering of Activity in fMRI Data", *IEEE Trans. Med. Imaging* **12** (2005) 987.

F. Wolf, "Symmetry, Multistability, and Long-Range Interactions in Brain Development", *Phys. Rev. Lett.* **95** (2005) 208701.

F. Wolf, "Symmetry Breaking and Pattern Selection in Visual Cortical Development", in École d'Été de Physique des Houches, 2003, Methods and Models in *Neurophysics*, Elsevier, Amsterdam (2005) 575.

2006

D. Brockmann, L. Hufnagel, and T. Geisel, "The scaling laws of human travel", *Nature* **439** (2006) 462.

M. Hiller et al., "Wavepacket Dynamics, Quantum Reversibility and Random Matrix Theory", *Annals of Physics* **321** (2006) 1025.

J. A. Méndez-Bermúdez, T. Kottos, and D. Cohen, "Parametric invariant random matrix model and the emergence of multifractality", *Physical Review E* **73** (2006) 036204.

B. Naundorf, F. Wolf, and M. Volgushev, "Unique features of action potential initiation in cortical neurons", *Nature* **440** (2006) 1060.

M. Prusty, and H. Schanz, "Signature of Directed Chaos in the Conductance of a Nanowire", *PRL* **96** (2006) 130601.

M. Timme, T. Geisel, and F. Wolf, "Speed of synchronization in complex networks of neural oscillators: Analytic results based on Random Matrix Theory", *Chaos* **16** (2006) 015108.

D. Cohen, T. Kottos, and H. Schanz, "Rate of energy absorption by a closed ballistic ring", *Journal of Physics A: Math. Gen.* **39** (2006) 11755.

R. Der, F. Hesse, and G. Martius, "Rocking stamper and jumping snake from a dynamical system approach to artificial life", *Adaptive Behaviour* **14** (2006) 105.

J. Hass, J. M. Herrmann, and T. Geisel, "Optimal mass distribution for passivity-based bipedal robots", *The Int. Journal of Robotics Research* **25** (2006) 1087.

M. Hiller, T. Kottos, and T. Geisel, "Complexity in parametric Bose-Hubbard Hamiltonians and structural analysis of eigenstates", *Physical Review A*, Rapid Communication **73** (2006) 061604(R).

M. Hiller, T. Kottos, and A. Ossipov, "Bifurcations in resonance widths of an open Bose-Hubbard dimer", *Physical Review A* **73** (2006) 063625.

G. S. Ng, J. D. Bodyfelt, and T. Kottos, "Critical Fidelity at the Metal-Insulator Transition", *Phys. Rev. Lett.* **97** (2006) 256404.

M. Weiss, A. Méndez-Bermúdez, and T. Kottos, "Resonance width distribution for high-dimensional random media", *Physical Review B* **73** (2006) 045103.

T. Kottos, "Quantum graphology", in *Proceedings of the 2nd Workshop on Quantum Chaos and Localisation Phenomena*, Warsaw, 2006.

R. Der, and G. Martius, "From motor babbling to purposive actions: Emerging self-exploration in a dynamical systems approach to early robot development", in *From Animals to Animats, Proceedings*, **4095** of Lecture Notes in Computer Science (2006) 406.

R. Der, G. Martius, and F. Hesse, "Let it roll – emerging sensorimotor coordination in a spherical robot" in *Artificial LifeX: Proceedings of the Tenth International Conference on the Simulation and Synthesis of Living Systems* (2006) 192.

A. Levina, J. M. Herrmann, and T. Geisel, "Dynamical synapses give rise to a power-law distribution of neuronal avalanches" in *Advances in Neural Information Processing Systems* **18** (2006) 771.

H. Schanz, "A relation between bond-scattering matrix and number counting function for quantum graphs", in *Quantum Graphs and Their Applications* **415** (2006)

2007

V. V. Belik and D. Brockmann, "Accelerating random walks by disorder", *New Journal of Physics* **9(3)** (2007) 54.

J. D. Bodyfelt, M. Hiller, and T. Kottos, "Engineering fidelity echoes in Bose-Hubbard Hamiltonians", *Europhys. Lett.* **78** (2007) 50003.

D. Brockmann and L. Hufnagel, "Front propagation in reaction-superdiffusion dynamics – taming Lévy flights with fluctuations", *Phys. Rev. Lett.* **98** (2007) 178301.

M. Denker, S. Rouxc, M. Timme, A. Riehle, and S. Grün, "Phase synchronization between lfp and spiking activity in motor cortex during movement preparation", *Neurocomputing* **70** (2007) 2096.

H. W. Gutch and F. Theis, "Independent Subspace Analysis Is Unique, Given Irreducibility", in Independent Component Analysis and Signal Separation **4666** of LNCS (2007) 49.

H. Hennig, R. Fleischmann, L. Hufnagel, and T. Geisel, "Fractal conductance fluctuations of classical origin", *Physical Review E* **76** (2007) 015202.

J. Hass, J. M. Herrmann, S. Blaschke, and T. Rammsayer, "A neurocomputational model of temporal processing", *BMC Neuroscience* **8(S2)** (2007) 25.

J. Hass, J.M. Herrmann, S. Blaschke, and T. Rammsayer, "Timing errors in a dynamical model of temporal processing", in *Neuroforum*, Supplement T37-3B, vol. XIII of 1. German Neuroscience Society (2007).

J. Hass, J.M. Herrmann, S. Blaschke, and T. Rammsayer, "Timing errors in a dynamical model of temporal processing", in *Kognitionsforschung 2007*, Gesellschaft für Kognitionswissenschaft, Shaker (2007) 67.

F. Hesse, R. Der, and J. M. Herrmann, "Reflexes from self-organizing control in autonomous robots", in *7th International Conference on Epigenetic Robotics*, **134** of Cognitive Studies (2007) 37.

A. Levina, U. Ernst, and J. M. Herrmann, "Criticality of avalanche dynamics in adaptive recurrent networks", *Neurocomputing* **70** (2007) 1877.

A. Levina, J. M. Herrmann, and T. Geisel, "Dynamical synapses causing self-organized criticality in neural networks", *Nature Physics* (2007).

N. M. Mayer, J. M. Herrmann, M. Asada, and T. Geisel, "Pinwheel stability in a non-euclidean model of pattern formation in visual cortex", *J. Korean Phys. Soc.* **50(S01)** (2007) 150.

B. Naundorf, F. Wolf, and M. Volgushev, "Hodgkin and Huxley model – still standing?", *Nature* **445** (2007) E2.

A. Neef, D. Khimich, P. Pirih, D. Riedel, F. Wolf, and T. Moser, "Probing the Mechanism of Exocytosis at the Hair Cell Ribbon Synapse", *Journal of Neuroscience* **27(47)** (2007) 12933.

M. Prusty and H. Schanz, "Self-pulsed electron transmission through a finite waveguide in a transversal magnetic field", *Phys. Rev. Lett.* **98** (2007) 176804.

M. Schnabel, M. Kaschube, S. Löwel, and F. Wolf, "Random waves in the brain: Symmetries and defect generation in the visual cortex", *European Physical Journal* **145** (2007) 137.

H. Schrobsdorff, M. Ihrke, J. Behrendt, M. Hasselhorn, and J. M. Herrmann, "Modeling selective attention using eeg data", *BMC Neuroscience* **8(S2)** (2007) 135.

H. Schrobsdorff, J. M. Herrmann, and T. Geisel, "A feature-binding model with localized excitations", *Neurocomputing* **70(10-20)** (2007) 1706.

H. Schrobsdorff, M. Ihrke, B. Kabisch, J. Behrendt, M. Hasselhorn, and J. M. Herrmann, "A Computational Approach to Negative Priming", *Connection Science* **19(3)** (2007) 203.

M. Voultsidou, S. Dodel, and J. M. Herrmann, "Feature extraction in fmri data using random matrix theory", *Comput. And Visualiz. in Science* **10(2)** (2007) 100.

K. Doubrovinski and J. M. Herrmann, "Stability of localized patterns in neural fields", Neural Computation, accepted 2008.

M. Kaschube, M. Schnabel, and F. Wolf, "Self-Organization and the selection of pinwheel density in visual cortical development", New Journal of Physics., in press

Department of Dynamics of Complex Fluids

2003

J. Becker et al., "Complex dewetting scenarios captured by thin film models", *Nature Materials* **2** (2003) 59.

J. Buehrle, S. Herminghaus, and F. Mugele, "Interface profiles near three-phase contact lines in electric fields", *Phys. Rev. Lett.* **91** (2003) 086101.

A. Dimakis and F. Müller-Hoissen, "Differential geometry of group lattices", *J. Math. Phys.* **44** (2003) 1781.

A. Dimakis and F. Müller-Hoissen, "Riemannian geometry of bicovariant group lattices", *J. Math. Phys.* **44** (2003) 4220.

H. M. Evans et al., "Structural polymorphism of DNA-dendrimer complexes", *Phys. Rev. Lett.* **91** (2003) 075501.

M.A.Z. Ewiss et al., "Molecular dynamics and alignment studies of silica-filled 4-pentyl-4'-cyanobiphenyl (5CB) liquid crystal", *Liquid Crystals* **30** (2003) 1.

D. Geromichalos et al., "Dynamic aspects of wetting in granular matter", *Contact Angle Wettability and Adhesion* **3** (2003) 385.

D. Geromichalos et al., "Mixing and condensation in a wet granular medium", *Phys. Rev. Lett.* **90** (2003) 168702.

S. Herminghaus, K. Jacobs, and R. Seemann, "Viscoelastic dynamics of polymer thin films and surfaces" *Eur. Phys. J.* E **12** (2003) 101.

S. Herminghaus, "Harnessing the unstable", *Nature Materials* **2** (2003) 11.

A. Klingner, S. Herminghaus, and F. Mugele, "Self-excited oscillatory dynamics of capillary bridges in electric fields", *Appl. Phys. Lett.* **82** (2003) 4187.

C. Neto et al., "Satellite hole formation during dewetting: Experiment and simulation", *J. Phys.: Condens. Matter* **15** (2003) 3355.

C. Neto et al., "Correlated dewetting patterns in thin polystyrene films", *J. Phys.: Condens. Matter* **15** (2003) 421.

T. Pfohl et al., "Trends in microfluidics with complex systems", *Chem. Phys. Chem.* **4** (2003) 1291.

T. Pfohl and S. Herminghaus, "Mikrofluidik mit komplexen Flüssigkeiten", *Physik Journal* **2** (2003) 35.

M. Schulz, B. Schulz, and S. Herminghaus, "Shear-induced solid-fluid transition in a wet granular medium", *Phys. Rev. E* **67** (2003) 052301.

R. Seemann, "Zerreißprobe für dünne Polymerfilme – Neue Erkenntnisse warum und wie dünne Flüssigkeitsfilme aufbrechen", *Chemie.de*, 19. August 2003.

A. Thoss et al., "Kilohertz sources of hard x rays and fast ions with femtosecond laser plasmas.", *Journal of the Optical Society of America - Optical Physics* B **20** (2003) 224.

A.A.M. Ward et al., "Effect of cyclic deformations on the dynamic-mechanical properties of Silica-filled Butyl Rubber", *Macromol. Mater. Eng.* **288** (2003) 971.

A.A.M. Ward et al., "Studies on the dielectric behavior of Silica-filled Butyl Rubber Vulcanizates after cyclic deformation", *J. of Macromol. Science* B **42** (2003) 1265.

2004

B. Abel et al., "Characterization of extreme utltraviolet light-emitting plasmas from laser excited fluorine containing liquid polymer jet target" *J. Appl. Phys.* **95** (2004) 7619.

A. Charvat et al., "New design for a time-of-flight mass spectrometer with a liquid beam laser desorption ion source for the analysis of biomolecules", *Rev. Sci. Instrum.* **75** (2004) 1209.

M. Chul Choi et al., „Ordered patterns of liquid crystal toroidal defects by microchannel confinement", *Proceedings of the National Academy of Sciences of the USA (PNAS)* **101** (2004) 17340.

A. Dimakis and F. Müller-Hoissen, "Extension of noncommutative soliton hierarchies", *J. Phys. A: Math. Gen.* **37** (2004) 4069.

A. Dimakis and F. Müller-Hoissen, "Explorations of the extended ncKP hierarchy", *J. Phys. A: Math. Gen.* **37** (2004) 10899.

A. Dimakis and F. Müller-Hoissen, "Extension of Moyal-deformed hierarchies of soliton equations", in XI International Conference Symmetry Methods in Physics, C. Burdik, O. Navratil and S. Posta (eds.), *JINR* (Dubna) (2004).

A. Dimakis and F. Müller-Hoissen, "Differential calculi on quantum spaces determined by automorphisms", *Czech. J. Phys.* **54** (2004) 1235.

A. Dimakis and F. Müller-Hoissen, "Automorphisms of associative algebras and noncommutative geometry", *J. Phys. A: Math. Gen.* **37** (2004) 2307.

S. Herminghaus, R. Seemann. and K. Landfester, "Polymer Surface Melting Mediated by Capillary Waves", *Phys. Rev. Lett.* **93** (2004) 017801.

M. Kohonen et al., "On Capilary Bridges in Wet Granular Materials", *Physica A* **339** (2004) 7.

A. Otten and S. Herminghaus: "How plants keep dry: a physicist's point of view", *Langmuir* **20** (2004) 2405.

M. Scheel, D. Geromichalos, and S. Herminghaus, "Wet granular matter under vertical agitation", *J. Phys.: Condens. Matter* **16** (2004) 1.

B. Struth et al.,"Application of microfocussing at a none specific beamline", *SRI 2003 Proceedings, AIP Conference Proceedings* **705** (2004) 804.

R. Weber et al., "Photoemission from aqueous alkali-iodine salt solutions, using EUV synchrotron radiation", *J. Phys. Chem.* B **108** (2004) 4729.

B. Winter et al., "Full valence band photoemission from liquid water, using EUV synchrotron radiation", *J. Phys. Chem.* A **108** (2004) 2625.

B. Winter et al., "Molecular structure of surface active salt solutions: photoelectron spectroscopy and molecular dynamics simulations of aqueous Tetrabutyl-Ammonium Iodide", *J. Phys. Chem.* B **108** (2004) 14558.

M.A. Zaki Ewiss et al., "Wetting behaviour of 5CB and 8CB and their binary mixtures above the isotropic transition", *Liquid Crystals* **31** (2004) 557.

2005

B. Abel et al., "Applications, features, and mechanistic aspects of liquid water beam desorption mass spectrometry", *International Journal of Mass Spectrometry* **243** (2005) 177.

A. Ahmad et al., "New multivalent cationic lipids reveal bell curve for transfection efficiency versus membrane charge density: lipid-DNA complexes for gene delivery", *Journal of Gene Medicine* **7** (2005) 739.

J.-C. Baret et al., "Electroactuation of Fluid Using Topographical Wetting Transitions", *Langmuir* **21** (2005) 12218.

M. Brinkmann, J. Kierfeld, and R. Lipowsky, "Stability of liquid channels or filaments in the presence of line tension", *J. Phys. Condens. Matter* **17** (2005) 2349.

A. Dimakis and F. Müller-Hoissen, "An algebraic scheme associated with the noncommutative KP hierarchy and some of its extensions", *J. Phys. A: Math. Gen.* **38** (2005) 5453.

A. Dimakis and F. Müller-Hoissen, "Algebraic identities associated with KP and AKNS hierarchies", *Czech. J. Phys.* **55** (2005) 1385.

T. v. Dorfmüller et al., Bergmann-Schaefer: *Lehrbuch der Experimentalphysik: Gase, Nanosysteme, Flüssigkeiten, 2. Aufl, Hrsg. v. K. Kleinermanns,* Walter de Gruyter -Verlagsgruppe, Berlin 2005.

K. Ewert et al., "Cationic lipid-DNA complexes for non-viral gene therapy: relating supramolecular structures to cellular pathways", *Expert Opinion on Biological Therapy* **5** (2005) 33.

A. Fingerle, S. Herminghaus, and V. Zaburdaev, "Kolmogorov-Sinai Entropy of the Dilute Wet Granular Gas", *Phys. Rev. Lett* **95** (2005) 198001.

Z. Fournier et al., "Mechanical properties of wet granular materials", *J. Phys.: Condens. Matter* **17** (2005) S477.

P. Heinig and D. Langevin, "Domain shape relaxation and local viscosity in stratifying foam films", *Eur. Phys. J. E* **18** (2005) 483.

S. Herminghaus, "A Generic Mechanism of Sliding Friction between Charged Soft Surfaces", *Phys. Rev. Lett.* **95** (2005) 264301.

S. Herminghaus (edtr.), *J. Phys.: Condens. Matter* **17** (2005) (special issue on wetting).

S. Herminghaus, "Dynamics of wet granular matter", *Advances in Physics* **54** (2005) 221.

K. Jacobs, R. Seemann, and H. Kuhlmann" Trendbericht: Mikrofluidik" *Nachrichten aus der Chemie* **53** (2005) 302 (eingeladener Beitrag).

S. Köster et al., "Microaligned collagen matrices by hydrodynamic focusing: controlling the pH-induced self-assembly", *MRS Proceedings* **898E** (2005) 0989-L05-21.

S. Köster, D. Steinhauser, T. Pfohl, "Brownian motion of actin filaments in confining microchannels", *J. Phys.: Condens. Matter* **17** (2005) S4091.

R. Lipowsky et al., "Droplets, bubbles, and vesicles at chemically structured surfaces", *J. Phys. Condens. Matter* **17** (2005) S537.

R. Lipowsky et al., "Wetting, budding, and fusion-morphological transitions of soft surfaces", *J. Phys. Condens. Matter* **17** (2005) S2885.

F. Mugele et al., "Electrowetting: A Convenient Way to Switchable Wettability Patterns", *J. Phys.: Condens. Matter* **17** (2005) S559.

A. Otten et al., "Microfluidics of soft matter investigated by small angle x-ray scattering", *Journal of Synchrotron Radiation* 12 (2005) 745.

R. Seemann et al., "Wetting morphologies at microstructured surfaces", *Proc. Natl. Acad. Sci.* USA **102** (2005) 1848.

R. Seemann et al., "Dynamics and structure formation in thin polymer melt films", *J. Phys.: Condens. Matter* **17** (2005) S267.

B. Winter et al., "Effect of bromide on the interfacial structure of aqueous tetrabutylammonium iodide: Photoelectron spectroscopy and molecular dynamics simulations", *Chemical Physics Letters* **410** (2005) 222.

B. Winter et al.,"Electron Binding Energies of Aqueous Alkali and Halide Ions: EUV Photoelectron Spectroscopy of Liquid Solutions and Combined Ab Initio and Molecular Dynamics Calculations", *J. Am. Chem. Soc.* **127** (2005) 2703.

2006

S. Arscott et al., "Capillary filling of miniaturized sources for electrospray mass spectrometry", *J. Phys.: Condens. Matter* 18 (2006) S677.

Ch. Bahr, "Surfactant-induced nematic wetting layer at a thermotropic liquid crystal/water interface", *Phys. Rev. E* **73** (2006) 030702(R).

J.-C. Baret and M. Brinkmann, "Wettability control of droplet deposition and detachment", *Phys. Rev. Letters* **96** (2006) 146106.

M. Brinkmann et al., "Fluidics of a nanogap", Langmuir **22** (2006) 9784.

V. Designolle et al., "AFM study of defect-induced depressions of the smectic-A/air interface", *Langmuir* **22** (2006) 362.

A. Dimakis and F. Müller-Hoissen, "Nonassociativity and integrable hierarchies", arXiv:nlin/0601001.

A. Dimakis and F. Müller-Hoissen, "Functional representations of integrable hierarchies", *J. Phys. A: Math. Gen.* **39** (2006) 9169.

A. Dimakis and F. Müller-Hoissen, "From AKNS to derivative NLS hierarchies via deformations of associative products", *J. Phys. A: Math. Gen.* **39** (2006) 14015.

A. Dimakis and F. Müller-Hoissen, "From nonassociativity to solutions of the KP hierarchy", *Czech. J. Phys.* **56** (2006) 1123.

R. Dootz et al., "Evolution of DNA compaction in microchannels", *J. Phys.: Condens. Matter* **18** (2006) S639.

R. Dootz et al., "Raman and surface enhanced Raman microscopy of microstructured PEI/DNA multilayers", *Langmuir* **22** (2006) 1735.

K. Ewert et al., "A columnar phase of dendritic lipid-based cationic liposome-DNA complexes for gene delivery: hexagonally ordered cylindrical micelles embedded in a DNA honeycomb lattice", *J. Am. Chem. Soc.* **128** (2006) 3998.

A. Fingerle and S. Herminghaus, "Unclustering transition in freely cooling wet granular matter", *Phys. Rev. Lett.* **97** (2006) 078001.

M. Fischer, P. Heinig, and P. Dhar, "The viscous drag of spheres and filaments moving in membranes or monolayers", *J. Fluid. Mech* **558** (2006) 451.

S. Herminghaus and F. Brochard: "Dewetting Through Nucleation", *C. R. Physique* **7** (2006) 1073

Y. Iwashita and H. Tanaka, "Self-organization in Phase Separation of a Lyotropic Liquid Crystal into Cellular, Network and Droplet Morphologies", *Nature Materials* 5 (2006) 147

C. Lutz et al., "Surmounting Barriers: The Benefit of Hydrodynamic Interactions", *Europhys. Lett.* **74** (2006) 719.

C. Priest, S. Herminghaus, and R. Seemann, "Generation of monodisperse gel emulsions in a microfluidic device", *Appl. Phys. Lett.* **88** (2006) 024106.

C. Priest, S. Herminghaus, and R. Seemann, "Controlled electrocoalescence in microfluidics: targeting a single lamella", *Appl. Phys. Lett.* **89** (2006) 134101.

C. Priest et al. "Gel emulsions for microfluidic processing", *Proceedings of the 4th world congress on emulsions* 2006.

M. Schmiedeberg and H. Stark, "Superdiffusion in a Honeycomb Billiard", *Phys. Rev. E.* **73** (2006) 031113.

R. Seemann et al., "Freezing of Polymer Thin Films and Surfaces: The Small Molecular Weight Puzzle", *J. Polymer Sci. B* **44** (2006) 2968

B. Winter and M. Faubel, "Photoemission from liquid aqueous solutions", *Chemical Reviews* **106** (2006) 1176.
B. Winter et al., "Electron binding energies of hy-

drated H3O + and OH-: Photoelectron spectroscopy of aqueous acid and base solutions combined with electronic structure calculations", *Journal of the American Chemical Society* **128** (2006) 3864.

V. Yu. Zaburdaev, M. Brinkmann, and S. Herminghaus, "Free Cooling of the One-Dimensional Wet Granular Gas", *Phys. Rev. Lett.* **97** (2006) 018001.

2007

Ch. Bahr, "Surface triple points and multiple-layer transitions observed by tuning the surface field at smectic liquid crystal/water interfaces", *Phys. Rev. Lett.* **99** (2007) 057801.

J.-C. Baret et al., "Transport Dynamics in Open Microfluidic Grooves", *Langmuir* **23** (2007) 5200.

M. Brinkmann, K. Khare, and R. Seemann, "Manipulation of Fluidic Interfaces by Control of Surface Energies", Buchbeitrag für *„Microfluidic Technologies for Miniaturized Analysis Systems"*, Springer Wien New York, ISBN 978-0-387-28597-9 (2007).

V. Chokkalingam et al., "Discrete Microfluidics: Production of Silica Particles with Emulsions"*Proc. µTAS2007 (Paris)* **Vol. 2** (2007) 1534 (CBM Society, San Diego, 2007).

A. Dimakis and F. Müller-Hoissen, "Burgers and KP hierarchies: A functional representation approach", *Theor. Math. Phys.* **152** (2007) 933.

A. Dimakis and F. Müller-Hoissen, "With a Cole-Hopf transformation to solutions of the noncommutative KP hierarchy in terms of Wronski matrices", *J. Phys. A: Math. Theor.* **40** (2007) F321.

A. Dimakis and F. Müller-Hoissen, "A new approach to deformation equations of noncommutative KP hierarchies", *J. Phys. A: Math. Theor.* **40** (2007) 7573.

A. Dimakis and F. Müller-Hoissen, "Weakly nonassociative algebras, Riccati and KP hierarchies", arXiv:nlin/0701010, to appear in Proc. AGMF Workshop, Lund, 2006.

A. Dimakis and F. Müller-Hoissen, "Dispersionless limit of the noncommutative potential KP hierarchy and solutions of the pseudodual chiral model in 2 + 1 dimensions", arXiv:0706.1373 [nlin.SI].

F. Müller-Hoissen, "Noncommutative Geometries and Gravity", arXiv:0710.4418 [gr-qc], to appear in Proc. Third Mexican Meeting on Mathematical and Experimental Physics.

R. Dootz et al., "Rapid Prototyping of X-Ray Microdiffraction Compatible Continuous Microflow Foils", *Small* **3** (2007) 96.

M. Engstler et al., "Hydrodynamic Flow-Mediated Protein Sorting on the Cell Surface of Trypanosomes", *Cell* **131** (2007) 505.

H. M. Evans et al., "X-ray Microdiffraction on Flow-controlled Biomolecular Assemblies", *Bulletin of the Polish Academy of Sciences: Technical Sciences* **55** (2007) 217.

R. Fetzer et al., "Thermal Noise Influences Fluid Flow in Thin Films during Spinodal Dewetting", *Phys. Rev. Lett.* **99** (2007) 114503.

A. Fingerle, S. Herminghaus, and V. Yu. Zaburdaev, "Chaoticity of the Wet Granular Gas" *Phys. Rev. E* **75** (2007) 061301.

A. Fingerle, "Relativistic fluctuation theorems", *C. R. Physique* **8** (2007) 696.

A. Fingerle and S. Herminghaus, "Equation of state of wet granular matter", *Phys. Rev. E* **76** (2007), in press.

S. Höfl et al., "Volume Phase Transition of ''Smart'' Microgels in Bulk Solution and Adsorbed at an Interface: A Combined AFM, Dynamic Light, and Small Angle Neutron Scattering Study", *Polymer* **48** (2007) 245.

Y. Iwashita and H. Tanaka, "Spontaneous onion formation from planar lamellar nuclei", *Phys. Rev. Lett.*, **98** (2007) 145703

E. Kadivar, Ch. Bahr, and H. Stark, "Cross-over in the wetting behavior at surfactant-laden liquid-crystal/water interfaces: experiment and theory", *Phys. Rev. E* **75** (2007) 061711.

K. Khare et al., "Dewetting of liquid filaments in wedge shaped grooves", *Langmuir* **23** (2007) 12138.

K. Khare et al., "Switching Liquid Morphologies on Linear Grooves", *Langmuir* **23** (2007) 12997.

S. Köster et al., "Fluctuations of Single Confined Actin Filaments" *Biophysical Reviews and Letters* **2** (2007) 155.

S. Köster et al., "Visualization of Flow-Aligned Type I Collagen Self-Assembly in Tunable pH Gradients", *Langmuir* **23** (2007) 357.

D. Nolting et al., "pH-Induced Protonation of Lysine in Aqueous Solution Causes Chemical Shifts in X-ray Photoelectron Spectroscopy", *J. Am. Chem. Soc.*, **129** (2007) 14068-14073.

A. Pelah, R. Seemann, and T. M. Jovin, "Reversible cell deformation by a polymeric actuator", *J. Am. Chem. Soc.* **129** (2007) 468.

S. Peter et al., “Slow dynamics and glass transition in simulated free-standing polymer films: a possible relation between global and local glass transition temperatures”, *Phys. Cond. Mat.* **19** (2007) 205119.

T. Pfohl et al., “Highly Packed and Oriented DNA Mesophases Identified Using in Situ Microfluidic X-ray Microdiffraction”, *Biomacromolecules* **8** (2007) 2167.

C. Priest et al., “Droplet-Based Microfluidics at High Dispersed-Phase Volume Fractions ” *Proc. µTAS2007 (Paris)* **Vol. 2** (2007) 931 (CBM Society, San Diego, 2007).

T. M. Schneider, B. Eckhardt, and J. Vollmer, “Statistical analysis of coherent structures in transitional pipe flow“, *Phys. Rev. E* **75** (2007) 066313

M. Scheel et al., “Morphological clues to wet granular pile stability”, *Nature Materials* (2007) in press.

R. Seemann, S. Herminghaus, and K. Jacobs, “Structure Formation in Thin Liquid Films: Interface Forces Unleashed” in *CISM Courses and Lectures* **Vol. 490**: “Thin Films of Soft Matter” (Springer, Wien 2007).

E. Surenjav et al., “Manipulation of Monodisperse Gel Emulsions in Microchannels”, *Proc. µTAS2007 (Paris)* **Vol. 1** (2007) 339 (CBM Society, San Diego, 2007).

J. Vollmer, G. K. Auernhammer, and D. Vollmer, “Minimal Model for Phase Separation under Slow Cooling” *Phys. Rev. Lett.* **98** (2007) 115701.

B.Winter et al., “Hydrogen bonds in liquid water studied by photoelectron spectroscopy”, *J. Chem. Phys.* **126** (2007)124504.

B. Winter et al., ”Hydrogen bonding in liquid water probed by resonant Auger-electron spectroscopy”, *J. Chem. Phys.* **127** (2007) 094501.

V. Yu. Zaburdaev and S. Herminghaus, “Dry and wet Granular Shockwaves”, *Phys. Rev E* **75** (2007) 031304.

Department of Fluid Dynamics, Pattern Formation and Nanobiocomplexity

2003

B. Abel et al., "Comment on 'Rate coefficients for photoinitiated NO_2 unimolecular decomposition: energy dependence in the threshold regime'", *Chem. Phys. Lett.* **368** (2003) 252.

T. Azzam et al., "The bound state spectrum of HOBr up to the dissociation limit: Evolution of saddle-node bifurcations", *J. Chem. Phys.* **118** (2003) 9643.

D. Babikov et al., "Quantum origin of an anomalous isotope effect in ozone formation", *Chem. Phys. Lett.* **372** (2003) 686.

D. Babikov et al., "Metastable states of ozone calculated on an accurate potential energy surface", *J. Chem. Phys.* **118** (2003) 6298.

D. Babikov et al., "Formation of ozone: Metastable states and anomalous isotope effect", *J. Chem. Phys.* **119** (2003) 2577.

A.M. Crawford, N. Mordant, and E. Bodenschatz, "Comment on Dynamical Foundations of Nonextensive Statistical Mechanics", arXiv: physics/0212080 (2003).

K.E. Daniels and E. Bodenschatz, "Statistics of Defect Motion in Spatiotemporal Chaos in Inclined Layer Convection", *Chaos* **13** (2003) 55.

K.E. Daniels, R.J. Wiener, and E. Bodenschatz, "Localized Transverse Bursts in Inclined Layer Convection", *Phys. Rev. Lett.* **91**, (2003) 114501.

P. Fleurat-Lessard et al., "Theoretical investigation of the temperature dependence of the $O + O_2$ exchange reaction", *J. Chem. Phys.* **118** (2003) 610.

P. Fleurat-Lessard et al., "Isotope dependence of the $O + O_2$ exchange reaction: Experiment and theory", *J. Chem. Phys.* **119** (2003) 4700. [Erratum: **120** (2004) 4993].

S. Yu. Grebenshchikov, "Van der Waals states in ozone and their influence on the threshold spectrum of $O_3(X^1A_1)$. I. Bound states", *J. Chem. Phys.* **119** (2003) 6512.

S. Yu. Grebenshchikov, R. Schinke, and W. L. Hase, "State-specific dynamics of unimolecular dissociation", in *Comprehensive Chemical Kinetics*, **39** Unimolecular Kinetics, Part 1. The Reaction Step, N. J. B. Green, ed. (Elsevier, Amsterdam, 2003).

M. V. Ivanov and R. Schinke, "Two-dimensional neutral donors in electric fields", *J. Phys: Condensed Matter* **15** (2003) 5909.

V. Kurkal, P. Fleurat-Lessard, and R. Schinke, "NO_2: Global potential energy surfaces of the ground ($^2A_1$) and the first excited ($^2B_1$) electronic states", *J. Chem. Phys.* **119** (2003) 1489.

L. Poluyanov and R. Schinke, "Theory of Molecular Bound States including $\sum$ - Π Vibronic Interaction", *Chem. Phys.* **288** (2003) 123.

Z.-W. Qu, H. Zhu, and R. Schinke, "The ultra-violet photodissociation of ozone revisited", *Chem. Phys. Lett.* **377** (2003) 359.

B.L. Sawford et al., "Conditional and Unconditional Acceleration Statistics in Turbulence", *Phys. Fluids* **15** (2003) 3478.

R. Schinke, P. Fleurat-Lessard, and S. Yu. Grebenshchikov, "Isotope dependence of the lifetime of ozone complexes formed in $O + O_2$ collisions", *Phys. Chem. Chem. Phys.* **5** (2003) 1966.

R. Siebert and R. Schinke, "The vibrational spectrum of cyclic ozone", *J. Chem. Phys.* **119** (2003) 3092.

M. Tashiro and R. Schinke, "The effect of spin-orbit coupling in complex forming $O(^3P) + O_2$ collisions", *J. Chem. Phys.* **119** (2003) 10186.

K.-L. Yeh et al., "A time-dependent wave packet study of the $O + O_2$ ($v = 0, j = 0$) exchange reaction", *J. Phys. Chem. A* **107** (2003) 7215.

2004

K.E. Daniels, C. Beck, and E. Bodenschatz, "Defect Turbulence and Generalized Statistical Mechanics", *Physica D* **193** (2004) 208.

S. F. Deppe et al., "Resonance spectrum and dissociation dynamics of ozone in the $^3B_2$ electronically excited state: Experiment and theory", *J. Chem. Phys.* **121** (2004) 5191.

C. Huepe et al., "Statistics of Defect Trajectories in Spatio-Temporal Chaos in Inclined Layer Convection and the Complex Ginzburg-Landau Equation", *Chaos* **14** (2004) 864.

M. V. Ivanov, and R. Schinke "Two-dimensional analogs of the H_2^+ ion in stationary electric fields", *Phys. Rev. B* **69** (2004) 165308-1.

M.V. Ivanov, S. Yu. Grebenshchikov, and R. Schinke "Intra- and intermolecular energy transfer in highly excited ozone complexes", *J. Chem. Phys.* **120** (2004) 10015.

M. Joyeux, R. Schinke, and S. Yu. Grebenshchikov "Semiclassical dynamics of the van der Waals states in $O_3(X^1A_1)$", *J. Chem. Phys.* **120** (2004) 7426.

S. Luther, J. Rensen, and S. Guet, "Aspect Ratio Measurement Using a Four-Point Fiber-Optical Probe", *Exp. Fluids* **36** (2004) 326.

N. Mordant, A.M. Crawford, and E. Bodenschatz, "Experimental Lagrangian Acceleration Probability Density Function Measurement", *Physica D* **193** (2004) 245.

N. Mordant, A.M. Crawford, and E. Bodenschatz, "Three-Dimensional Structure of Lagrangian Acceleration in Turbulent Flows", *Phys. Rev. Lett.* **93** (2004) 214501.

Z.-W. Qu et al., "The Huggins band of ozone: Unambiguous electronic and vibrational assignment", *J. Chem. Phys.* **120** (2004) 6811.

Z.-W. Qu, "The Huggins band of ozone: A theoretical analysis", *J. Chem. Phys.* **121**, (2004) 11731.

D.S. Rhoads et al., "Using Microfluidic Channel Networks to Generate Gradients for Studying Cell Migration", In Cell Migration: Developmental Methods and Protocols (J.-L. Guan, ed.), *Humana Press*, Totowa, NJ **294** (2004) 347.

R. Schinke, and P. Fleurat-Lessard "On the transition-state region of the $O(^3P) + O_2(^3\Sigma^-_g)$ potential energy surface", *J. Chem. Phys.* **121** (2004) 5789.

R. Schinke, "Quantum mechanical studies of photodissociation dynamics using accurate global potential energy surfaces", In *Conical Intersections: Electronic Structure, Dynamics and Spectroscopy*, W. Domcke ed. (2004) 473.

E.A. Variano, E. Bodenschatz, and E.A. Cowen, "A Random Synthetic Jet Array Driven Turbulence Tank", *Exp. Fluids* **37** (2004) 613.

C. Voelz and E. Bodenschatz, "Experiments with Dictyostelium Discoidium Amoebae in Different Geometries", in Dynamics and Bifurcation of Patterns in Dissipative Systems G. Dangelmayr and I. Oprea (eds.), World Scientific Series on Nonlinear Science **12**, *World Scientific* (Singapore) (2004) 372.

T. Walter, E. Bodenschatz, and W. Pesch, "Dislocation Dynamics in Rayleigh-Bénard Convection", *Chaos* **14** (2004) 933.

H. Zhu et al., "On spin-forbidden processes in the ultra-violet photodissociation of ozone", *Chem. Phys. Lett.* **384** (2004) 45.

2005

L. Adam et al., "Experimental and theoretical investigation of the reaction $NH(X^3\Sigma^-) + H(^2S) \rightarrow N(^4S) + H_2(X^1\Sigma^+_g)$", *J. Chem. Phys.* **122** (2005) 114301-1.

M.M. Afonso and D. Vincenzi, "Non Linear Elastic Polymers in Random Flow", *J. Fluid Mech.* **540** (2005) 99.

J. Bluemink et al., "Asymmetry Induced Particle Drift in Rotational Flow", *Phys. Fluids* **17** (2005) 072106.

A.M. Crawford, N. Mordant, and E. Bodenschatz, "Joint Statistics of the Lagrangian Acceleration and Velocity in Fully Developed Turbulence", *Phys. Rev. Lett.* **94** (2005) 024501.

S. Guet, S. Luther, and G. Ooms, "Bubble Shape and Orientation Determination with a Four-Point Optical Fiber Probe", *Exp. Therm. Fluid Sci.* **29** (2005) 803.

W. L. Hase and R. Schinke "Role of computational chemistry in the theory of unimolecular reaction rates", In *Theory and Applications of Computational Chemistry: The first 40 years*, C.E. Dykstra et al. eds. (Elsevier, New York, 2005) 397.

M. V. Ivanov, and R. Schinke, "Temperature dependent energy transfer in Ar – O_3 collisions", *J. Chem. Phys.* **122** (2005) 234318-1.

M. Joyeux et al., "Intramolecular dynamics along isomerization and dissociation pathways", *Adv. Chem. Phys.* **130** (2005) 267.

R.F. Katz, R. Ragnarsson, and E. Bodenschatz, "Tectonic Microplates in a Wax Model of Sea-Floor Spreading", *New J. Phys.* **7** (2005) 37.

R.F. Katz and E. Bodenschatz, "Taking Wax for a Spin: Microplates in an Analog Model of Plate Tectonics", *Europhysics News* **5** (2005) 155.

S. Luther et al., "Data Analysis for Hot-Film Anemometry in Turbulent Bubbly Flow", *Exp. Therm. Fluid Sci.* **29** (2005) 821.

K. Mauersberger et al., "Assessment of the ozone isotope effect", *Adv. Atom. Mol. and Opt. Phys.* **50** (2005) 1.

H. Nobach, K. Chang, and E. Bodenschatz, "Transformation von zeitlichen in räumliche Statistiken – zwei Alternativen zur Taylor-Hypothese". Tagungsband 13. Fachtagung "Lasermethoden in der Strömungsmesstechnik", Cottbus, 6.-8. Sept.2005.

H. Nobach et al., "Full-Field Correlation-Based Image Processing for PIV", Proc. 6th International Symposium on Particle Image Velocimetry, Pasadena, California, USA, September 21-23, 2005.

Z.-W. Qu et al., "Experimental and theoretical investigation of the reactions NH($X^3\Sigma^-$) + D(^2S) → ND($X^3\Sigma^-$) + H(^2S) and NH($X^3\Sigma^-$) + D(^2S) → N(^4S) + HD($X^1\Sigma^+_g$)", *J. Chem. Phys.* **122** (2005) 204313-1.

Z.-W. Qu. et al., "The photodissociation of ozone in the Hartley band: A theoretical analysis", *J. Chem. Phys.* **123** (2005) 074305-1.

Z.-W. Qu, H. Zhu, and R. Schinke, "Infrared spectrum of cyclic ozone: A theoretical investigation", *J. Chem. Phys.* **123** (2005) 204324-1.

Z.-W. Qu et al., "The triplet channel in the photodissociation of ozone in the Hartley band: Classical trajectory surface hopping analysis", *J. Chem. Phys.* **122** (2005) 191102-1.

J. Rensen et al., "Hot-Film Anemometry in Two Phase Flows I: Bubble-Probe Interaction", *Int. J. Multiphase Flow* **31** (2005) 285.

J. Rensen, S. Luther, and D. Lohse, "The Effect of Bubbles on Developed Turbulence", *J. Fluid Mech.* **548** (2005) 153.

A.M. Reynolds et al., "On the Distribution of Lagrangian Accelerations in Turbulent Flows", *New J. Phys.* **7** (2005) 58.

R. Schinke, and P. Fleurat-Lessard, "The effect of zero-point energy differences on the isotope dependence of the formation of ozone: A classical trajectory study.
J. Chem. Phys. **122** (2005) 094317.

B. Utter, R. Ragnarsson, and E. Bodenschatz, "Experimental Apparatus and Sample Preparation Techniques for Directional Solidification", *Rev. Sci. Inst.* **76** (2005) 013906.

B. Utter and E. Bodenschatz, "Double Dendrite Growth in Solidification", *Phys. Rev. E* **72** (2005) 011601.

T.H. van der Berg et al., "Drag Reduction in Bubbly Taylor-Couette Turbulence", *Phys. Rev. Lett.* **94** (2005) 044501.

H. Varela et al., "Transitions to Electrochemical Turbulence", *Phys. Rev. Lett.* **94** (2005) 174104.

H. Varela et al., "A Hierarchy of Global Coupling Induced Cluster Patterns During the Oscillatory H2-Electrooxidation Reaction on a Pt Ring-Electrode", *Phys. Chem. Chem. Phys.* **7** (2005) 2429.

H. Zhu et al., "The Huggins band of ozone. Analysis of hot bands", *J. Chem. Phys.* **122** (2005) 024310-1.

2006

S. Ayyalasomayajula et al., "Lagrangian Measurements of Inertial Particle Accelerations in Grid Generated Wind Tunnel Turbulence", *Phys. Rev. Lett.* **97** (2006) 144507.

C. Beta et al., "Defect-Mediated Turbulence in a Catalytic Surface Reaction", *Europhys. Lett.* **75** (2006) 868.

M. Bourgoin et al., "The Role of Pair Dispersion in Turbulent Flow", *Science* **311** (2006) 835.

A. Celani, A. Mazzino, and D. Vincenzi, "Magnetic Field Transport and Kinematic Dynamo Effect: A Lagrangian Interpretation", *Proc. R. Soc. A* **462** (2006) 137.

S. C. Farantos et al., "Reaction paths and elementary bifurcations tracks: The diabatic $^1B_2$-state of ozone", *Int. J. of Bifurcation and Chaos*, **16** (2006) 1913.

M. Kinzel et al., "Measurement of Lagrangian Acceleration Using the Laser Doppler Technique", Proc. of the 13th International Symposium on Applications of Laser Techniques to Fluid Mechanics, Lisbon, Portugal, June 26-29, 2006.

M. Kinzel et al., "Messung Lagrange'scher Beschleunigungen mittels Laser-Doppler-Anemometrie", Tagungsband 14. Fachtagung "Lasermethoden in der Strömungsmesstechnik", Braunschweig, 5.-7. Sept. 2006.

H. Nobach, M. Kinzel, and C. Tropea, "Measurement of Lagrangian Acceleration in Turbulent Flows Using the Laser Doppler Technique Optical Methods of Flow Investigation", *Proc. of SPIE* **6262** (2006) 1.

H. Nobach and E. Bodenschatz, "New resolution limits in PIV image processing", Proc. of the 13th International Symposium on Applications of Laser Techniques to Fluid Mechanics, Lisbon, Portugal, June 26-29, 2006.

H. Nobach and E. Bodenschatz, "Neue Auflösungsgrenzen von PIV", Tagungsband 14. Fachtagung "Lasermethoden in der Strömungsmesstechnik", Braunschweig, 5.-7. Sept. 2006.

N.T. Ouellette, H. Xu, and E. Bodenschatz, "A Quantitative Study of Three-Dimensional Lagrangian Particle Tracking Algorithms", *Exp. Fluids* **40** (2006) 301.

N.T. Ouellette et al., "Small-Scale Anisotropy in Lagrangian Turbulence", *New J. Phys.* **8** (2006) 102.

N.T. Ouellette et al., "An Experimental Study of Turbulent Relative Dispersion Models", *New J. Phys.* **8** (2006) 109.

N.T. Ouellette et al., "Statistical Geometry in Intensely Turbulent Flow", Proc. 12th Int. Sym. Flow Visualization, ed. I. Grant (2006) 167.

R. Schinke et al., "Dynamical studies of the ozone isotope effect: A status report", *Ann. Rev. Phys. Chem.* **57** (2006) 625.

M. V. Ivanov and R. Schinke, "Recombination of ozone via the chaperon mechanism", *J. Chem. Phys.* **124** (2006) 104303.

E. Scifoni et al., "Energies and spatial features for the rotationless bound states of $^4He_3^+$ ($^2\Sigma_g^+$): A cationic core from helium cluster ionization", *J. Chem. Phys.* **125** (2006) 164304.

L. Song et al., "Dictyostelium Discoideum Chemotaxis: Threshold for Directed Motion", *Eur. J. Cell Biol.* **85** (2006) 981.

R. Toegel, S. Luther, and D. Lohse, "Viscosity Destabilizes Bubbles", *Phys. Rev. Lett.* **96** (2006) 114301.

T.H. van der Berg, S. Luther, and D. Lohse, "Energy Spectra in Microbubbly Turbulence", *Phys. Fluids* **18** (2006) 038103.

T.H. van der Berg et al., "Bubbly Turbulence", *J. Turbul.* **7** (2006) 1.

D. Vincenzi and E. Bodenschatz, "Single Polymer Dynamics in Elongational Flow and the Confluent Heun Equation", *J. Phys. A: Math. Gen.* **39** (2006) 10691.

H. Xu et al., "High Order Lagrangian Velocity Statistics in Turbulence", *Phys. Rev. Lett.* **96** (2006) 024503.

H. Xu, N.T. Ouellette, and E. Bodenschatz, "Multifractal Dimension of Lagrangian Turbulence", International Collaboration for Turbulence Research, *Phys. Rev. Lett.* **96** (2006) 114503.

S. Yu. Grebenshchikov et al., "Absorption spectrum and assignment of the Chappuis band of ozone", *J. Chem. Phys.* **124** (2006) 204313.

S. Yu. Grebenshchikov et al., "Spin-orbit mechanism of predissociation in the Wulf band of ozone", *J. Chem. Phys.* **125** (2006) 021102.

2007

L. Adam et al., "Exploring Renner-Teller induced quenching in the reaction $H(^2S) + NH(a^1\Delta)$: A combined experimental and theoretical study", *J. Chem. Phys.* **126** (2007) 034304.

C. Beta et al., "Flow Photolysis for Spatiotemporal Stimulation of Single Cells", *Anal. Chem.* **79** (2007) 3940.

P.S. Bodega et al., "High Frequency Periodic Forcing of the Oscillatory Catalytic CO Oxidation on Pt (110)", *New J. Phys.* **9** (2007) 61.

S. Yu. Grebenshchikov et al., "New theoretical investigations of the photodissociation of ozone in the Hartley, Huggins, Chappuis, and Wulf bands", *Phys. Chem. Chem. Phys.* **9** (2007) 2044

S. Yu. Grebenshchikov and R. Schinke, "Comment on: 'Theory of the photodissociation of ozone in the Hartley continuum: Potential energy surfaces, conical intersections, and the photodissociation dynamics'[*J. Chem. Phys.* **123** (2005) 014306]", *J. Chem. Phys.* **126** (2007) 247101.

M. V. Ivanov, H. Zhu, and R. Schinke, "Theoretical investigation of exchange and recombination reactions in $O(^3P) + NO(^2\Pi)$ collisions", *J. Chem. Phys.* **126** (2007) 054304.

M. V. Ivanov, R. Schinke, and G. C. McBane, "Theoretical investigation of vibrational relaxation of $NO(^2\Pi)$, $O_2(^3\Sigma_g^-)$, and $N_2(^1\Sigma_g^+)$ in collisions with $O(^3P)$", *Mol. Phys.* **105** (2007) 1183.

L. Lammich et al., "Electron-impact dissociation and transition properties of a stored LiH_2^- beam", *Eur. Phys. J. D* **41** (2007) 103.

E. van Nierop et al., "Drag and lift forces on bubbles in a rotating flow", *J. Fluid. Mech.* **571** (2007) 439.

H. Nobach and E. Bodenschatz, "Grenzen von PIV durch individuelle Intensitätsänderung von Streuteilchen", Tagungsband, 15. Fachtagung "Lasermethoden in der Strömungsmesstechnik", Rostock, 4.-6. Sept. 2007.

H. Nobach and E. Bodenschatz, "Limitations of Accuracy in PIV due to Individual Variations of Particle Image Intensities", Proc. 7th International Symposium on Particle Image Velocimetry, Rome, Italy, Sept. 11-14, 2007.

H. Nobach, "Gegen Wavelets & Co. – Vorteile klassischer Signal- und Datenverarbeitungsverfahren in der optischen Strömungsmesstechnik", Shaker Verlag Aachen (2007) ISBN 978-3-8322-6564-9 (Zugl.: TU Darmstadt, Habil., 2007).

N.T. Ouellette, H. Xu, and E. Bodenschatz, "Measuring Lagrangian Statistics in Intense Turbulence", *Handbook of Experimental Fluid Dynamics*, Springer, C. Tropea, J. Foss, & A. Yarin ed. (2007) 789.

A. Pumir et al., "Wave Emission from Heterogeneities Opens a Way to Controlling Chaos in the Heart", *Phys. Rev. Lett.* **99** (2007) 208101.

R. Schinke and S. Yu. Grebenshchikov, "Comment on: 'Theory of the photodissociation of ozone in the Hartley continuum; effect of vibrational excitation and O(^1D) atom velocity disribution'" [Phys. Chem. Chem. Phys. 7, 3829 (2005)]«, *Phys. Chem. Chem. Phys*. **9** (2007) 4026.

R. Schinke and S. Yu. Grebenshchikov, "On the photodissociation of ozone in the range of 5 – 9 eV", *Chem. Phys.*, in print.

G. Seiden, M. Ungarish, and S.G. Lipson, "Formation and Stability of Band Patterns in a Rotating Suspension-Filled Cylinder", *Phys. Rev. E* **76** (2007) 026221.

K. Shirai et al., "Application of Laser Doppler Velocity Profile Sensor to Turbulent Flows: Measurement of Water Channel Flow and Two-Point Correlation", Tagungsband 15. Fachtagung "Lasermethoden in der Strömungsmesstechnik", Rostock, 4.-6. Sept. 2007.

D. Vincenzi et al., "Stretching of Polymers in Isotropic Turbulence: A Statistical Closure", *Phys. Rev. Lett.* **98** (2007) 024503.

D. Vincenzi et al., "Statistical Closures for Homogeneous Shear Flow Turbulence of Dilute Polymer Solutions", *Progress in Turbulence II*, Springer Proceedings in Physics **109** (2007) 261.

H. Xu, N.T. Ouellette, and E. Bodenschatz, "Curvature of Lagrangian Trajectories in Turbulence", *Phys. Rev. Lett.* **98** (2007) 050201.

H. Xu et al., "Experimental Measurements of Lagrangian Statistics in Intense Turbulence", J.M.L.M. Palma & A. Silva Lopes ed. *Advances in Turbulence XI: Proc. 11th Euro. Turb. Conf.* (2007) 1.

H. Xu, N.T. Ouellette, and E. Bodenschatz, "Multi-Particle Statistics - Lines, Shapes, and Volumes in High Reynolds Number Turbulence", W.-Z. Chien ed. *Proc. 5th Int. Conf. Nonlinear Mech.* (2007) 1155.

H. Xu et al., "Acceleration Correlations and Pressure Structure Functions in High-Reynolds Number Turbulence", *Phys. Rev. Lett.* **99** (2007) 204501.

K. Chang et al., "Lagrangian Particle Tracking in High Reynolds Number Turbulence", Particle-Laden Flow: From Geophysical to Kolmogorov Scales, *ERCOFTAC Ser* **11** (2007) 299.

K.E. Daniels et al., "Competition and Bistability of Ordered Undulations and Undulation Chaos in Inclined Layer Convection", *J. Fluid Mech.*, in press.

H. Xu, N.T. Ouellette, and E. Bodenschatz, "Evolution of Geometric Structures in Intense Turbulence", *New J. Phys.*, in press.

M. Stich et al., "Control of Spatiotemporal Chaos in Catalytic CO Oxidation by Laser-induced Pacemakers", *Phil. Trans. R. Soc. A* **366** (2008) 419.

Independent Junior Research Group Network Dynamics

2003

M. Timme, F. Wolf, and T. Geisel, "Unstable attractors induce perpetual synchronization and desynchronization", *Chaos* **13** (2003), 377.

2004

M. Denker, M. Timme, M. Diesmann, F. Wolf, and T. Geisel, "Breaking Synchrony by Heterogeneity in Complex Networks", *Phys. Rev. Lett.* **92** (2004), 074103.

M. Timme, F. Wolf, and T. Geisel, "Topological Speed Limits to Network Synchronization" *Phys. Rev. Lett.* **92** (2004), 074101.

A. Zumdieck, M. Timme, T. Geisel, and F. Wolf, "Long Chaotic Transients in Complex Networks", *Phys. Rev. Lett.* **93** (2004), 244103.

2005

P. Ashwin and M. Timme, "Unstable attractors: existence and robustness in networks of oscillators with delayed pulse coupling", *Nonlinearity* **18** (2005), 2035.

P. Ashwin and M. Timme, "Nonlinear dynamics: When instability makes sense", *Nature* **436** (2005) 36.

2006

M. Timme, T. Geisel, and F. Wolf, "Speed of synchronization in complex networks of neural oscillators: Analytic results based on Random Matrix Theory", *Chaos* **16** (2006) 015108.

M. Timme, "Does Dynamics Reflect Topology in Directed Networks?" *Europhys. Lett.* **76** (2006) 367.

R.-M. Memmesheimer and M. Timme, "Designing Complex Networks", *Physica D* **224** (2006) 182.

R.-M. Memmesheimer and M. Timme, "Designing the Dynamics of Spiking Neural Networks", *Phys. Rev. Lett.* **97** (2006) 188101.

2007

M. Denker, S. Roux, M. Timme, A. Riehle, and S. Grün, "Phase Synchronization between LFP and Spiking Activity in Motor Cortex During Movement Preparation", *Neurocomputing* **70** (2007) 2096.

M. Timme, "Revealing Network Connectivity From Response Dynamics", *Phys. Rev. Lett.* **98** (2007) 224101.

D. Kozen and M. Timme, "Indefinite summation and the Kronecker delta". Technical Report, Computing and Information Science, Cornell University (2007).

S. Jahnke, R.-M. Memmesheimer, and M. Timme, "Stable Irregular Dynamics in Complex Neural Networks", *Phys. Rev. Lett.* (2007) in press.

Independent Junior Research Group Nonlinear Dynamics and Arrhythmias of the Heart

2004

S. Luther, J. Rensen, and S. Guet, "Aspect ratio measurement using a four-point fiber-optical probe", *Exp. Fluids* **36** (2004) 326.

2005

J. Rensen, et al., "Hot-film anemometry in two phase flows I: Bubble-probe interaction", *Int. J. Multiphase Flow* **31** (2005) 285.

J. Rensen, S. Luther, and D. Lohse, "The effect of bubbles on developed turbulence", *J. Fluid Mech.* **548** (2005) 153.

T.H. van den Berg et al., "Drag reduction in bubbly Taylor-Couette turbulence", *Phys. Rev. Lett.* **94** (2005) 044501.

S. Luther et al., "Data analysis for hot-film anemometry in turbulent bubbly flow", *Exp. Thermal and Fluid Science* **29** (2005) 821.

S. Guet, S. Luther, and G. Ooms, "Bubble shape and orientation determination with a four-point optical fiber probe", *Exp. Thermal and Fluid Science* **29** (2005) 803.

J. Bluemink et al., "Asymmetry induced particle drift in rotational flow", *Phys. Fluids* **17** (2005) 072106-1.

2006

R. Toegel, S. Luther, and D. Lohse, "Viscosity destabilizes bubbles", *Phys. Rev. Lett.* **96** (2006) 114301.

T.H. van den Berg, S. Luther, and D. Lohse, "Energy spectra in microbubbly turbulence", *Phys. Fluids* **18** (2006) 038103

T.H. van der Berg et al., "Bubbly turbulence", *J. of Turbulence* **7** (2006) 1.

2007

E. van Nierop et al., "Drag and lift forces on bubbles in a rotating flow", *J. Fluid Mech.* **571** (2007) 439.

Independent Junior Research Group Onset of Turbulence and Complexity

2003

B. Hof, A. Juel , and T. Mullin, "Magnetohydrodynamic damping of convective flows in gallium", *J. Fluid Mech.* **482** (2003) 163.

B. Hof, A. Juel, and T. Mullin, "Scaling of the turbulence transition threshold in a pipe" *Phys. Rev. Lett.* **91** (2003) 244502.

2004

B. Hof et al., "Stability of convective flows in molten gallium." *J. Fluid Mech.*, **515** (2004) 391.

B. Hof et al., "Experimental observation of nonlinear travelling waves in turbulent pipe flow" *Science* **305** (2004) 1594.

2005

B. Hof, A. Juel, and T.Mullin, "Magnetohydrodynamic damping of oscillations in low Prandtl number convection", *J. Fluid. Mech.* **545**(2005) 193.

B. Hof et al., " Turbulence regeneration in pipe flow at moderate Reynolds numbers" *Phys. Rev. Lett.* **95 (**2005) 214502.

B.Hof, "Transition to Turbulence in pipe flow", In Proc. IUTAM Symp. on Laminar-Turbulent Transition and Finite Amplitude Solutions (T.Mullin, and R.R. Kerswell, eds) Springer (Dordrecht) (2005) 221.

2006

B. Eckhardt, B. Hof, and H. Faisst, "Die Lösung eines alten Rätsels", *Physik in unserer Zeit*, **37** (2006) 212

B. Hof et al., "Finite Lifetime of Turbulence in Pipe Flow." *Nature* **443** (2006) 59.

2007

B. Eckhardt et al., "Turbulence Transition in Pipe flow", *Annual Revue Fluid Mechanics*, **39** (2007) 447.

Max Planck Fellow Group

2003

T. Aspelmeier and M.A. Moore, "Free energy fluctuations in Ising spin glasses", *Phys. Rev. Lett.* **90** (2003) 177201.

T. Aspelmeier, M.A. Moore, and A.P. Young, "Interface energies in spin glasses", *Phys. Rev. Lett.* **90** (2003) 127202.

M. Küntzel et al., "Diffusion of gelation clusters in the Zimm model", *Eur. Phys. J. E* **12** (2003) 325.

J. Trommershäuser et al., "Heterogeneous presynaptic release probabilities: Functional relevance for short-term plasticity", *Biophys. J.* **84** (2003) 1563.

2004

T. Aspelmeier and M.A. Moore, "Generalized Bose-Einstein phase transition in large-m component spin glasses", *Phys. Rev. Lett.* **92** (2004) 077201.

T. Aspelmeier, A.J. Bray, and M.A. Moore, "Complexity of Ising spin glasses", *Phys. Rev. Lett.* **92** (2004) 087203.

O. Herbst et al., "Local equation of state and velocity distributions of a driven granular gas", *Phys. Rev. E* **70** (2004) 051313.

S. Mukhopadhyay, P. M. Goldbart, and A. Zippelius, "Goldstone fluctuations in the amorphous solid state", *Europhys. Lett.* **67** (2004) 49.

P. M. Goldbart, S. Mukhopadhyay, and A. Zippelius, "Goldstone-type fluctuations and their implications for the amorphous solid state", *Phys. Rev. B* **70** (2004) 184201.

2005

J. Yeo, M.A. Moore, and T. Aspelmeier, "Nature of perturbation theory in spin glasses", *J. Phys. A* **38** (2005) 4027.

O. Herbst et al., "A driven two-dimensional granular gas with coulomb friction", *Phys. Fluids* **17** (2005) 107102.

O. Herbst, P. Müller, and A. Zippelius, "Local heat flux and energy loss in a two-dimensional vibrated granular gas", *Phys. Rev. E* **72** (2005) 041303.

H. Löwe, P. Müller, and A. Zippelius, "Dynamics of gelling liquids: a short survey", *J. Phys. Cond. Mat.* **17** (2005) S1659.

H. Löwe, P. Müller, and A. Zippelius, "Rheology of gelling polymers in the Zimm model", *J. Chem. Phys.* **122** (2005) 014905.

K. Vollmayr-Lee and A. Zippelius, "Heterogeneities in the glassy state", *Phys. Rev. E* **72** (2005) 041507.

C. Wald, A. Zippelius, and P. M. Goldbart, "Glassy states and microphase separation in cross-linked homopolymer blends", *Europhys. Lett.* **70** (2005) 843.

2006

T. Aspelmeier et al., "Free energy landscapes, dynamics, and the edge of chaos in mean-field models of spin glasses", *Phys. Rev. B* **74** (2006) 184411.

A. Braun and T. Aspelmeier, "The m-component spin glass on a Bethe lattice", *Phys. Rev. B* **74** (2006) 144205.

M. Otto, T. Aspelmeier and A. Zippelius, "Microscopic dynamics of thin hard rods", *J. Chem. Phys.* **124** (2006) 154907.

S. Ulrich et al., "Elasticity of highly cross-linked random networks", *Europhys. Lett.* **76** (2006) 677.

C. Wald, P. M. Goldbart, and A. Zippelius, "Glassy correlations and microstructures in randomly cross-linked homopolymer blends", *J. Chem. Phys.* **124** (2006) 214905.

A. Zippelius, "Granular gases", *Physica A* **369** (2006) 143.

2007

P. Benetatos and A. Zippelius, "Anisotropic random networks of semiflexible polymers", *Phys. Rev. Lett.* **99** (2007) 198301.

E. Ben-Naim and A. Zippelius, "Singular energy distributions in driven and undriven granular media", *J. Stat. Phys.* **129** (2007) 677.

N. V. Brilliantov et al., "Translations and rotations are correlated in granular gases", *Phys. Rev. Lett.* **98** (2007) 128001.

C. H. Köhler et al., "Variational bounds for the shear viscosity of gelling melts", *Europhys. Lett.* **78** (2007) 46002.

R. Kühn et al., "Finitely coordinated models for low-temperature phases of amorphous systems", *J. Phys. A* **40** (2007) 9227.

X. M. Mao et al., "Elastic heterogeneity of soft random solids", *Europhys. Lett.* **80** (2007) 26004.

Emeritus Group

2003

G. Benedek, et al., "Deep penetration of vacancies into a solid", *Journal of Electron Spectroscopy and Related Phenomena* **129** (2003) 201.

M. Farnik and J. P. Toennies, "The influence of embedded atoms, molecules and clusters on the lifetimes of electron bubbles in large ^{4}He droplets", *J. Chem. Phys.* **118** (2003) 4176.

A. P. Graham and J. P. Toennies, "The adsorption of xenon on crystalline ice surfaces grown on Pt(111) studied with helium atom scattering", *J. Chem. Phys.* **118** (2003) 2879.

P. Graham and J. P. Toennies, "The adsorption of xenon on crystalline ice surfaces grown on Pt(111) studied with helium atom scattering", *J. Chem. Phys.* **118** (2003) 2879.

S. Grebenev et al., "High resolution infra-red spectra of the OCS-H_2 -HD and -D_2 van der Waals complexes in liquid helium droplets", *J. Chem. Phys.* **118** (2003) 8656.

R. E. Grisenti and J. P. Toennies, "Cryogenic Microjet Source for Orthotropic Beams of Ultra-Large Superfluid Helium Droplets", *Phys. Rev. Lett.* **90** (2003) 234501-1.

L. Y. Rusin, M. B. Sevruyk, and J. P. Toennies, "Angular distribution features of the reaction F^+H_2 products at low energies", *Russian Chemical Physics* **22** (2003) 10.

J. G. Skofronick et. al., "Helium atom scattering studies of the structure and vibrations of H2 physisorbed on MgO(001) single crystals", *Phys. Rev. B* **67** (2003), 035413-1.

K. T. Tang and J. P. Toennies, "The van der Waals potentials between all the rare gas atoms from He to Rn", *J. Chem. Phys.* **118** (2003) 4976.

Á. Vibók et al., "Ab-initio conical intersections for the Na^+H_2 system: A four-state study", *J. Chem. Phys.* **119** (2003) 6588.

2004

R. Brühl et al., "Diffraction of neutral helium clusters: Evidence for "magic numbers" *Phys. Rev. Lett.* **92** (2004) 185301-1.

R.B. Doak et al., "Field ionization detection of supersonic molecular beams", *Rev. Sci. Instrum.* **75** (2004) 405.

Y. Ekinci and J.P. Toennies, "Thermal expansion of the LiF(001) surface", *Surf. Sci.* **563** (2004) 127.

A.P. Graham, J.P. Toennies, and G. Benedek, "Evidence for long-range surface state mediated interaction between sodium atoms on copper (001)", *Surf. Sci. Lett.* **556** (2004) L143.

A. Kalinin et al., "Evidence for a bound HeH_2 halo molecule by diffraction from a transmission grating", *J. Chem. Phys.* **121** (2004) 625.

A. Kalinin et al., "Eclipse" effect in the scattering of weakly bound helium clusters", *Phys. Rev. Lett.* **93** (2004) 163402-1.

E. Knuth, S. Schaper, and J.P. Toennies, "Impurity-stimulated heterogeneous nucleation of supercooled H_2 clusters", *J. Chem. Phys.* **120** (2004) 235.

A. Lindinger, J.P. Toennies, and A.F. Vilesov, "The effects of isotope substitution and nuclear spin modifications on the spectra of complexes of tetracene with hydrogen molecules in ultracold 0.37 K He droplets", *J. Chem. Phys.* **121** (2004) 12282.

L.Y. Rusin, M.B. Sevryuk, and J.P. Toennies, "Simulation of the reactive scattering of $F + D_2$ on a model family of potential energy surfaces with various topographies: The correlation approach", *J. Chem. Phys.* **120 (2004)**

W. Schöllkopf, R. E. Grisenti, and J.P. Toennies, "Time-of-flight resolved transmission-grating diffraction of molecular beams", *Eur. Phys. J. D* **28** (2004) 125.

G. Tejeda et al., "Raman spectroscopy of small para-H_2 clusters formed in cryogenic free jets", *Phys. Rev. Lett.* **92** (2004) 223401-1.

J.P. Toennies, "Serendipitous meanderings and adventures with molecular beams" *Ann. Rev. Phys. Chem.* **55** (2004) 1.

J.P. Toennies and A.F. Vilesov, "Superfluid helium droplets: A uniquely cold nano-matrix for molecules and molecular complexes", *Angew. Chem. Int. Ed.* **43** (2004) 2622.

J.P. Toennies und A.F. Vilesov, "Suprafluide Heliumtröpfchen: außergewöhnlich kalte Nanomatrices für Moleküle und molekulare Komplexe", *Angew. Chem.* **116** (2004) 2674.

J.P. Toennies et al., "Low-energy electron induced restructuring of water monolayers on NaCl(100)", *J. Chem. Phys.* **120** (2004) 11347.

J.P. Toennies, "A short history of the surphon workshop series", *J. Phys.: Condens. Matter* **16** (2004) Preface.

F. Träger and J.P. Toennies, "Helium atom scattering studies of the structures and vibrations of the H_2, HD and D_2 monolayers on NaCl(001)", *J. Phys. Chem. B* **108** (2004) 14710.

2005

G. Benedek, F. Traeger, and J.P. Toennies, "Spectroscopy of shear-horizontal surface phonons by rotation-flip scattering of ortho-H_2 molecules", *Phys. Rev. Lett.* **94** (2005) 086103-1.

G. Benedek et al., "Oscillations in the expansion of solid ^{4}He into vacuum", *Phys. Rev. Lett.* **95** (2005) 095301-1.

R. Brühl et al., "Matter wave diffraction from an inclined transmission grating: Searching for the elusive ^{4}He trimer Efimov state", *Phys. Rev. Lett.* **95** (2005) 063002-1.

U. Buck, R. Düren, and J.P. Toennies, "Obituary Hans Pauly", *Physics Today* **58** (2005) 76.

F. Buyvol-Kot et al., "Magnetic moments in small hydrogen clusters", *Solid State Communications* **135** (2005) 532.

Y. Ekinci and J.P. Toennies, "Elastic and rotationally inelastic diffraction of D_2 molecules from the LiF(001) surface", *Phys. Rev. B* **72** (2005) 205430-1.

M. Fárnik. and J.P. Toennies, "Ion-molecule reactions in ^{4}He droplets: Flying nano-cryo-reactors",
J. Chem. Phys. **122** (2005) 014307-1.

M. Grams, B. Stasicki, and J.P. Toennies, "Production and characterization of micron-sized filaments of solid argon", *Rev. Sci. Instrum.* **76** (2005) 123904-1

A. Kalinin et al., "Observation of mixed fermionic/bosonic helium clusters by transmission grating diffraction", *Phys. Rev. Lett.* **95** (2005) 113402-1.

O. Kornilov et al., "Liquid drop excitations and the size dependent surface tension of small ^{4}He clusters", *J. Low Temp. Phys.* **138** (2005) 235.

L.Yu. Rusin, M. B. Sevryuk, and J.P. Toennies, "Comparison of experimental time-of-flight spectra of the HF products from the F + H_2 reaction with quantum mechanical calculations",
J. Chem. Phys. **122** (2005) 134314-1.

2006

J. Chaiken et al., "Application of scaling and kinetic equation to helium cluster size distribution: Homogeneous nucleation of a nearly ideal gas", *J. Chem. Phys.* **125** (2006) 74305.

P. Estrup, J. P. Toennies, and P. Weber, "Obituary Edward F. Greene", *Physics Today* **59** (2006) 79.

R. Guardiola et al., "Magic numbers, excitation levels and other properties of small neutral ^{4}He clusters (N≤50)", *J Chem. Phys.* **124** (2006) 084307-1.

G. C. Hegerfeldt et al., "He-atom diffraction from nanostructure transmission gratings", *Russian journal: Chemical Physics* **25** (2006) 3.

A. V. Kalinin, L. Yu. Rusin, and J. P. Toennies, "Ion source with longitudinal ionization of a molecular beam by an electron beam in a magnetic field", *Prob. Tech. Eksp.* **5**, (2006) 125. [*Instruments and Experimental Techniques* **49**, (2006) 709]

A. Lindinger, J.P. Toennies, and A.F. Vilesov, "Laser-induced fluorescence spectra of tetracene complexes with Ne, H_2O, D_2O inside He droplets", *Chem Phys. Lett.* **429** (2006) 1.

J. Lobo et al., "Phonon dispersion curves of the Ge(111)-c(2x8) surface determined by helium atom scattering", *Phys. Rev. B* **74** (2006) 035303–1.

C. Nyeland and J.P. Toennies, "Electron gas-density functional calculations of intermolecular potentials between noble gas atoms and noble metal surfaces", *Chem. Phys.* **321** (2006) 285.

L. Y. Rusin and J.P. Toennies, "An improved source of intense beams of fluorine atoms",
J. Phys. D: Appl. Phys. **39** (2006) 4186.

R. Valero et al., "Rotational transitions and diffraction in D_2 scattering from the LiF (001) surface: Theory and experiment", *J. Chem. Phys.* **124** (2006) 234707.

2007

M. H. Alexander et al., "Elastic and inelastic F + D_2 scattering: experiment and simulation on various potential energy surfaces", *Phys. ad Chem. Kinetics in Gas Dynamics* **5** (2007)

G. Benedek et al., "The effects of ^{3}He impurities on the oscillations in the expansion of solid ^{4}He", *Journal of Low Temperature Physics* **146** (2007) 393.

V. Chis et al., "Evidence of longitudinal resonance and optical subsurface phonons in Al(001)", *J. Phys. Condens. Matter* **19** (2007).

S. A. Khairallah et at., “Interplay between magic number stabilities and superfluidity of small parahydrogen clusters”, *Phys. Rev. Lett.* **98** (2007) 183401.

O. Kornilov and J. P. Toennies; “Matter-wave diffraction studies of quantum magic helium clusters”, *Europhysics News* **38** (2007) 22.

C. Peth et al., “XUV laser-plasma source based on solid Ar filament”, *Rev. Sci. Instr.*, in print

L. Y. Rusin, M. B. Sevryuk, and J. P. Toennies, “The special features of rotationally resolved differential cross sections of the F + H_2 reaction at small scattering angles”, *Russian J. of Phys. Chem. B* **1** (2007) 452.

J. P. Toennies and F. Traeger, “Simularities and differences within the H_2 monolayers on NaCl, MgO and H_2O”, *J. Phys. Condens. Matter* **19** (2007).

J. P. Toennies, “Molecular Low Energy Collisions: past, presend and future”, *Physica Scripta* **76** (2007) C15.

Services

The service groups of the institute are headed by the institute manager, relieving the board of directors and its managing director from a range of management tasks. The institute manager and her team support the scientific departments and research groups, ensuring that all staff and guests enjoy an excellent research environment. In addition to financial affairs, human resources, grant administration, and coordination with the central administration of the Max Planck Society, the institute management is in charge of the library and bookbindery, information technology services, facility management including machine and electronics shops, and all outreach activities. Further tasks arise for all services due to the construction activities at the new location "Am Fassberg" as well as general continual support of the two locations "Bunsenstraße" and "Am Fassberg".

MPIDS Courtyard at Bunsenstraße

Workshops – Design and Engineering

Based on the requests from the scientific departments, the mechanical design group develops and engineers solutions for scientific apparatuses. The group uses the most advanced software tools that allow the design of complex parts in three dimensions. This includes three-dimensional assembly and the simulation of the assembled components. Once the technical design has been finished, technical drawings are generated or the design is directly entered into the CAD engine that generates instruction sets understood by the CNC-machines.

The research workshop not only trains apprentices to become precision mechanics, but every scientist can acquire practical know-how here.

The design group works in close collaboration with the electronics shop that designs all electrical components including digital and analog electronics. The design group also certifies in collaboration with the mechanical and electronic shop the conformity of the apparatuses with the European and German laws.

New parts and electronics are manufactured in the respective workshop. The machine shop also assembles components and apparatuses. It is equipped with conventional as well as computer controlled lathes, milling and EDM (electrical discharge) machines. The associated metal shop manufactures frames and other large metal parts, and has state-of-the-art welding equipment for handling steel and aluminum.

The machine and electronics shops are also responsible for the maintenance and repair of the existing machines and apparatuses.

Precision Mechanics Interns

Central IT Services

64bit HPC Linux cluster with HA AIX file server in air-conditioned racks. The systems shown provide 112 CPUs, 872GB RAM and more than 25TB disk space

While each scientific department operates its own computing facilities which are tailored to its specific applications and thus allow for the flexibility of small organizational units and a rapid response to changing scientific needs, common necessities and organisational structures are provided by the central IT service group. Headed by a board formed by the IT coordinators of the scientific departments and the coordinator of the service group, one of the main responsibilities of the central IT services is the maintenance and extension of a reliable and secure network infrastructure with all its technological and legal challenges.
The other responsibilities are diverse. But predominantly the group has to meet the rapidly growing needs for IT resources of the non-scientific staff, as information technology proliferates in all areas. Everything from administration and public relations, to the design and manufacture in the institute‘s workshops, communication facilities, and outreach – computer based services and equipment are utilized throughout and need installation, integration and management.

Facility Management

Members of the MPIDS Facility Management Team

The members of the facility management team handle all technical and infrastructural issues. They support the departments and research groups during the installation of special experimental equipment or constructions, and care for the unobstructed handling of all facilities.

Administration

Guest Apartment

The administration supports all departments and research groups for the accomplishment of personnel and financial management tasks. This includes: purchasing, accounting and bookkeeping, contract management, payroll accounting, calculation of travel expenses, administration of sponsored research and the management of 10 guest apartments and 14 guest rooms within 3 guest houses. To perform these tasks the administration uses modern office tools such as SAP.

Library and Bookbindery

The library of the institute provides researchers, guests and visitors with all necessary printed and online information focussing on the main research topics of the institute. Due to the fact that the Max Planck Institute for Dynamics and Self-Organization was founded only in November 2004 as the successor of the 80-year-old Max Planck Institute for Fluid Dynamics, the existing inventory mainly contains literature from the former institute and some books even have antiquarian value. Due to the upcoming move of the institute the inventory of the library will be moved to the Otto Hahn Library at the Max Planck Campus as soon as the extension of the Otto Hahn Library is completed.
Currently the institute library, together with the library of the Department of Nonlinear Dynamics, contains more than 7,700 volumes, subscribes to 24 printed research journals, and is part of the Max Planck electronic library system.
The library will still be supported by a bookbinder until the end of 2008, so that especially old books can be restored by hand.

MPIDS Bookbindery

Outreach Activities

All departments of the institute highly value the dissemination of their research results to the general public both locally and on a national/international level. Major findings are highlighted in internationally distributed press releases which are usually coordinated with the central press office of the Max Planck Society. To further professionalize public relations, a science journalist will be supporting the institute beginning 2008.
The institute is also actively reaching out to the local community with multiple activities. We initiated the column **Frag`den Wissenschaftler** ("Ask the Scientist") in cooperation with the weekly regional newsprint and advertising paper "Extra Tip". Extra Tip is distributed every Sunday free of charge to 190,000 households in the larger Göttingen area. Since January 2006 "Frag` den Wissenschaftler" has been published weekly. The general public (typically students from Grade 7-13) can ask questions about topics on science in general. A scientist from the institute (or other research institutions in Göttingen) answers the question at a simple but precise level. The answer is then published together with a picture and a short introduction of the corresponding scientist. Previously published "Frag` den Wissenschaftler" questions and answers can be found on the website of the journal (http://www.extratip-goettingen.de/fraeg-den-wissenschaeftler.html) and that of the institute.

MPIDS Girl´s Days 2007 at the Machine Shop

To better inform young people about science, the institute offers internships to students from local high-schools and undergraduates from Germany and abroad. The institute also regularly participates in the

The award is given as a landmark in the Land of Ideas on September 24, 2007.

worldwide initiative **Girl´s Day**. In 2006 for the first time, a special one-day program was offered: 10 girls and boys, mainly children of staff members, had the opportunity to inform themselves about different jobs within the machine shops, bookbindery, administration, and research laboratories. In 2007 we enjoyed an even larger number of participants – 19 children. The positive feedback encourages us to work even more intensively on this project and to also consider other student programs.

A special highlight this year was having the experiment hall named as one of the winners in the competition **365 Landmarks in the Land of Ideas**. The nation-branding initiative and Deutsche Bank have launched this event series. At an open house in December, the hall, its architecture and its future use as a research facility were presented to the general public.

In 2007 the Max Planck Institute for Dynamics and Self-Organization participated jointly with other Max Planck institutes in Göttingen in a special scientific event held at the **Göttingen Literaturherbst**, a literature festival held yearly in Göttingen. In addition to podium discussions on the perspectives of stem cell research in international comparison, the program included 10 scientific lectures given by speakers such as Richard Dawkins, Sir Peter Atkins and Schwer B. Nuland.

As international contacts and research stays at foreign institutions are an important part of the everyday life of today's scientist, networking plays a significant role. The MPIDS is part of an initiative that is establishing an **ALUMNI network** using the novel IT-tools of the public relations office of the Max Planck Society.

How to get to the Max Planck Institute for Dynamics and Self-Organization

Location 1

Bunsenstraße 10
D-37073 Göttingen

Departments: Nonlinear Dynamics (Prof. Geisel)
Dynamics of Complex Fluids (Prof. Herminghaus)
Fluid Dynamics, Pattern Formation and Nanobiocomplexity (Prof. Bodenschatz)
Research Groups: Network Dynamics (Dr. Timme)
Onset of Turbulence and Complexity (Dr. Hof)
Max Planck Fellow Group: Polymers, Complex Fluids and Disordered Systems (Prof. Zippelius)
Emeritus Group: Molecular Interactions (Prof. Toennies)

Services: Institute Management, Administration, Facility Management, Electronic and Mechanic Workshop, IT-Services, Library, Outreach Office, Stock Rooms, Lecture Hall, and Guest Houses.

By plane

From Frankfurt am Main Airport (FRA): Use one of the railway stations at the airport. Trains to Göttingen (direct or via Frankfurt main station) leave twice an hour during daytime (travel time: 2 hours).
From Hannover Airport (HAJ): Take the suburban railway (S-Bahn) to the Central Station (»Hannover Hauptbahnhof«). From here direct ICE trains to Göttingen depart every 1/2 hour.

By train

Göttingen Station is served by the following ICE routes: Hamburg-Göttingen-Munich, Hamburg-Göttingen-Frankfurt, and Berlin-Göttingen-Frankfurt.
From Göttingen railway station:
From the Göttingen station you can take a taxi (5 minutes) or walk (20 minutes). If you walk, you need to leave the main exit of the station and walk to the right. Follow the main street, which after the traffic lights turns into Bürgerstraße. Keep walking until you come to the Bunsenstraße. Turn right – you will reach the entrance gate of the MPIDS after about 300m.

By car

Leave the freeway A7 (Hanover–Kassel) at the exit »Göttingen«, which is the southern exit. Follow the direction »Göttingen Zentrum« (B3). After about 4 km you will pass through a tunnel. At the next traffic light, turn right (direction »Eschwege« B27) and follow the »Bürgerstraße« for about 600 m. The fourth junction to the right is the »Bunsenstraße«. You will reach the institute's gate after about 300m.

Location 2

Am Fassberg 17
D-37077 Göttingen

Departments: Fluid Dynamics, Pattern Formation and Nanobiocomplexity (Prof. Bodenschatz)
Research Group: Nonlinear Dynamics and Cardiac Arrhythmias (Dr. Luther)
(hosted at MPI for Experimental Medicine)
Services: Experimental Hall, Clean Room, and Cell Biology Laboratories

By plane

From Frankfurt am Main Airport (FRA): Use one of the railway stations at the airport. Trains to Göttingen (direct or via Frankfurt main station) leave twice an hour during daytime (travel time: 2 hours).
From Hannover Airport (HAJ): Take the suburban railway (S-Bahn) to the Central Station (»Hannover Hauptbahnhof«). From here direct ICE trains to Göttingen depart every 1/2 hour.

By train

Göttingen Station is served by the following ICE routes: Hamburg-Göttingen-Munich, Hamburg-Göttingen-Frankfurt am Main, and Berlin-Göttingen-Frankfurt.
From Göttingen railway station:
On arrival at Göttingen station take a taxi (15 minutes) or the bus (35 minutes). At platform A take the bus No. 8 (direction: »Geismar-Süd«) or No 13 (direction: »Weende-Ost/Papenberg«). At the second stop »Groner Straße« change to bus No. 5 (direction »Nikolausberg« and get off at the »Faßberg« stop, which is directly in front of the entrance of the Max Planck Campus (MPISDS and MPI for Biophysical Chemistry). Ask at the gate to get directions.

By car

Leave the freeway A7 (Hanover-Kassel) at the exit »Göttingen-Nord«, which is the northern of two exits. Follow the direction for Braunlage (B 27). Leave town – after about 1.5 km at the traffic light (Chinese restaurant on your right) turn left and follow the sign »Nikolausberg«. The third junction on the left is the entrance to the Max Planck Campus (MPIDS and MPI for Biophysical Chemistry). Ask at the gate to get directions.